

**New Double-Responsive Micelles of Block Copolymers
Based on *N,N*-Diethylacrylamide: Synthesis, Kinetics,
Micellization, and Application as Emulsion Stabilizers**

DISSERTATION

zur Erlangung des akademischen Grades eines

Doktors der Naturwissenschaften (Dr. rer. nat.)

in Fach Chemie der Fakultät für Biologie, Chemie und Geowissenschaften

der Universität Bayreuth

und

Docteur de l'Université Pierre et Marie Curie, Paris VI

(Ecole Doctorale Physique et Chimie des Matériaux)

vorgelegt von

Xavier André

Geboren in Lyon / Frankreich

Bayreuth, 2005

Die vorliegende Arbeit wurde in der Zeit von September 2001 bis Juni 2005 in Bayreuth am Lehrstuhl Makromolekulare Chemie II unter der Betreuung von Herrn Prof. Dr. Axel H. E. Müller und in Paris an dem Laboratoire de Chimie des Polymères (Université Pierre et Marie Curie, ParisVI, Frankreich) unter der Betreuung von Frau Prof. Dr. Bernadette Charleux angefertigt.

Vollständiger Abdruck der von der Fakultät für Biologie, Chemie und Geowissenschaften der Universität Bayreuth zur Erlangung des akademischen Grades eines Doktors der Naturwissenschaften genehmigten Dissertation.

Dissertation eingereicht am: 29. Juni 2005

Zulassung durch die Promotionskommission: 6. Juli 2005

Wissenschaftliches Kolloquium: 18. Oktober 2005

Amtierender Dekan: Prof. Dr. O. Meyer

Prüfungsausschuss:

Prof. Dr. H. Alt (Universität Bayreuth)

Prof. Dr. B. Charleux (Zweitgutachter, Université Pierre et Marie Curie, Frankreich)

Prof. Dr. D. Hourdet (Université Pierre et Marie Curie, Frankreich)

Prof. Dr. Robert Jérôme (Drittgutachter, Université de Liège, Belgien)

Prof. Dr. A. H. E. Müller (Erstgutachter, Universität Bayreuth)

THESE en co-tutelle

présentée

à l'Université Pierre et Marie Curie, Paris VI

(Ecole Doctorale Physique et Chimie des Matériaux)

et à la Fakultät für Biologie, Chemie und Geowissenschaften

der Universität Bayreuth

pour l'obtention des grades de:

Docteur de l'Université Pierre et Marie Curie, Paris VI

et

Doktor der Naturwissenschaften (Dr. rer. nat.)

par **Xavier André**

New Double-Responsive Micelles of Block Copolymers Based on *N,N*-Diethylacrylamide: Synthesis, Kinetics, Micellization, and Application as Emulsion Stabilizers

soutenue le 18 octobre 2005, à Bayreuth, Allemagne

Devant le jury composé de:

Prof. Dr. Helmut Alt (Universität Bayreuth, Allemagne)

Prof. Dr. Bernadette Charleux (Université Pierre et Marie Curie, France)

Prof. Dr. Dominique Hourdet (Université Pierre et Marie Curie, France)

Prof. Dr. Robert Jérôme (Rapporteur, Université de Liège, Belgique)

Prof. Dr. Axel H. E. Müller (Rapporteur, Universität Bayreuth, Allemagne)

A ma famille

Table of Contents

1. Introduction	1
1.1 Concept of smart (co)polymers	1
1.2 Thermo-responsive (co)polymers	2
1.3 Synthetic ways to well-defined (co)polymers	4
1.4 Living/controlled polymerization of functionalized monomers	6
1.5 Block copolymers micelles in aqueous solutions	8
1.6 Amphiphilic block copolymers in emulsion polymerization	12
1.7 Aim of the thesis	16
1.8 References	17
2. Overview of the thesis	25
2.1 Kinetics studies using in-line FT-NIR spectroscopy	26
2.2 Synthesis of bishydrophilic block copolymers	30
2.3 Characterization of the thermo- and pH-responsive micelles	32
2.4 Thermo- and pH-responsive micelles as stabilizer in emulsion polymerization	35
2.5 Individual contributions to joint publications	38
2.6 References	40
3. Kinetic Investigation of the Anionic Polymerization of <i>N,N</i>-Diethylacrylamide in the Presence of Triethylaluminium Using In-line FT-NIR Spectroscopy	43
3.1 Introduction	44
3.2 Experimental section	48
3.3 Results and discussion	51
3.4 Conclusions	80
3.5 References	82
3.6 Supporting Information	85
4. Thermo- and pH-Responsive Micelles of Poly(Acrylic acid)-<i>block</i>-Poly(<i>N,N</i>-Diethylacrylamide)	99
4.1 Introduction	100
4.2 Experimental section	101

4.3 Results and discussion	103
4.4 Conclusions	110
4.5 References	111
5. Solution Properties of Double-Stimuli Poly(acrylic Acid)-<i>block</i>-Poly(<i>N,N</i>-Diethylacrylamide) Copolymer	113
5.1 Introduction	114
5.2 Experimental section	118
5.3 Results and discussion	123
5.4 Conclusions	150
5.5 References	152
5.6 Supporting Information	156
6. Remarkable Stabilization of Latex Particles by a New Generation of Double-Stimuli Responsive Poly[(Meth)acrylic Acid]-<i>block</i>-Poly(<i>N,N</i>-Diethylacrylamide) Copolymers	161
6.1 Introduction	162
6.2 Experimental section	165
6.3 Results and discussion	169
6.4 Conclusions	190
6.5 References	192
6.6 Supporting Information	194
7. Summary/Zusammenfassung/Résumé	197
8. Appendix	203
8.1 Fundamentals of anionic polymerization	203
8.2 Fundamentals of free-radical emulsion polymerization	212
8.3 Curriculum vitae	215
8.4 List of publications	216
8.5 Presentations at international conferences	218

Acknowledgments

1. Introduction

In this thesis, the synthesis, characterization, and applications of a new generation of double-stimuli responsive block copolymers is presented. Well-defined polymers and block copolymers based on *N,N*-diethylacrylamide (DEAAM), acrylic acid (AA), and methacrylic acid (MAA) are synthesized via anionic polymerization. Their behavior in water can be easily tuned by controlling the pH, the temperature and the ionic strength of the solution. These block copolymers might be a promising material for emulsions and miniemulsions stabilizers, drug-encapsulation, or for domains related to biotechnology.

1.1 Concepts of smart (co)polymers

The classification ‘smart or intelligent’ (co)polymers defines new materials, which exhibit reversible large properties changes in response to small physical or chemical changes in their environment. Two nomenclatures can be used to classify the different stimulus-responsive materials.¹ The most intuitive classification is related to the stimulus or the stimuli which the materials respond to. Different stimuli can be cited: such as the exposition to light (UV irradiation), a mechanic constraint, the application of an electric or magnetic field, and a change in environmental conditions (pH, ionic strength, temperature).²⁻⁶ Similarly, smart materials can be characterized according to their physical form. They can be either in a molecularly dispersed state in solutions (‘free chains’),⁷ grafted or adsorbed on a surface (‘smart surfaces’ also in the dispersed state),⁸⁻¹⁰ or cross-linked to form a gel (‘hydrogels’).^{11,12} All these transitions ruled by the appropriate stimulus are reversible. The concept of intelligent or smart materials takes its entire signification when the possibility to switch on/off a structural change in the material at the molecular level, inducing a determined function.¹³

The applications of smart or intelligent materials cover a wide range of domains relative to the environment (depollution of water),^{14,15} biomedical (implants),¹⁶ biotechnology (protein-polymer conjugates,¹⁷⁻²⁰ oligonucleotide-polymer conjugates,²¹⁻²³ biological molecules recognition²⁴, pharmaceuticals (drug-delivery systems,²⁵⁻²⁷ anti-tumor therapeutics¹⁰), and personal care products.²⁸ The design of intelligent hydrogels whose degree of swelling varies considerably with different temperature, solvents, electric fields, or pH opens a wide range of news applications, including smart absorbents for solvent

extraction or drug delivery systems.²⁹⁻³⁴ As it was reported by several authors, amphiphilic copolymers are of interest in the colloids and latexes industries (paints and pigments).^{35,36} The possibility to synthesize intelligent latex particles was reported recently by using a stimulus-responsive polymer. Thermo-responsive hairy latex particles based on PNIPAAm,³⁷⁻³⁹ and pH-responsive latex particles were recently described.⁴⁰⁻⁴² Such new compounds has revealed good properties for biomedical applications.^{38,43} Other applications may include domains, which are not related to medical and biological areas. They can cover fields where amphiphilic copolymers are encountered. For example, the remarkable 'thermoviscosifying' properties of such copolymers are of interest in oil industry.⁴⁴ The thermo-responsive latexes can also be used for dye encapsulation and the stimulus-dependent surface activity suggests potential applications as stimulus-responsive emulsifiers for oil-in-water emulsions. Over the wide range of compounds (monomers) available for a specific response, the only limitation is the synthetic chemist ability as well as the toxicity of some compounds, regarding the targeted application (biocompatibility).

1.2 Thermo-responsive (co)polymers

Among the different classes of stimulus-responsive (co)polymers mentioned above, the thermo- and/or pH-responsive polymers and copolymers are of interest, especially for the biomedical and pharmaceutical applications. The most studied thermo-responsive polymer is the poly (*N*-isopropylacrylamide), but other poly (*N*-alkylacrylamide)s polymers also undergo the coil-to-globule phase transition above their respective *Lower Critical Solution Temperature* (LCST). Polymers exhibiting an LCST are characterized by an inverse temperature dependence of their solubility in aqueous solution. Below the LCST, there are hydrogen bonds between hydrophilic groups and water. The polymer is soluble (coiled structure). When temperature rises, hydrogen bonds weaken and hydrophobic interactions between adjacent groups increase. Consequently, water becomes a poor solvent, and the polymer starts to self-aggregate. Precipitation is an endothermic transition and the system is ruled by the decrease of entropy. In all cases reported in literature, the phase separation and precipitation are reversible. The LCST corresponds to the minimum of the phase separation curve.^{45,46} Thus, the values reported commonly in the literature are in fact cloud points.

Depending on their substitution, poly(*N*-alkylacrylamide)s can either be soluble in water: poly(acrylamide), poly(*N*-methylacrylamide), and poly(*N,N*-dimethylacrylamide), or insoluble in water: poly(*N-n*-butylacrylamide), poly(*N-tert*-butylacrylamide), poly(*N*-ethyl, *N*-propylacrylamide), and poly(*N,N*-dipropylacrylamide). In contrast, other poly(*N*-alkylacrylamide)s exhibit a cloud point in water at various temperatures: poly(*N*-acryloylpyrrolidine) ($T_c = 5\text{ }^\circ\text{C}$), poly(*N-n*-propylacrylamide) ($T_c = 22\text{ }^\circ\text{C}$), poly(*N*-isopropyl, *N*-methylacrylamide) ($T_c = 25\text{ }^\circ\text{C}$), poly(*N,N*-diethylacrylamide) ($T_c = 29\text{-}40\text{ }^\circ\text{C}$, depending on the microstructure), poly(*N*-isopropylacrylamide) ($T_c = 32\text{-}34\text{ }^\circ\text{C}$), poly(*N*-cyclopropylacrylamide) ($T_c = 47\text{ }^\circ\text{C}$), poly(*N*-acryloylpiperidine) ($T_c = 55\text{ }^\circ\text{C}$), poly(*N*-ethyl, *N*-methylacrylamide) ($T_c = 56\text{ }^\circ\text{C}$), poly(*N*-ethylacrylamide) ($T_c = 82\text{ }^\circ\text{C}$). Other polymers exhibit this coil-to-globule transition in water, i.e. poly(ethylene oxide) (PEO, $T_c \sim 95\text{ }^\circ\text{C}$),⁴⁷ poly[2-(dimethylamino)ethyl methacrylate] (PDMAEMA, $T_c \sim 50\text{ }^\circ\text{C}$),^{48,49} poly(propylene oxide) (PPO, $T_c \sim 5\text{ }^\circ\text{C}$),⁵⁰ poly(vinylcaprolactam) (PVCL, $T_c \sim 33\text{ }^\circ\text{C}$),⁵¹ poly(methylvinylether) (PMVE, $T_c \sim 36\text{ }^\circ\text{C}$).⁵² Some polymers respond to a combination of two or more stimuli like the PDMAEMA which responds to the pH and the temperature.^{49,53}

A few thermo-responsive (co)polymers are characterized by an *Upper Critical Solution Temperature* (UCST). In aqueous solution the compound is soluble at a temperature above its transition temperature and is insoluble below it. Polymers made from the zwitterionic monomer 2-[*N*-(3-methacryl-amidopropyl)-*N,N*-dimethyl]ammoniopropane sulfonate (SPP) exhibits a UCST in water;⁵⁴ the same behavior is observed for gels of poly(*N,N*-dimethylacrylamide) (PDMAAm) in mixed solvents (water with methanol, dioxane, or acetone).⁵⁵ Bishydrophilic block copolymers based on NIPAAm and SPP exhibit a double thermo-responsive behavior in water as they combine both LCST and UCST effects.⁵⁴ Thermo-responsive smart materials can successfully be used in separation techniques, i.e. as surface modifiers for novel 'green' chromatography,^{56,57} for affinity separation of proteins and nucleotides,⁵⁸ microfiltration membranes,⁵⁹ as well as for therapeutics, i.e. polymer-drug,⁶⁰ or polymer-protein conjugates,⁶¹ polymeric micelles,⁶² and polymeric liposomes.⁶³

The parameters influencing the LCST can be classified in two categories: firstly the parameters inherent to the polymer itself: its molecular weight, polydispersity, and tacticity,⁶⁴ and secondly, the external factors such as the added salt,⁶⁵ cosolvent,^{66,67} and

surfactant.^{68,69} No precipitation is observed in the case of PNIPAAm in 1 wt.-% sodium dodecyl sulfate (SDS) solution even in boiling solution.⁷⁰ The interactions between PNIPAAm with the charged micelles lead to the formation of a negatively charged complex which prevents the PNIPAAm from aggregation.

Another approach consists in tuning the transition temperature between 0 and 100 °C by copolymerization with a non-ionic comonomer (hydrophobic or hydrophilic). Ethylene oxide (EO),⁷ *N*-acryloxy succinimide (AS),⁷¹ *N,N*-dimethylacrylamide (DMAAm),⁷² were successfully used as comonomers in combination with NIPAAm. Furthermore, ionic pH- and thermo-responsive copolymers can be obtained by copolymerization of NIPAAm or DEAAm with acrylic acid,⁷³⁻⁷⁵ methacrylic acid,^{11,76,77} itaconic acid,⁷⁸ and acrylamide-derivatives bearing a carboxylic function (anionic),⁷⁹ or cationizable 2-vinylpyridine,⁸⁰ and amino-derivative methacrylamide (*N,N'*-dimethylaminopropylmethacrylamide).⁸¹

1.3 Synthetic ways to well-defined (co)polymers

The synthesis of polymers and copolymers with well-defined structures, architectures, and functionalities remains a continuous challenge for polymer chemists both in academic and industrial areas. The term ‘well-defined’, which is commonly used nowadays, requires the prediction of the molecular weight and the obtention of narrow molecular weight distributions. Most of the polymers used so far for the applications mentioned above, have broad molecular weight distributions and their composition is not uniform. In order to get a better control of the targeted application, narrow molecular weight distributions as well as homogeneous structures and compositions are required. Indeed, many applications are based on the response kinetics. It is obvious that the structure has to be perfectly known (controlled drug encapsulation and release after a change in pH or in temperature, distinct retention time of a conjugate in the body, uniform pore-size). A broad molecular weight distribution can affect the macroscopic response of a thermo-responsive material, where lower molecular weight chains still remain soluble even if the stimulus is applied.⁸² In the field of emulsion polymerization, the effect of chemical or physical cross-linkages assured by higher molecular weight chains of the stabilizer made of amphiphilic block copolymer (ionic or neutral) can compete with the (electro-) steric stabilization, leading to the flocculation. Furthermore, the direct synthesis of pure (co)polymers without any purification method and/or requirement of a protecting group remains a challenge for

number of applications. For example, the deprotection under acidic or basic conditions of polymer protein conjugates melting leads to the denaturation of the protein.⁸²

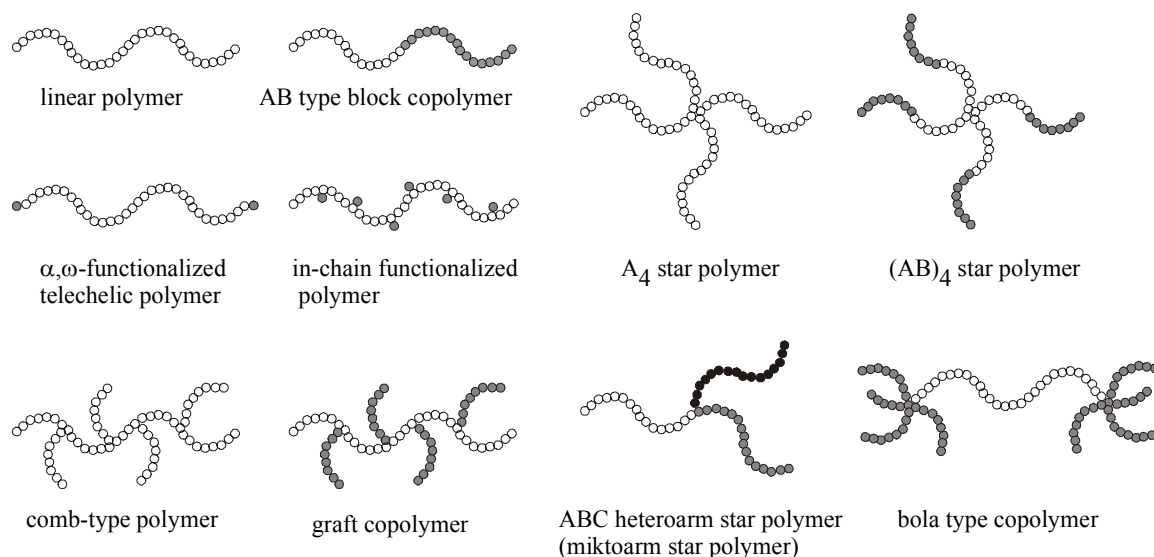


Figure 1-1. Examples for polymer architectures accessible via living polymerization.

The solution to this problem seems to be the polymerization under 'living' conditions that yields polymers with low polydispersities and defined molecular weights. The term 'living' was first introduced to define the anionic polymerization process in 1956 as Szwarc and coworkers discovered the livingness of polydienyl-lithium and polystyryl-sodium chains in hydrocarbon media.⁸³ The term 'living' is used to describe systems where no irreversible chain transfers and chain terminations occur during the course of the polymerization. The molecular weight is controlled by the stoichiometry of the reaction (ratio of monomer concentration to initiator concentration), and the monomer conversion. Thus it provides the maximum degree of control for the synthesis of polymers with predictable molecular weight. The living conditions require also that the growing chains keep their activity long until complete monomer conversion. The possibility of post-polymerization reactions with the active chain ends allows the design of copolymer of different architectures (*block-*, *star-*, and *comb-shape*) with different functionalities by choosing the appropriate quenching agent. Figure 1-1 shows some (co)polymer architectures accessible by living polymerization processes. Narrow molecular weight

distributions can be obtained only if the relative rate of initiation is higher than the rate of monomer incorporation.

The major drawbacks of anionic living polymerization are the limited choice of monomers and the stringent reaction conditions, where polymerization should occur in the absence of impurities (protic species, oxygen), which can lead to chain termination and/or chain transfer. Living methods may include anionic, cationic,⁸⁴⁻⁸⁷ group transfer polymerization,⁸⁸ and coordinative polymerizations.⁸⁹

To circumvent the inconveniences due to the stringent reactions required for living processes, Controlled Radical Polymerization (CRP) systems were introduced by several groups. All these processes tend to approach the living conditions by decreasing as much as possible the irreversible chain termination occurring in free-radical polymerization. The main strategy employed consists in decreasing the concentration of active centers and in compensating the irreversible termination by introducing a competing reversible termination. Since the irreversible bimolecular termination can be reduced but not completely suppressed, these new systems of polymerization should be considered as controlled polymerizations rather than living ones.⁹⁰ CRP methods may include polymerization initiated by the 'INIFERTERS' (Initiation, Transfer, Termination),⁹¹ Nitroxide Mediated Radical Polymerization (NMRP),⁹²⁻⁹⁴ Atom-Transfer Radical Polymerization (ATRP),^{95,96} degenerative transfer,⁹⁷ and Reversible Addition-Fragmentation Chain Transfer (RAFT) polymerization processes.⁹⁸⁻¹⁰⁰ CRP methods allow the synthesis of well-defined polymers and copolymers of different architectures but suffer from some limitations.

1.4 Living/controlled polymerization of functionalized monomers

The direct production of poly(acrylic acid) and poly(methacrylic acid) via anionic polymerization is not possible because of the acidic proton born by the carboxylic function. A precursor such as poly(*tert*-butyl acrylate) or poly(*tert*-butyl methacrylate) has to be synthesized first, which leads to the desired product after an hydrolysis under acidic conditions. Generally two methods are used, i.e. trifluoroacetic acid in dichloromethane for one day at room temperature,¹⁰¹ or hydrochloric acid in dioxane at reflux for one day.^{102,103} Similarly, the direct polymerization of acrylic acid or methacrylic acid by ATRP can not

be attempted. The transition metal ions complexed to a ligand (containing nitrogen) contaminate the final product and can also complex monomers bearing hydroxyl, amine, or carboxyl function. In this case, polymerization is possible only if the group is protected,^{95,104} or by the appropriate monomer/solvent ratio choice.¹⁰⁵ Recently, Du Prez et al. reported the facile obtention of monodisperse poly[(meth)acrylic acid] after removal by thermolysis of the hemiacetal ester on a precursor of poly[1-ethoxyethyl (meth)acrylate], firstly synthesized by Atom Transfer Radical Polymerization (ATRP).¹⁰⁶ RAFT processes allow the direct polymerization of acrylic acid (AA) without any protection.¹⁰⁷ Furthermore, block copolymers based on AA can be obtained but it is restricted to monomers and copolymers both soluble in the solvent used for the polymerization, i.e. well-defined PNIPAAm-*block*-PAA copolymers.¹⁷ After hydrolysis of the dithiocarbonyl-derived chain end, RS(C=S)Z, a thiol-terminated can be easily obtained and is of interest for the conjugation with proteins (attached to cysteine residue). In addition, the R group of the chain transfer agent can be chosen to obtain a second functionality at the other chain end of the polymer, interesting for some biomedical applications. Similarly, NMRP strategies allow the direct polymerization of functional monomer like styrene sulfonate using TEMPO,¹⁰⁸ and AA using an alkoxyamine initiator based on the *N-tert*-butyl-*N*-(1-diethyl phosphono-2,2-dimethyl propyl) nitroxide, SG1.¹⁰⁹

Beside acrylic acid, other functionalized monomers containing reactive hydrogen atoms, such as monoalkyl-acrylamides, or monomer like hydroxyethylmethacrylate (HEMA) can not be polymerized via anionic method in a living fashion. In order to polymerize these monomers, protecting groups have to be introduced which necessitates the deprotection of the functional groups after polymerization.¹¹⁰ As it was the case for poly[alkyl (meth)acrylate], the living/controlled polymerization of alkylacrylamide monomers was during several decades not described. Parallel to the increasing applications of the materials based on such monomers, the interests have increased considerably. The living/controlled polymerization of *N,N*-dialkylacrylamide monomers was achieved by anionic polymerization and Group Transfer Polymerization (GTP).^{111,112} Recently, Nakahama et al. reported the successful synthesis of *N,N*-dimethylacrylamide and *N,N*-diethylacrylamide via anionic polymerization in the presence of Lewis acids in tetrahydrofuran at low temperature.¹¹³ The crucial influence of the choice of the initiating group/Lewis acid was demonstrated and the influence on the microstructure as well as the solubility of the final polymer obviously showed. Beside the dialkylacrylamide monomers,

NIPAAm still remains the most studied and the most used of its family. As a monoalkylacrylamide, it presents an acidic proton in the alpha position of the carbonyl group and the nucleophilic attack by the initiator can occur as it is observed for alkyl (meth)acrylate monomers. Recently, two groups reported the anionic polymerization of a protected NIPAAm.^{114,115} The deprotection is easy and pure PNIPAAm can be obtained. The relatively poor solubility of such polymers makes their analysis difficult and no final conclusions on the living /controlled fashion could be done. The poor solubility still remains a recurrent problem for those confronted with the analysis of poly(alkylacrylamide)s and their derivatives. The main interest on these compounds is based on their thermo-responsive properties in water. They exhibit a LCST in water which varies with the monomer nature. In some cases the thermo-responsive behavior disappears as a highly stereoregular PDEAAm rich in syndiotactic (rr) triads is soluble in water and does not present any phase-transition.¹¹³ The controlled-radical polymerization of alkylacrylamide monomers was successfully attempted by CRP methods, using ATRP,¹¹⁶⁻¹¹⁸ RAFT,¹¹⁹ and NMRP.¹²⁰⁻¹²³

Regardless of the new synthetic systems described in the literature, anionic polymerization remains the best synthetic way to obtain polymers and copolymers of determined mass, highly pure composition and perfect chain architecture. Furthermore, the control of the microstructure (tacticity) still remains a predominant feature of ionic processes, i.e. in the case of polydienes, poly(alkyl acrylate)s, poly(alkyl methacrylate)s, and poly(alkylacrylamide)s. Different microstructures do not only affect the properties in bulk (T_g , isotactic PMMA ≈ 40 °C, T_g , syndiotactic PMMA ≈ 140 °C, and T_g , cis-1,4-polybutadiene ≈ -110 °C, T_g , 1,2-polybutadiene ≈ -10 °C),¹²⁴ but also have a tremendous influence on the solution properties of the resulting polymer. In the case of PDEAAm, it was reported that atactic PDEAAm and PDEAAm rich in isotactic and heterotactic triads exhibit a LCST in aqueous solutions whereas PDEAAm rich in syndiotactic triads is always soluble and does not exhibit a LCST.¹¹³

1.5 Block copolymer micelles in aqueous solutions

Micellization phenomena have interested chemists from different fields, like physical-chemistry, biochemistry and polymer chemistry. Research has been essentially devoted to the low molecular weight surface-active molecules, i.e. sodium dodecyl sulfate (SDS).¹²⁵

Since two decades it has been expanded to the association of copolymers of different architectures (block-, stat- or graft-) but more attention was devoted to block copolymers since their structure mimics the low-molecular weight structure (hydrophilic head, hydrophobic tail).¹²⁶ Similarly to low-molecular weight surfactants, amphiphilic block copolymers self-assemble in aqueous solutions.¹²⁷ In most cases, the association phenomenon leads to the formation of multi-molecular entities of different shape. For biotechnological/therapeutics applications and for ecological considerations the demand on water-soluble (co)polymers has been increased. Beside the biotechnological area, where micelles can be used as drug carriers,^{128,129} polymer micelles can be used in the field of nanoscience. Antonietti and Armes used polymer micelles as 'nanoreactors' to produce highly dispersed metal or semiconductor particles.¹³⁰⁻¹³² Similarly, mineralization of gold was performed using micelles made of polystyrene-*block*-poly(2-vinylpyridine).¹³³

In aqueous media, amphiphilic molecules made of AB block copolymer self-assemble to form micelles. The micellar aggregates can adopt different morphologies, such as spherical, rod-like, core-corona, vesicle, and worm-like micelles. As water is a poor solvent for the hydrophobic segment, it forms the core of the entity as the corona made of the water-soluble block stabilizes the system. Triblock- and graft- copolymers can adopt in aqueous solutions additional morphologies like core-shell-corona micelles with a compartmentalized core, micelles with a mixed corona (no chain segregation), core-shell-corona micelles with a compartmentalized corona (radial chain segregation), Janus micelles with an asymmetric corona (lateral chain segregation), and vesicles.^{134,135}

As reported for low-molecular weight surfactants, the critical phenomena play an important role for micelles of block copolymers. Below its *Critical Micellar Concentration* (CMC), an amphiphilic block copolymer in aqueous solution can be observed as an isolated molecularly block copolymer (unimer). Above its CMC, micelles made of amphiphilic molecules are formed and are in equilibrium with the non-associated molecules (unimers). The number of aggregation, N_{agg} , can be defined as the number of unimers self-assembling to form a supramolecular assembly (micelle) made of N_{agg} unimers. Generally this system is under, thermodynamic equilibrium. For a 'closed association' scheme, dynamic equilibrium between micelles and unimers is observed where the unimer concentration is constant ($c = CMC$). There is also a mechanism called 'open association' that comprises a series of equilibria between unimers, dimers, trimers

etc.^{136,137} However, for a micelle with a glassy core, i.e. with a glass transition temperature of the core-constituting block that is sufficiently high, as is the case for polystyrene, the structure is 'kinetically frozen' and may not represent the thermodynamic equilibrium.¹³⁸ Due to the high degree of incompatibility between the soluble and the insoluble block, the CMCs observed for amphiphilic block copolymers ($10^{-5} - 10^{-8} \text{ mol}\cdot\text{L}^{-1}$) are smaller than those observed for low-molecular weight surfactant ($\text{CMC}_{\text{SDS}} = 7.6 \cdot 10^{-3} \text{ mol}\cdot\text{L}^{-1}$ at 23°C).¹³⁹⁻¹⁴¹ The block lengths of the copolymers have a considerable impact on the CMC, where the length of the insoluble block affects the CMC much more than that of the soluble block. Förster et al. have postulated a universal scaling relation $N_{\text{agg}} \propto N_A^2 \cdot N_B^{-0.8}$ for strongly segregated diblock and triblock copolymer systems that was derived from micellization experiments with polystyrene-*block*-poly(4-vinylpyridine) in toluene,^{142,143} where N_A is the length of the insoluble block and N_B that of the soluble block.

Depending on their composition micelles made of block copolymers can be classified according to the ratio of core radius, R_c , to corona thickness, d_{corona} .¹⁴⁴ Crew-cut micelles possess large cores and short coronal 'hair' and are observed for $R_{\text{core}} \gg d_{\text{corona}}$,¹⁴⁵⁻¹⁴⁷ whereas star micelles are spherical with small cores and expanded coronas ($R_{\text{core}} \ll d_{\text{corona}}$).¹⁴⁸ For star micelles, the radius of the core seems to be independent of the length of the soluble block and scales as $N_B^{3/5}$, where N_B is the number of units in the insoluble block.¹⁴⁴ Under certain restrictions (hydrophobic/hydrophilic balance), the reverse micelles can be theoretically observed.⁵⁰ Numerous studies on the influence of some parameters on the structure of star-like micelles were reported by Eisenberg et al. in the case of poly(acrylic acid)-*block*-polystyrene (PAA-*b*-PS). The CMC and the aggregation number are influenced by the PAA block length for a short PS block and by the PS block when this is long.¹⁴⁹⁻¹⁵¹ The ionic strength exerts also a strong influence on both the CMC and the aggregation number. The addition of salt is comparable to a diminution of the solvent quality and its influence increases with the PAA block length. A maximum is observed where the salt concentration has no more influence for both the CMC and N_{agg} .¹⁴⁹ The main differences in comparison to low-molecular weight surfactant may include the slower exchange equilibrium between micelles and the heterogeneity of composition and size of block copolymers. Fluorescence studies were reported in the case of poly(methacrylic acid)-*block*-poly(dimethylaminoalkyl methacrylate) and an equilibrium constant of 10^{-3} s^{-1} was found,^{152,153} which can be easily compared to the value reported for low molecular weight surfactant ($10^6 - 10^8 \text{ s}^{-1}$).¹³⁹ Additionally the exchange

rate between unimers (non-associated copolymer) and micelles decreases when the hydrophobic content increases. In this case frozen micelles can be observed in pure water in the case of PS-*b*-PAA copolymers (styrene mol.-% > 45) where no equilibrium takes place.¹⁵⁴ By increasing the temperature, by addition of cosolvent, or by addition of a cosurfactant, it was possible to tune the exchange dynamics of unimers between block copolymer micelles.¹⁵⁵

Ionic amphiphilic block copolymers can be either anionic or cationic. In the case of anionic polyelectrolyte block, poly(acrylic acid),^{156,157} poly(methacrylic acid),^{158,159} poly(sodium styrenesulfonate),¹⁶⁰ and poly(malic acid)¹⁶¹ can be used in combination with a block made of polystyrene,¹⁶²⁻¹⁶⁴ poly(methyl methacrylate),^{157,165} or poly(isobutylene).^{166,167} Cationic polyelectrolyte blocks can be either protonated tertiary amines where ionization degree depends on the pH, like poly(2-vinyl pyridine),^{168,169} and poly[2-(dimethylamino)ethyl methacrylate] (PDMAEMA)¹⁷⁰⁻¹⁷² or modified polymer bearing a permanent charge, like the quaternized-poly(chloromethyl-styrene),¹⁷³ quaternized-poly(4-vinylpyridine),¹⁷⁴⁻¹⁷⁸ and betainized-PDMAEMA.^{179,180}

The geometry and architecture of the micelles obtained is closely dependent on the micellization procedure. This is only true for systems where no exchange between unimers and micelles is observed. It is observed in the case of frozen micelles or when the hydrophobic/hydrophilic balance is too high (quasi non-soluble block copolymers).¹⁰¹ Their preparation may include the use of a common solvent which is removed by distillation, or dialysis. The time factor, stirring conditions as well as the temperature of preparation are of importance. Depending on their hydrophilic content, micelles of polystyrene-*block*-poly(acrylic acid) can be obtained by direct dissolution in water or by using *N,N*-dimethylformamide (DMF) as a common solvent. Water is added dropwise to DMF, which is a good solvent for both blocks, and DMF is removed by dialysis.¹⁸¹ THF was used as a cosolvent in the case of poly(ethylene glycol)-*block*-poly(ϵ -caprolactone).¹⁸² Polystyrene-*block*-poly(bromo-vinylpyridinium) obtained after quaternization of PS-*b*-P4VP with bromoethyl, dissolves instantaneously in water when the hydrophilic content is higher than 75 wt.-%.¹⁷⁴⁻¹⁷⁸ Some systems does not require the use of dialysis like the micelles made of poly(vinyl pyrrolidone)-*block*-poly(ethylene oxide) which self-assemble instantaneously in aqueous solutions on titration from pH = 1 to 10,¹⁸³ or micelles of

poly(*N*-vinylpyrrolidone)-*block*-poly(*D,L*-lactide) which are formed by direct dissolution in water.¹⁸⁴

The formation of ‘schizophrenic micelles’ was reported by Armes for block copolymers based of 2-(dimethylamino)ethyl methacrylate (DMAEMA), 4-vinylbenzoic acid (VBA), propylene oxide (PPO), and 2-(*N*-morpholino)ethyl methacrylate (MEMA).^{43,50,185} Some of the studied copolymers display a response to the pH, the temperature, and other stimuli like the ionic strength. Under certain restrictions, such AB block copolymers can form either the so-called ‘direct’ A-core micelle and by changing one parameter the B-core ‘inverse’ micelle. Depending on the pH value the zwitterionic poly(4-vinyl benzoic acid)-*block*-poly(2-(diethylamino)ethyl methacrylate) (PVBA-*b*-PDMAEMA) copolymer can form direct PVBA-core micelles (pH = 2) and inverse PDMAEMA-core micelles (pH = 10).⁴³ The authors mentioned the possible applications as pigment dispersant or in the field of biotechnology for proteins purification and separation.

1.6 Amphiphilic block copolymers in emulsion polymerization

Aqueous free-radical emulsion polymerization still remains the synthetic way of choice for number of industrial applications.¹⁸⁶⁻¹⁸⁸ As the polymerization occurs in water, there is no need to use organic solvent (environmental aspects, cost of recycling), the heat of the reaction is controlled by the medium, and the final product has a low viscosity and is easy to handle.¹⁸⁹ It leads to stable polymer particles aqueous suspensions (particle diameter \approx 50 to 500 nm). High molecular weights can be obtained with high polymerization rates, and high monomer conversions are reachable which limits the presence of unreacted monomer in the final product.¹⁹⁰ A direct use of the latex is possible for paintings, coatings and adhesives applications, alike, the polymer can be isolated for other applications.¹⁸⁶

The stabilizer (surfactant or emulsifier) plays a key-role from the nucleation step to the final application. As it participates to the nucleation step and contributes to the creation of new particles, polymerization kinetics is directly affected by it. The obtention of stable latexes is the first criterion of an efficient stabilizer. As the particle number is related to the stabilizer efficiency, for a given amount of stabilizer and monomer, the best stabilization is observed for the latex where the particles size is smaller.¹⁹¹ Three modes of stabilization can be cited. By using ionic low-molecular weight surfactant, i.e. SDS, the electrostatic

stabilization of the latex occurs by repulsive interaction. The presence of low molecular weight surfactant in the latex is an impurity when regarding the final application (paints, coatings). They ensure ions-rich zones within the film and are more sensitive to water. Furthermore, the intrinsic mobility of the surfactant in a polymer film can lead to desorption and bad adhesive properties. The second strategy consists in introducing a neutral water-soluble polymer which adsorbs on the particles to ensure a steric stabilization. Steric stabilizers based on poly(vinyl acetate), poly(ethylene oxide) (PEO) and partially hydrophobically-modified cellulose can be cited as example.¹⁹² *Statistic-, block- and graft-*copolymers of ethylene oxide, styrene and alkyl acrylate monomers were described in the academic area.¹⁹³⁻¹⁹⁵ The third mode of stabilization is a combination of both electrostatic and steric effects.¹⁹⁶ The use of an ionic or ionizable comonomer (acrylic acid, sodium sulfonate styrene) allows the *in-situ* formation of amphiphilic copolymer chains which participate in the stabilization (emulsifier-free latex).¹⁹⁷ But the ionic units can be either buried inside the latex particle or lost by solubilization in water, and the stabilization can not occur in an efficient way.¹⁹⁸

To bypass this problem, macromolecular stabilizer made of neutral or ionic amphiphilic copolymers were introduced.¹⁹⁹ Their use allows a better stabilization of the latex as well as a better control of the polymerization process.²⁰⁰ The introduction of amphiphilic (co)polymers of different architectures (*stat, block, brush, graft*) to replace the low molecular weight surfactant and the hydrophilic comonomer presents several advantages: use of smaller amount because of their lower critical micellar concentration, better properties of the final latex because of their lower diffusion coefficient (lower mobility), better stabilization by the combination of a steric with an electrostatic stabilization when the copolymer contains a polyelectrolyte segment, the so-called 'electrosteric' stabilization.²⁰¹ In the case of block copolymers, the properties can be easily tuned by the appropriate choice of blocks nature, and length. Among the various block copolymers which were investigated, those containing a polyelectrolyte segment showed their remarkable efficiency. They impart good stability of the latex during the polymerization and during the storage because they combine the electrostatic repulsion and the steric effect.^{199,202-204} The presence of one or more hydrophobic block allows a better anchorage on the latex particles and suppresses desorption processes. It can be either by adsorption where the hydrophobic units are localized on the surface, by absorption where entanglements are observed, or by covalent bonding. The latter is observed by the use of

polymerizable surfactant,^{205,206} or by transfer to the hydrophobic block during the polymerization as it was described for the formation of branching by transfer to the polymer during the emulsion polymerization process.^{207,208}

Anionic polyelectrolyte- and cationic-polyelectrolyte copolymers of different architectures and morphologies were described. Statistic copolymers based on acrylic acid, methacrylic acid, acrylonitrile, dodecyl acrylate, methyl methacrylate, and styrene were synthesized by free-radical copolymerization and used as stabilizer in the emulsion polymerization of styrene, methyl methacrylate, and butyl acrylate.²⁰⁹⁻²¹² They present a lower efficiency in contrast to low-molecular weight surfactant because stable latexes can be only obtained with important copolymer-to-monomer weight ratio (up to 30 wt.-%). This is due to their heterogeneous structure and composition and to their broad molecular weight distribution. In the case of acrylic acid-based copolymer, the presence of low molecular weight pure poly(acrylic acid) chains in the copolymer tends also to destabilize the latex by depletion. In the opposite case, longer chains can lead to the formation of bonds between particles which lead to the flocculation. Similarly, graft-copolymers and polysoaps have been used, but have not presented any remarkable advantages in comparison to classical surfactant. As they mimic the structure of low-molecular weight surfactant, the interests of block copolymers have been increased in the last decades. Living-ionic and controlled-radical processes allow the formation of well-defined structures and composition. The first studies were reported on neutral amphiphilic copolymers, mostly based on polystyrene, poly(alkyl acrylate)s, and poly(ethylene oxide).¹⁹⁵ They present some advantages due to their insensibility to variation of pH. But some drawbacks were reported such as the influence of the temperature (POE: $T_c \approx 90$ °C) on the partition of the emulsifier between aqueous and organic phases, leading to a bimodal particle size distribution.²¹³ On the other hand, the copolymer can be buried or entrapped in the particle which reduces its stabilization efficiency.¹⁹⁸ As already reported above, anionically charged block copolymers are based on monomers bearing a carboxylate function (acrylic acid, methacrylic acid), or sulfonate function. Only a few examples are reported in the literature concerning the use of cationic or cationizable amphiphilic block copolymers in emulsion polymerization stabilization. Generally, they are based on monomers bearing a protonated or quaternized tertiary amine function, such as 2-(dimethylamino)ethyl methacrylate,^{214,215} or quaternized (chloromethylstyrene).^{204,216}

The characteristics of the block copolymers were investigated. Typically molecular weight between 5000 and 50000 g·mol⁻¹ were used and stable latexes with a solid content of 10 to 20 wt.-% can be obtained by using typically 1 wt.-% copolymer-to-monomer ratio. In some cases, only 0.15 wt.-% of copolymer were sufficient to stabilize the latex.²¹⁷ Nevertheless, some drawbacks can be cited for the use of ionic block copolymer which are due to their polyelectrolyte-nature. By increasing the ionic strength, the electrostatic repulsion is screened because the corona made of the polyelectrolyte segment can not be expanded in aqueous phase. It leads to a destabilization of the latex.²¹⁷ Poly(methacrylic acid)-*block*-poly(methyl methacrylate) under its acidic form can not lead to stable latex.

Similarly to the control of the particle size (by the appropriate choice of emulsifier), one another determining factor in emulsion polymerization is the control of the molecular weight as well as the molecular weight distribution of the polymer chains. For that purpose, controlled-radical fashions were introduced to the polymerization processes in dispersed media.²¹⁸⁻²²⁰ The first attempts were successfully described in the case of mini-emulsion polymerization, because the complexity of the emulsion system does not allow a complete control (exchange dynamics between the different compartments of the system). In the case of miniemulsion the initial droplet size is smaller than the size observed in conventional process. The resulting increase in the interfacial area of the droplet phase and the reduced number of micelles ensure that entry into the droplets becomes the predominant particle nucleation mechanism. In the ideal case the system at t_{∞} is the same as at t_0 (particles size and number).¹⁸⁶ Recently, nitroxide-mediated controlled radical emulsion polymerization (NMRP) of styrene and *n*-butyl acrylate was reported using water-soluble alkoxyamine as initiator.²²¹

One way of investigation for the future seems to be the synthesis of smart or intelligent latexes whose properties can be tuned by the application of one or more stimuli. Two strategies can be mentioned: first the grafting of stimuli-responsive hairs onto PS or PMMA preformed particles, secondly, the use of stimuli-responsive block copolymer as dispersant and particles stabilizer. The second strategy is a one-pot method which could be interesting for various applications.

1.7 Aim of the thesis

The first objective of this thesis was to obtain well-defined poly(*N,N*-diethylacrylamide), poly(*tert*-butyl acrylate)-*block*-poly(*N,N*-diethylacrylamide) and poly(*tert*-butyl methacrylate)-*block*-poly(*N,N*-diethylacrylamide) (PDEAAm, *Pt*BA-*b*-PDEAAm, *Pt*BMA-*b*-PDEAAm) via sequential anionic polymerization. For that purpose, we introduced the use of triethylaluminum as Lewis acid to complex ester amido enolate-lithium in tetrahydrofuran at low temperature. Polymerization kinetics was monitored via *in-line* Fourier Transform Near Infra-Red spectroscopy (FT-NIR) and computational chemistry results have completed the study. Selective hydrolysis of the *Pt*BA or *Pt*BMA segments rendered stimuli-responsive poly(acrylic acid)- and poly(methacrylic acid)-*block*-PDEAAm copolymers. The solution properties of such bishydrophilic copolymer could be tuned by the temperature, the pH, and the ionic strength of the aqueous solution. Direct and inverse-micellar structures were observed by means of different physical-chemistry investigations. Additionally, batch free-radical emulsion polymerizations were carried out using these stimuli-responsive block copolymers in order to evaluate their emulsifying and latex stabilizing efficiency.

1.8 References

- (1) Roy, I.; Gupta, M. N. *Chemistry & Biology* **2003**, *10*, 1161-1171.
- (2) Wallace, G. G.; Spinks, G. M.; Teasdale, P. R.; Editors. *Conductive Electroactive Polymers: Intelligent Materials Systems*, 1996.
- (3) Seki, T.; Kojima, J.-y.; Ichimura, K. *Journal of Physical Chemistry B* **1999**, *103*, 10338-10340.
- (4) Chee, C. K.; Rimmer, S.; Soutar, I.; Swanson, L. *ACS Symposium Series* **2001**, *780*, 223-237.
- (5) Durand, A.; Herve, M.; Hourdet, D. *ACS Symposium Series* **2001**, *780*, 181-207.
- (6) Patil, A. O.; Ikenoue, Y.; Wudl, F.; Heeger, A. J. *Journal of the American Chemical Society* **1987**, *109*, 1858-1859.
- (7) Topp, M. D. C.; Dijkstra, P. J.; Talsma, H.; Feijen, J. *Macromolecules* **1997**, *30*, 8518-8520.
- (8) Mahltig, B.; Gohy, J.-F.; Antoun, S.; Jérôme, R.; Stamm, M. *Colloid and Polymer Science* **2002**, *280*, 495-502.
- (9) Nath, N.; Chilkoti, A. *Adv. Mater.* **2002**, *14*, 1243-1247.
- (10) Prazeres, T. J. V.; Santos, A. M.; Martinho, J. M. G.; Elaessari, A.; Pichot, C. *Langmuir* **2004**, *20*, 6834-6840.
- (11) Stile, R. A.; Healy, K. E. *Biomacromolecules* **2001**, *2*, 185-194.
- (12) Zhang, X.-Z.; Yang, Y.-Y.; Wang, F.-J.; Chung, T.-S. *Langmuir* **2002**, *18*, 2013-2018.
- (13) Hoffman, A. S.; Stayton, P. S.; Bulmus, V.; Chen, G.; Chen, J.; Cheung, C.; Chilkoti, A.; Ding, Z.; Dong, L.; Fong, R.; Lackey, C. A.; Long, C. J.; Miura, M.; Morris, J. E.; Murthy, N.; Nabeshima, Y.; Park, T. G.; Press, O. W.; Shimoboji, T.; Shoemaker, S.; Yang, H. J.; Monji, N.; Nowinski, R. C.; Cole, C. A.; Priest, J. H.; Harris, J. M.; Nakamae, K.; Nishino, T.; Miyata, T. *J. Biomed. Mater. Res.* **2000**, *52*, 577-586.
- (14) Pandit, P.; Basu, S. *Environmental Science and Technology* **2004**, *38*, 2435-2442.
- (15) Pandit, P.; Basu, S. *Journal of Colloid and Interface Science* **2002**, *245*, 208-214.
- (16) Hiratani, H.; Alvarez-Lorenzo, C. *Journal of Controlled Release* **2002**, *83*, 223-230.
- (17) Schilli, C. M.; Müller, A. H. E.; Rizzardo, E.; Thang, S. H.; Chong, Y. K. *ACS Symposium Series* **2003**, *854*, 603-618.
- (18) Maeda, H. *Adv. Drug Delivery Rev.* **2001**, *46*, 169-185.
- (19) Nucci, M. L.; Shorr, R.; Abuchowski, A. *Adv. Drug Delivery Rev.* **1991**, *6*, 133-151.
- (20) Bromberg, L.; Levin, G. *Bioconjugate Chemistry* **1998**, *9*, 40-49.
- (21) Murata, M.; Kaku, W.; Anada, T.; Soh, N.; Katayama, Y.; Macda, M. *Chemistry Letters* **2003**, *32*, 266-267.
- (22) Gerst, M.; Schuch, H.; Urban, D. *ACS Symposium Series* **2000**, *765*, 37-51.
- (23) Kabanov, A. V.; Alakhov, V. Y. *J. Control. Release* **1994**, *28*, 15-35.
- (24) Elaessari, A.; Delair, T.; Pichot, C. *Progress in Colloid & Polymer Science* **2004**, *124*, 82-87.
- (25) Ringsdorf, H. *J. Polym. Sci. Polymer Symp.* **1975**, *51*, 135-153.
- (26) Hussein, G. A.; Christensen, D. A.; Rapoport, N. Y.; Pitt, W. G. *Journal of Controlled Release* **2002**, *83*, 303-305.
- (27) Pruitt, J. D.; Hussein, G.; Rapoport, N.; Pitt, W. G. *Macromolecules* **2000**, *33*, 9306-9309.

- (28) Brannon-Peppas, L. *ACS Symposium Series* **1993**, 520, 42-52.
- (29) Bajpai, S. K.; Dubey, S. *Reactive & Functional Polymers* **2005**, 62, 93-104.
- (30) Bajpai, S. K.; Dubey, S. *Polymer International* **2004**, 53, 2178-2187.
- (31) Tanaka, T.; Fillmore, D. J.; Sun, T.; Nishio, I.; Swislow, G.; Shah, A. *Phys. Rev. Lett.* **1980**, 45, 1636.
- (32) Osada, Y. *Adv. Polym. Sci.* **1987**, 82, 1.
- (33) Osada, Y.; Kishi, R.; Hasebe, M. *Journal of Polymer Science, Part C: Polymer Letters* **1987**, 25, 481-485.
- (34) Lim, Y. H.; Kim, D.; Lee, D. S. *J. Appl. Polym. Sci.* **1997**, 64, 2647-2655.
- (35) Ayoub, M. M. H.; Nasr, H. E.; Rozik, N. N. *Journal of Macromolecular Science, Pure and Applied Chemistry* **1998**, A35, 1415-1432.
- (36) Berger, M.; Richtering, W.; Mülhaupt, R. *Polymer Bulletin (Berlin)* **1994**, 33, 521-528.
- (37) Duracher, D.; Veyret, R.; Elaissari, A.; Pichot, C. *Polymer International* **2004**, 53, 618-626.
- (38) Pichot, C.; Elaissari, A.; Duracher, D.; Meunier, F.; Sauzedde, F. *Macromol. Symp.* **2001**, 175 (Polymerization Processes and Polymer Materials II), 285-297.
- (39) Tsuji, S.; Kawaguchi, H. *Langmuir* **2004**, 20, 2449-2455.
- (40) Amalvy, J. I.; Armes, S. P.; Binks, B. P.; Rodrigues, J. A.; Unali, G. F. *Chemical Communications (Cambridge, United Kingdom)* **2003**, 1826-1827.
- (41) Amalvy, J. I.; Unali, G. F.; Li, Y.; Granger-Bevan, S.; Armes, S. P.; Binks, B. P.; Rodrigues, J. A.; Whitby, C. P. *Langmuir* **2004**, 20, 4345-4354.
- (42) Read, E. S.; Fujii, S.; Amalvy, J. I.; Randall, D. P.; Armes, S. P. *Langmuir* **2004**, 20, 7422-7429.
- (43) Liu, S.; Armes, S. P. *Angewandte Chemie, International Edition* **2002**, 41, 1413-1416.
- (44) Hwang, F. S.; Hogen-Esch, T. E. *Macromolecules* **1995**, 28, 3328-3335.
- (45) Heskins, M.; Guillet, J. E. *Journal of Macromolecular Science, Chemistry* **1968**, 2, 1441-1455.
- (46) Durand, A.; Hourdet, D. *Polymer* **2000**, 41, 545-557.
- (47) Bailey, F. E., Jr.; Callard, R. W. *Journal of Applied Polymer Science* **1959**, 1, 56-62.
- (48) Bütün, V.; Armes, S. P.; Billingham, N. C. *Polymer* **2001**, 42, 5993-6008.
- (49) Bütün, V.; Armes, S. P.; Billingham, N. C. *Macromolecules* **2001**, 34, 1148-1159.
- (50) Liu, S.; Billingham, N. C.; Armes, S. P. *Angewandte Chemie, International Edition* **2001**, 40, 2328-2331.
- (51) Shtanko, N. I.; Lequieu, W.; Goethals, E. J.; Du Prez, F. E. *Polymer International* **2003**, 52, 1605-1610.
- (52) Verdonck, B.; Goethals, E. J.; Du Prez, F. E. *Macromolecular Chemistry and Physics* **2003**, 204, 2090-2098.
- (53) Rungsardthong, U.; Ehtezazi, T.; Bailey, L.; Armes, S. P.; Garnett, M. C.; Stolnik, S. *Biomacromolecules* **2003**, 4, 683-690.
- (54) Arotcarena, M.; Heise, B.; Ishaya, S.; Laschewsky, A. *Journal of the American Chemical Society* **2002**, 124, 3787-3793.
- (55) Pagonis, K.; Bokias, G. *Polymer* **2004**, 45, 2149-2153.
- (56) Kikuchi, A.; Okano, T. *Progress in Polymer Science* **2002**, 27, 1165-1193.
- (57) Kikuchi, A.; Okano, T. *Macromolecular Symposia* **2004**, 207, 217-227.
- (58) Costioli, M. D.; Fisch, I.; Garret-Flaudy, F.; Hilbrig, F.; Freitag, R. *Biotechnology and Bioengineering* **2003**, 81, 535-545.

- (59) Ying, L.; Kang, E. T.; Neoh, K. G. *Langmuir* **2002**, *18*, 6416-6423.
- (60) Lackey, C. A.; Murthy, N.; Press, O. W.; Tirrell, D. A.; Hoffman, A. S.; Stayton, P. S. *Bioconjugate Chemistry* **1999**, *10*, 401-405.
- (61) Kulkarni, S.; Schilli, C.; Müller, A. H. E.; Hoffman, A. S.; Stayton, P. S. *Bioconjugate Chemistry* **2004**, *15*, 747-753.
- (62) Katayama, Y.; Sonoda, T.; Maeda, M. *Macromolecules* **2001**, *34*, 8569-8573.
- (63) Stauch, O.; Uhlmann, T.; Froehlich, M.; Thomann, R.; El-Badry, M.; Kim, Y.-K.; Schubert, R. *Biomacromolecules* **2002**, *3*, 324-332.
- (64) Lessard, D. G.; Ousalem, M.; Zhu, X. X. *Canadian Journal of Chemistry* **2001**, *79*, 1870-1874.
- (65) Freitag, R.; Garret-Flaudy, F. *Langmuir* **2002**, *18*, 3434-3440.
- (66) Costa, R. O. R.; Freitas, R. F. S. *Polymer* **2002**, *43*, 5879-5885.
- (67) Winnik, F. M.; Ottaviani, M. F.; Bossman, S. H.; Garcia-Garibay, M.; Turro, N. J. *Macromolecules* **1992**, *25*, 6007-6017.
- (68) Garret-Flaudy, F.; Freitag, R. *J. Polym. Sci., Part A: Polym. Chem.* **2000**, *38*, 4218-4229.
- (69) Garret-Flaudy, F.; Freitag, R. *Langmuir* **2001**, *17*, 4711-4716.
- (70) Eliassaf, J. *J. Appl. Polym. Sci.* **1978**, *22*, 873-874.
- (71) Shah, S. S.; Wertheim, J.; Wang, C. T.; Pitt, C. G. *J. Control. Release* **1997**, *45*, 95-101.
- (72) Escobar, J. L.; Garcia, D.; Valerino, A.; Zaldivar, D.; Hernaez, E.; Katime, I. *Journal of Applied Polymer Science* **2004**, *91*, 3433-3437.
- (73) Bokias, G.; Staikos, G.; Iliopoulos, I. *Polymer* **2000**, *41*, 7399-7405.
- (74) Kobayashi, J.; Kikuchi, A.; Sakai, K.; Okano, T. *Analytical Chemistry* **2001**, *73*, 2027-2033.
- (75) Kobayashi, J.; Kikuchi, A.; Sakai, K.; Okano, T. *Journal of Chromatography, A* **2002**, *958*, 109-119.
- (76) Freitas, R. F. S.; Cussler, E. L. *Separation Science and Technology* **1987**, *22*, 911-919.
- (77) Liu, S.; Liu, M. *Journal of Applied Polymer Science* **2003**, *90*, 3563-3568.
- (78) Katime, I.; Valderruten, N.; Quintana, J. R. *Polymer International* **2001**, *50*, 869-874.
- (79) Kuckling, D.; Adler, H.-J. P.; Arndt, K.-F.; Ling, L.; Habicher, W. D. *Macromolecular Chemistry and Physics* **2000**, *201*, 273-280.
- (80) Kuckling, D.; Wohlrab, S. *Polymer* **2001**, *43*, 1533-1536.
- (81) Park, T. G.; Hoffman, A. S. *Journal of Applied Polymer Science* **1992**, *46*, 659-671.
- (82) Costioli, M. D. *Ph. D. Thesis*; Swiss Federal Institute of Technology: Lausanne, Switzerland, 2004.
- (83) Szwarc, M. *Nature* **1956**, *178*, 1168-1169.
- (84) Miyamoto, Y.; Sawamoto, M.; Higashimura, T. *Macromolecules* **1984**, *17*, 265.
- (85) Sawamoto, M.; Higashimura, T. *Macromol. Chem. Symp.* **1986**, *3*, 83.
- (86) Faust, R.; Kennedy, J. P. *Polym. Bull.* **1986**, *15*, 317.
- (87) Kennedy, J. P. *J. Macromol. Sci.* **1987**, *A24*, 933.
- (88) Müller, A. H. E. *Makromol. Chem., Macromol. Symp.* **1990**, *32*, 87.
- (89) Webster, O. *Science* **1991**, *251*, 887.
- (90) Matyjaszewski, K.; Müller, A. H. E. *Polym. Prepr. (Am. Chem. Soc., Div. Polym. Chem.)* **1997**, *38*, 6.
- (91) Otsu, T.; Yoshida, M. *Makromol. Chem. Rapid Commun.* **1982**, *3*, 127-132.

- (92) Georges, M. K.; Veregin, R. P. N.; Kazmaier, P. M.; Hamer, G. K. *Macromolecules* **1993**, *26*, 2987-2988.
- (93) Georges, M. K.; Saban, M.; Veregin, R. P. N.; Hamer, G. K.; Kazmaier, P. M. *Polym. Prepr. (Am. Chem. Soc., Div. Polym. Chem.)* **1994**, *35*, 737-738.
- (94) Georges, M. K.; Veregin, R. P. N.; Kazmaier, P. M.; Hamer, G. K. *Polym. Prepr. (Am. Chem. Soc., Div. Polym. Chem.)* **1994**, *35*, 870-871.
- (95) Wang, J. S.; Matyjaszewski, K. *Macromolecules* **1995**, *28*, 7901-7910.
- (96) Wang, J. S.; Matyjaszewski, K. *J. Am. Chem. Soc.* **1995**, *117*, 5614-5615.
- (97) Matyjaszewski, K.; Gaynor, S.; Wang, J.-S. *Macromolecules* **1995**, *28*, 2093-2095.
- (98) Meijs, G. F.; Morton, T. C.; Rizzardo, E.; Thang, S. H. *Macromolecules* **1991**, *24*, 3689-3695.
- (99) Rizzardo, E.; Meijs, G. F.; Thang, S. H. *Macromol. Symp.* **1995**, *98*, 101-123.
- (100) Moad, C. L.; Moad, G.; Rizzardo, E.; Thang, S. H. *Macromolecules* **1996**, *29*, 7717-7726.
- (101) Burguière, C.; Pascual, S.; Bui, C.; Vairon, J.-P.; Charleux, B.; Davis, K. A.; Matyjaszewski, K.; Bétrémieux, I. *Macromolecules* **2001**, *34*, 4439-4450.
- (102) Mori, H.; Müller, A. H. E. *Progress in Polymer Science* **2003**, *28*, 1403-1439.
- (103) Müller, A. H. E.; Cai, Y.; Hartenstein, M.; Gradzielski, M.; Zhang, M.; Mori, H.; Pergushov, D. V. *Polymer Preprints (American Chemical Society, Division of Polymer Chemistry)* **2004**, *45*, 267-268.
- (104) Matyjaszewski, K.; Xia, J. *Chem. Rev.* **2001**, *101*, 2921-2990.
- (105) Godwin, A.; Hartenstein, M.; Müller, A. H. E.; Brocchini, S. *Angew. Chem. Int. Ed.* **2001**, *40*, 594.
- (106) Camp, W. V.; Du Prez, F. E.; Bon, S. A. F. *Macromolecules* **2004**, *37*, 6673-6675.
- (107) Loiseau, J.; Doeerr, N.; Suau, J. M.; Egraz, J. B.; Llauro, M. F.; Ladaviere, C.; Claverie, J. *Macromolecules* **2003**, *36*, 3066-3077.
- (108) Bouix, M.; Gouzi, J.; Charleux, B.; Vairon, J.-P.; Guinot, P. *Macromolecular Rapid Communications* **1998**, *19*, 209-213.
- (109) Couvreur, L.; Lefay, C.; Belleney, J.; Charleux, B.; Guerret, O.; Magnet, S. *Macromolecules* **2003**, *36*, 8260-8267.
- (110) Breiner, T.; Schmidt, H.-W.; Muller, A. H. E. *e-Polymers* **2002**, Paper No. 22.
- (111) Eggert, M.; Freitag, R. *Journal of Polymer Science, Part A: Polymer Chemistry* **1994**, *32*, 803-813.
- (112) Xie, X.; Hogen-Esch, T. E. *Macromolecules* **1996**, *29*, 1746-1752.
- (113) Kobayashi, M.; Okuyama, S.; Ishizone, T.; Nakahama, S. *Macromolecules* **1999**, *32*, 6466-6477.
- (114) Kitayama, T.; Shibuya, W.; Katsukawa, K.-I. *Polymer Journal (Tokyo, Japan)* **2002**, *34*, 405-409.
- (115) Ishizone, T.; Ito, M. *Journal of Polymer Science, Part A: Polymer Chemistry* **2002**, *40*, 4328-4332.
- (116) Teodorescu, M.; Matyjaszewski, K. *Polymer Preprints (American Chemical Society, Division of Polymer Chemistry)* **1999**, *40*, 428-429.
- (117) Teodorescu, M.; Matyjaszewski, K. *Macromolecules* **1999**, *32*, 4826-4831.
- (118) Teodorescu, M.; Matyjaszewski, K. *Macromolecular Rapid Communications* **2000**, *21*, 190-194.
- (119) Ray, B.; Isobe, Y.; Matsumoto, K.; Habae, S.; Okamoto, Y.; Kamigaito, M.; Sawamoto, M. *Macromolecules* **2004**, *37*, 1702-1710.
- (120) Benoit, D.; Chaplinski, V.; Braslau, R.; Hawker, C. J. *Journal of the American Chemical Society* **1999**, *121*, 3904-3920.

- (121) Diaz, T.; Fischer, A.; Jonquieres, A.; Brembilla, A.; Lochon, P. *Macromolecules* **2003**, *36*, 2235-2241.
- (122) Schierholz, K.; Givehchi, M.; Fabre, P.; Nallet, F.; Papon, E.; Guerret, O.; Gnanou, Y. *Macromolecules* **2003**, *36*, 5995-5999.
- (123) Müller, A. H. E.; Andre, X.; Schilli, C. M.; Charleux, B. *Polymeric Materials: Science and Engineering* **2004**, *91*, 252-253.
- (124) Brandrup, J.; Immergut, E. H.; Grulke, E. A. *Polymer Handbook*; Wiley: New YORK, 1999.
- (125) Clint, J. H. *Surfactant Aggregation*, 1992.
- (126) Alexandridis, P.; Lindman, B. *Amphiphilic Block Copolymers: Self-Assembly and Applications*; Elsevier: Amsterdam, 2000.
- (127) Riess, G. *Progress in Polymer Science* **2003**, *28*, 1107-1170.
- (128) Bader, H.; Ringsdorf, H.; Schmidt, B. *Angew. Makromol. Chem.* **1984**, *123/124*, 457-485.
- (129) Chung, J. E.; Yokoyama, M.; Aoyagi, T.; Sakurai, Y.; Okano, T. *J. Controlled Release* **1998**, *53*, 119-130.
- (130) Antonietti, M.; Wenz, E.; Bronstein, L.; Seregina, M. *Advanced Materials (Weinheim, Germany)* **1995**, *7*, 1000-1005.
- (131) Antonietti, M.; Förster, S.; Hartmann, J.; Oestreich, S. *Macromolecules* **1996**, *29*, 3800-3806.
- (132) Liu, S.; Weaver, J. V. M.; Save, M.; Armes, S. P. *Langmuir* **2002**, *18*, 8350-8357.
- (133) Spatz, J. P.; Mössmer, S.; Möller, M. *Angew. Chem., Int. Ed.* **1996**, *35*, 1510-1512.
- (134) Fustin, C. A.; Abetz, V.; Gohy, J. F. *Eur. Phys. J. E* **2005**, ASAP.
- (135) Kotz, J.; Kosmella, S.; Beitz, T. *Progress in Polymer Science* **2001**, *26*, 1199-1232.
- (136) Elias, H.-G. In *Light Scattering from Polymer Solutions*; Huglin, M. B., Ed.; Academic Press: London, 1972; pp 397-457.
- (137) Elias, H.-G. *J. Macromol. Sci.* **1973**, *A7*, 601.
- (138) Tuzar, Z. *Solvents and Self-Organization of Polymers*; Kluwer: Dordrecht, 1996; Vol. E 327.
- (139) Malliaris, A.; Boens, N.; Luo, H.; Van der Auweraer, M.; De Schryver, F. C.; Reekmans, S. *Chemical Physics Letters* **1989**, *155*, 587-592.
- (140) Wilhelm, M.; Zhao, C. L.; Wang, Y.; Xu, R.; Winnik, M. A. *Macromolecules* **1991**, *24*, 1033.
- (141) Quintana, J. R.; Villacampa, M.; Katime, I. A. *Macromolecules* **1993**, *26*, 606.
- (142) Förster, S.; Zisenis, M.; Wenz, E.; Antonietti, M. *Journal of Chemical Physics* **1996**, *104*, 9956-9970.
- (143) Förster, S.; Abetz, V.; Müller, A. H. E. *Advances in Polymer Science* **2004**, *166*, 173-210.
- (144) Moffitt, M.; Khougaz, K.; Eisenberg, A. *Accounts of Chemical Research* **1996**, *29*, 95-102.
- (145) Gao, Z.; Varshney, S. K.; Wong, S.; Eisenberg, A. *Macromolecules* **1994**, *27*, 7923-7927.
- (146) Nagarajan, R.; Ganesh, K. *J. Phys. Chem.* **1989**, *90*, 5843.
- (147) Nagarajan, R.; Ganesh, C. *Macromolecules* **1989**, *22*, 4312.
- (148) Halperin, A. *Macromolecules* **1989**, *22*, 3806.
- (149) Astafieva, I.; Khougaz, K.; Eisenberg, A. *Macromolecules* **1995**, *28*, 7127-7134.
- (150) Khougaz, K.; Astafieva, I.; Eisenberg, A. *Macromolecules* **1995**, *28*, 7135-7147.
- (151) Astafieva, I.; Zhong, X. F.; Eisenberg, A. *Macromolecules* **1993**, *26*, 7339-7352.

- (152) Creutz, S.; van Stam, J.; Antoun, S.; De Schryver, F. C.; Jérôme, R. *Macromolecules* **1997**, *30*, 4078-4083.
- (153) Creutz, S.; van Stam, J.; De Schryver, F. C.; Jérôme, R. *Macromolecules* **1998**, *31*, 681-689.
- (154) Munk, P.; Ramireddy, C.; Tian, M.; Webber, S. E.; Prochazka, K.; Tuzar, Z. *Makromolekulare Chemie, Macromolecular Symposia* **1992**, *58*, 195-199.
- (155) van Stam, J.; Creutz, S.; De Schryver, F. C.; Jérôme, R. *Macromolecules* **2000**, *33*, 6388-6395.
- (156) Kriz, J.; Plestil, J.; Tuzar, Z.; Pospisil, H.; Brus, J.; Jakes, J.; Masar, B.; Vlcek, P.; Doskocilova, D. *Macromolecules* **1999**, *32*, 397-410.
- (157) Kriz, J.; Masar, B.; Pospisil, H.; Plestil, J.; Tuzar, Z.; Kiselev, M. A. *Macromolecules* **1996**, *29*, 7853-7858.
- (158) Tuzar, Z.; Prochazka, K.; Zuzkova, I.; Munk, P. *Polymer Preprints (American Chemical Society, Division of Polymer Chemistry)* **1993**, *34*, 1038-1039.
- (159) Schuch, H.; Klingler, J.; Rossmanith, P.; Frechen, T.; Gerst, M.; Feldthusen, J.; Müller, A. H. E. *Macromolecules* **2000**, *33*, 1734-1740.
- (160) Nowakowska, M.; Karewicz, A.; Klos, M.; Zapotoczny, S. *Macromolecules* **2003**, *36*, 4134-4139.
- (161) Cammas-Marion, S.; Bear, M.-M.; Harada, A.; Guerin, P.; K., K. *Macromol. Chem. Phys.* **2000**, *201*, 355.
- (162) Qin, A.; Tian, M.; Ramireddy, C.; Webber, S. E.; Munk, P.; Tuzar, Z. *Macromolecules* **1994**, *27*, 120-126.
- (163) Zhang, L.; Eisenberg, A. *Science (Washington, D. C.)* **1995**, *268*, 1728-1731.
- (164) Zhang, L. F.; Eisenberg, A. *Macromolecular Symposia* **1997**, *113*, 221-232.
- (165) Rager, T.; Meyer, W. H.; Wegner, G. *Macromol. Chem. Phys.* **1999**, *200*, 1672-1680.
- (166) Feldthusen, J.; Ivan, B.; Müller, A. H. E. *Macromolecules* **1998**, *31*, 578-585.
- (167) Pergushov, D. V.; Remizova, E. V.; Gradzielski, M.; Lindner, P.; Feldthusen, J.; Zezin, A. B.; Müller, A. H. E.; Kabanov, V. A. *Polymer* **2004**, *45*, 367-378.
- (168) Prochazka, K.; Martin, T. J.; Munk, P.; Webber, S. E. *Macromolecules* **1996**, *29*, 6518-6525.
- (169) Martin, T. J.; Prochazka, K.; Munk, P.; Webber, S. E. *Macromolecules* **1996**, *29*, 6071-6073.
- (170) Lee, A. S.; Gast, A. P.; Bütün, V.; Armes, S. P. *Macromolecules* **1999**, *32*, 4302-4310.
- (171) Bütün, V.; Billingham, N. C.; Armes, S. P. *Chem. Commun. (Cambridge)* **1997**, 671-672.
- (172) Narrainen, A. P.; Pascual, S.; Haddleton, D. M. *Journal of Polymer Science, Part A: Polymer Chemistry* **2002**, *40*, 439-450.
- (173) Wendler, U.; Bohrisch, J.; Jaeger, W.; Rother, G.; Dautzenberg, H. *Macromolecular Rapid Communications* **1998**, *19*, 185-190.
- (174) Selb, J.; Gallot, Y. *Makromolekulare Chemie* **1981**, *182*, 1775-1786.
- (175) Selb, J.; Gallot, Y. *Makromolekulare Chemie* **1981**, *182*, 1513-1523.
- (176) Selb, J.; Gallot, Y. *Makromolekulare Chemie* **1981**, *182*, 1491-1511.
- (177) Selb, J.; Gallot, Y. *Makromolekulare Chemie* **1980**, *181*, 2605-2624.
- (178) Selb, J.; Gallot, Y. *Makromolekulare Chemie* **1980**, *181*, 809-822.
- (179) Baines, F. L.; Billingham, N. C.; Armes, S. P. *Macromolecules* **1996**, *29*, 3416-3420.

- (180) Tuzar, Z.; Pospisil, H.; Plestil, J.; Lowe, A. B.; Baines, F. L.; Billingham, N. C.; Armes, S. P. *Macromolecules* **1997**, *30*, 2509-2512.
- (181) Zhang, L.; Eisenberg, A. *Journal of the American Chemical Society* **1996**, *118*, 3168-3181.
- (182) Kim, K. H.; Cui, G. H.; Lim, H. J.; Huh, J.; Cheol-Hee, A.; Jo, W. H. *Macromolecular Chemistry and Physics* **2004**, *205*, 1684-1692.
- (183) Webber, S. E. *J. Phys. Chem. B* **1998**, *102*, 2618-2626.
- (184) Luo, L.; Ranger, M.; Lessard, D. G.; Le Garrec, D.; Gori, S.; Leroux, J.-C.; Rimmer, S.; Smith, D. *Macromolecules* **2004**, *37*, 4008-4013.
- (185) Bütün, V.; Armes, S. P.; Billingham, N. C.; Tuzar, Z.; Rankin, A.; Eastoe, J.; Heenan, R. K. *Macromolecules* **2001**, *34*, 1503-1511.
- (186) Lovell, P. *Emulsion Polymerization and Emulsion Polymers*, 1997.
- (187) Lovell, P. A. *Macromolecular Symposia* **1995**, *92*, 71-81.
- (188) Halary, J.; Cookson, P.; Stanford, J. L.; Lovell, P. A.; Young, R. J. *Advanced Engineering Materials* **2004**, *6*, 729-733.
- (189) Gilbert, R. *Emulsion Polymerization - A Mechanistic Approach*; Academic Press: London, 1995.
- (190) Odian, G. *Principles of Polymerization*, 3rd ed.; John Wiley & Sons, Inc.: New York, 1991.
- (191) Perrin, P.; Millet, F.; Charleux, B. *Surfactant Science Series* **2001**, *99*, 363-445.
- (192) Brown, R.; Stützel, B.; Sauer, T. *Macromolecular Chemistry and Physics* **1995**, *196*, 2047-2064.
- (193) Jialanella, G. L.; Firer, E. M.; Piirma, I. *Journal of Polymer Science, Part A: Polymer Chemistry* **1992**, *30*, 1925-1933.
- (194) Piirma, I.; Lenzotti, J. R. *British Polymer Journal* **1989**, *21*, 45-51.
- (195) Piirma, I. *Surfactant Science Series, Vol. 42: Polymeric Surfactants*, 1992.
- (196) Sung, A.-M.; Piirma, I. *Langmuir* **1994**, *10*, 1393-1398.
- (197) Xu, X.-J.; Chen, F. *Journal of Applied Polymer Science* **2004**, *92*, 3080-3087.
- (198) Mura, J.-L.; Riess, G. *Polymers for Advanced Technologies* **1995**, *6*, 497-508.
- (199) Riess, G.; Labbe, C. *Macromolecular Rapid Communications* **2004**, *25*, 401-435.
- (200) Gaillard, N.; Guyot, A.; Claverie, J. *Journal of Polymer Science, Part A: Polymer Chemistry* **2003**, *41*, 684-698.
- (201) Riess, G. *Colloids and Surfaces, A: Physicochemical and Engineering Aspects* **1999**, *153*, 99-110.
- (202) Kukula, H.; Schlaad, H.; Tauer, K. *Macromolecules* **2002**, *35*, 2538-2544.
- (203) Lamb, D. J.; Anstey, J. F.; Fellows, C. M.; Monteiro, M. J.; Gilbert, R. G. *Biomacromolecules* **2001**, *2*, 518-525.
- (204) Save, M.; Manguian, M.; Chassenieux, C.; Charleux, B. *Macromolecules* **2005**, *38*, 280-289.
- (205) Guyot, A.; Tauer, K. *Surfactant Science Series* **2001**, *100*, 547-575.
- (206) Tauer, K.; Zimmermann, A.; Schlaad, H. *Macromolecular Chemistry and Physics* **2002**, *203*, 319-327.
- (207) Britton, D. J.; Lovell, P. A.; Heatley, F.; Venkatesh, R. *Macromolecular Symposia* **2001**, *175*, 95-104.
- (208) Ahmad, N. M.; Britton, D.; Heatley, F.; Lovell, P. A. *Macromolecular Symposia* **1999**, *143*, 231-241.
- (209) Roe, C. P. *Journal of Colloid and Interface Science* **1971**, *37*, 93-101.
- (210) Ito, K.; Sabao, K.; Kawaguchi, S. *Polym. Prepr. (Am. Chem. Soc., Div. Polym. Chem.)* **1993**, *34(2)*, 620-621.

- (211) Kuo, P. L.; Chen, C. J. *Journal of Polymer Science, Part A: Polymer Chemistry* **1993**, *31*, 99-111.
- (212) Moustafa, A. B.; Faizalla, A. *Journal of Applied Polymer Science* **2000**, *78*, 1209-1215.
- (213) Hergeth, W. D.; Bloss, P.; Biedenweg, F.; Abendroth, P.; Schmutzler, K.; Wartewig, S. *Makromolekulare Chemie* **1990**, *191*, 2949-2955.
- (214) Leemans, L.; Jérôme, R.; Teyssie, P. *Macromolecules* **1998**, *31*, 5565-5571.
- (215) Liu, Q.; Yu, Z.; Ni, P. *Colloid and Polymer Science* **2004**, *282*, 387-393.
- (216) Jäger, W.; Wendler, U.; Lieske, A.; Bohrisch, J. *Langmuir* **1999**, *15*, 4026-4032.
- (217) Müller, H.; Leube, W.; Tauer, K.; Förster, S.; Antonietti, M. *Macromolecules* **1997**, *30*, 2288-2293.
- (218) Farcet, C.; Lansalot, M.; Charleux, B.; Pirri, R.; Vairon, J. P. *Macromolecules* **2000**, *33*, 8559-8570.
- (219) Farcet, C.; Charleux, B.; Pirri, R. *Macromolecular Symposia* **2002**, *182*, 249-260.
- (220) Cunningham, M. F. *Progress in Polymer Science* **2002**, *27*, 1039-1067.
- (221) Nicolas, J.; Charleux, B.; Guerret, O.; Magnet, S. *Angewandte Chemie, International Edition* **2004**, *43*, 6186-6189.

2. Overview of the thesis

This thesis consists of seven chapters and an additional appendix including four publications which are presented in Chapters 3 to 6.

Kinetic investigations of the anionic polymerization of *N,N*-diethylacrylamide (DEAAM) were performed in the presence of triethylaluminum in THF at -78 °C. The results are correlated with quantum chemistry results to propose a mechanism (Chapter 3).

Bishydrophilic block copolymers based on acrylic acid or methacrylic acid and DEAAM were obtained by extending the developed synthetic strategy to sequential copolymerization in the presence of Et₃Al. Their remarkable pH- and thermo-responsive properties in water were initially studied and demonstrated by means of Dynamic Light Scattering (Chapter 4).

Subsequently, the schizophrenic behavior of the asymmetric poly(acrylic acid)₄₅-*block*-poly(*N,N*-diethylacrylamide)₃₆₀ in water was extensively investigated by further experimental procedures including Small Angle Neutron Scattering, Static/Dynamic Light Scattering, and cryo-Transmission Electron Microscopy (Chapter 5).

Such poly[(meth)acrylic acid]-*block*-poly(*N,N*-diethylacrylamide) copolymers were used as pH- and thermo-responsive surfactants in the formulation of batch free-radical emulsion polymerization of various monomers. The ability of these block copolymers to replace usual surfactants and to produce stable latexes was investigated as well as the effects of various factors, i.e. the temperature, the pH, the block copolymer concentration, the hydrophobic block length, and the monomer nature (Chapter 6).

Fundamentals of anionic and free-radical emulsion polymerization are presented in Appendices 8.1, and 8.2, respectively.

In the following, summaries of the main results together with descriptions of the experimental methods are presented.

2.1 Kinetic studies using in-line FT-NIR spectroscopy

Method. Since one decade the development of in-line methods in combination with mid- and near- infra-red spectroscopy (mid-IR, NIR) has taken a great importance for polymer chemists. It is now possible to transfer the light source to the probe immersed in the reaction mixture via optical fibers, light guides, or conduits.¹ The sensor attached to the probe is based either on transmittance (TR) or on Attenuated Total Reflectance (ATR) method. Depending on the sample characteristics (transparency, viscosity) one of the two principles may be applied. The ATR method is less sensitive than the TR one, but can be successfully used to monitor polymerization kinetics in dispersed media (emulsion, suspension).²

The main advantage is the possibility to follow the monomer conversion with a non-destructive tool and without the periodic sample removal, as in the case of classical gravimetric analysis. This is of importance for many systems, which are highly sensitive to the reaction conditions (water, oxygen), like anionic and cationic living polymerizations.³ It remains also particularly beneficial for polymerization of highly hazardous toxic monomers, such as ethylene oxide,⁴ as well as for fast reactions, for which high sampling rates are required. Monitoring kinetics in the mid and near IR region can be conducted easily, because well-defined primary resonance bands are detectable and their peak area or peak height can be followed with time. Thus, copolymerization parameters can be directly measured from one single experiment.⁵ In the case of mid-IR investigations the user is limited to apply the ATR method, whereas for near IR measurements a classical transmission setup can be used. Hence, in-line kinetic monitoring in the near infrared region remains the tool of choice for the polymer chemists.

As shown in Figure 2-1, light is transmitted by means of fiber-optic cables. The collimated light beam passes the solution once and is then collected by the spectrometer via a second fiber-optic cable. Numerous overtones and combination vibrations can be observed in the near-infrared region of the spectrum from about 0.7 μm (ca. 14,000 cm^{-1}) to 2.5 μm (4,000 cm^{-1}). Taking into account the number of overtone and combination frequencies possible from a large molecule like a polymer it might appear that this region would be complex to analyze. In fact, only the overtone or combination bands of vibrations involving hydrogen such as C-H, O-H, N-H are observed at appreciable intensities.⁶ FT-NIR allows thus the continuous monitoring of monomer conversion in living/controlled

polymerization by following the intensity change of these resonance bands.^{3,7} The determination of the monomer conversion can be more reliable with inline spectroscopic methods than with gravimetric analysis or gas chromatography. In the first case, soluble oligomeric fractions are not taken into account whereas gas chromatography needs the use of a volatile external standard (e.g. *n*-alkane) whose evaporation leads to truncated results.

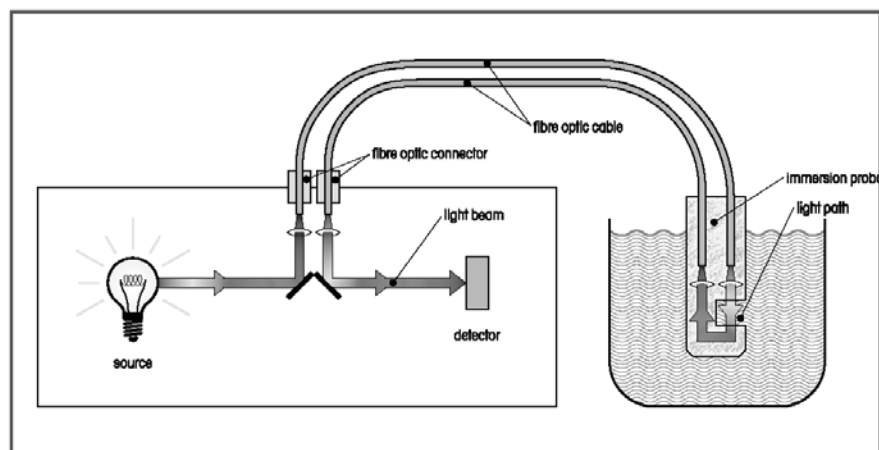


Figure 2-1. Measurement principle (Hellma[©]).

Setup. The anionic polymerizations were performed in a sealed laboratory autoclave (Büchi, 1L) equipped with a mechanic stirrer and a cooling jacket. As it is shown in Figure 2-2, the complete system is hermetically closed and can be evacuated for the direct injection of dry solvents from the distillations. The polymerizations were carried out under dry nitrogen pressure allowing withdrawing of samples via a capillary plunging at the bottom of the reactor. Ampoules containing monomers, additives, or initiator, equipped with Rotaflo seals were directly connected to the setup for injection into the reactor. Via a septum, small quantities of initiator can be injected. This technique may present some advantages in comparison to other synthetic methods. High vacuum technique is generally used for anionic polymerization,⁸ but it is time-consuming and only small quantities of product can be obtained. Furthermore, for safety reasons, it is advantageous to work inside a closed reactor system, e.g. for highly toxic gaseous monomers like ethylene oxide.⁴ Another advantage remains the possibility to follow polymerization kinetics using a FT-NIR probe immersed in the reactor, as described previously. This method allows the monitoring of fast polymerizations ($t_{1/2} \approx 10\text{-}60$ s) but is inappropriate for ultra-fast

reactions, which have to be carried out using a flow-tube reactor.⁹⁻¹³ During the reaction, a constant stirring rate of 300 rpm was used which allowed the recording of NIR spectra of acceptable quality.

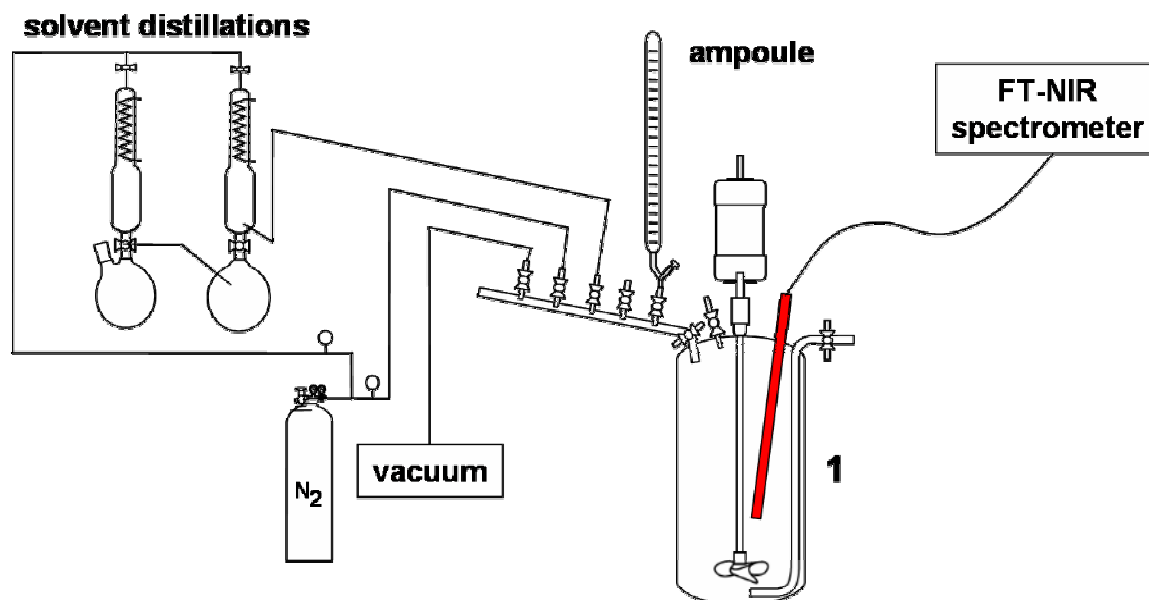


Figure 2-2. Upscaling reactor setup used to perform the kinetic studies.

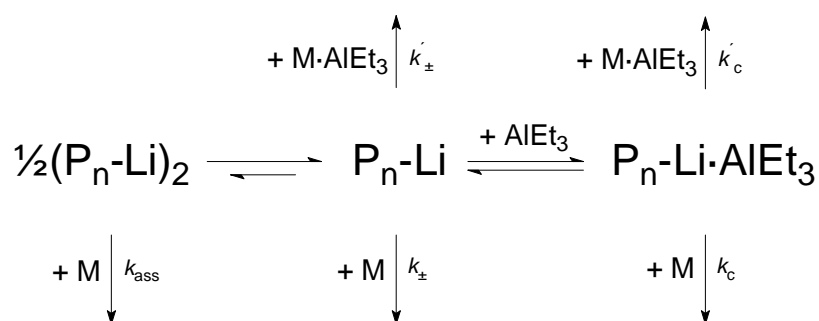
Molecular characterization. The absolute determination of the molecular weights is of importance for the polymer chemist confronted to kinetic investigations. Only with the knowledge of the exact molecular weights it is possible to deduce parameters, like the initiator or blocking efficiency, the effective concentration of chain ends, $[P^*]_0$, and finally the absolute polymerization rate constants.

For the determination of absolute weight-average and number-average molecular weights, as well as for the determination of the end groups, Matrix-Assisted Laser Desorption/Ionization Time-of-Flight (MALDI-TOF) mass spectrometry has proven to be an extremely reliable and precise method.¹⁴ It is noteworthy, however, that a quantitative evaluation of the distribution is only possible for polymers having low polydispersity indices ($M_w/M_n \leq 1.1$). If this requirement is not fulfilled, the number-average, M_n , and weight-average molecular weights, M_w are underestimated due to the fact that discrimination of the higher molecular weight chains occurs during the ionization. Since narrowly distributed polymers and copolymers could be synthesized in the present work,

the error for M_n is negligibly small. Consequently, MALDI-TOF MS was used in this work to measure the absolute M_n values. For checking and comparing the polydispersity index values, the polymer distributions were additionally investigated by Size Exclusion Chromatography (SEC) in appropriate solvents. In this context it should be noted that the characterization via Size Exclusion Chromatography (SEC) of polymers bearing an amide function like PNIPAAm in THF involves various problems due to chain aggregation after complete drying of the polymer samples and adsorption onto the columns.^{15,16}

Results. Based on the experimental results, which were obtained by the kinetic investigations using *in-situ* Fourier-transform near-infrared (FT-NIR) fiber-optic spectroscopy, we were able to propose the first and very detailed mechanistic study of the anionic polymerization of a dialkylacrylamide.

Scheme 2-1. Postulated mechanism of DEAAm polymerization in THF with $k_{\pm} \gg k_c \gg k_{\text{ass}}, k'_{\pm} \gg k_{\pm}$, and $k'_c \gg k_c$



The polymerization follows first order kinetics with respect to the effective concentration of active chains, $[\text{P}^*]_0$, but shows complex kinetics with respect to the actual monomer and initial aluminum concentrations. The mechanism involves two equilibria: between noncoordinated and Al-coordinated chain ends (deactivation of chain ends) as well as between free and Et_3Al -activated monomer (activated monomer mechanism). These two effects are in a delicate balance that depends on the ratio of the concentrations of Et_3Al , monomer, and chain ends. Thus, the polymerization rate of this system is governed simultaneously by the complex interplay between the activation of monomer (dependent on monomer and Et_3Al concentrations) and the deactivation of chain ends

(dependent on the ratio of concentrations of Et_3Al to initiator). The existence of the more reactive unimeric aluminate complex, $\text{P-Li}\cdot\text{AlEt}_3$ as well as that of the dimeric aggregates of free amidoenolate chain ends is indicated by quantum-chemical calculations via Density Functional Theory (DFT).¹⁷ The postulated mechanism is presented in Scheme 2-1 and further details with the complete kinetic studies can be found in chapter 3.

2.2 Synthesis of bishydrophilic block copolymers

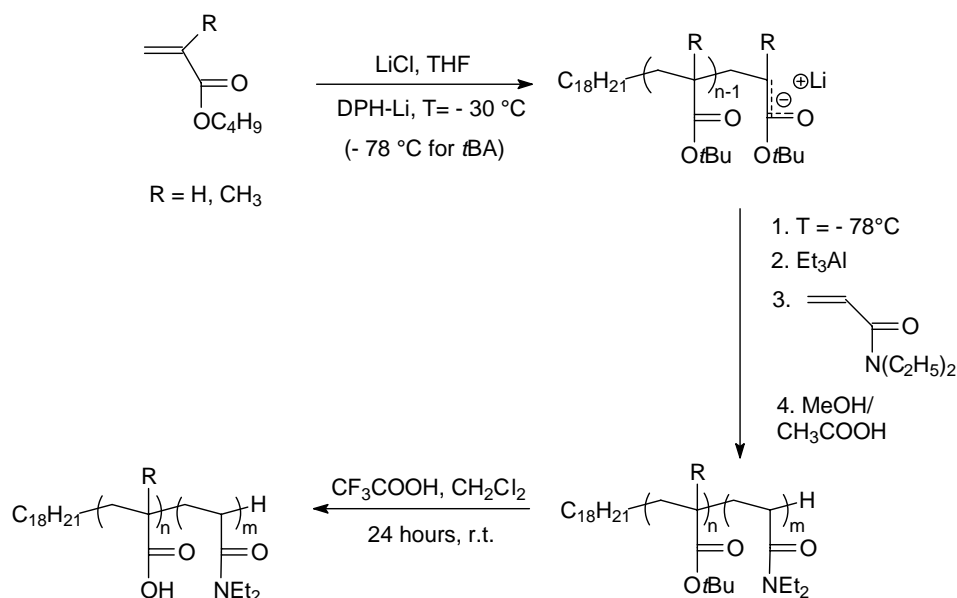
There are only few examples of the synthesis of bishydrophilic block copolymers in the literature. For instance, the synthesis of double hydrophilic statistical di- and triblock copolymers of acrylamide and acrylic acid was reported using the MADIX process.¹⁸ Besides, it was also attempted by RAFT polymerization to obtain well-defined poly(acrylic acid)-*block*-poly(*N*-isopropylacrylamide) copolymers,^{19,20} tapered triblock copolymers made of a poly(acrylic acid) inner block and poly(ethylene oxide) comb-like outer blocks (PEO),²¹ and by ATRP to obtain star-block copolymers $(\text{PEO-}b\text{-PAA})_3$, and dendrimer-like copolymers $(\text{PEO}_3\text{-}star\text{-PAA}_6)$.²²

Results. With the help of the fundamental kinetic and microstructure studies presented in chapter 3, we were able to elaborate a synthetic pathway for the polymerization of well-defined bishydrophilic block copolymers. Certainly, anionic polymerization remains the method of choice for the control of the microstructure, which has a great influence on the thermo-responsive and solubility properties of PDEAAM.²³⁻³⁰ Therefore, in order to obtain block copolymers with PDEAAM segments exhibiting an LCST behavior, lithiated initiators in combination with Et_3Al were used in THF at -78°C . We demonstrated that the mainly heterotactic PDEAAM blocks and homopolymers indeed undergo a coil-to-globule transition above their cloud point, $T_c \sim 31^\circ\text{C}$.

Applying the concept of sequential monomer addition, we were able to synthesize a variety of different bishydrophilic block copolymers, with (meth)acrylic acid blocks. For that purpose, the polymerization of DEAAm was initiated by poly(*tert*-butyl acrylate)-Li, and poly(*tert*-butyl methacrylate)-Li as macroinitiators in the presence of Et_3Al to render the desired poly(*tert*-butyl acrylate)-*block*-PDEAAM and poly(*tert*-butyl methacrylate)-*block*-PDEAAM copolymers (Scheme 2-2). Usually, the blocking efficiencies remained

low ($f < 0.70$), which is presumably due to a backbiting reaction occurring after incorporation of one or two units of DEAAm. Nevertheless, it was possible to remove the precursor traces by a simple precipitation in *n*-hexane and pure diblock copolymers were obtained. The main advantage in comparison to other drastic methods using organocesium initiator³¹ is that this method does not need the synthesis of expensive and highly sensitive initiators. Indeed, the well-known diphenylhexyl-lithium (DPH-Li) formed *in-situ* by the reaction of diphenylethylene and *n*-butyl lithium (both commercially available) can be used as initiator.

Scheme 2-2. Synthetic strategy for the synthesis of well-defined poly[(meth)acrylic acid]-*block*-poly(*N,N*-diethylacrylamide) copolymers



The post-polymerization treatment of the *Pt*B(M)A-*b*-PDEAAm copolymers with CF_3COOH in dichloromethane leads to poly[(meth)acrylic acid]-*b*-PDEAAm (PAA-*b*-PDEAAm, PMAA-*b*-PDEAAm). This procedure allows the selective hydrolysis of the *Pt*BMA or *Pt*BA block without affecting the PDEAAm segment.

In conclusion, it was shown that different comonomers can be used and varying block lengths can be achieved using this method.

2.3 Characterization of the thermo- and pH-responsive micelles

The synthesized bishydrophilic block copolymers open an elegant way to prepare micelles in a simple and reversible way (see Chapters 4 and 5), as it was assumed that different external stimuli can lead to the formation of various kinds of micelles.³² Precisely speaking, the poly[(meth)acrylic acid]-*block*-poly(*N,N*-diethylacrylamide) copolymers [P(M)AA-*b*-PDEAAm] can exist in four states in aqueous solution, depending on both the temperature and the pH, namely, direct PDEAAm-core micelles, inverse P(M)AA-core micelles, precipitated copolymer, and molecularly dissolved chains (unimers), as it shown in Figure 2-3 in the particular case of the asymmetric (AA)₄₅-*b*-(DEAAm)₃₆₀ block copolymer.

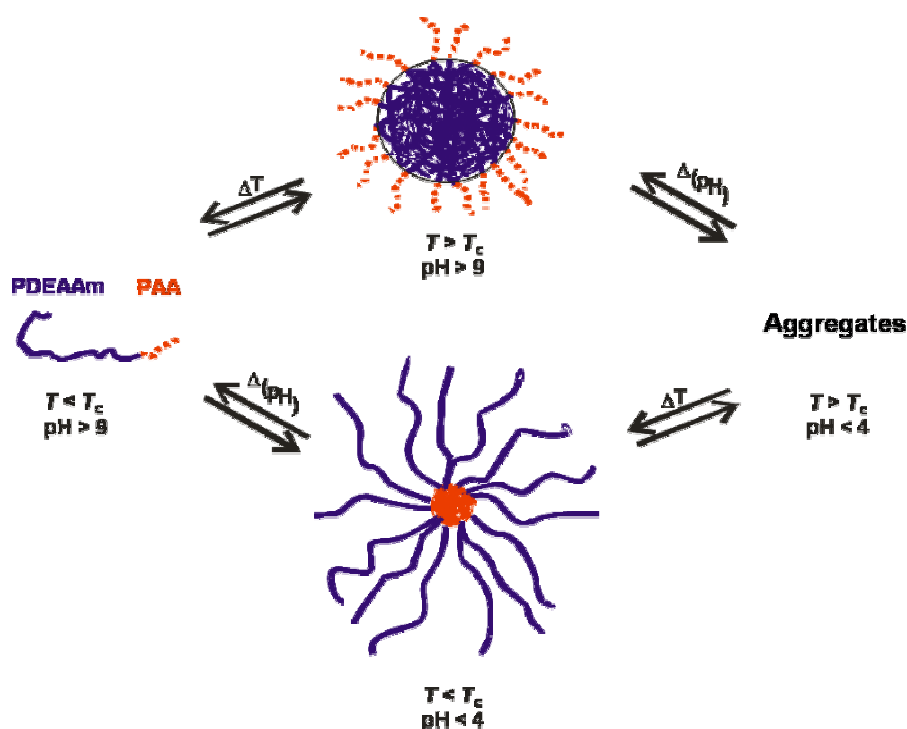


Figure 2-3. Modes of micelle formation for poly(acrylic acid)₄₅-*block*-poly(*N,N*-diethylacrylamide)₃₆₀ in aqueous solution in dependence of pH and temperature.

Its ‘schizophrenic’^{32,33} aggregation behavior was investigated with Static and Dynamic Light Scattering methods (SLS, DLS), NMR, Small-angle neutron scattering (SANS) as well as cryogenic-Transmission Electron Microscopy (cryo-TEM) experiments. It could be shown that the type, the size and the internal structure of the micelles can be fine-tuned by changes in pH, temperature and ionic strength. In the following, a few characterization

results of both types of micelles are highlighted, whereas for a full coverage of the results the reader is kindly referred to chapter 5.

Results. For $\text{pH} \geq 7.7$, the block copolymer is molecularly dissolved at room temperature and ‘direct’ spherical PDEAAm-core micelles are formed upon heating the solution above the cloud point which was found to be $T_c \approx 35 \text{ }^\circ\text{C}$. The occurrence of this transition could be clearly demonstrated by DLS and SANS (Figure 2-4).

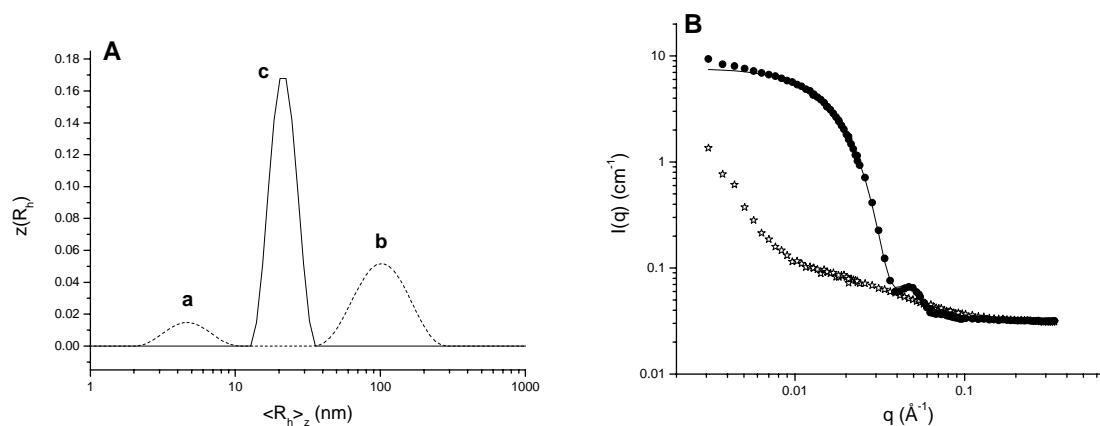


Figure 2-4. (A) Intensity-weighted hydrodynamic radius distribution (CONTIN) in water at $T = 21 \text{ }^\circ\text{C}$ (---) showing unimers (a) and loose aggregates (b); at $T = 45 \text{ }^\circ\text{C}$ (—) showing PDEAAm-core micelles (c); conditions: $c = 1.3 \text{ g}\cdot\text{L}^{-1}$, $\text{pH} = 12.8$, $[\text{NaCl}] = 0.1 \text{ mol}\cdot\text{L}^{-1}$, $\theta = 30^\circ$. (B) SANS in NaOD/D₂O at $T = 23$ (☆) and $45 \text{ }^\circ\text{C}$ (●); conditions: $c = 1.5 \text{ g}\cdot\text{L}^{-1}$, $\text{pH} = 12.8$, $[\text{NaCl}] = 0.1 \text{ mol}\cdot\text{L}^{-1}$. The solid line represents the fit of the experimental data points at $45 \text{ }^\circ\text{C}$ using a polydisperse spherical model.

Generally, the block copolymerization of PDEAAm with a hydrophilic comonomer (acrylic acid or methacrylic acid) shifts the cloud point to higher temperature, as compared to PDEAAm homopolymers. This transition is thus closer to the human body temperature, making these materials and their derivatives very interesting classes of water-soluble thermo-responsive polymers.³⁴

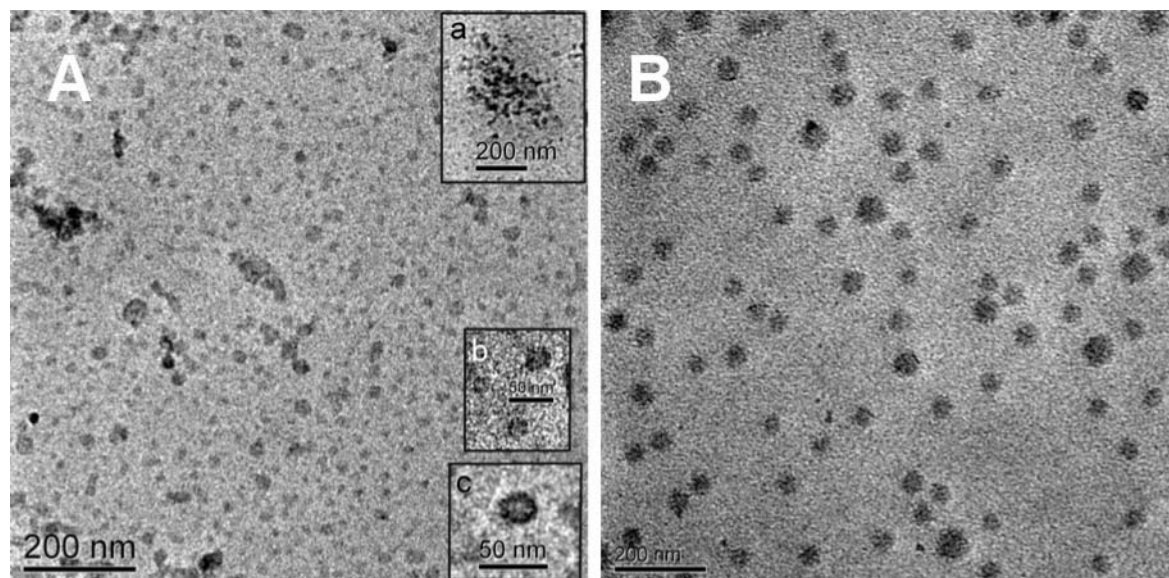


Figure 2-5. Cryo-TEM image of the $(AA)_{45}\text{-}b\text{-(DEAAm)}_{360}$ vitrified from an aqueous solution at $T = 23\text{ }^{\circ}\text{C}$ and $\text{pH} = 4.0$ (A, $c = 2.1\text{ g}\cdot\text{L}^{-1}$), and at $T = 45\text{ }^{\circ}\text{C}$ and $\text{pH} = 12.6$ (B, $c = 4.9\text{ g}\cdot\text{L}^{-1}$).

In order to gain further information about the internal micellar structure, the data of different scattering experiments, DLS, SLS and SANS, were evaluated and compared. From the light scattering measurements at $T = 45\text{ }^{\circ}\text{C}$ and $\text{pH} \geq 8$, a ratio $R_g/R_h = 0.77 \pm 0.19$ could be calculated. This result gave a first indication for the existence of spherical micelles with a dense core as the value is very close to the theoretically predicted one of 0.775.³⁵ A subsequent computational treatment of the SANS data obtained at different pH and salt concentrations could further clarify the structure. It was found that a polydisperse spherical model fits perfectly the experimental curves (see Figure 2-4B). According to the fitting parameters, a core/corona structure was obviously demonstrated, e.g. a relatively compact, and pH- and salt-independent PDEAAm-core, $11 \leq R_c \leq 14\text{ nm}$, surrounded by a PAA-corona. The thickness of the latter could be tuned by the pH and the added salt concentration in a range of $2 \leq \delta_c \leq 10\text{ nm}$. Additionally, it was possible to confirm the spherical structure by means of cryo-TEM in a straight forwarded manner (see Figure 2-5B).

In summary, all different analytical investigations gave a clear proof for the existence of crew-cut micelles.³⁶ This elegant preparation procedure, via simply increasing the

temperature, is one of the rare examples for the direct formation of crew-cut micelles without the use of intermediate solvents or dialysis procedures.³⁷

A completely different type of micelle was however formed at room temperature and low pH. Under these acidic conditions, polydisperse PAA-core micelles are observed by DLS with a z-average hydrodynamic radius, $\langle R_h \rangle_z \approx 50$ nm. The PAA-core micelles are constituted of 69 ± 5 unimers, independently of the ionic strength of the aqueous media, indicating that indeed the PAA block is the inner part of the micelles. In this case, the structure is stabilized by expanded PDEAAM chains and a star-like structure is suggested. A successful visualization of the micellar aggregates could also be accomplished by cryo-TEM and the corresponding image can be seen in Figure 2-5A. These micelles disappear progressively upon heating above the cloud point of the PDEAAM block resulting in a macroscopic phase separation. The loss of the micellar stability is obviously caused by the desolvation of the PDEAAM segment at high temperature.

2.4 Thermo- and pH-responsive block copolymers used as stabilizer in emulsion polymerization

The last part of the thesis deals with the application of the previously investigated smart block copolymers for emulsion polymerization. Several $[(M)AA]_x-b-(DEAAM)_y$ copolymers of various block lengths were used for this study.

For the evaluation of the process efficiency, the obtention of stable latexes is the main criterion.³⁸ Furthermore, for comparable amounts of stabilizer the formation of smaller particle sizes with narrow particle size distributions is desirable. Emulsion polymerization dispersants yielding narrowly dispersed small particles are generally considered to be of high efficiency.³⁹

Results. Due to their bishydrophilic nature at room temperature, the synthesized PAA-*b*-PDEAAM block copolymers represent a considerable advantage in comparison to usual amphiphilic copolymers. In general, only block copolymers of high hydrophilic content can be used due to the difficulty encountered solubilizing them in aqueous solutions. In the approach presented here, block copolymers of all kinds of compositions can be molecularly dissolved in alkaline water at room temperature without further complicated

procedures. Upon heating these solutions above the cloud point of the PDEAAm segments, the copolymer becomes amphiphilic and can be employed as stabilizer in emulsion polymerization processes. Due to the relative high T_g of the PDEAAm block, the micelles formed above the PDEAAm block cloud point, T_c , are in a frozen-state. However it was found that even in a very simple ‘one-pot’ procedure the monomer droplet nucleation can be avoided.

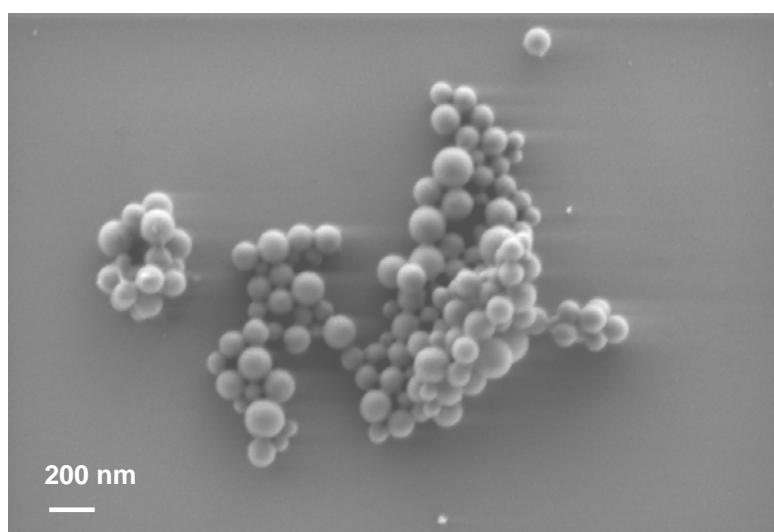


Figure 2-6. SEM image of the polystyrene latex stabilized with 1.9 % of $(AA)_{45}$ - b - $(DEAAm)_{360}$ copolymer-to-styrene weight ratio.

Using these in-situ generated amphiphilic copolymers, conventional batch emulsion polymerizations were successfully carried out using different monomers (styrene, methyl methacrylate and *n*-butyl acrylate) at 70 °C (see Figure 2-6). In all cases, stable latexes could be obtained independently of the monomer nature. One of the remarkable features is that the latexes remain stable at room temperature for months. Indeed, this is surprising as the pure block copolymers are totally water soluble at room temperature under alkaline conditions and were therefore expected to have a strong tendency to desorb from the particle surface.

The particle sizes and particle size distributions of the resulting latexes were investigated using different methods including Dynamic Light Scattering (DLS),

Transmission Electron Microscopy (TEM), and Asymmetric Flow Field-Flow Fractionation (AF-FFF). For latexes with low polydispersities the results of the different methods coincide fairly well. In the case of broadly distributed latexes a detailed discussion of differences in the obtained average diameter values can be found in chapter 6. The systematic study of the block copolymer concentration and the block copolymer composition reveals that the best efficiency is found for symmetric diblock copolymers at a concentration of 2 wt.-% relative to the amount of monomer. Here the particle size reached a minimum (i.e. the particle number reached a maximum).

Furthermore, stable monomer emulsions at room temperature can be obtained using $(AA)_{45-b}-(DEAAM)_{360}$ copolymer after heating the solution above T_c . This allows the production of stable submicrometer particles via miniemulsion procedure.

In order to understand the remarkable long-term stability of the produced latexes during the storage at room temperature, further investigations and experiments were carried out. They indicate that the stabilization is purely electrostatic, the P(M)AA segment being located at the particle surface, whereas the PDEAAM one is buried inside the particle by strong entanglements (PS and PMMA latexes) or by covalent linkages to the polymer chains in the case of the *Pn*BA latex. Thus, the PDEAAM block can not act as steric stabilizer anymore. The produced latexes are highly pH-responsive and their flocculation can be triggered by the diminution of the pH value.

The herein developed strategy demonstrates a new and highly effective way to produce stable latexes with remarkable stabilities and opens a new pathway towards the formation of hybrid particles via miniemulsion procedure (see chapter 6 for more details).

2.5 Individual contributions to joint publications

The results presented in this thesis were obtained in collaboration with others, and published or submitted to publication as indicated below. In the following, the contributions of my coauthors to the different publications are specified.

Chapter 3

This work has been published in *Macromolecules* **2006**, *39*, p. 2773-2787, under the title ‘Anionic Polymerization and Block Copolymerization of *N,N*-Diethylacrylamide in the Presence of Triethylaluminum. Kinetic Investigation Using In-line FT-NIR Spectroscopy’ by Xavier André, Khaled Benmohamed, Alexander V. Yakimansky, Galina I. Litvinenko, and Axel H. E. Müller.* Kinetic experiments as well as their full interpretation were performed by me. Under my supervision, K. Benmohamed performed some kinetic experiments and block copolymer syntheses during his ‘Erasmus’ internship in spring-summer 2003. I included the results of A. Yakimanski in my discussion of the experimental results. Galina Litvinenko participated to the calculation of the fraction of activated monomer and complexed chain ends.

Chapter 4

This work has been published in *Macromolecular Rapid Communication* **2005**, *26*, p. 558-563, under the title ‘Thermo- and pH-Responsive Micelles of Poly(acrylic acid)-*block*-Poly(*N,N*-diethylacrylamide)’ by Xavier André, Mingfu Zhang and Axel H. E. Müller.* I performed all the experiments presented in this work. Mingfu Zhang introduced me the know-how for Light Scattering measurements and participated in the discussion of the LS results.

Chapter 5

This work is to be submitted to *Langmuir* under the title ‘Solution Properties of Double-Stimuli Responsive Micelles of Poly(acrylic acid)-*block*-Poly(*N,N*-diethylacrylamide)’ by Xavier André, Markus Burkhardt, Markus Drechsler, Peter Lindner, Michael Gradzielski, and Axel H. E. Müller.* The synthesis of the block copolymer was done by me as reported

in chapter 4. Together with Markus Burkhardt I performed the SANS measurements at the Institut Max von Laue- Paul Langevin (ILL, Grenoble, France). Peter Lindner was the local contact at the D11 beam line. The radialization of the rough data and the fits of the experimental data were performed by Markus Burkhardt with the help of Michael Gradzielski. Together with them, I evaluated and discussed the scattering curves. Markus Drechsler conducted the cryo-TEM measurements.

Chapter 6

This work is to be submitted to *Macromolecules* under the title ‘Remarkable Stabilization of Latex particles by a New Generation of Double-Stimuli Responsive Poly[(Meth)acrylic Acid)-*block*-Poly(*N,N*-Diethylacrylamide) Copolymers’ by Xavier André, Khaled Benmohamed, Sabine Wunder, Axel H. E. Müller, and Bernadette Charleux.* I performed all the experiments and their evaluation during my different stays at the Laboratoire de Chimie des Polymères at the Université Pierre et Marie Curie (Paris, France) under the supervision of Bernadette Charleux. Some of the block copolymers synthesized by K. Benmohamed during his ‘Erasmus’ internship in spring-summer 2003 were used for the study. Sabine Wunder performed the AF-FFF measurements.

* marks the corresponding authors of the papers

2.6 References

- (1) Shaikh, S.; van Zanden, S.; Puskas, J. E. In *In Situ Spectroscopy of Monomer and Polymer Synthesis*; Puskas, J. E.; Storey, R., Eds.; Kluwer Academic/Plenum: New York / Dordrecht, 2003; pp 1-7.
- (2) Tauer, K.; Padtberg, K.; Dessy, C. *ACS Symposium Series* **2002**, *801*, 93-112.
- (3) Lanzendörfer, M. G.; Schmalz, H.; Abetz, V.; Müller, A. H. E. In *In Situ Spectroscopy of Monomer and Polymer Synthesis*; Puskas, J. E.; Storey, R., Eds.; Kluwer Academic/Plenum: New York / Dordrecht, 2003; pp 67-82.
- (4) Schmalz, H.; Lanzendoerfer, M. G.; Abetz, V.; Müller, A. H. E. *Macromolecular Chemistry and Physics* **2003**, *204*, 1056-1071.
- (5) Shaikh, S.; Puskas, J. E.; Kaszas, G. *Journal of Polymer Science, Part A: Polymer Chemistry* **2004**, *42*, 4084-4100.
- (6) Siesler, H. W.; Holland-Moritz, K. *Infrared and Raman Spectroscopy of Polymers*, 1980.
- (7) Lanzendörfer, M.; Schmalz, H.; Abetz, V.; Müller, A. H. E. *Polym. Prepr. (Am. Chem. Soc., Div. Polym. Chem.)* **2001**, *42*, 329-330.
- (8) Hadjichristidis, N.; Iatrou, H.; Pispas, S.; Pitsikalis, M. *Journal of Polymer Science, Part A: Polymer Chemistry* **2000**, *38*, 3211-3234.
- (9) Charleux, B.; Rives, A.; Vairon, J.-P.; Matyjaszewski, K. *Macromolecules* **1998**, *31*, 2403-2408.
- (10) Liu, B.; Matsuoka, H.; Terano, M. *Macromolecular Symposia* **2001**, *165*, 3-10.
- (11) Mori, H.; Yamahiro, M.; Terano, M.; Takahashi, M.; Matsukawa, T. *Macromolecular Chemistry and Physics* **2000**, *201*, 289-295.
- (12) Janata, M.; Lochmann, L.; Vlcek, P.; Dybal, J.; Müller, A. H. E. *Makromolekulare Chemie* **1992**, *193*, 101-112.
- (13) Baskaran, D.; Müller, A. H. E.; Sivaram, S. *Macromolecules* **1999**, *32*, 1356-1361.
- (14) Montaudo, G., Montaudo, M. S., Samperi, F. *Mass Spectrometry of Polymers*; CRC Press: Boca Raton, London, New York, Washington D.C., 2002.
- (15) Yang, H. J.; Cole, C.-A.; Monji, N.; Hoffman, A. S. *J. Polym. Sci., Part A: Polym. Chem.* **1990**, *28*, 219-226.
- (16) Ganachaud, F.; Monteiro, M. J.; Gilbert, R. G.; Dourges, M.-A.; Thang, S. H.; Rizzardo, E. *Macromolecules* **2000**, *33*, 6738-6745.
- (17) Yakimansky, A. V.; Müller, A. H. E. *Macromolecules* **2005**, *in preparation*.
- (18) Taton, D.; Wilczewska, A.-Z.; Destarac, M. *Macromolecular Rapid Communications* **2001**, *22*, 1497-1503.
- (19) Schilli, C. M.; Müller, A. H. E.; Rizzardo, E.; Thang, S. H.; Chong, Y. K. *ACS Symposium Series* **2003**, *854*, 603-618.
- (20) Schilli, C. M.; Zhang, M.; Rizzardo, E.; Thang, S. H.; Chong, Y. K.; Edwards, K.; Karlsson, G.; Müller, A. H. E. *Macromolecules* **2004**, *37*, 7861-7866.
- (21) Khouzakoun, E.; Gohy, J.-F.; Jérôme, R. *Polymer* **2004**, *45*, 8303-8310.
- (22) Hou, S.; Chaikof, E. L.; Taton, D.; Gnanou, Y. *Macromolecules* **2003**, *36*, 3874-3881.
- (23) Nakahama, S.; Kobayashi, M.; Ishizone, T.; Hirao, A. *Polymeric Materials Science and Engineering* **1997**, *76*, 11-12.
- (24) Kobayashi, M.; Okuyama, S.; Ishizone, T.; Nakahama, S. *Macromolecules* **1999**, *32*, 6466-6477.
- (25) Kobayashi, M.; Ishizone, T.; Nakahama, S. *Journal of Polymer Science, Part A: Polymer Chemistry* **2000**, *38*, 4677-4685.

-
- (26) Kobayashi, M.; Ishizone, T.; Nakahama, S. *Macromolecules* **2000**, *33*, 4411-4416.
- (27) Eggert, M.; Freitag, R. *Journal of Polymer Science, Part A: Polymer Chemistry* **1994**, *32*, 803-813.
- (28) Freitag, R.; Baltes, T.; Eggert, M. *Journal of Polymer Science, Part A: Polymer Chemistry* **1994**, *32*, 3019-3030.
- (29) Baltes, T.; Garret-Flaudy, F.; Freitag, R. *J. Polym. Sci., Part A: Polym. Chem.* **1999**, *37*, 2977-2989.
- (30) Garret-Flaudy, F.; Freitag, R. *Langmuir* **2001**, *17*, 4711-4716.
- (31) Ishizone, T.; Yoshimura, K.; Hirao, A.; Nakahama, S. *Macromolecules* **1998**, *31*, 8706-8712.
- (32) Bütün, V.; Armes, S. P.; Billingham, N. C.; Tuzar, Z.; Rankin, A.; Eastoe, J.; Heenan, R. K. *Macromolecules* **2001**, *34*, 1503-1511.
- (33) Liu, S.; Billingham, N. C.; Armes, S. P. *Angewandte Chemie, International Edition* **2001**, *40*, 2328-2331.
- (34) Liu, S.; Liu, M. *Journal of Applied Polymer Science* **2003**, *90*, 3563-3568.
- (35) Moffitt, M.; Yu, Y.; Nguyen, D.; Graziano, V.; Schneider, D. K.; Eisenberg, A. *Macromolecules* **1998**, *31*, 2190-2197.
- (36) Zhang, L.; Eisenberg, A. *Science (Washington, D. C.)* **1995**, *268*, 1728-1731.
- (37) Zhang, L.; Eisenberg, A. *Journal of the American Chemical Society* **1996**, *118*, 3168-3181.
- (38) Lovell, P. *Emulsion Polymerization and Emulsion Polymers*, 1997.
- (39) Gilbert, R. *Emulsion Polymerization - A Mechanistic Approach*; Academic Press: London, 1995.

3. Anionic Polymerization and Block Copolymerization of *N,N*-Diethylacrylamide in the Presence of Triethylaluminum. Kinetic Investigation Using In-line FT-NIR Spectroscopy

Xavier André, Khaled Benmohamed, Alexander V. Yakimansky,
Galina I. Litvinenko, and Axel H. E. Müller*

*Makromolekulare Chemie II, and Bayreuther Zentrum für Kolloide und Grenzflächen,
Universität Bayreuth, D-95440 Bayreuth, Germany. Email: axel.mueller@uni-bayreuth.de*

Abstract

We present the first kinetic study of the anionic polymerization of a *N,N*-dialkylalkylacrylamide, i.e. *N,N*-diethylacrylamide (DEAAm). The polymerization was initiated by ethyl α -lithioisobutyrate (EiBLi), poly(*tert*-butyl acrylate)-Li, and poly(*tert*-butyl methacrylate)-Li in the presence of triethylaluminum (Et₃Al) in tetrahydrofuran at -78 °C. In-situ Fourier transform near-infrared (FT-NIR) fiber-optic spectroscopy was successfully used to follow the polymerization kinetics to elucidate its mechanism. The kinetics of this process are very complex. They involve two equilibria: activation of the monomer and deactivation of chain ends by Et₃Al. These two effects are in a delicate balance that depends on the ratio of the concentrations of Et₃Al, monomer, and chain ends. Polymers with narrow molecular weight distribution are produced, whereas broadly distributed polymer is obtained in the absence of Et₃Al. By using this method, well-defined poly(*N,N*-diethylacrylamide) (PDEAAm), poly(*tert*-butyl acrylate)-*block*-PDEAAm, and poly(*tert*-butyl methacrylate)-*block*-PDEAAm (co)polymers were successfully synthesized, although the initiator or blocking efficiencies remained low ($f < 0.70$). The polymers obtained in the presence of Et₃Al are rich in heterotactic triads, whereas highly isotactic polymer is obtained in the absence of Et₃Al. In both cases, the polymers exhibit a lower critical solution temperature (LCST) with a cloud point at $T_c \approx 31$ °C in water.

Published in *Macromolecules* **2006**, *39*, 2773-2787.

3.1 Introduction

The interest in the living/controlled polymerization of mono- and dialkylacrylamides has been increasing due to their thermoresponsive properties in aqueous solution. Homopolymers of *N*-isopropylacrylamide (NIPAAm), and *N,N*-diethylacrylamide (DEAAm) exhibit a lower critical solution temperature (LCST) with a cloud point at ca. 32 °C, making these materials and their derivatives a very interesting class of polymers.^{1,2}

The control of the stereostructure in anionic polymerization was described by early work on poly(*N,N*-dimethylacrylamide) (PDMAAm) synthesized using alkylolithium initiators. The polymers were reported to be highly crystalline and rich in isotactic (mm) triads.^{3,4} Several groups have investigated the effect of counterions and temperature on the tacticity of the resulting polymer in the absence of additives. Xie and Hogen-Esch used different organometallic initiators in tetrahydrofuran (THF) at -78 °C in the absence of additives.⁵ Only large counterions such as cesium gave homogeneous reaction mixtures, leading to narrowly distributed polymers. Neither transfer nor terminations were observed and the experimental number-average molecular weights, M_n , were in accordance with calculated ones. The living character was lost when the polymerization was carried out at 0 °C. Under the same conditions, *N,N*-dimethylmethacrylamide did not polymerize, presumably due to an insufficient stabilization of the propagating amidoenolate. Kobayashi et al. observed a heterogeneous polymerization of DMAAm and DEAAm by using organolithium initiator in the presence of LiCl, leading to broadly distributed polymers (PDI > 3).⁶ Nakhmanovich et al. polymerized DMAAm with several initiators containing alkaline earth metal compounds (Mg, Ca, Ba) and they reported the influence of the counterion size on the tacticity but no evidence on the living character.⁷ Freitag et al. reported the polymerization of DEAAm via anionic and Group Transfer Polymerization (GTP) methods and reported the influence of the tacticity on the measured cloud point, T_c .^{8,9} In comparison to the value of $T_c = 32$ °C claimed for PDEAAm synthesized via free-radical polymerization (atactic polymer), a value of 30 °C was observed for predominantly syndiotactic polymers synthesized via GTP, whereas a value of 36 °C was measured for predominantly isotactic polymers synthesized via anionic polymerization using butyllithium as initiator without additive.

Major advances were reported by Nakahama et al. for the anionic polymerization of DMAAm and DEAAm by the use of organolithium and organopotassium initiators in the presence of Lewis acids (Et_2Zn , Et_3B).^{6,10,11} The great influence of the system initiator/additive/solvent on the tacticity and the solubility of the resulting polymer was

clearly demonstrated. The authors suggested that the coordination of the amidoenolate with the Lewis acid leads to a change of the stereostructure of the final polymer along with the retardation of the polymerization. Highly isotactic PDEAAm was obtained by using LiCl with an organolithium initiator whereas highly syndiotactic, and atactic polymers were obtained in the presence of Et_2Zn , and Et_3B , respectively. Indeed, the polymers produced in the presence of Et_3B show a very broad distribution of the carbonyl carbon resonance and their degree of syndiotacticity increases with the ratio B/Li, but it does not reach as high a level as that observed with Et_2Zn . Polymers rich in syndiotactic triads were not soluble in water, whereas other microstructures lead to hydrophilic polymers.¹¹ Ishizone et al. also reported the use of Lewis acids (Et_2Zn , Et_3B) for the controlled polymerization of *tert*-butyl acrylate initiated by organocesium compounds in THF.^{12,13} They reported the successful synthesis of poly(*tert*-butyl acrylate)-*block*-poly(*N,N*-diethylacrylamide) in THF at $-78\text{ }^\circ\text{C}$. For that purpose, *tert*-butyl acrylate was first initiated by an organocesium initiator (Ph_2CHCs) in the presence of Me_2Zn , and DEAAm was then initiated by the poly(*tert*-butyl acrylate)-Cs macroinitiator leading to a well-defined block copolymer ($M_w/M_n = 1.17$).¹²

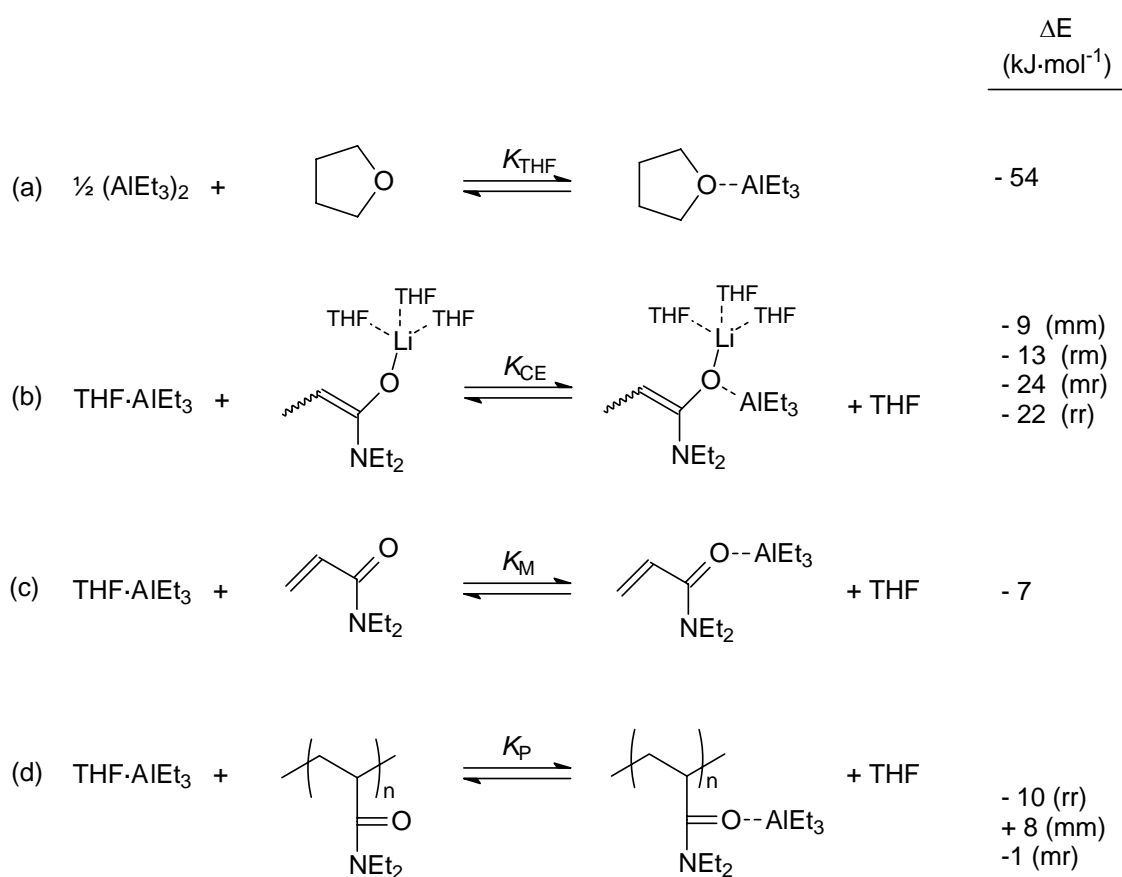
Only one example was reported recently by Kitayama et al. for the polymerization of DMAAm in toluene. Living character was observed by using a system based on *tert*-butyllithium/*bis*(2,6-di-*tert*-butylphenoxy)ethylaluminum in toluene at $0\text{ }^\circ\text{C}$.¹⁴ Well-defined block copolymers PDMAAm-*block*-poly(methyl methacrylate) could be obtained in good yield but no kinetic studies were performed. Using ^{13}C NMR spectroscopy, the authors observed the preferential coordination of $\text{EtAl}(\text{ODBP})_2$ to the carbonyl group of DMAAm and suggested an activated monomer mechanism where the adduct $\text{R}_3\text{Al}\cdot\text{DMAAm}$ propagates first until complete conversion followed by the polymerization of activated methyl methacrylate ($\text{R}_3\text{Al}\cdot\text{MMA}$). Aluminum alkyl derivatives were also introduced for the polymerization of alkyl (meth)acrylates in toluene.¹⁵⁻¹⁸ Living and stereospecific polymerizations were observed using *tert*-butyllithium/*bis*(2,6-di-*tert*-butylphenoxy)-methylaluminum,^{19,20} and *sec*-butyllithium/diisobutyl(2,6-di-*tert*-butyl-4-methylphenoxy)-aluminum.²¹ Living/ controlled polymerizations of alkyl (meth)acrylates were also reported using simple trialkylaluminum compounds in the presence of Lewis bases (12-crown-4, methyl pivalate, methyl benzoate, and *N,N,N',N'*-tetramethylenediamine),²²⁻²⁷ or tetraalkylammonium salts.^{22,28} Recently, the use of triisobutylaluminum in combination with potassium *tert*-butoxide was successfully reported for the living anionic polymerization of *tert*-butyl acrylate (*t*BA) and methyl methacrylate (MMA) in toluene at $0\text{ }^\circ\text{C}$.^{29,30}

Because of their acidic proton, the direct anionic polymerization of monoalkylacrylamides such as NIPAAm is not possible. By using *N*-methoxymethyl-substituted NIPAAm, well-defined polymers were synthesized using an organopotassium initiator in the presence of Et₂Zn, but no living character was described.³¹ The use of *N*-trimethylsilyl-substituted NIPAAm leads to highly isotactic polymers but no molecular weight distributions were shown due to the poor solubility of the resulting polymers in common solvents.³² However, these promising methods have opened new synthetic strategies to polymerize *N*-monosubstituted acrylamide monomers with the advantages of anionic polymerization.

By using controlled radical polymerization (CRP) processes, well-defined PNIPAAm and PDMAAm have been synthesized recently. reversible addition fragmentation transfer (RAFT),³³⁻³⁵ atom transfer radical polymerization (ATRP),^{36,37} and nitroxide mediated radical polymerization (NMRP)^{38,39} were used. More recently, several groups reported the control of tacticity by CRP in the presence of yttrium- and ytterbium-based Lewis acid for NIPAAm via RAFT,^{40,41} and for DMAAm via RAFT and ATRP.⁴² Nevertheless, anionic polymerization remains the best synthetic way to obtain well-defined (co)polymers up to complete monomer conversion, high molecular weight, and with desired microstructure.

To our knowledge, no kinetic investigations of the anionic polymerization of alkylacrylamides have been published so far. Besides the interesting properties of PDEAAm in aqueous solution, the monomer DEAAm is an ideal compound for Fourier transform near-infrared (FT-NIR) measurements, as it shows a distinct overtone of the vinylic C-H stretching at ca. 6156 cm⁻¹.⁴³ The variation of the peak height at this wavenumber can be followed throughout the reaction until the peak disappears at complete monomer conversion.

Herein, we report kinetic studies of the anionic polymerization of DEAAm in THF at -78 °C. Ethyl α -lithioisobutyrate (EiBLi), poly(*tert*-butyl methacrylate)-Li, and poly(*tert*-butyl acrylate)-Li (PtBMA-Li, PtBA-Li) were used as (macro)initiators in the presence of Et₃Al. The influence of the reaction parameters ([DEAAm]₀, [Initiator]₀, [Et₃Al]₀) are investigated independently to propose a polymerization mechanism. The influence of the additive on the tacticity and solubility of the resulting polymers is also discussed.

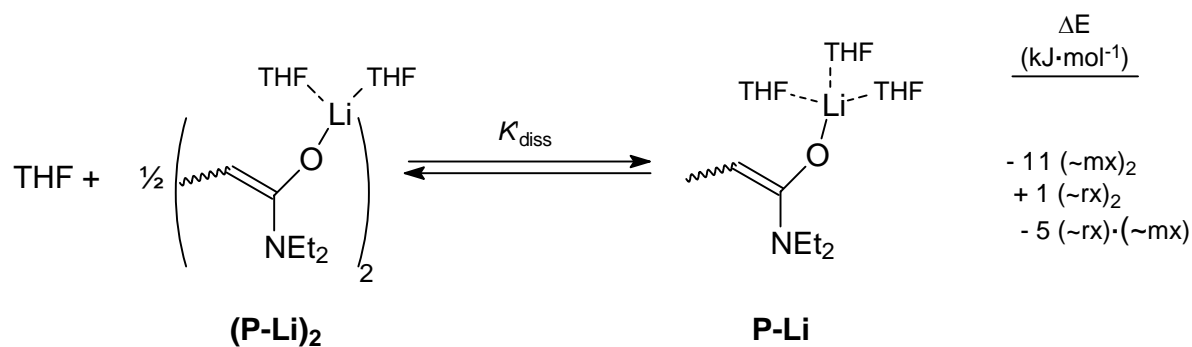
Scheme 3-1. Competing interactions of Et₃Al and DFT-calculated energy differences⁴⁴

Being a Lewis acid, Et₃Al might coordinate with all the Lewis bases present in the reaction medium. Amidoenolate chain ends, monomer, and polymer carbonyl groups as well as THF compete for coordination with Et₃Al. The possible interactions are shown in Scheme 3-1, together with the energy gains calculated by density functional theory (DFT).⁴⁴ The calculations on the trimeric model compound, i.e., an amidoenolate having two penultimate units, showed a strong tendency to coordinate with Et₃Al (stronger than the binding of Et₃Al to THF), this tendency being dependent on the tacticity of the chain end ($\Delta E = -9$ to -24 kJ·mol⁻¹). The tendency of noncoordinated chain ends to aggregate to dimers is very weak and also depends on the tacticity (Scheme 3-2); the dimers are regarded to be much less reactive than unimers or even inactive (dormant). Previous kinetic and quantum-chemistry investigations on aluminum alkyl-esterenolate complexes in nonpolar solvent also indicated the existence of an ester enol aluminate and a less-reactive dimeric associate.^{22,28,45}

The DFT calculations also indicate the coordination of Et₃Al with the carbonyl group of DMAAm; however, this bond is not as strong as that of the chain end ($\Delta E = -7$ kJ·mol⁻¹). It

may indicate that free monomer and activated monomer are in equilibrium. Binding of Et_3Al to the carbonyl groups of the polymer is calculated to be less favorable than the other coordination modes ($\Delta E = +8 \text{ kJ}\cdot\text{mol}^{-1}$ for *mm* triads, $-10 \text{ kJ}\cdot\text{mol}^{-1}$ for *rr* triads, and $-1 \text{ kJ}\cdot\text{mol}^{-1}$ for *mr* triads). Because the resulting polymers are mainly heterotactic, we assume that $\Delta E \cong 0$. The effect of Et_3Al on the microstructure of the final polymer is discussed further below.

Scheme 3-2. Aggregation of the amidoenolate chain ends in the absence of Et_3Al



3.2 Experimental Part

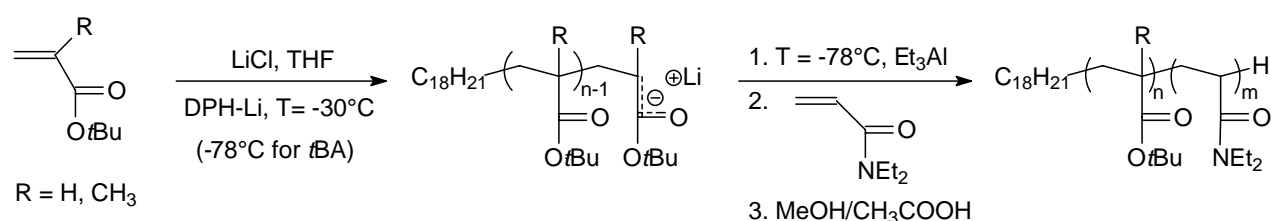
Materials. Tetrahydrofuran (THF, Merck) was purified by refluxing over CaH_2 and distilled from potassium before use. Triethylaluminum (Et_3Al , Aldrich, 1M in hexane) was used as received. The monomers *tert*-butyl methacrylate, and *tert*-butyl acrylate (*t*BMA, *t*BA, BASF) were three times degassed under high vacuum (10^{-5} mbar), and Et_3Al was added dropwise until a yellowish color appeared. The mixture was stirred and condensed into an ampule and stored under dry nitrogen atmosphere. DEAAm was synthesized by the reaction at $T < 10^\circ\text{C}$ in toluene (Merck) of a 2-fold excess of diethylamine and acryloyl chloride (96%, Aldrich). The crude DEAAm was then purified five times from CaH_2 by fractional distillation under reduced pressure, and it was three times degassed prior to the polymerization. Ethyl α -lithioisobutyrate (EiBLi) was synthesized according to the method of Lochmann and Lim.⁴⁶ Diphenylhexyl-lithium (DPHLi) was prepared by the reaction of *n*-butyllithium (*n*-BuLi, Acros, 1.3M in cyclohexane/hexane, 92:8) and 1,1-diphenylethylene (DPE, 97%, Aldrich, freshly distilled over *n*-BuLi) in situ ($[\text{DPE}]/[n\text{-BuLi}] = 1.1$). LiCl (Fluka, anhydrous $\geq 98\%$) was dried in high vacuum at 300°C for 3 days and dissolved in dry THF.

Equipment and In-Line FT-NIR Spectroscopy. The sequential anionic polymerizations were performed under dry nitrogen pressure in a thermostated glass reactor (Büchi) equipped

with an all-glass immersion transmission probe (Hellma) with an optical path length of 10 mm connected via fiberoptics to a Nicolet Magna 560 FT-IR spectrometer equipped with a white light source and a PbS detector.⁴⁷ Data processing of NIR spectra was performed with Nicolet's OMNIC Series software version 5.2. Each spectrum was constructed with 16 scans with a resolution of 8 cm⁻¹ and recorded every 3.7 s. Prior to the measurement, a blank spectrum of the solution containing the initiator, and eventually the additive, was recorded in the absence of a monomer at the working temperature. The measurement was started before injection of the first monomer. The baseline for signal height determination was drawn from 7000 to 6300 cm⁻¹, and the FT-NIR spectra of DEAAm were obtained after solvent subtraction to yield a pure component spectrum and to determine conversions because THF has strong absorptions close to the overtone vibrations of DEAAm. For the block copolymerization, *t*BMA and *t*BA polymerizations kinetics (precursors) were monitored using the same procedure.

Homopolymerization of DEAAm. The reactor containing ca. 600 mL of dry THF was cooled to -78 °C. The appropriate amount of Et₃Al was injected to the reactor via a syringe (12.0 mmol; 18.8 mmol·L⁻¹, run C). The initiator, EiBLi (49.4 mg, 0.63 mmol·L⁻¹) was dissolved in 10 mL of dry toluene in a Rotaflo-sealed ampule and introduced into the reactor. Polymerization was started after stabilization of the temperature at $T = -78$ °C by injection of DEAAm (28.6 mmol; 44.9 mmol·L⁻¹) via a syringe ($t = 0$). A degassed solution of methanol/acetic acid (9:1 v/v) was used as a quenching agent. Experiments with varying the initial concentrations of EiBLi and Et₃Al were performed using the same procedure at $T = -78$ °C.

Scheme 3-3. Anionic polymerization of *N,N*-diethylacrylamide initiated by a poly(*tert*-butyl (meth)acrylate]-Li macroinitiator in the presence of Et₃Al



Block Copolymerization. As shown in Scheme 3-3, the initiator (DPHLi, 1.1 mmol; 1.8 mmol·L⁻¹, run L) was formed by the reaction of DPE and *n*-BuLi in the THF solution of LiCl at -30 °C (11.8 mmol; 18.5 mmol·L⁻¹). The monomer *t*BMA (55.4 mmol; 87.0 mmol·L⁻¹) was

injected via a syringe into the reactor to start the polymerization of the precursor. The characteristic red color of the DPHLi initiator disappeared instantaneously. After full conversion of *t*BMA, the temperature was cooled to $-78\text{ }^{\circ}\text{C}$ (ca. 1 h), and then Et_3Al (8 mmol; $12.6\text{ mmol}\cdot\text{L}^{-1}$) and DEAAm (57.2 mmol; $89.9\text{ mmol}\cdot\text{L}^{-1}$) ($t = 0$) were added successively. A degassed solution of methanol/acetic acid (9:1 v/v) was used as a quenching agent. An aliquot of the final solution was taken and dried for 2 days under vacuum to result in the crude copolymer. The rest of the copolymer was recovered by precipitation into a large excess of *n*-hexane, filtered and dried for 2 days under vacuum. This process removes unreacted *Pt*BMA precursor, leading to the purified copolymer. Traces of LiCl were removed from *Pt*BMA precursor by 1 day of stirring in benzene followed by a filtration. The clear solutions were freeze-dried from benzene. Experiments with varying the initial concentrations of DEAAm were performed using the same procedure at $-78\text{ }^{\circ}\text{C}$. The synthesis and purification of *Pt*BA-*b*-PDEAAm copolymer were carried out using the same experimental conditions, except that both monomers *tert*-butyl acrylate (*t*BA) and DEAAm were polymerized at the same temperature ($-78\text{ }^{\circ}\text{C}$).

Characterization of Polymers. Polymers were characterized by size exclusion chromatography (SEC) using a Waters 510 HPLC Pump, a Bischoff 8110 RI detector, a Waters 486 UV detector ($\lambda = 270\text{ nm}$), and a 0.05 M solution of LiBr in 2-*N*-methylpyrrolidone (NMP) as eluent. PSS GRAM columns (300 x 8 mm, $7\mu\text{m}$): 10^3 , 10^2 \AA (PSS, Mainz, Germany) were thermostated at $70\text{ }^{\circ}\text{C}$. A $20\mu\text{L}$ of a 0.4 wt.-% polymer solution was injected at an elution rate of $1\text{ mL}\cdot\text{min}^{-1}$. Polystyrene standards were used to calibrate the columns, and methyl benzoate was used as an internal standard. A second SEC setup was performed in pure THF at an elution rate of $1\text{ mL}\cdot\text{min}^{-1}$ using a Shodex RI-101 detector, a Waters 996 photodiode array detector (PDA), and PSS SDVgel columns (300 x 8 mm, $5\mu\text{m}$): 10^5 , 10^4 , 10^3 , and 10^2 \AA . Poly(*tert*-butyl methacrylate) standards were used to calibrate the columns. MALDI-TOF mass spectrometry was performed on a Bruker Reflex III equipped with a 337 nm N_2 laser and 20 kV acceleration voltage. Dihydroxybenzoic acid (DHB) or dithranol were used as matrix. Samples were prepared from dimethylacetamide solution by mixing matrix ($10\text{ g}\cdot\text{L}^{-1}$), and sample ($10\text{ g}\cdot\text{L}^{-1}$) in a ratio 10:1. No additional salt was needed for the measurement. The number-average molecular weights, M_n , were determined in the linear mode. The MALDI measurements were reproducible in the range of $\pm 3\%$. ^1H and ^{13}C NMR spectra were recorded on a Bruker AC-250 spectrometer in $\text{THF-}d_8$ or CDCl_3 at room

temperature. To ensure a good resolution of the ^{13}C NMR spectra for the determination of the polymer microstructure, 13,000 scans were accumulated.

3.3 Results and Discussion

3.3.1 Polymerization of DEAAm

Table 3-1. Anionic Polymerization of DEAAm initiated by ethyl α -lithioisobutyrate (EiBLi) in the presence of Et_3Al in THF at $-78\text{ }^\circ\text{C}$ ^a

Run	$[\text{EiBLi}]_0$ $\text{mmol}\cdot\text{L}^{-1}$	$[\text{Et}_3\text{Al}]_0$ $\text{mmol}\cdot\text{L}^{-1}$	$r =$ $[\text{Et}_3\text{Al}]_0/[\text{I}]_0$	$10^{-3}\cdot M_{n,\text{theo}}$ ^b	$10^{-3}\cdot M_{n,\text{exp}}$ ^c (MALDI)	$10^{-3}\cdot M_{n,\text{exp}}$ ^d (SEC)	M_w/M_n ^d (SEC)	f ^e
A	0.87	0	0	6.8	16.5 ^f	12.1	2.13	0.41
B	0.65	4.7	7.2	8.8	26.0	17.6	1.03	0.34
C	0.63	18.8	29.8	9.1	39.4	30.8	1.05	0.23
D	0.74	30.8	41.6	7.7	39.2 ^f	28.7	1.10	0.20
E	1.14	19.0	16.7	5.2	22.4	14.0	1.06	0.23
F	1.69	18.8	11.1	3.5	7.2	5.1	1.05	0.49

^a Full conversions observed in all cases, $X_p = 1$, $[\text{M}]_0 = [\text{DEAAm}]_0 = 44.1\text{-}45.4\text{ mmol}\cdot\text{L}^{-1}$. ^b $M_{n,\text{theo}} = X_p\cdot[\text{M}]_0/[\text{I}]_0\cdot M_{\text{DEAAm}} + M_{\text{initiator}}$. ^c After precipitation in *n*-hexane, linear mode. ^d After precipitation in *n*-hexane, PS calibration. ^e Initiator efficiency, $f = M_{n,\text{theo}}/M_{n,\text{MALDI}}$. ^f Using Equation 3-1.

(i) Initiation with EiBLi. A series of PDEAAm were synthesized using ethyl α -lithioisobutyrate (EiBLi) as an initiator in the presence and absence of Et_3Al in THF at $-78\text{ }^\circ\text{C}$ (Table 3-1). EiBLi is known as a unimeric model of the poly(alkyl methacrylate) living chains and was used as an initiator in numerous kinetic studies on alkyl acrylates and alkyl methacrylates.^{28,48,49} PDEAAm synthesized in the absence or in the presence of Et_3Al were obtained in quantitative yield and the polymerization media were clear and transparent up to 100% monomer conversion. Polymer produced in the absence of Et_3Al showed a broad molecular weight distribution ($M_w/M_n = 2.1$), whereas in the presence of Et_3Al , well-defined polymers were obtained ($M_w/M_n \leq 1.10$). Figure 3-1 shows the SEC traces of PDEAAm obtained at various Et_3Al and EiBLi initial concentrations. The SEC characterization of polymers bearing an amide function like PNIPAAm in THF involves various problems⁵⁰ due to chain aggregation after complete drying of the polymer samples and adsorption on the

columns.⁵¹ To circumvent this problem, the addition of salt (Bu_4NBr),⁵² or triethylamine/methanol to THF was proposed.⁵³ Furthermore, because of their stereoregular structure, PDEAAm or PNIPAAm produced by anionic polymerization are poorly soluble in common solvents and their characterization is commonly performed in *N,N*-dimethylformamide (DMF) or in *N,N*-dimethylacetamide (DMAc).^{11,31} We have obtained good results by using 2-*N*-methylpyrrolidinone (NMP) with LiBr (0.05 M) as an eluent in combination with polar PSS GRAM columns thermostated at 70 °C. As the columns were calibrated against linear polystyrene standards, the molecular weight of each narrowly distributed PDEAAm sample was measured additionally by MALDI-TOF mass spectrometry.

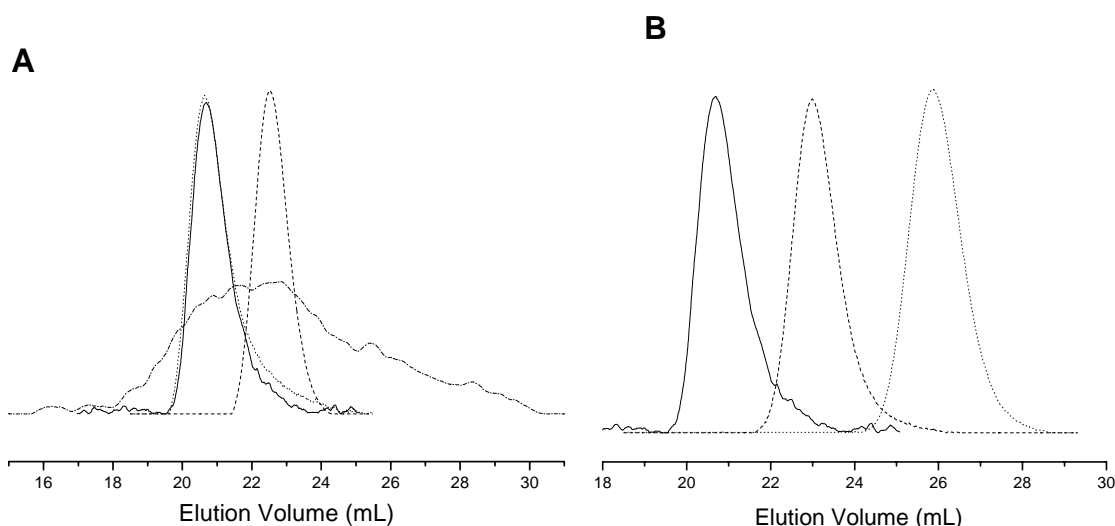


Figure 3-1. (A) SEC traces of the PDEAAm obtained with $\text{EiBLi}/\text{Et}_3\text{Al}$ in THF at -78 °C by varying $[\text{Et}_3\text{Al}]_0$: (---) 0, (---) 4.7, (---) 18.8, and (—) 30.8 $\text{mmol}\cdot\text{L}^{-1}$. (B) Variation of the initial initiator concentration, $[\text{EiBLi}]_0$: (—) 0.63, (---) 1.14, and (---) 1.69 $\text{mmol}\cdot\text{L}^{-1}$. Experimental conditions: see Table 3-1.

Figure 3-2 shows the MALDI-TOF mass spectrum of a PDEAAm of lower molecular weight (run F), measured without any added salt. The spectrum (Figure 3-2A) shows a second peak of lower intensity at ca. $m/z = 3500$, which is attributed to doubly charged chains that are often observed for polar polymers ($z = 2$).⁵⁴ Thus, a multi-peak Gaussian fitting procedure was used to calculate the molecular weights. The expanded spectrum from 6000 to 6300 Da is shown in Figure 3-2C, and the series of observed masses are in good agreement with the

expected chain structure $[C_6H_{11}O_2 + DP_n \cdot (C_7H_{13}NO)]$ with a repeat unit of 127.09 Da = monoisotopic mass (average mass = 127.19) corresponding to one DEAAm unit and a residual fragment of 115.08 Da, monoisotopic mass (average mass = 115.15 Da) corresponding to the initiator fragment.

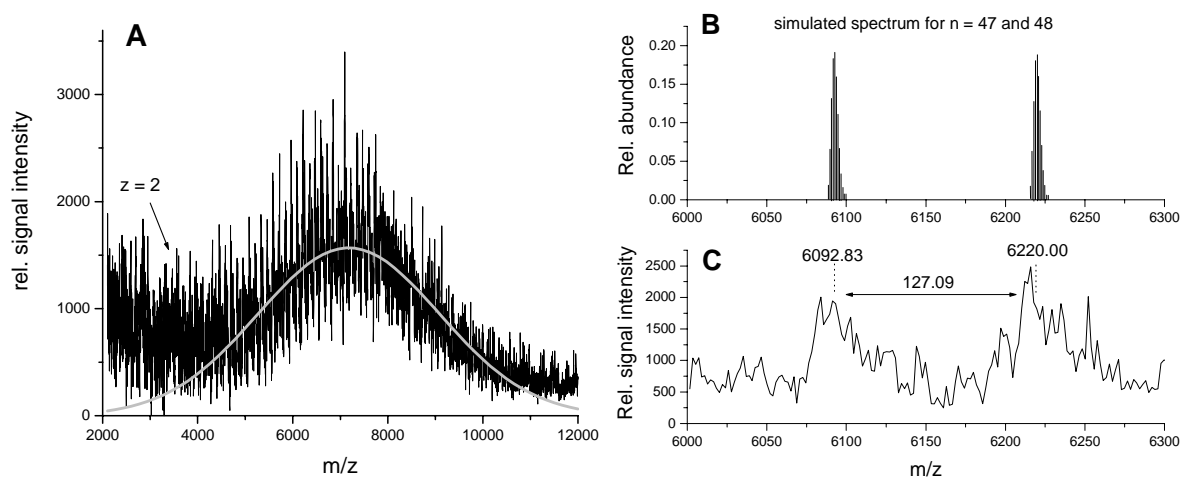


Figure 3-2. MALDI-TOF mass spectrum of PDEAAm (run F). (A) Complete spectrum measured without salt in the linear mode. The grey line corresponds to a multi-peak Gaussian fit. (B) Simulated peak distribution due to isotopic abundance. (C) Expanded experimental spectrum.

The number-average molecular weights, M_n , determined by SEC using a PS calibration underestimate the real molecular weights (Table 3-1, Figure 3-3). A linear fit of the plot of $M_n(\text{MALDI})$ vs $M_n(\text{SEC})$ for the PDEAAm samples obtained with organolithium initiators in the presence of Et_3Al results in the relation,

$$M_n(\text{MALDI}) = (1.40 \pm 0.05) \cdot M_n(\text{SEC}) \quad (3-1)$$

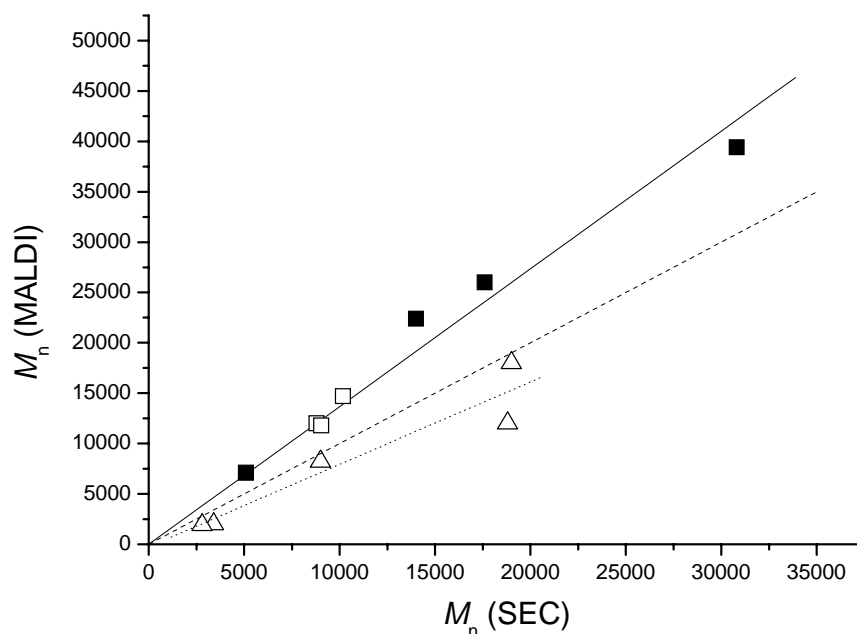


Figure 3-3. Plot of $M_n(\text{MALDI})$ vs $M_n(\text{SEC})$, SEC in NMP for PDEAAm obtained with (■) EiBLi/Et₃Al, and (□) DPHLi/Et₃Al in THF at $-78\text{ }^\circ\text{C}$. (—) Linear fit of data points; (---) line expected for $M_n(\text{MALDI}) = M_n(\text{SEC})$. For comparison well-defined PNIPAAm⁵⁵ are shown (△). The characterization of PDEAAm obtained with DPHLi/Et₃Al is shown in the Supporting Information, Table 3-7.

It was reported by Ganachaud et al., and by Schilli et al. that the SEC evaluation of linear PNIPAAm in pure THF, and in THF + tetrabutylammonium bromide (Bu₄NBr), respectively, gives significantly higher molecular weights than those obtained from MALDI-TOF analysis.^{35,51} These atactic polymers were obtained via RAFT polymerization. The characterization of well-defined linear PNIPAAm obtained by RAFT using benzyl 1-pyrrolocarbodithioate as a chain transfer agent⁵⁵ are also plotted in Figure 3-3. Their absolute molecular weights are slightly overestimated in NMP but not as much as it was reported by Schilli et al. in THF + salt. Even if the direct comparison of PNIPAAm and PDEAAm is not possible, this observation may be attributed to the intrinsic difference of the chemical structure of both polymers. As a monoalkylacrylamide, PNIPAAm may form hydrogen bonds with NMP. In contrast, PDEAAm does not bear an amide proton and hydrogen bonding is not possible. Thus, for a given absolute molecular weight, the hydrodynamic volume in NMP of a PDEAAm coil is smaller than that of PNIPAAm and it therefore shows an apparently lower

M_n . PDEAAm synthesized via anionic polymerization is rich in heterotactic triads (see below), and therefore, should have a microstructure comparable to PNIPAAm.

Relatively low initiator efficiencies, $0.23 \leq f \leq 0.49$, are calculated from the M_n obtained by MALDI-TOF MS. With increasing ratio $r = [\text{Et}_3\text{Al}]_0/[\text{I}]_0$, f decreases as it is suggested in Figure 3-4, reaching a plateau at $f \approx 0.20$ for $r \geq 10$. The effect of Et_3Al on polymerization rates will be discussed in details below.

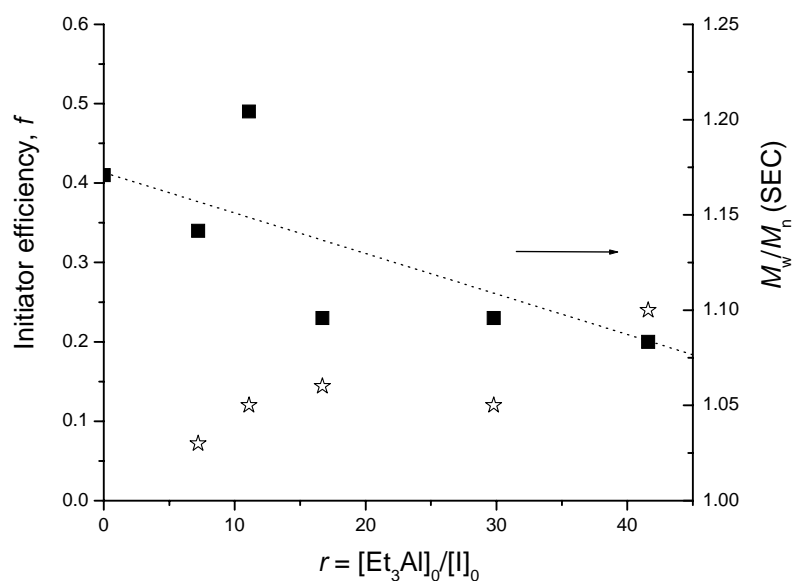


Figure 3-4. Dependence of the initiator efficiency, f (■), and the polydispersity index, M_w/M_n (☆) on the ratio $r = [\text{Et}_3\text{Al}]_0/[\text{I}]_0$ synthesized using EiBLi in the presence of Et_3Al in THF at $-78\text{ }^\circ\text{C}$. Experimental conditions; see Table 3-1.

A few attempts were carried out using DPHLi as an initiator in the presence of Et_3Al . Narrowly distributed polymers were obtained at $-78\text{ }^\circ\text{C}$ ($M_w/M_n = 1.15\text{-}1.19$) while broad molecular weight distributions (MWD) were observed at $0\text{ }^\circ\text{C}$ ($M_w/M_n > 1.7$). For details, see Table 3-7 in the Supporting Information. However, the living polymers were unable to initiate the polymerization of *tert*-butyl acrylate (*tBA*) or *tert*-butyl methacrylate (*tBMA*). This was attributed to the coordination of Et_3Al to the amidoenolate active chain which decreases the nucleophilicity of the resulting ate-complex.

(ii) **Initiation by Poly[*tert*-butyl (meth)acryloyl]-Li/LiCl.** *tert*-Butyl methacrylate (*t*BMA) was polymerized in a living way using the system DPHLi/LiCl in THF at $-30\text{ }^{\circ}\text{C}$.⁵⁶ Full conversion was obtained after ca.15-20 min. A sample was withdrawn from the reaction mixture and analyzed by SEC and MALDI-TOF MS (see Figures 3-22 and 3-23 in the Supporting Information). The precursor polymers had molecular weights between 7000 and 9000 $\text{g}\cdot\text{mol}^{-1}$ and their MWDs were very narrow ($M_w/M_n = 1.04\text{-}1.05$). As we reported earlier, well-defined *Pt*BA precursors could be obtained in a similar way,⁵⁷ and their molecular weights were between 4000 and 6000 $\text{g}\cdot\text{mol}^{-1}$ with narrow MWD, $M_w/M_n = 1.10\text{-}1.18$ (see Figures 3-24 and 3-25 in the Supporting Information). Polymerization of *t*BA occurred within 1 minute at $-78\text{ }^{\circ}\text{C}$. By using the absolute number-average molecular weights, M_n , measured by MALDI-TOF MS, high initiator efficiencies were calculated and are in the range between 0.8 and 1.0. The effective *Pt*BMA-Li, and *Pt*BA-Li chain end concentrations for the initiation of the second monomer can be calculated by taking the molecular weight given by MALDI-TOF (see Table 3-7 in the Supporting Information). The livingness of the *t*BMA polymerization was investigated by in-line FT-NIR spectroscopy coupled with SEC and MALDI-TOF mass spectrometry. The same treatment is not possible for the *t*BA polymerization because the half-lives are too short to allow for sample withdrawing during the course of the polymerization ($t_{1/2} \approx 10\text{ s}$).

As shown in Figure 3-5 for the polymerization of *t*BMA at $-30\text{ }^{\circ}\text{C}$ (run J), a linear first-order time-conversion plot is observed, and the molecular weight determined by MALDI increases linearly with the conversion, X_p , while the polydispersity index, M_w/M_n , decreases with conversion. It indicates the livingness of the *t*BMA polymerization under these conditions. An apparent polymerization rate, $k_{\text{app}} = 4.9\cdot 10^{-3}\text{ s}^{-1}$, and an absolute polymerization rate constant, $k_p = k_{\text{app}}/(f\cdot[I]_0) = 3.0\text{ L}\cdot\text{mol}^{-1}\cdot\text{s}^{-1}$, can be calculated. The latter compares well to the previously reported data by Kunkel et al., $k_p = 3.5\text{ L}\cdot\text{mol}^{-1}\cdot\text{s}^{-1}$ for the polymerization of *t*BMA initiated by methyl α -lithioisobutyrate (MiBLi) in THF at $-30\text{ }^{\circ}\text{C}$ using a similar ratio $[\text{LiCl}]/(f\cdot[\text{MiBLi}]_0) = 16.6$.⁵⁸

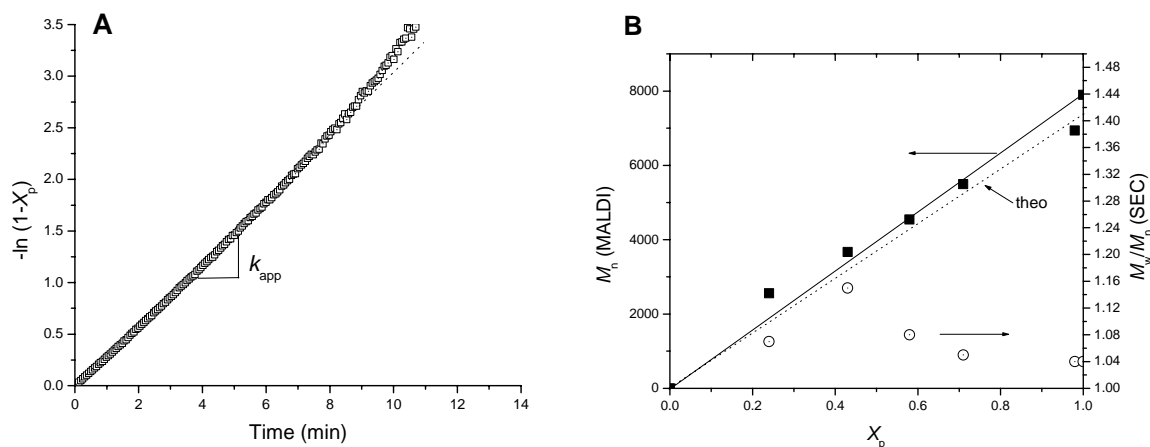


Figure 3-5. (A) First-order time-conversion plot for the polymerization of *t*BMA initiated by DPHLi/LiCl in THF at $-30\text{ }^{\circ}\text{C}$, run J. (B) Corresponding dependence of M_n (MALDI) (■), and of the polydispersity index, M_w/M_n (SEC) (○), on *t*BMA conversion, X_p . Experimental conditions: $[t\text{BMA}]_0 = 86.4\text{ mmol}\cdot\text{L}^{-1}$, $[\text{DPHLi}]_0 = 1.74\text{ mmol}\cdot\text{L}^{-1}$, $[\text{LiCl}]/(f[\text{DPHLi}]_0) = 11.3$.

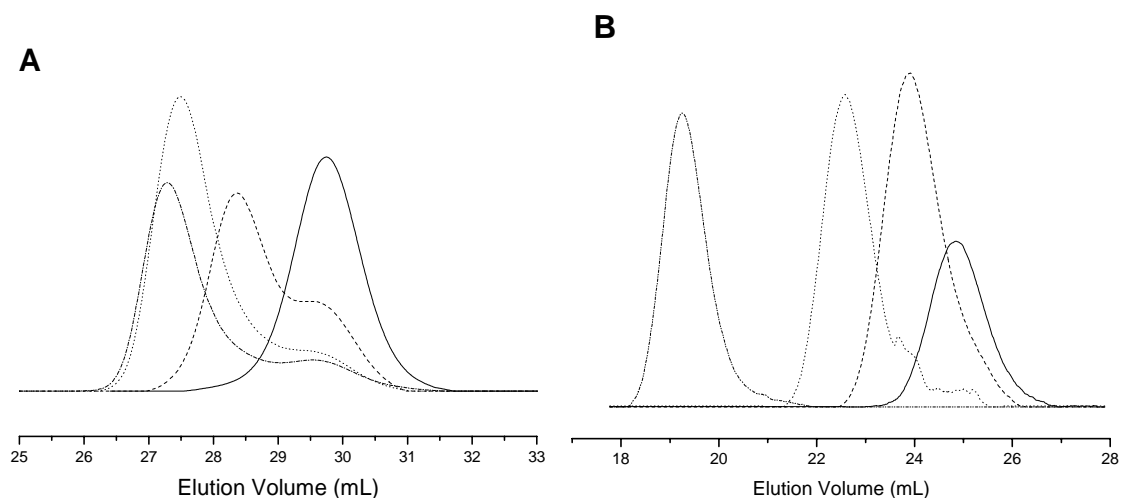


Figure 3-6. (A) SEC traces (normalized RI signal) of the *Pt*BA precursor (—), and the crude *Pt*BA-*b*-PDEAAm copolymers before purification at 0.34 (---), 0.84 (···), and 1.0 (— · —) of DEAAm conversion for run G. The SEC measurements were performed in THF + 0.25 wt.-% tetrabutylammonium bromide (TBAB) at $23\text{ }^{\circ}\text{C}$.⁵⁷ (B) SEC traces of purified *Pt*BMA-*block*-PDEAAm copolymers synthesized in THF at $-78\text{ }^{\circ}\text{C}$ using different initial DEAAm concentrations: $[\text{DEAAm}]_0 = 11.2$ (—, run J), 44.7 (---, run K), 89.9 (···, run L), 202.4 $\text{mmol}\cdot\text{L}^{-1}$ (— · —, run M). Experimental conditions see Table 3-2.

Table 3-2. Anionic polymerization of DEAAm initiated by a poly(*tert*-butyl acrylate)-Li and poly(*tert*-butyl methacrylate)-Li [PtB(M)A-Li] macroinitiators in the presence of Et₃Al and LiCl in THF at $-78\text{ }^{\circ}\text{C}^{\text{a,b}}$

Run	Initiator	[I] ₀ ^c mmol·L ⁻¹	[DEAAm] ₀ mmol·L ⁻¹	[Et ₃ Al] ₀ mmol·L ⁻¹	$r =$ [Et ₃ Al] ₀ /[I] ₀	$r^* =$ [Et ₃ Al] ₀ /[P*] ₀ ^d	$10^{-3} \cdot$ $M_{n,\text{theo}}$ ^e	$10^{-3} \cdot M_{n,\text{exp}}$ ^f (MALDI)	f^g	$10^{-3} \cdot M_{n,\text{exp}}$ ^h (SEC)	M_w/M_n ^h (SEC)
G	PtBA-Li	1.77	94.0	12.9	7.30	48.6	12.7	51.8	0.15	28.5	1.12
H	PtBA-Li	2.35	137	13.9	5.90	23.7	11.4	45.2	0.25	29.7	1.08
I	PtBA-Li	0.55	92.0	3.2	5.80	18.8	24.3 ⁱ	77.6	0.31	48.9	1.09
J	PtBMA-Li	1.62	11.2	12.5	7.72	11.0	8.8	11.5	0.70	9.3	1.05
K	PtBMA-Li	1.71	44.7	12.5	7.31	18.3	10.8	16.0	0.40	11.7	1.05
L	PtBMA-Li	1.51	89.9	12.6	8.34	15.7	16.1	22.7	0.53	18.1	1.06
M	PtBMA-Li	1.38	202	12.6	9.13	21.7	27.9	79.0	0.42	57.4	1.04

^a Full conversions observed in all cases, $X_p = 1$, from FT-NIR data. ^b *t*BA and *t*BMA were polymerized by DPHLi/LiCl at -78 , and $-30\text{ }^{\circ}\text{C}$, respectively, $[\text{LiCl}]/[\text{DPHLi}]_0 = 7.10\text{-}15.9$. ^c Effective macroinitiator concentration, see Table 3-6 in the Supporting Information. ^d $[\text{P}^*]_0$, active chain end concentration, calculated using the blocking efficiency, f . ^e $M_{n,\text{theo}} = X_p \cdot [\text{M}]_0 / [\text{I}]_0 \cdot M_{\text{DEAAm}} + M_{\text{precursor}}$. ^f After precipitation in *n*-hexane, linear mode. ^g Blocking efficiency, $f = (M_{n,\text{theo}} - M_{n,\text{prec}}) / (M_{n,\text{exp}} - M_{n,\text{prec}})$. ^h After precipitation in *n*-hexane, PS calibration. ⁱ $X_p = 0.88$.

The initiation of DEAAm by various *Pt*BA-Li macroinitiators was observed in THF at $-78\text{ }^{\circ}\text{C}$, and *Pt*BA-*b*-PDEAAm copolymers were obtained. Nevertheless, the method suffered from a low blocking efficiency ($f = 0.15\text{--}0.31$), as summarized in Table 3-2 (runs G, H, and I). We initially attributed this to the short livingness of *Pt*BA-Li active chains after complete monomer conversion, leading to the deactivation of the active centers by backbiting termination before addition of the second monomer.⁵⁷ This can be easily observed in the SEC traces of the block copolymer at different DEAAm conversions where a second peak attributed to the remaining precursor is present (Figure 3-6A). To circumvent this crucial problem, we decided to use *Pt*BMA-Li as a macroinitiator, which is known to be more stable than *Pt*BA-Li in THF at low temperature. *t*BMA was polymerized at $-30\text{ }^{\circ}\text{C}$ in order to achieve complete *t*BMA conversion in a reasonable time. Despite the fact that the polymerization of *t*BMA occurs in a living fashion in THF at $-30\text{ }^{\circ}\text{C}$, and that DEAAm was consumed quantitatively, blocking efficiencies are in the range $0.40 \leq f \leq 0.70$ only. The SEC traces of the resulting crude copolymer are bimodal (Figure 3-7), corresponding to a considerable amount of *Pt*BMA homopolymer. This might suggest that significant self-termination takes place before initiation of the polymerization by *Pt*BMA-Li, as it was observed using *Pt*BA precursors. However, *Pt*BMA-Li chain ends were reported to be quite stable at $T \leq -30\text{ }^{\circ}\text{C}$. For both *Pt*BA-Li and *Pt*BMA-Li macroinitiators, the lowest blocking efficiencies are observed with the highest ratios $r^* = [\text{Et}_3\text{Al}]_0/[\text{P}^*]_0$.

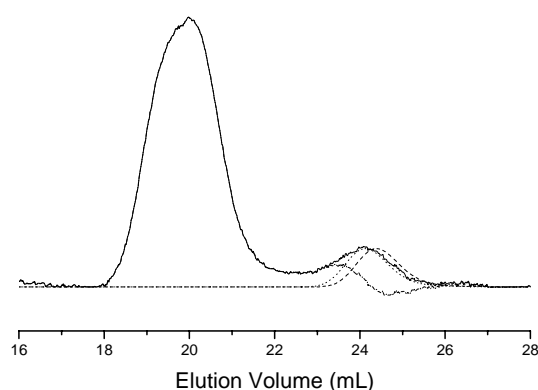


Figure 3-7. SEC (in THF, RI signal) traces of the *Pt*BMA precursor (---), and the crude *Pt*BMA-*b*-PDEAAm (---) for $X_p = 0.56$. A shift of the precursor peak by 0.30 mL (····) enables the subtraction from the block copolymer peak (-·-·-); run M. Experimental conditions, see Table 3-2.

The SEC traces (RI detection) indicate a shift of the maximum attributed to the *Pt*BMA precursor from $V_{\max} = 24.4$ to 24.1 mL in the copolymer trace (Figure 3-7), i.e., subtraction of the precursor peak is only possible, if the precursor is somewhat shifted toward higher molecular weights, indicating that it could have added one or two DEAAm units before terminating.

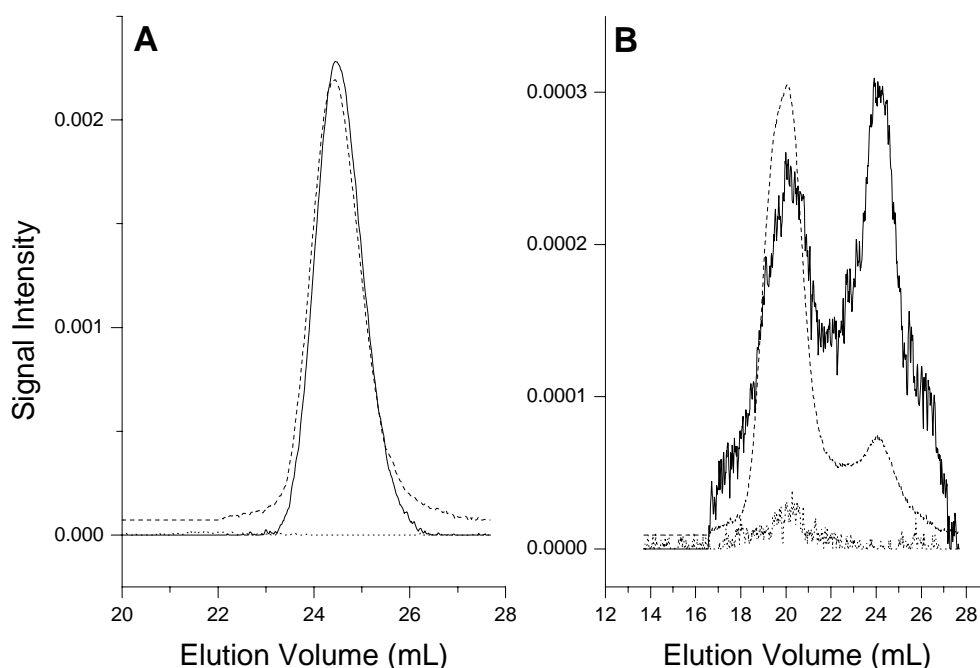
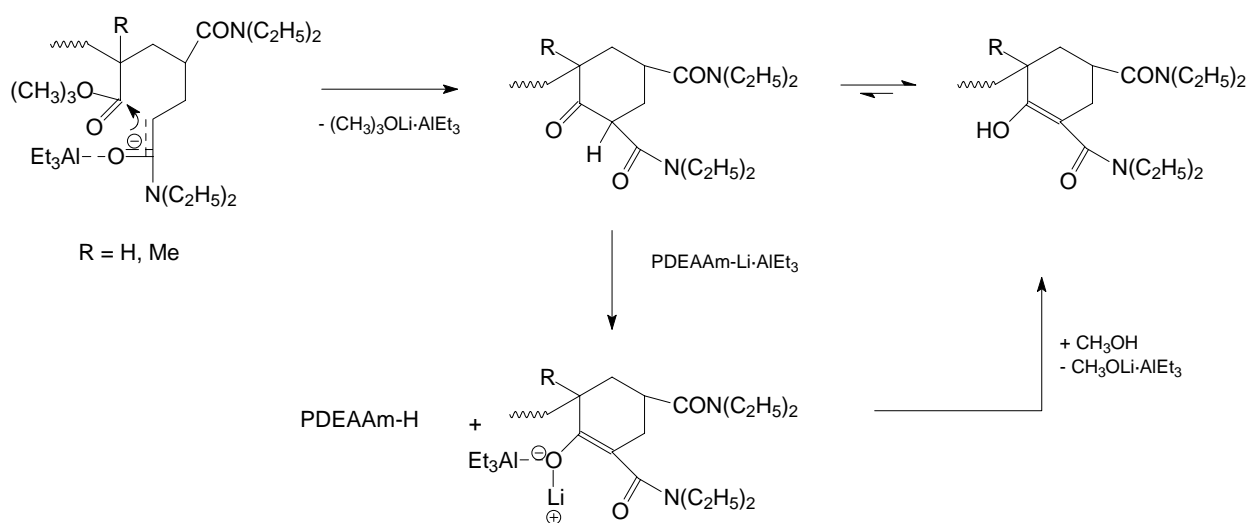


Figure 3-8. SEC traces of the *Pt*BMA precursor (A) and the crude *Pt*BMA-*b*-PDEAAm for $X_{p,DEAAm} = 0.56$ (B) in NMP+LiBr at 70 °C. RI detection (---), UV detection at $\lambda = 270$ (—) and 300 nm (···). Run M, experimental conditions, see Table 3-2.

The UV traces at $\lambda = 270$ and 300 nm are shown in Figure 3-8. No signal at $\lambda = 300$ nm is observed for the *Pt*BMA precursor, whereas a noisy signal of low intensity is observed in the crude block copolymer that we attribute to the backbiting product of amidoenolate chains, i.e., a cyclic, enolized β -ketoamide,⁵ similar to the enolized cyclic β -ketoester observed in the polymerization of *n*-butyl acrylate⁵⁹ and *t*BA,⁶⁰ having strong UV absorption at 260 nm. Similarly, the formation of cyclic β -ketoesters was reported as a backbiting product for the polymerization of MMA with an absorption at 300 nm.⁶¹ The

low signal-to-noise ratio is due to the relatively low absorbance of this cyclic product. We speculate that backbiting may occur after incorporation of one or two DEAAm units in the chain, as shown in Scheme 3-4. Indeed, the molecular weight at peak maximum is shifted from 9,200 to 10,600 using a PS calibration, as shown in Figure 3-7. As indicated in Scheme 3-4, the driving force for the termination process is probably due to the presence of the acidic α -proton ($pK_a = 12-14$)⁶² in the newly formed cyclic β -ketoamide, which induces the termination of a second PDEAAm-Li growing chain, the resulting anion of the cyclic β -ketoamide being not nucleophilic enough to initiate the polymerization. The residual active chain end concentration is assumed to remain stable during the polymerization of DEAAm allowing living polymerization as discussed below. Nevertheless, by precipitation of the reaction mixture in *n*-hexane after quenching, it is possible to eliminate the remaining precursor and the copolymer chains containing a few units of DEAAm to yield pure diblock copolymers, as shown in Figure 3-6B.

Scheme 3-4. Proposed termination mechanism after incorporation of two DEAAm units



3.3.2 Polymerization kinetics

The course of the polymerization was followed by in-situ FT-NIR spectroscopy, and samples were taken at various monomer conversions for the experiments with $t_{1/2} > 1$ min. The decrease of the intensity of the bands with time was followed. Specific monomer absorptions for DEAAm were detected at ca. 6156, 6071, 6001, 4748, 4713, 4686, 4621, and 4574 cm^{-1} (Figure 3-9). In contrast to the RAFT polymerization of NIPAAm in

dioxane, no absorption attributed to the polymer at ca. 6700 cm^{-1} was found.³⁵ The strongest vibration located at ca. 6156 cm^{-1} was attributed to the first overtone of C–H vinylic stretching of DEAAm. Furthermore, this specific vibration is well separated from other vibrations or solvent cutoff and therefore, its peak height was chosen for conversion determination. Peak heights are generally used instead of peak areas for evaluation because they usually give less noise. The monomer conversions, X_p , were calculated using Equation 3-2:

$$X_p = \frac{A_0 - A_t}{A_0 - A_\infty} \quad (3-2)$$

where A_t is the absorbance at time t , A_0 is the initial absorbance and A_∞ is the absorbance at full conversion.

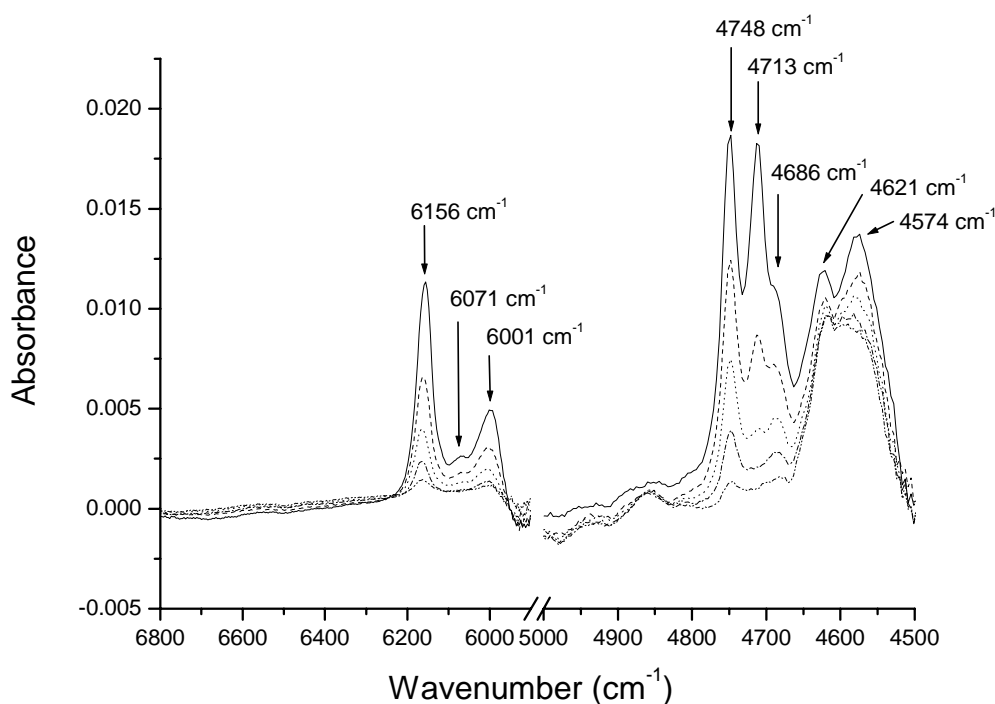


Figure 3-9. Evolution of various NIR vibration overtone bands obtained after solvent subtraction at $t = 0, 7.4$ (---), 14.8 (···), 22.3 (-·-), and 33.3 s (- - -) for the polymerization of DEAAm initiated by $\text{EiBLi}/\text{Et}_3\text{Al}$ in THF at $T = -78\text{ }^\circ\text{C}$ (run E). Experimental conditions: $[\text{DEAAm}]_0 = 45.4\text{ mmol}\cdot\text{L}^{-1}$, $[\text{EiBLi}]_0 = 1.14\text{ mmol}\cdot\text{L}^{-1}$, $[\text{Et}_3\text{Al}]_0 = 19.0\text{ mmol}\cdot\text{L}^{-1}$.

(i) Effect of Monomer Concentration. Four different kinetic runs were carried out using *Pt*BMA-Li living chains as a macroinitiator for the anionic polymerization of DEAAm in the presence of Et₃Al. The effect of the initial monomer concentration on the polymerization kinetics was examined, keeping the other concentrations ($[PtBMA-Li]_0$, $[Et_3Al]_0$) constant. These series of experiments were carried out in the presence of LiCl, the effect of which is a priori considered as negligible in contrast to the strong effect of aluminum alkyl. This assumption is confirmed below. Table 3-3 summarizes the experimental conditions and the kinetic data obtained for the four different experiments. The plots of monomer conversion vs time show a high linearity up to high conversion $X_p \leq 0.9$ (Figure 3-10). At first glance, this suggests an internal zeroth order with respect to $[DEAAm]_0$. Moreover, the slopes in this plot decrease with increasing initial monomer concentration, which can be regarded as a negative reaction order with respect to monomer.

The first-order time-conversion plots show an upward curvature for all runs except for the lowest $[DEAAm]_0$, where $[Et_3Al]_0 \approx [DEAAm]_0$ (Figure 3-10B). The same feature was observed using a *Pt*BA-Li macroinitiator (see Figure 3-28 in the Supporting Information). The number-average molecular weights increase linearly with monomer conversion (Figure 3-11), and the final block copolymers after purification have narrow MWDs. This excludes the hypothesis of a slow initiation, which also would result in a sigmoidal shape of the linear plot of conversion vs time that is not observed.

The observed polymerization rate constants in the final state, $k_{p,exp} = k_{app}^{(2)}/[P^*]_0$, only show a slight decrease when $[DEAAm]_0$ increases, but this is only due the effective active chain end concentration, $[P^*]_0 = f[I]_0$, which varies for each run. Figure 3-12 shows that the rates, when normalized to the effective chain end concentration, $[P^*]_0 = f[I]_0$, are constant within the limits of experimental error. Thus, only the *initial* rates (at higher monomer concentrations) depend on $[DEAAm]_0$.

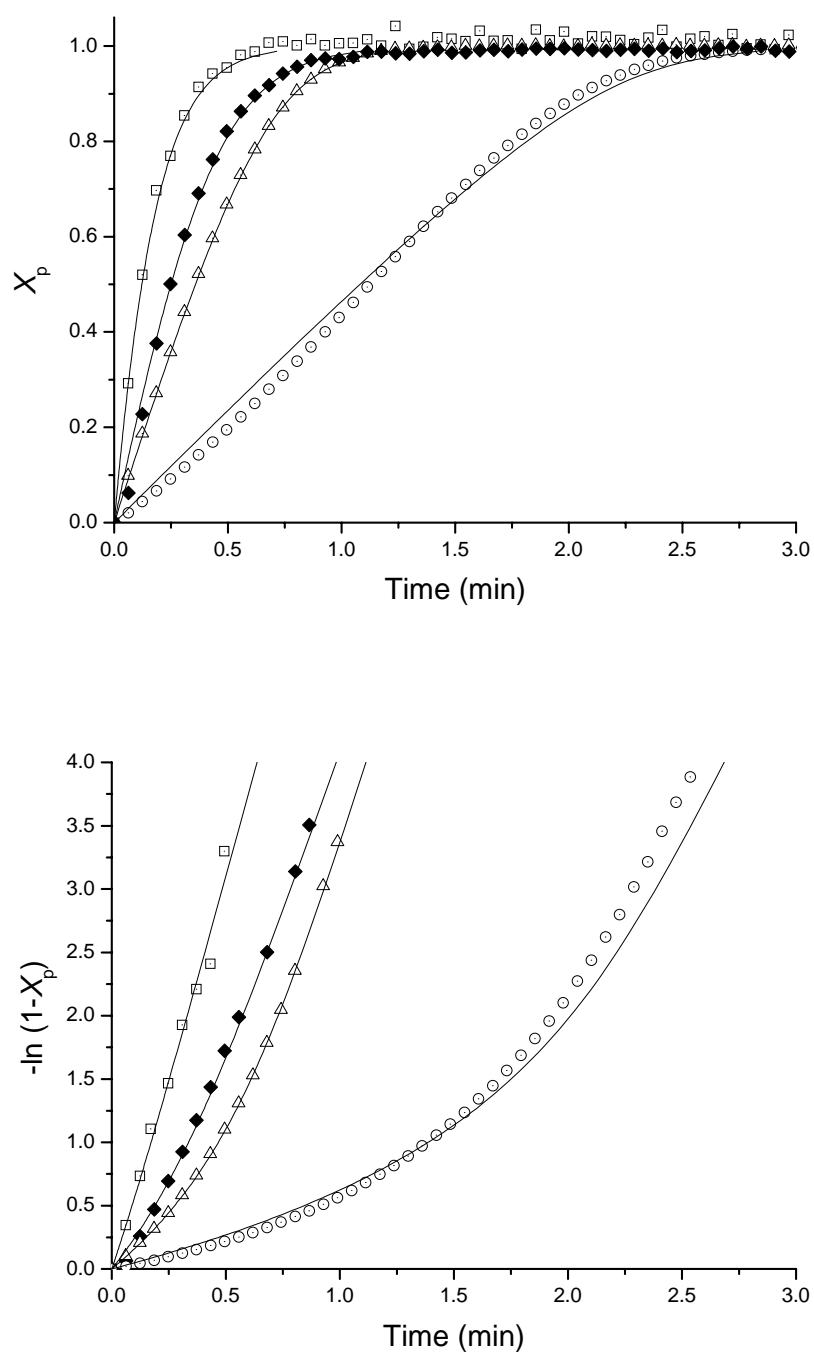


Figure 3-10. Linear (top) and first-order (bottom) time-conversion plots for the anionic polymerization of DEAAm at $-78\text{ }^\circ\text{C}$ with $\text{PrBMA-Li/Et}_3\text{Al}$ in THF using different initial monomer concentrations: $[\text{DEAAm}]_0 = 11.2$ (\square), 44.7 (\blacksquare), 89.9 (\triangle), 202.4 (\circ) $\text{mmol}\cdot\text{L}^{-1}$ (runs J, K, L, and M). For reaction conditions, see Table 3-3. The lines are fits according to the kinetic model outlined below (Scheme 3-6) with $K_M = 10^3$ and $K_{\text{CE}} = 10^2$, $k'_{\pm} = 220$ $\text{L}\cdot\text{mol}^{-1}\cdot\text{s}^{-1}$.

Table 3-3. Experimental conditions and kinetic results of DEAAm polymerization using various initial monomer concentrations in THF at $-78\text{ }^{\circ}\text{C}^{\text{a}}$

run	$[\text{I}]_0^{\text{b}}$ $\text{mmol}\cdot\text{L}^{-1}$	$[\text{M}]_0$ $\text{mmol}\cdot\text{L}^{-1}$	$r =$ $[\text{Et}_3\text{Al}]_0/[\text{I}]_0$	$[\text{M}]_0/$ $[\text{Et}_3\text{Al}]_0$	f^{c}	$[\text{P}^*]_0^{\text{d}}$ $\text{mmol}\cdot\text{L}^{-1}$	$10^2\cdot k_{\text{app}}^{(1)\text{e}}$ s^{-1}	$10^2\cdot k_{\text{app}}^{(2)\text{e}}$ s^{-1}	$k_{\text{p,exp}}^{\text{f}}$ $\text{L}\cdot(\text{mol}\cdot\text{s})^{-1}$
J	1.62	11.2	7.72	0.89	0.70	1.13	11.2	11.2	99.4
K	1.71	44.7	7.31	3.54	0.40	0.68	4.60	7.82	115
L	1.51	89.9	8.34	7.19	0.53	0.80	3.13	7.67	95.9
M	1.38	202	9.13	16.2	0.42	0.58	0.73	5.18	89.3

^a $[\text{Et}_3\text{Al}]_0 = 12.6\text{ mmol}\cdot\text{L}^{-1}$. ^b $[\text{I}]_0 = [\text{PtBMA-Li}]_0$, see Table 3-2. ^c Blocking efficiency, see Table 3-2, $f = (M_{\text{n,theo}} - M_{\text{n,MALDI,prec}})/(M_{\text{n,MALDI}} - M_{\text{n,MALDI,prec}})$. ^d Effective chain end concentration, $[\text{P}^*]_0 = f[\text{I}]_0$. ^e Initial and final slopes of the first-order plots. ^f Observed rate constant at high conversion, $k_{\text{p,exp}} = k_{\text{app}}^{(2)}/[\text{P}^*]_0$.

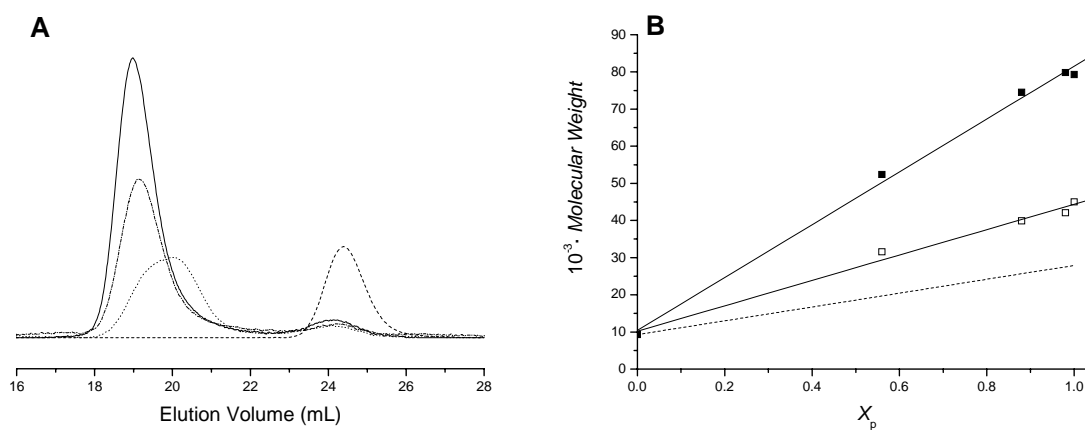


Figure 3-11. (A) SEC traces of the PtBMA precursor (---), and of the crude PtBMA-*b*-PDEAAm at $X_{\text{p}} = 0.56$ (···), 0.88 (-·-), 1.0 (—) (run M) in NMP+LiBr at $70\text{ }^{\circ}\text{C}$. The RI signals are normalized according to the weight of incorporated DEAAm. (B) Dependence of M_{n} (\square) and M_{peak} (\blacksquare) (SEC) on DEAAm conversion for run M using PtBMA-Li as macroinitiator in the presence of Et_3Al and LiCl in THF at $-78\text{ }^{\circ}\text{C}$. For experimental conditions, see Table 3-3. The absolute molecular weights are corrected from the molecular weights obtained with a PS calibration in NMP+LiBr, using Equation 1. The theoretical evolution of the molecular weights is shown as a dotted line.

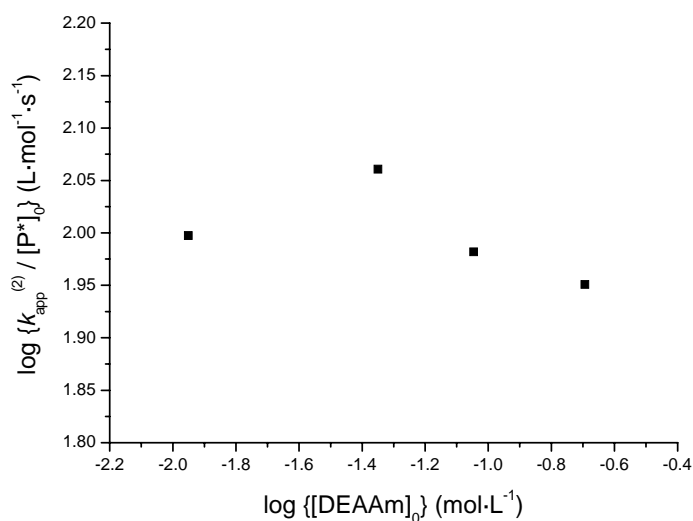


Figure 3-12. Determination of the external reaction order with respect to the initial monomer concentration, $[DEAAm]_0$, for the anionic polymerization of DEAAm with $PtBMA-Li/Et_3Al$ in THF at $-78\text{ }^\circ\text{C}$. The apparent rate constants, $k_{app}^{(2)}$, were determined at high conversion. Slope = $-0.04 \pm 0.05 \approx 0$. Experimental conditions: $[DEAAm]_0 = 11.2\text{--}202\text{ mmol}\cdot\text{L}^{-1}$, $[PtBMA-Li]_0 = 1.38\text{--}1.71\text{ mmol}\cdot\text{L}^{-1}$, $[Et_3Al]_0 = 12.6\text{ mmol}\cdot\text{L}^{-1}$.

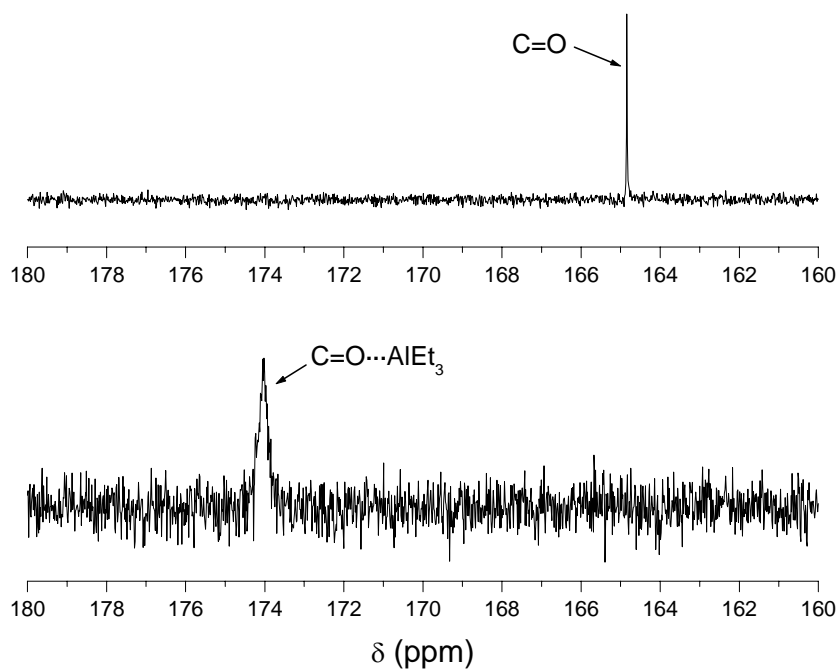


Figure 3-13. ^{13}C NMR spectra of the carbonyl region of DEAAm in the absence (top) and presence of Et_3Al (bottom) in $\text{THF-}d_8$, $[Et_3Al]_0/[DEAAm]_0 \approx 1$.

The observation that an internal zeroth order with respect to the actual monomer concentration $[\text{DEAAM}]_t$ might be explained by the activation of DEAAM by Et_3Al , i.e., mainly activated monomer contributing to propagation and the concentration of *activated* monomer being constant up to high conversion, if Et_3Al is liberated after monomer addition to activate another monomer molecule. The ^{13}C NMR spectra of the carbonyl region of DEAAM are shown in Figure 3-13. In the absence of Et_3Al , the chemical shift of the peak attributed to the DEAAM carbonyl carbon is 164.82 ppm. In $\text{THF-}d_8$, the $\text{Et}_3\text{Al}/\text{DEAAM}$ solution is slightly turbid ($[\text{Et}_3\text{Al}]_0/[\text{DEAAM}]_0 = 1$), and the peak attributed to the carbonyl group is shifted downfield ($\delta = 174.05$ ppm), indicating that the electron density of the carbonyl carbon is lowered due to the coordination to Et_3Al . A similar effect was observed by Aida et al. and by Schlaad et al. for methyl methacrylate (MMA) complexed by bis[triisobutyl(phenoxy)]methylaluminum in dichloromethane⁶³ or trimethyl- and triisobutylaluminum in toluene,⁶⁴ respectively. The slight turbidity as well as the relatively broad shape of the peak may be attributed to the possible initiation of DEAAM by Et_3Al in the absence of an initiator. Indeed, precipitation of polymer was observed at the end of the measurement. Similarly, the slow polymerization of DEAAM in the presence of Et_3B in THF at 25 °C was reported by Kobayashi et al.¹¹ The relatively high concentration used for ^{13}C NMR measurement ($c = 100 \text{ g}\cdot\text{L}^{-1}$) may explain the occurrence of this phenomenon.

However, the assumption that mainly activated monomer is polymerized neither explains the increase of polymerization rates with the conversion nor the apparent negative reaction order of the initial reaction rates with respect to $[\text{DEAAM}]_0$. The experimental results indicate that the apparent rate constants increase constantly during the polymerization, i.e., with decreasing *actual* monomer concentration, $[\text{DEAAM}]_t$. This is shown in Figure 3-14, where the slopes of the first-order time-conversion plots, i.e. that *instantaneous* observed rate constants, $k_{\text{app}}(t)$, normalized to the same chain end concentration, $[\text{P}^*]_0$, are plotted versus the *instantaneous* monomer conversion $[\text{DEAAM}]_t$ at that time (this implies that polymerization kinetics is first-order with respect to the effective concentration of active centers, $[\text{P}^*]_0$, which is shown further below). Identical instantaneous rate constants are observed for $[\text{DEAAM}]_t < [\text{Et}_3\text{Al}]_0$, whereas they decrease at higher concentrations. This observation can be explained by taking into account that the equilibrium between free and activated monomer (Scheme 3-1c) has a DFT-calculated energy gain of ca. $7 \text{ kJ}\cdot\text{mol}^{-1}$, indicating that the equilibrium is not completely shifted to

the right-hand side, but depends on the ratio of monomer to Et_3Al , as shown in Scheme 3-5.

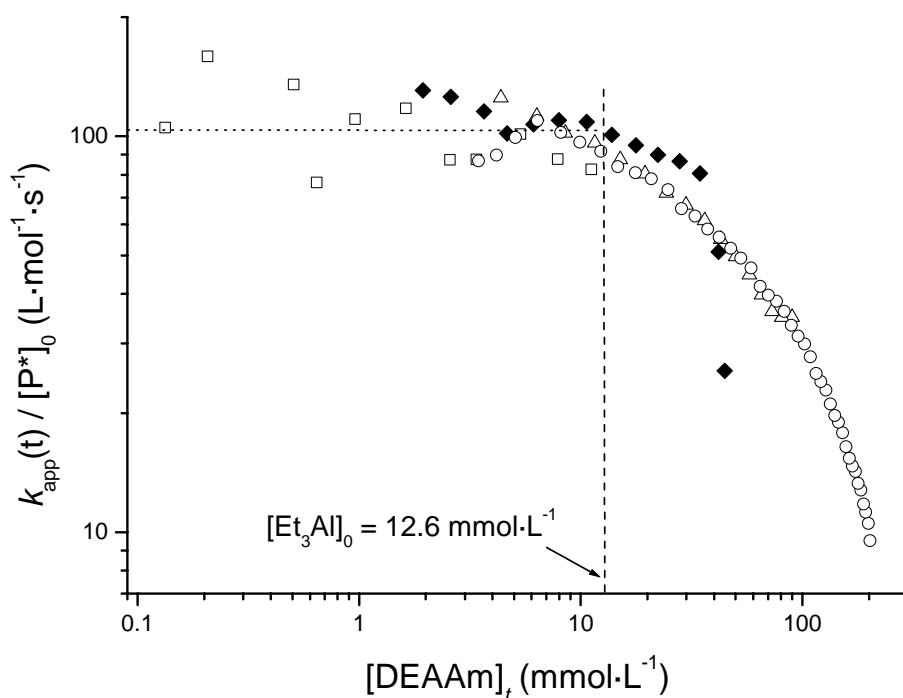
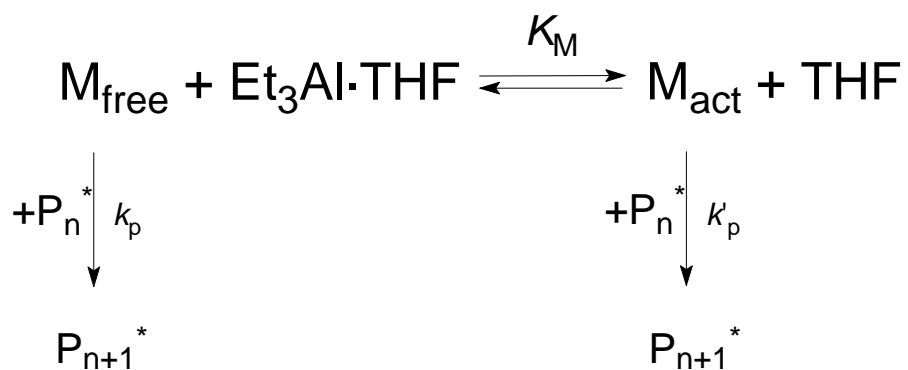


Figure 3-14. Dependence of the instantaneous observed rate constant, $k_{p,\text{exp}} = k_{\text{app}}(t)/[\text{P}^*]_0$, on the actual monomer concentration $[\text{DEAAm}]_t$. Symbols see Figure 3-10; experimental conditions, see Table 3-3.

Scheme 3-5. Equilibrium between free and activated monomer



Because $[\text{THF}] = \text{const}$, we introduce the equilibrium constant $K = K_M/[\text{THF}] = K_M/12.5$ M. Then we can set up the mass action law,

$$K = \frac{[\text{M}]_{\text{act}}}{[\text{M}]_{\text{free}} \cdot [\text{Et}_3\text{Al} \cdot \text{THF}]} \quad (3-3)$$

and define the fraction of activated monomer, $\alpha_M = [\text{M}]_{\text{act}}/[\text{M}]_t$. The solution of the corresponding quadratic equation (for a more detailed discussion, see Supporting Information) renders

$$\alpha_M = \frac{1}{2} \cdot \left(1 + \frac{[\text{Et}_3\text{Al}]_0 + K^{-1}}{[\text{M}]_t} \right) - \sqrt{\left[\frac{1}{4} \cdot \left(\frac{[\text{Et}_3\text{Al}]_0 + K^{-1}}{[\text{M}]_t} \right)^2 - \frac{[\text{Et}_3\text{Al}]_0}{[\text{M}]_t} \right]} \quad (3-4)$$

The limiting relationships are

$$\begin{aligned} [\text{M}]_t \gg [\text{Et}_3\text{Al}]_0 &\Rightarrow \alpha_M \sim [\text{M}]_t^{-1} \\ [\text{M}]_t \ll [\text{Et}_3\text{Al}]_0 &\Rightarrow \alpha_M \sim K \cdot [\text{Et}_3\text{Al}]_0 / (1 + K \cdot [\text{Et}_3\text{Al}]_0) \approx K \cdot [\text{Et}_3\text{Al}]_0 \end{aligned} \quad (3-5)$$

The observed instantaneous rate constant, $k_{p,\text{exp}} = k_{\text{app}}/[\text{P}^*]_0$, can then be seen as composed of those of the activated and the free monomer, k'_p and k_p , respectively:

$$k_{p,\text{exp}} = \alpha_M \cdot k'_p + (1 - \alpha_M) \cdot k_p \quad (3-6)$$

For $k'_p \gg k_p$ and not too small α_M this leads to $k_{p,\text{exp}} \cong \alpha_M \cdot k'_p$, i.e., the observed rate constant, should be directly proportional to α_M .

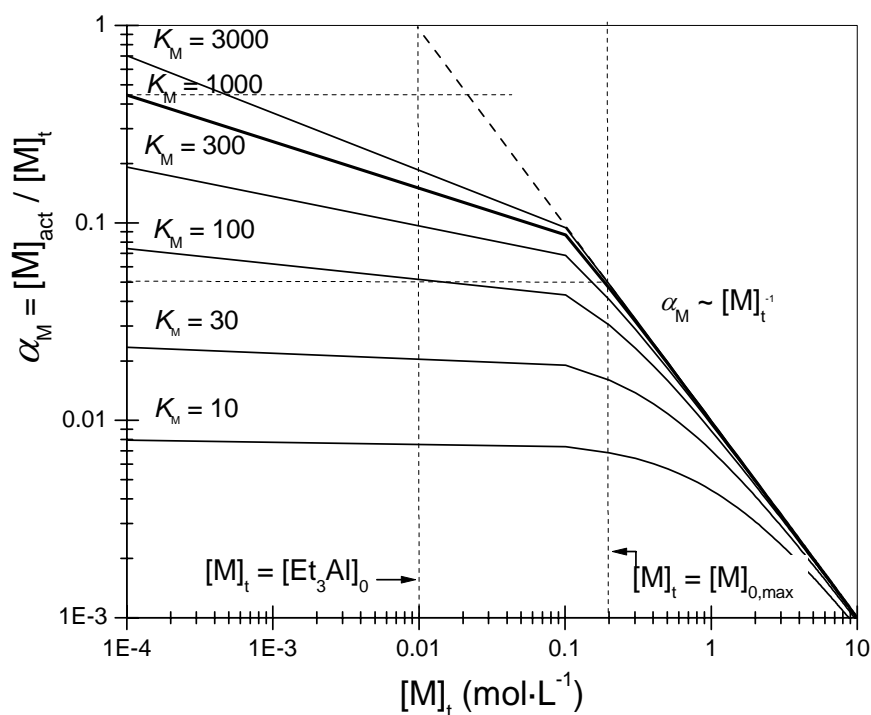


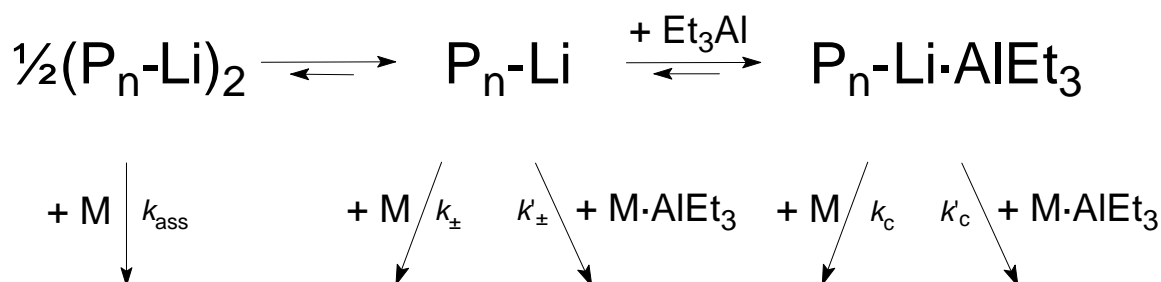
Figure 3-15. Dependence of the fraction of activated monomer on the instantaneous monomer concentration, calculated according to Equation 4 for $[\text{Et}_3\text{Al}]_0 = 10 \text{ mM}$. The dotted vertical lines indicate the maximum monomer concentration used in our experiments and the point, where the monomer concentration is equal to $[\text{Et}_3\text{Al}]_0$, the horizontal dotted lines show that α_M drops from 0.45 to 0.05 for $K_M = 1000$ for the highest initial monomer concentration investigated.

The dependence of the fraction of activated monomer, α_M , is plotted in Figure 3-15 for various values of K . It is seen that α_M increases with decreasing monomer concentration and levels off when the monomer concentration reaches the level of $[\text{Et}_3\text{Al}]_0$. A reasonable fit of the data in Figure 3-14 is obtained for $K_M \cong 10^3$, where both the k_{app} and α_M values at the highest and lowest monomer concentration span 1 order of magnitude. Moreover, a very good fit of the time-conversion plots (Figure 3-10) is observed with this value of equilibrium constant (as will be seen in Part iii, the shape of the time-conversion plot also depends on the equilibrium constant related to the complexation of the chain end, K_{CE}). The observation that a linear first-order time-conversion plot is observed for the lowest-initial-monomer concentration (run J, $[\text{DEAAM}]_0 = 11 \text{ mM} \cong [\text{Et}_3\text{Al}]_0$) can easily be

explained by the fact that, below that, α_M does not change very much any more. For the estimated equilibrium constant, $K_M \cong 10^3$, we can calculate the free energy difference as $\Delta G \cong -11 \text{ kJ}\cdot\text{mol}^{-1}$. Assuming that there is no large entropy change (same number of reagents in educts and products), this coincides quite well with the value of $\Delta E = -7 \text{ kJ}\cdot\text{mol}^{-1}$ calculated by DFT for the reaction of DMAAm with $\text{Et}_3\text{Al}\cdot\text{THF}$ (Scheme 3-1c).

Up to now, our experimental observations are in agreement with a combination of Schemes 3-5 and 3-6, the latter Scheme illustrating the various equilibria the chain end is involved in. In the absence of a Lewis acid, we have a coexistence of associated and free ion pairs, which are believed to be in a slow equilibrium, similar to the case of acrylates and methacrylates in THF;^{65,66} however, according to the DFT calculations the equilibrium is quite shifted towards the free ion pairs. Thus, the main contribution to propagation is related to the rate constant of noncomplexed ion pairs, k_{\pm} . In the presence of the Lewis acid this equilibrium will shift to the right-hand side, and aggregates disappear completely. How much the equilibrium of complexation with Et_3Al is shifted to the right-hand side will be discussed further below (Part iii). Because the complexed chain end is much less reactive than the free one, the main contribution will be related to the rate constant of addition of activated monomer to noncomplexed ion pairs, k'_{\pm} .

Scheme 3-6. Postulated mechanism of DEAAM polymerization in THF with $k_{\pm} \gg k_c \gg k_{\text{ass}}, k'_{\pm} \gg k_{\pm}$, and $k'_c \gg k_c$



(ii) Effect of Initiator Concentration. The initial concentrations of Et_3Al , and DEAAM were maintained constant while varying the initial concentration of EtBLi in THF at $-78 \text{ }^\circ\text{C}$. These series of experiments were carried out in the absence of LiCl . The results are collected in Table 3-4. Linear first-order time-conversion plots are observed in all the

cases (Figure 3-16). Here, the ratio, $[\text{DEAAm}]_0/[\text{Et}_3\text{Al}]_0 = 2.4$ is constant, i.e., the initial monomer concentration is not much higher than $[\text{Et}_3\text{Al}]_0$ and strong deviations from linearity are not expected. Because of the very fast polymerizations obtained using EiBLi as an initiator ($t_{1/2} < 22$ s), withdrawing samples was impossible. Using PtBMA-Li or PtBA-Li as macroinitiator, the observed polymerization rate constant, $k_{p,\text{exp}} = k_{\text{app}}/[\text{P}^*]_0$ is lower than those observed with EiBLi as initiator. This is attributed to the presence of LiCl in the solution for the polymerization of DEAAm initiated by PtB(M)A-Li macroinitiator. Even if LiCl tends to dissociate the aggregates in the polymerization of alkyl methacrylate monomers in THF,⁶⁵ this effect was not observed for DEAAm and DMAAm, where broad MWDs were found even in the absence of Lewis acid.⁶

The bilogarithmic plot in Figure 3-17 indicates that the reaction is first-order with respect to the effective concentration of active centers, $[\text{P}^*]_0 = f[\text{I}]_0$. This is expected, since the initiator concentration does not enter into the equation for α_M .

Table 3-4. Experimental conditions and kinetic results of DEAAm polymerization using various initial initiator concentrations, $[\text{EiBLi}]_0$, in THF at -78 °C^a

run	$[\text{I}]_0^b$ mmol·L ⁻¹	$r =$ $[\text{Et}_3\text{Al}]_0/[\text{I}]_0$	$r^* =$ $[\text{Et}_3\text{Al}]_0/[\text{P}^*]_0$	f^c	$[\text{P}^*]_0^d$ mmol·L ⁻¹	$t_{1/2}$ s	$10^2 \cdot k_{\text{app}}^e$ s ⁻¹	$k_{p,\text{exp}}^f$ L·(mol·s) ⁻¹
C	0.63	29.8	134	0.23	0.14	21.6	3.63	259
E	1.14	16.7	73.1	0.23	0.26	6.6	9.50	365
F	1.69	11.1	22.7	0.49	0.83	3.0	31.6	381

^a Initial monomer concentration, $[\text{DEAAm}]_0 = 44.8\text{--}45.4$ mmol·L⁻¹, $[\text{Et}_3\text{Al}]_0 = 18.8\text{--}19.0$ mmol·L⁻¹, $[\text{DEAAm}]_0/[\text{Et}_3\text{Al}]_0 = 2.4$. ^b Initial initiator concentration, $[\text{I}]_0 = [\text{EiBLi}]_0$. ^c Initiator efficiency. ^d Effective chain end concentration, $[\text{P}^*]_0 = f[\text{I}]_0$. ^e Slope of the first-order plot. ^f Observed rate constant, $k_{p,\text{exp}} = k_{\text{app}}/[\text{P}^*]_0$.

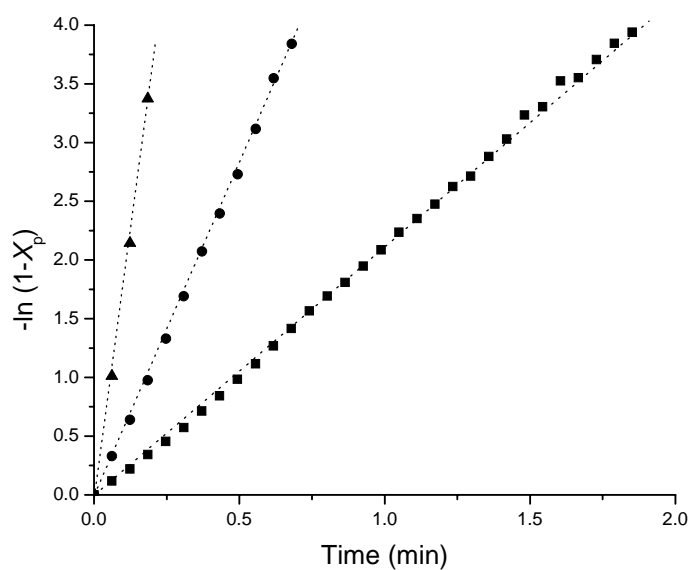


Figure 3-16. First-order time-conversion plots for the anionic polymerization of DEAAm initiated by $\text{EiBLi}/\text{Et}_3\text{Al}$ in THF at $-78\text{ }^\circ\text{C}$ using various initial initiator concentrations: (\blacktriangle) 1.69 , (\bullet) 1.14 , and (\blacksquare) $0.63\text{ mmol}\cdot\text{L}^{-1}$. Reaction conditions, see Table 3-4.

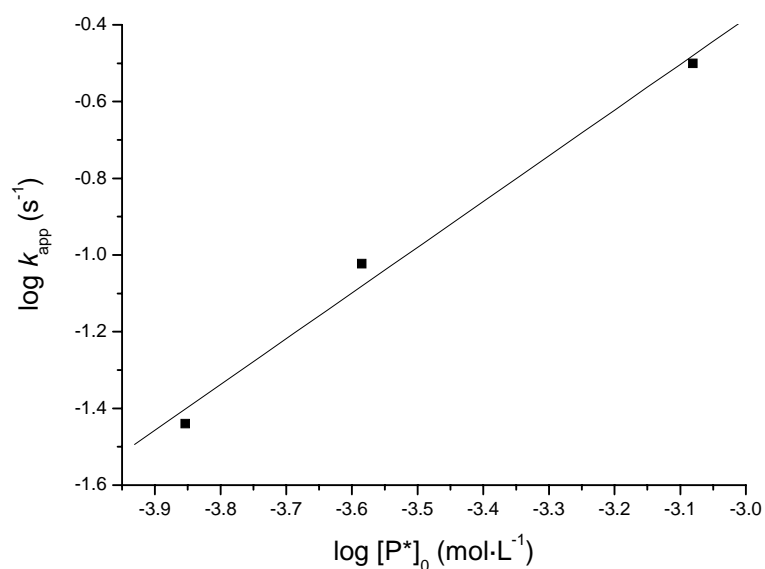


Figure 3-17. Determination of the external reaction order with respect to the effective concentration of active centers, $[\text{P}^*]_0$, for the anionic polymerization of DEAAm with $\text{EiBLi}/\text{Et}_3\text{Al}$ in THF at $-78\text{ }^\circ\text{C}$. Slope = 1.19 ± 0.13 .

(iii) **Effect of Et₃Al Concentration.** In a third series of experiments, the initial concentration of Et₃Al was varied, keeping the other concentrations constant. EiBLi was used as initiator in THF at -78 °C in the absence of LiCl. The results are given in Table 3-5. The first-order time-conversion plots are always linear in the absence or in the presence of Et₃Al except for run B ([Et₃Al]₀ = 4.7 mmol·L⁻¹), where [DEAAM]₀/[Et₃Al]₀ = 9.5 (Figure 3-18). At this ratio, a similar behavior as in Part (i) is expected, whereas, in the other two cases, the ratio [DEAAM]₀/[Et₃Al]₀ < 2.4, similar to the case in Part (ii). In the absence of Et₃Al, a very fast reaction occurs and a broad MWD is observed (Table 3-1, run A). Because association should not be very pronounced, the broad MWD might be explained by the poor solubility of the polymers in THF, leading to a heterogeneous reaction.

Table 3-5. Experimental and kinetic data of DEAAM polymerization using different Et₃Al concentration in THF at -78 °C^a

run	[I] ₀ ^b mmol·L ⁻¹	[Et ₃ Al] ₀ mmol·L ⁻¹	$r =$ [Et ₃ Al] ₀ /[I] ₀	$r^* =$ [Et ₃ Al] ₀ /[P*] ₀	[M] ₀ / [Et ₃ Al] ₀	f^c	[P*] ₀ ^d mmol·L ⁻¹	$t_{1/2}$ s	$10^2 \cdot k_{app}^e$ s ⁻¹	$k_{p,exp}^f$ L·(mol·s) ⁻¹
A	0.87	0	0	0	-	0.41	0.36	1.20	24.6	680
B	0.65	4.7	7.23	21.3	9.51	0.34	0.22	18.6	14.7 ^g (3.28) ^h	670 (150) ⁱ
C	0.63	18.8	29.8	130	2.37	0.23	0.14	21.6	3.63	260
D	0.74	30.8	41.6	160	1.45	0.20	0.15	21.6	2.95	200

^a Initial monomer concentration, [DEAAM]₀ = [M]₀ = 44.1-45.3 mmol·L⁻¹. ^b Initial initiator concentration, [EiBLi]₀ = [I]₀. ^c Initiator efficiency, $f = M_{n,theo}/M_{n,MALDI}$, see Table 3-1. ^d Effective chain end concentration, [P*]₀ = $f[I]_0$. ^e Slope of the first-order plot. ^f Observed rate constant at high conversion, $k_{p,exp} = k_{app}/[P^*]_0$. ^g At high conversion. ^h At low conversion. ⁱ Calculated with the slope at low conversion.

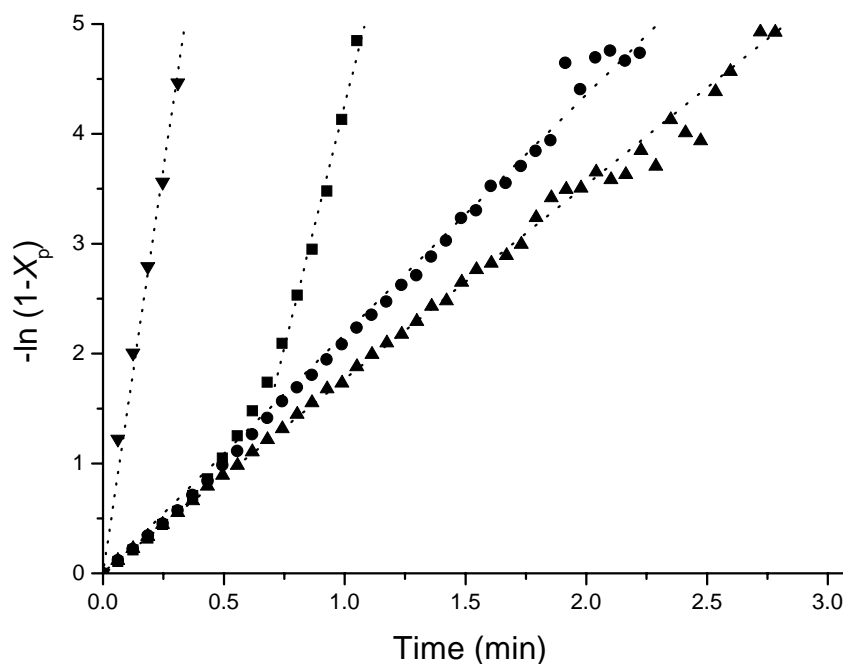


Figure 3-18. First-order time-conversion plots for the anionic polymerization of DEAAm initiated by EtBLi in THF at $-78\text{ }^\circ\text{C}$ using various Et_3Al concentrations, $[\text{Et}_3\text{Al}]_0$: (\blacktriangledown) 0, (\blacksquare) 4.7, (\bullet) 18.8, and (\blacktriangle) 30.8 $\text{mmol} \cdot \text{L}^{-1}$. Reaction conditions: $[\text{DEAAm}]_0 = 44.1\text{--}45.3\text{ mmol} \cdot \text{L}^{-1}$, $[\text{I}]_0 = 0.65\text{--}0.87\text{ mmol} \cdot \text{L}^{-1}$ (runs A, B, C, and D).

Upon addition of Et_3Al , narrow MWDs are observed (Figure 3-1), and the polymerization rates decrease, which is in accordance with previous work on aluminum-esterenolate complexes in toluene that are known to polymerize more slowly than noncoordinated esterenolate.²⁸ The dependence of the polymerization rate constant on $[\text{Et}_3\text{Al}]_0$ was examined. For $[\text{Et}_3\text{Al}]_0/[\text{P}^*]_0 > 5$, the observed rate constants (calculated at high monomer conversion), $k_{\text{p,exp}}$, gradually decrease to ca. 30% of the initial value without Et_3Al with an external order of -0.7 (Figure 3-19).

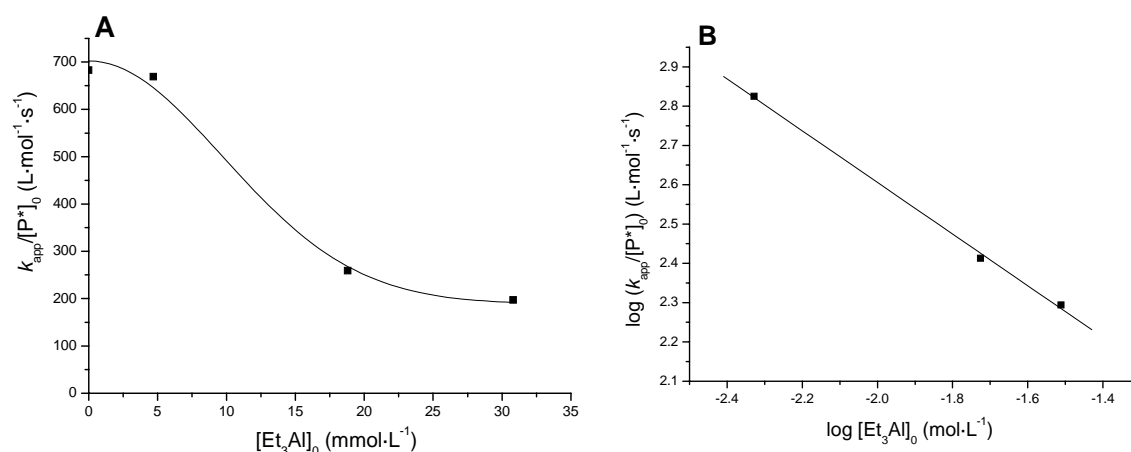


Figure 3-19. (A) Dependence of the observed rate constant (at high conversion), $k_{p,exp} = k_{app}/[P^*]_0$, on $[Et_3Al]_0$. (B) Determination of the external reaction order with respect to the concentration of Et_3Al for the anionic polymerization of DEAAm with EiBLi in THF at -78 °C. Slope = -0.66 ± 0.03 .

However, this observation is in contradiction to the calculations on the fraction of activated monomer (Equations 3-4, 3-5, and 3-6). Equation 3-5 predicts that the concentration of activated monomer increases with increasing $[Et_3Al]_0$ and consequently, the rate should increase, too. Thus, we must now examine how the concentration of complexed (less active) chain ends depends on $[Et_3Al]_0$. Based on Scheme 3-1b (see also the right part of Scheme 3-6), we can calculate the fraction of complexed chain ends, α' , in a similar way as for the fraction of activated monomer (see Supporting Information, Equation 3-15). Unfortunately, the equation is more complex and depends on both equilibrium constants for the activation of monomer, K_M (Scheme 3-5), and deactivation of chain ends, K_{CE} (Scheme 3-6). The fraction of active, noncomplexed species, $1-\alpha'$, is given in Figure 3-20. We see that the dependence is similar to the observation in Figure 3-19, with a slope of -1 in the bilogarithmic plot. Thus, we must conclude that the kinetics of this system is governed by a complex interplay between the activation of monomer and the deactivation of chain ends. At low ratios $r = [Et_3Al]_0/[I]_0$, the effects of monomer activation seem to approximately cancel, whereas at higher r values, the fraction of activated monomer is close to unity and the effect of chain end deactivation prevails.

Thus, at a given set of initial concentrations of monomer, initiator, and Et₃Al, the observed rate constant depends on six parameters (see Scheme 3-6), α_M , α' , k_{\pm} , k'_{\pm} , k_c and k'_c :

$$k_{p,\text{exp}} = [\alpha_M \cdot k'_{\pm} + (1 - \alpha_M) \cdot k_{\pm}] \cdot (1 - \alpha') + [\alpha_M \cdot k'_c + (1 - \alpha_M) \cdot k_c] \cdot \alpha' \quad (3-7a)$$

where both α_M and α' , (and consequently $k_{p,\text{exp}}$) depend on monomer conversion. Even if we neglect the contribution of the deactivated chain ends to propagation (i.e., k_c and $k'_c = 0$), we end up with the four-parameter equation,

$$k_{p,\text{exp}} = [\alpha_M \cdot k'_{\pm} + (1 - \alpha_M) \cdot k_{\pm}] \cdot (1 - \alpha') \quad (3-7b)$$

We tried to fit the various constants to the data in Figure 3-19. However, the number of data points and their accuracy is not high enough to allow for a reasonable fit. More measurements are necessary and will be performed in the future. In addition, even more can be learned from the temperature dependence of the various parameters.

The DFT-calculated energies of complexation range from -9 to -24 kJ·mol⁻¹, depending on the tacticity of the chain end (the implications for tacticity are discussed in a separate publication).⁴⁴ Again, neglecting entropy contributions, this translates into the equilibrium constant, K_{CE} , being in the range from 10^2 to 10^6 . As is seen from Figure 3-20, K_{CE} values are in the range from 10^2 to 10^4 , leading to a significant decrease of the concentration of noncomplexed chain ends, in the range of Et₃Al concentrations investigated. It must be noted, that the calculations in Figure 3-20 are simplified in neglecting the effect of monomer complexation (in fact, the fraction of active chain ends decreases with conversion, see Figures 3-30, Supporting Information) but they may serve for a semiquantitative estimation. The time-conversion plots in Figure 3-10 could, however, be fitted using $K_M = 10^3$ and $K_{CE} = 10^2$, but it should be noted that other sets of equilibrium constants also give a satisfactory fit.

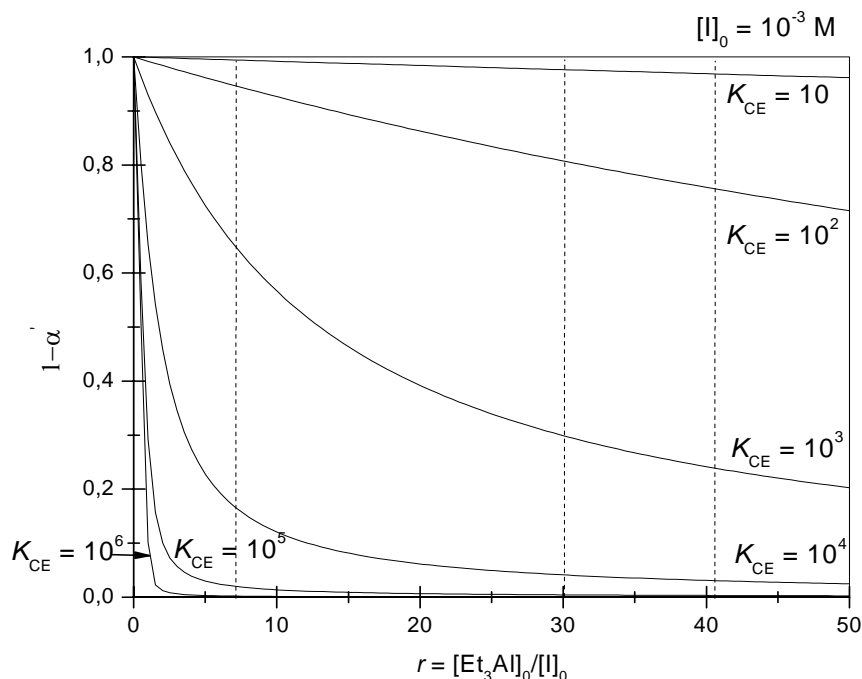


Figure 3-20. Calculated fraction of active (noncomplexed) chain ends, $1-\alpha'$, as a function of the ratio $r = [\text{Et}_3\text{Al}]_0/[\text{I}]_0$ at high monomer conversion ($[\text{M}]_t \ll [\text{Et}_3\text{Al}]_0$). The dotted lines correspond to the experimental ratios.

3.3.3 Tacticity of PDEAAm

Previous studies indicated that the stereostructure of PDMAAm cannot be characterized by the *N*-methyl proton resonance, which shows complex patterns due to the combination of both the tacticity effect and the partially hindered rotation around the amide bond.⁶⁷ ¹³C NMR spectroscopy of the carbonyl carbon gave better results for the assignment of configurations.⁶⁸ This methodology has been used in an efficient way to investigate the stereostructure of poly(*N,N*-dialkylacrylamide)s.^{5,11} It is possible to assign the resonances of isotactic (*mm*, 173.3–173.6 ppm), heterotactic (*mr+rm*, 173.6–174.1 ppm), and syndiotactic triads (*rr*, 174.1–174.5 ppm) of PDEAAm carbonyl carbon signals.⁶ In the absence of an additive, it was reported by Hogen-Esch that the isotactic triad fraction of PDMAAm decreased by decreasing the counterion size from cesium to lithium.⁵ According to McGrath's, Hogen-Esch's, and Kobayashi's results,^{4,6} PDEAAm produced with lithiated initiator in the presence or in the absence of LiCl is rich in isotactic configurations.

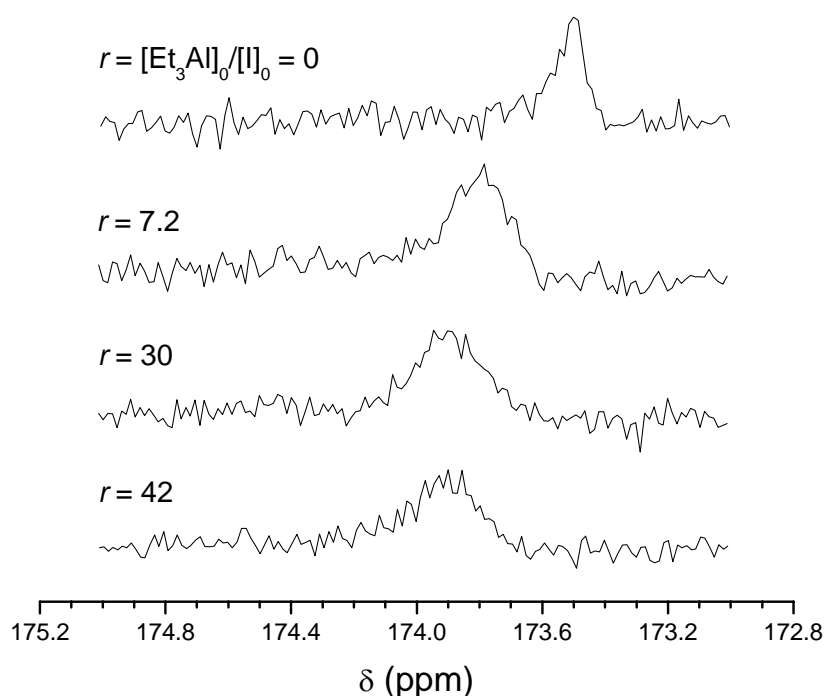


Figure 3-21. ^{13}C NMR spectra of the carbonyl region of the PDEAAs obtained with $\text{EtBLi}/\text{Et}_3\text{Al}$ using various concentrations of Et_3Al . Reaction conditions: $[\text{EtBLi}]_0 = 0.65\text{--}0.87 \text{ mmol}\cdot\text{L}^{-1}$, $[\text{DEAAm}]_0 = 44.1\text{--}45.3 \text{ mmol}\cdot\text{L}^{-1}$ (runs A, B, C, and D).

Figure 3-21 shows the ^{13}C NMR spectra of PDEAAm's produced with EtBLi in the absence and presence of various amount of Et_3Al . The polymers produced with EtBLi in the absence of Et_3Al (run A) exhibit well-resolved carbonyl carbon signals in the region of 173.4-173.6 ppm, which are attributed to isotactic triads. Upon addition of Et_3Al ($r = 7.2$), a broad peak from 173.6 to 174.3 ppm emerges, which is attributed to heterotactic triads. This clearly indicates the influence of the additive on the monomer addition and the formation of the coordinated amidoenolate species. Similarly, Nakhmanovich et al. and Martinez-Castro et al. reported the highly heterotactic content of PDEAAm produced with $\text{DPHLi}/\text{Et}_3\text{Al}$,⁶⁹ and PDMAAm produced with thienyllithium/ Et_3Al , respectively.⁷⁰ An increase of r to 42 results in a slight shift towards the syndiotactic region (Figure 3-21). No change in the tacticity is observed for further addition of Et_3Al . These results are discussed in the light of DFT calculations in a separate publication.⁴⁴

3.4 Conclusions

We have demonstrated that DEAAm could be successfully initiated by monomeric or polymeric lithium esterenolates in the presence of Et₃Al in THF at low temperature. For the synthesis of block copolymers, a poly(*tert* butyl acrylate)-Li or poly(*tert*-butyl methacrylate)-Li can be used as macroinitiator. The blocking efficiencies are rather low and attributed to a self-termination reaction occurring after incorporation of one or two DEAAm units. Kinetic studies, supported by quantum-chemical calculations, indicate a complicated mechanism involving equilibria between noncoordinated and Al-coordinated chain ends as well as between free and Et₃Al-activated monomer. The observed kinetics of this system is governed by a complex interplay between the activation of monomer (dependent on monomer and Et₃Al concentrations) and the deactivation of chain ends (dependent on the ratio of concentrations of Et₃Al to initiator). Well-defined polymers rich in heterotactic (*mr+rm*) triads were synthesized, and they exhibit a cloud point in water at ca. 31 °C. Consequently, the poly[(meth)acrylic acid]-*block*-PDEAAm copolymers obtained after hydrolysis of the poly[*tert*-butyl(meth)acrylate] block, are promising pH- and thermo-responsive materials for various applications related to biotechnology and stabilization of dispersions.⁵⁷

Acknowledgement. This work was supported by the European Union within MC RTN POLYAMPHI and by DFG within the ESF EUROCORES Programme SONS. We would like to express our gratitude to the reviewers for their constructive criticism on the mechanism we proposed in the first version of this manuscript. This helped to considerably improve the mechanism and make it self-consistent. We thank Sabine Wunder (SEC), Cornelia Rettig, Kerstin Matussek, Manuela Schumacher, and Denise Danz (MALDI) for their help. X. A. acknowledges financial support by the French Research Ministry, and the French-Bavarian University Center. Kh. B. acknowledges an 'Erasmus-Socrates' exchange grant from the European Union. Michael Lanzendörfer[†] is gratefully acknowledged for fruitful discussions.

Supporting Information Available: Tables with results of *t*BA and *t*BMA polymerization with DPHLi/LiCl, SEC traces and MALDI-TOF mass spectra of the poly[*tert*-butyl

(meth)acrylate] precursors, and of the poly(*N,N*-diethylacrylamide)s synthesized using diphenylhexyl-Li/Et₃Al. Linear and first-order time-conversion plots for the polymerization of DEAAm initiated by a poly(*tert*-butyl acrylate)-Li macroinitiator; calculation of the fraction of activated monomer and complexed chain ends (11 pages). This material is available free of charge via the Internet at <http://pubs.acs.org>.

3.5 References

- (1) Park, T. G.; Hoffman, A. S. *Journal of Applied Polymer Science* **1992**, *46*, 659-671.
- (2) Liu, H. Y.; Zhu, X. X. *Polymer* **1999**, *40*, 6985-6990.
- (3) Butler, K.; Thomas, P. R.; Tyler, G. J. *Journal of Polymer Science* **1960**, *48*, 357-366.
- (4) Huang, S. S.; McGrath, J. E. *Journal of Applied Polymer Science* **1981**, *26*, 2827-2839.
- (5) Xie, X.; Hogen-Esch, T. E. *Macromolecules* **1996**, *29*, 1746-1752.
- (6) Kobayashi, M.; Okuyama, S.; Ishizone, T.; Nakahama, S. *Macromolecules* **1999**, *32*, 6466-6477.
- (7) Nakhmanovich, B. I.; Urman, Y. G.; Arest-Yakubovich, A. A. *Macromol. Chem. Phys.* **2001**, *202*, 1327-1330.
- (8) Freitag, R.; Baltes, T.; Eggert, M. *Journal of Polymer Science, Part A: Polymer Chemistry* **1994**, *32*, 3019-3030.
- (9) Eggert, M.; Freitag, R. *Journal of Polymer Science, Part A: Polymer Chemistry* **1994**, *32*, 803-813.
- (10) Kobayashi, M.; Ishizone, T.; Nakahama, S. *Journal of Polymer Science, Part A: Polymer Chemistry* **2000**, *38*, 4677-4685.
- (11) Kobayashi, M.; Ishizone, T.; Nakahama, S. *Macromolecules* **2000**, *33*, 4411-4416.
- (12) Ishizone, T.; Yoshimura, K.; Hirao, A.; Nakahama, S. *Macromolecules* **1998**, *31*, 8706-8712.
- (13) Ishizone, T.; Yoshimura, K.; Yanase, E.; Nakahama, S. *Macromolecules* **1999**, *32*, 955-957.
- (14) Kitayama, T.; Katsukawa, K.-i. *Polymer Bulletin (Berlin)* **2004**, *52*, 117-124.
- (15) Ute, K.; Nishimura, T.; Hatada, K. *Polymer Journal (Tokyo, Japan)* **1989**, *21*, 1027-1041.
- (16) Haddleton, D. M.; Muir, A. V. G.; O'Donnell, J. P.; Richards, S. N.; Twose, D. L. *Macromolecular Symposia* **1995**, *91*, 93-105.
- (17) Uchiumi, N.; Hamada, K.; Kato, M.; Ono, T.; Yaginuma, S.; Ishiura, K. *EP 945470* **1999**, Kuraray Co., Ltd., Japan.
- (18) Ballard, D. G. H.; Bowles, R. J.; Haddleton, D. M.; Richards, S. N.; Sellens, R.; Twose, D. L. *Macromolecules* **1992**, *25*, 5907-5913.
- (19) Hirano, T.; Kitayama, T.; Cao, J.; Hatada, K. *Polymer Journal (Tokyo)* **2000**, *32*, 961-969.
- (20) Kitayama, T.; Tabuchi, M.; Hatada, K. *Polymer Journal (Tokyo)* **2000**, *32*, 796-802.
- (21) Hamada, K.; Shachi, K.; Ono, T.; Ishiura, K.; Takahashi, A. *JP 2002088109* **2002**, Kuraray Co., Ltd., Japan.
- (22) Schlaad, H.; Schmitt, B.; Müller, A. H. E.; Jüngling, S.; Weiss, H. *Macromolecules* **1998**, *31*, 573-577.
- (23) Schmitt, B.; Schlaad, H.; Müller, A. H. E. *Macromolecules* **1998**, *31*, 1705-1709.
- (24) Schmitt, B.; Schlaad, H.; Müller, A. H. E.; Mathiasch, B.; Steiger, S.; Weiss, H. *Macromolecules* **2000**, *33*, 2887-2893.
- (25) Baskaran, D.; Müller, A. H. E.; Sivaram, S. *Macromolecular Chemistry and Physics* **2000**, *201*, 1901-1911.
- (26) Marchal, J.; Gnanou, Y.; Fontanille, M. *Makromol. Chem., Macromol. Symp.* **1996**, *107*, 27.

- (27) Anderson, B. C.; Andrews, G. D.; Arthur Jr., P.; Jacobson, H. W.; Melby, L. R.; Playtis, A. J.; Sharkey, W. H. *Macromolecules* **1981**, *14*, 1599.
- (28) Schlaad, H.; Müller, A. H. E. *Macromolecules* **1998**, *31*, 7127-7132.
- (29) Ihara, E.; Ikeda, J.-i.; Inoue, K. *Macromolecules* **2002**, *35*, 4223-4225.
- (30) Ihara, E.; Ikeda, J.; Itoh, T.; Inoue, K. *Macromolecules* **2004**, *37*, 4048-4054.
- (31) Ishizone, T.; Ito, M. *Journal of Polymer Science, Part A: Polymer Chemistry* **2002**, *40*, 4328-4332.
- (32) Kitayama, T.; Shibuya, W.; Katsukawa, K.-I. *Polymer Journal (Tokyo, Japan)* **2002**, *34*, 405-409.
- (33) Donovan, M. S.; Sanford, T. A.; Lowe, A. B.; Sumerlin, B. S.; Mitsukami, Y.; McCormick, C. L. *Macromolecules* **2002**, *35*, 4570-4572.
- (34) Donovan, M. S.; Lowe, A. B.; Sumerlin, B. S.; McCormick, C. L. *Macromolecules* **2002**, *35*, 4123-4132.
- (35) Schilli, C.; Lanzendörfer, M. G.; Müller, A. H. E. *Macromolecules* **2002**, *35*, 6819-6827.
- (36) Teodorescu, M.; Matyjaszewski, K. *Macromolecules* **1999**, *32*, 4826-4831.
- (37) Kizhakkedathu, J. N.; Kumar, K. R.; Goodman, D.; Brooks, D. E. *Polymer* **2004**, *45*, 7471-7489.
- (38) Schierholz, K.; Givehchi, M.; Fabre, P.; Nallet, F.; Papon, E.; Guerret, O.; Gnanou, Y. *Macromolecules* **2003**, *36*, 5995-5999.
- (39) Diaz, T.; Fischer, A.; Jonquieres, A.; Brembilla, A.; Lochon, P. *Macromolecules* **2003**, *36*, 2235-2241.
- (40) Ray, B.; Isobe, Y.; Morioka, K.; Habaue, S.; Okamoto, Y.; Kamigaito, M.; Sawamoto, M. *Macromolecules* **2003**, *36*, 543-545.
- (41) Ray, B.; Isobe, Y.; Matsumoto, K.; Habaue, S.; Okamoto, Y.; Kamigaito, M.; Sawamoto, M. *Macromolecules* **2004**, *37*, 1702-1710.
- (42) Lutz, J.-F.; Neugebauer, D.; Matyjaszewski, K. *Journal of the American Chemical Society* **2003**, *125*, 6986-6993.
- (43) André, X.; Benmohamed, K.; Yakimansky, A. V.; Müller, A. H. E. *Proceedings, 40th IUPAC International Symposium on Macromolecules*: Paris, France, 2004.
- (44) Yakimansky, A. V.; Müller, A. H. E. *Macromolecules* **2005**, *in preparation*.
- (45) Weiss, H.; Yakimanski, A. V.; Müller, A. H. E. *Journal of the American Chemical Society* **1996**, *118*, 8897-8903.
- (46) Lochmann, L.; Lim, D. *Journal of Organometallic Chemistry* **1973**, *50*, 9-16.
- (47) Long, T. E.; Liu, H. Y.; Schell, B. A.; Teegarden, D. M.; Uerz, D. S. *Macromolecules* **1993**, *26*, 6237-6242.
- (48) Schmitt, B.; Stauf, W.; Müller, A. H. E. *Macromolecules* **2001**, *34*, 1551-1557.
- (49) Schlaad, H.; Müller, A. H. E. *Macromolecular Symposia* **1996**, *107*, 163-176.
- (50) Yang, H. J.; Cole, C.-A.; Monji, N.; Hoffman, A. S. *J. Polym. Sci., Part A: Polym. Chem.* **1990**, *28*, 219-226.
- (51) Ganachaud, F.; Monteiro, M. J.; Gilbert, R. G.; Dourges, M.-A.; Thang, S. H.; Rizzardo, E. *Macromolecules* **2000**, *33*, 6738-6745.
- (52) Schilli, C.; Lanzendoerfer, M. G.; Mueller, A. H. E. *Macromolecules* **2002**, *35*, 6819-6827.
- (53) Da, J.; Hogen-Esch, T. E. *Journal of Polymer Science, Part A: Polymer Chemistry* **2003**, *42*, 360-373.
- (54) Montaudo, G.; Montaudo, M. S.; Samperi, F. *Mass Spectrometry of Polymers*; CRC Press: Boca Raton, London, New York, Washington D.C., 2002.
- (55) Litvinenko, G. I.; André, X.; Müller, A. H. E. *in Preparation* **2005**.

- (56) Fayt, R.; Forte, R.; Jacobs, C.; Jérôme, R.; Ouhadi, T.; Teyssie, P.; Varshney, S. K. *Macromolecules* **1987**, *20*, 1442-1444.
- (57) André, X.; Zhang, M.; Müller, A. H. E. *Macromolecular Rapid Communications* **2005**, *26*, 558-563.
- (58) Kunkel, D. *Ph. D. Thesis*; Johannes-Gutenberg Universität: Mainz, 1992.
- (59) Schmitt, B.; Müller, A. H. E. *Macromolecules* **2001**, *34*, 2115-2120.
- (60) Janata, M.; Lochmann, L.; Mueller, A. H. E. *Makromolekulare Chemie* **1990**, *191*, 2253-2260.
- (61) Janata, M.; Lochmann, L.; Vlcek, P.; Dybal, J.; Müller, A. H. E. *Makromolekulare Chemie* **1992**, *193*, 101-112.
- (62) Zagala, A. P.; Dimov, D.; Hogen-Esch, T. E. *Macromolecular Symposia* **1998**, *132*, 309-336.
- (63) Aida, T.; Kuroki, M.; Sugimoto, H.; Watanabe, T.; Adachi, T.; Kawamura, C.; Inoue, S. *Makromolekulare Chemie, Macromolecular Symposia* **1993**, *67*, 125-135.
- (64) Schlaad, H.; Müller, A. H. E. *Macromolecular Symposia* **1995**, *95*, 13-26.
- (65) Kunkel, D.; Müller, A. H. E.; Janata, M.; Lochmann, L. *Makromolekulare Chemie, Macromolecular Symposia* **1992**, *60*, 315-326.
- (66) Kunkel, D.; Müller, A. H. E.; Janata, M.; Lochmann, L. *Polym. Prepr. (Am. Chem. Soc., Div. Polym. Chem.)* **1991**, *32*, 301-302.
- (67) Gia, H.; McGrath, J. E. *Polym. Bull.* **1980**, *2*, 837-840.
- (68) Huang, S. S.; McGrath, J. E. *Polymer Preprints (American Chemical Society, Division of Polymer Chemistry)* **1983**, *24*, 138-140.
- (69) Nakhmanovich, B. I.; Urman, Y. G.; Krystal'nyi, E. V.; Arest-Yakubovich, A. A. *Vysokomolekulyarnye Soedineniya, Seriya A i Seriya B* **2003**, *45*, 978-981.
- (70) Martinez-Castro, N.; Zhang, M.; Pergushov, D. V.; Müller, A. H. E. *Designed Monomers and Polymers, accepted*.

3.6 Supporting Information

Table 3-6. Polymerization of *tert*-butyl acrylate (*t*BA) and *tert*-butyl methacrylate, (*t*BMA) using DPHLi / LiCl as initiating agent in THF^a

Monomer	Temp,	[DPHLi] ₀	[<i>t</i> B(M)A] ₀	Time ^b	10 ³ ·	10 ³ · <i>M</i> _{n,exp} ^d	<i>M</i> _w / <i>M</i> _n ^d	10 ³ · <i>M</i> _{n,exp} ^e	<i>f</i> ^f
Run	°C	mmol·L ⁻¹	mmol·L ⁻¹	min	<i>M</i> _{n,theo} ^c	SEC	SEC	MALDI	
<i>t</i> BA-G	-78	1.77	88.1	1.2	6.6	10.0	1.10	6.0	1.10
<i>t</i> BA-H	-78	2.35	94.0	1.3	5.4	6.4	1.18	4.0	1.35
<i>t</i> BA-I	-78	0.56	23.0	1.0	5.5	7.8	1.10	5.6	0.98
<i>t</i> BMA-J	-30	1.74	86.44	13.8	7.3	6.9	1.04	7.9	0.93
<i>t</i> BMA-K	-30	1.74	86.49	16.3	7.3	6.5	1.05	7.5	0.98
<i>t</i> BMA-L	-30	1.75	86.95	12.9	7.3	7.6	1.05	8.5	0.86
<i>t</i> BMA-M	-30	1.75	87.05	19.5	7.3	8.5	1.04	9.3	0.79

^a [LiCl]/[DPHLi]₀ = 7.1-15.9. ^b Time at complete monomer conversion, *X*_p = 1. ^c *M*_{n,theo} = *X*_p · *M*_{*t*B(M)A} · [*t*B(M)A]₀ / [DPHLi]₀ + *M*_{initiator}. ^d PtBMA calibration in THF at +40 °C. ^e Linear mode. ^f Initiator efficiency, *f* = *M*_{n,theo} / *M*_{n,MALDI}.

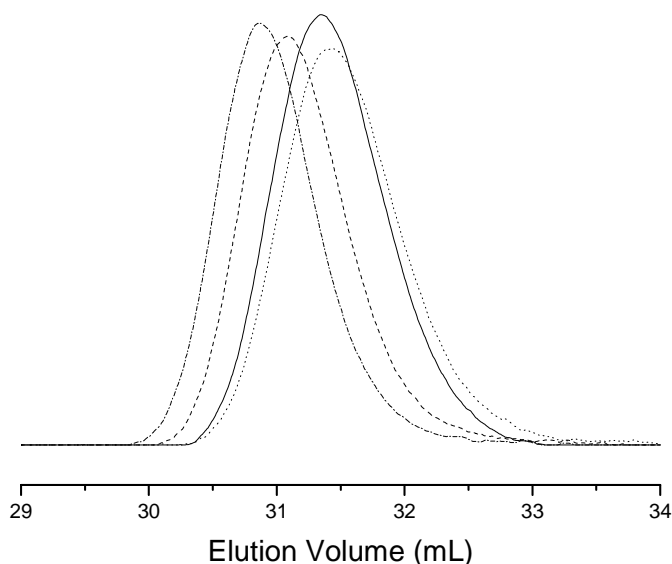


Figure 3-22. SEC traces of the PtBMA precursors obtained via the anionic polymerization of *t*BMA with DPHLi/LiCl at -30 °C in THF: run J (—), run K (---), run L (---), run M (···). Reaction conditions: [DPHLi]₀ = 0.5–1.8 mmol·L⁻¹, [*t*BMA]₀ = 25.6–87.1 mmol·L⁻¹, [LiCl]/[DPHLi]₀ = 10.5.

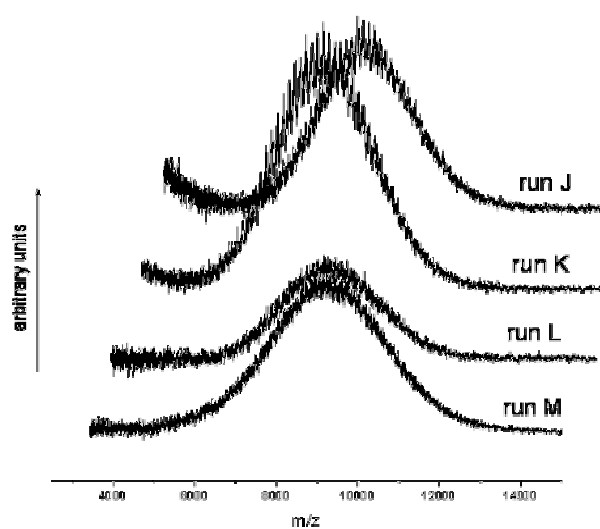


Figure 3-23. MALDI-TOF mass spectra of the *PtBMA* precursors obtained via the anionic polymerization of *tBMA* with DPHLi/LiCl at $-30\text{ }^{\circ}\text{C}$ in THF (see Table 3-1). Reaction conditions: $[\text{DPHLi}]_0 = 0.5\text{--}1.8\text{ mmol}\cdot\text{L}^{-1}$, $[\text{tBMA}]_0 = 25.6\text{--}87.1\text{ mmol}\cdot\text{L}^{-1}$, $[\text{LiCl}]/[\text{DPHLi}]_0 = 10.5$.

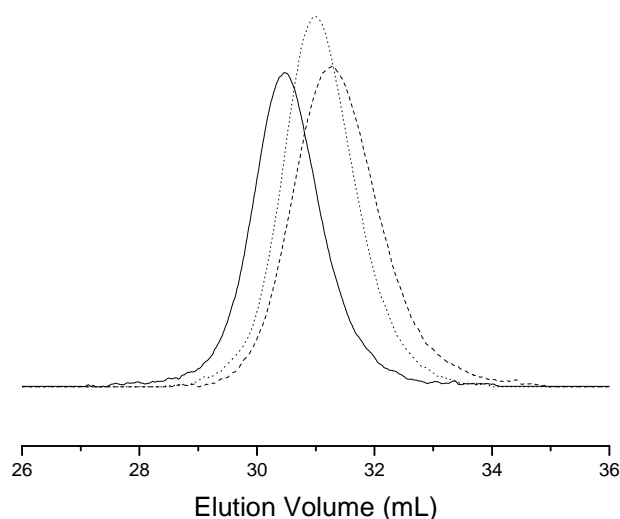


Figure 3-24. SEC traces of the *PtBA* precursors obtained via the anionic polymerization of *tBA* with DPHLi/LiCl at $-78\text{ }^{\circ}\text{C}$ in THF: run G (—), H (---), and I (···). Reaction conditions: $[\text{DPHLi}]_0 = 0.6\text{--}2.4\text{ mmol}\cdot\text{L}^{-1}$, $[\text{tBA}]_0 = 23.0\text{--}94.0\text{ mmol}\cdot\text{L}^{-1}$, $[\text{LiCl}]/[\text{DPHLi}]_0 = 7.4\text{--}15.9$.

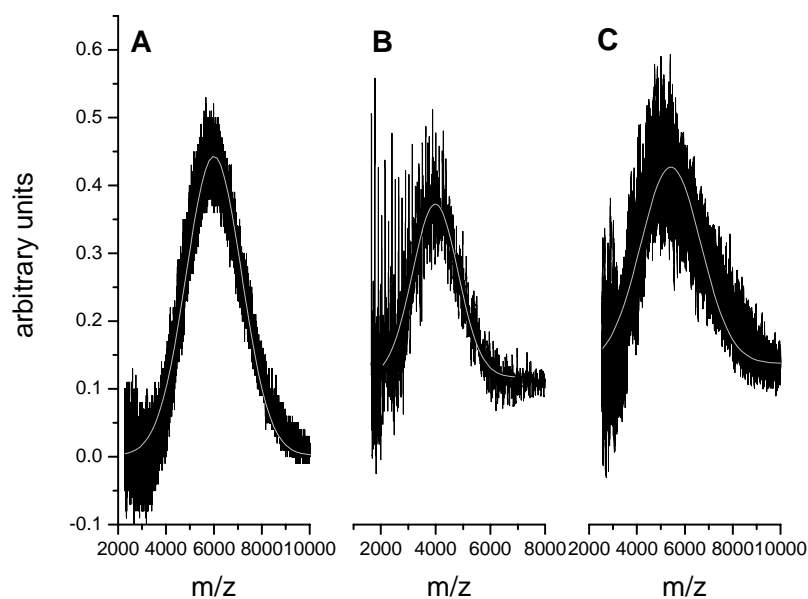


Figure 3-25. MALDI-TOF mass spectra of the PtBA precursors obtained via the anionic polymerization of *t*BA with DPHLi/LiCl at $-78\text{ }^{\circ}\text{C}$ in THF: run G, H, and I. Reaction conditions: $[\text{DPHLi}]_0 = 0.6\text{--}2.4\text{ mmol}\cdot\text{L}^{-1}$, $[\text{tBA}]_0 = 23.0\text{--}94.0\text{ mmol}\cdot\text{L}^{-1}$, $[\text{LiCl}]/[\text{DPHLi}]_0 = 7.4\text{--}15.9$. The solid grey lines represent a Gaussian fit of the data points.

Table 3-7. Anionic polymerization of DEAAm initiated by diphenylhexyllithium (DPHLi) in the presence of Et_3Al in THF at $-78\text{ }^{\circ}\text{C}$ ^{a,b}

run	$M_{n,\text{theo}}^c$	$M_{n,\text{SEC}}^d$	M_w/M_n^d	$M_{n,\text{MALDI}}^e$	f^f
N	9200	8790	1.19	12000	0.77
O	10000	9030	1.19	11800	0.85
P	9500	10180	1.15	14700	0.65
Q ^g	4800 ^h	45400 ⁱ	2.34	-	-
R ^g	4500 ^j	67800 ⁱ	1.71	-	-

^a Complete monomer conversion in all cases, $X_p = 1$. ^b $[\text{DPHLi}]_0 = 1.80\text{--}2.06\text{ mmol}\cdot\text{L}^{-1}$, $[\text{DEAAm}]_0 = 140\text{--}150\text{ mmol}\cdot\text{L}^{-1}$, $[\text{Et}_3\text{Al}]_0/[\text{DPHLi}]_0 = 6.20\text{--}12.8$, ^c $M_{n,\text{theo}} = M_{\text{DEAAm}} \cdot X_p \cdot [\text{DEAAm}]_0/[\text{Initiator}]_0 + MW_{\text{initiator}}$. ^d SEC in NMP + LiBr ($T = 70\text{ }^{\circ}\text{C}$) as eluent and calibrated with linear PS standards. ^e Linear mode. ^f Initiator efficiency, $f = M_{n,\text{theo}}/M_{n,\text{MALDI}}$. ^g At $0\text{ }^{\circ}\text{C}$. ^h $X_p = 0.98$. ⁱ SEC in THF + 0.25 wt.-% tetrabutylammonium bromide as eluent and calibrated with linear PS standards. ^j $X_p = 0.88$.

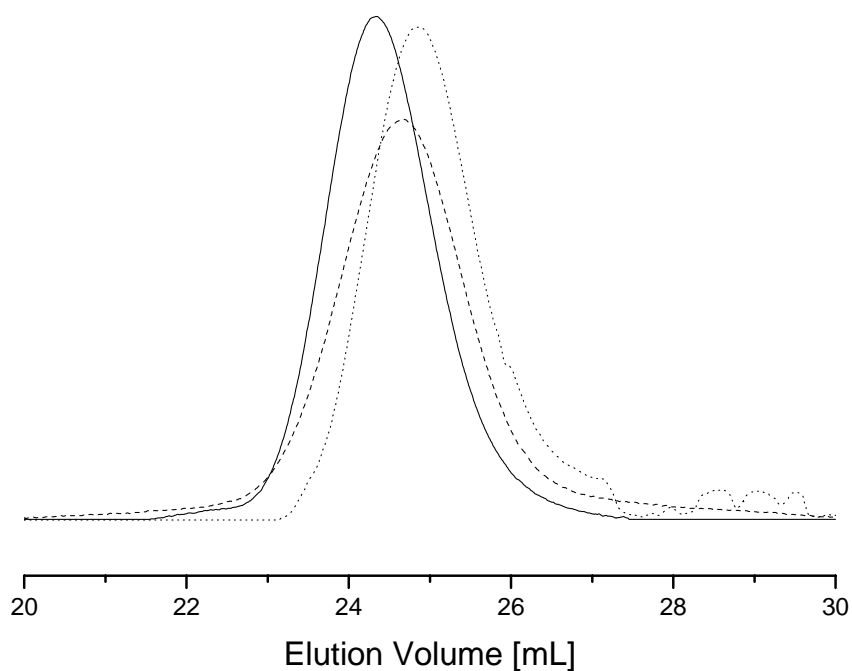


Figure 3-26. SEC traces of the PDEAAm synthesized by DPHLi/Et₃Al in THF at -78 °C. (---) Run N, (—) run P, and (...) run O measured in NMP+LiBr at 70 °C. Experimental conditions: [DEAAm]₀ = 144-150 mmol·L⁻¹, [DPHLi]₀ = 2.0-2.1 mmol·L⁻¹, [Et₃Al]₀ = 13.0-26.9 mmol·L⁻¹.

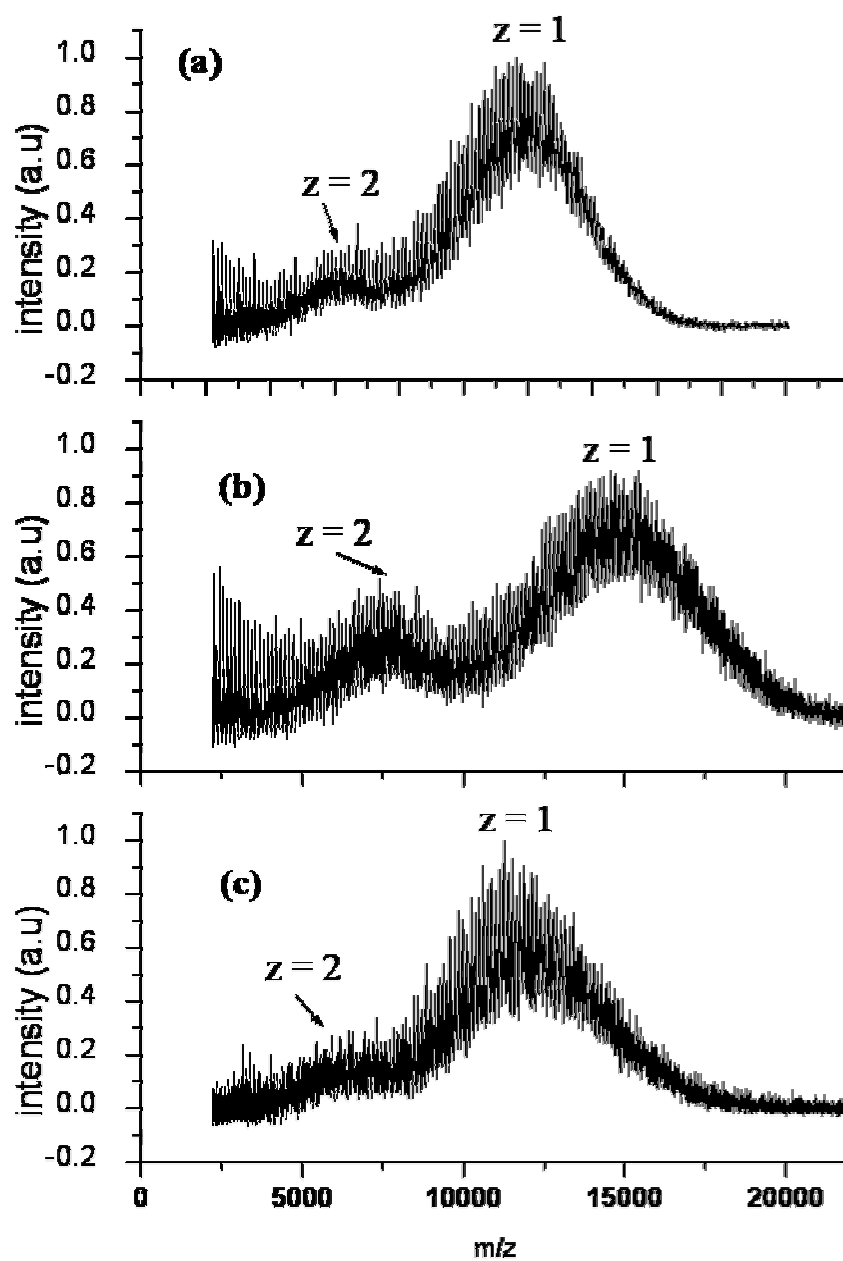


Figure 3-27. MALDI-TOF mass spectra of the PDEAAm synthesized by DPHLi/Et₃Al in THF at -78 °C. (a) run N, (b) run P, and (c) run O. Experimental conditions: [DEAAm]₀ = 144-150 mmol·L⁻¹, [DPHLi]₀ = 2.0-2.1 mmol·L⁻¹, [Et₃Al]₀ = 13.0-26.9 mmol·L⁻¹.

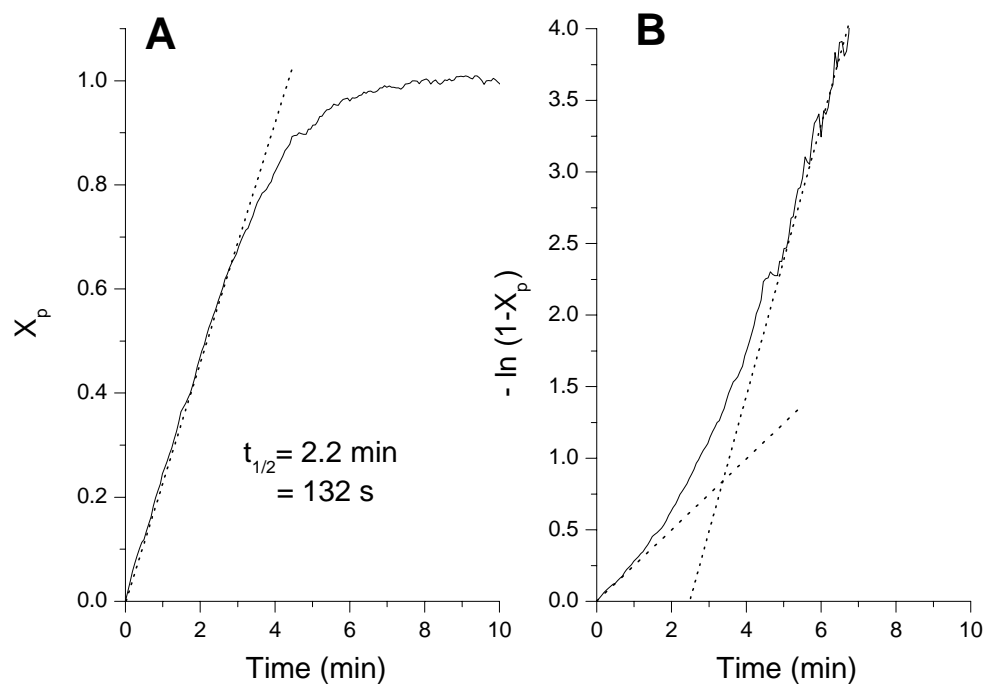


Figure 3-28. (A) Linear and (B) first-order time-conversion plots for the polymerization of DEAAm initiated by *Pt*BA-Li macroinitiator in THF at $-78 \text{ }^\circ\text{C}$ (run G, see Table 3-1). Experimental conditions: $[\text{DEAAm}]_0 = 94.0 \text{ mmol}\cdot\text{L}^{-1}$, $[\text{PtBA-Li}]_0 = 1.80 \text{ mmol}\cdot\text{L}^{-1}$, $[\text{Et}_3\text{Al}]_0 = 12.9 \text{ mmol}\cdot\text{L}^{-1}$.

Calculation of the effect of coordination of Et₃Al to monomer and chain ends on the kinetics of DEAAm polymerization

In order to make the equations in this derivation more easily readable, we use abbreviations for the various concentrations given in Scheme 3-7. Here, X denotes the adduct Et₃Al·THF, P_n and P'_n stand for an active and a deactivated (Et₃Al adduct) polymer chain, respectively, with n monomer units, M_{free} and M_{act} are free and activated (Et₃Al adduct) monomer, respectively.

Scheme 3-7

Reaction	Equilibrium constants	Modified constants
$X + P_n \xrightleftharpoons{K_{CE}} P'_n + \text{THF}$ <p>(Scheme 3-1b)</p>	$K_{CE} = \frac{P'_n \cdot \text{THF}}{X \cdot P_n}$	$K_1 = \frac{K_{CE}}{\text{THF}} = \frac{P'_n}{X \cdot P_n}$
$X + M_{\text{free}} \xrightleftharpoons{K_M} M_{\text{act}} + \text{THF}$ <p>(Scheme 3-1c)</p>	$K_M = \frac{M_{\text{act}} \cdot \text{THF}}{X \cdot M_{\text{free}}}$	$K = \frac{K_M}{\text{THF}} = \frac{M_{\text{act}}}{X \cdot M_{\text{free}}}$

For the various reagents the following mass balances are valid:

$$Al_0 = Al + X + P' + M_{\text{act}} \quad (3-8)$$

$$M_{\text{free}} + M_{\text{act}} = M = M_0 \cdot (1 - x) \quad (3-9)$$

$$I_0 = P + P' \quad (3-10)$$

Al_0 , M_0 and I_0 are the initial concentrations of Et₃Al, monomer and initiator, Al and X stand for free and THF-coordinated Et₃Al, respectively, and x is the monomer conversion. Because of extremely exothermic reaction of Et₃Al with THF ($\Delta E = -54 \text{ kJ}\cdot\text{mol}^{-1}$, see Scheme 3-1a) the fraction of free Et₃Al is extremely low and will be neglected.

By using the equilibrium constants and Equations (3-9) and (3-10) one can express P' and M_{act} via the concentration of $\text{Et}_3\text{Al}\cdot\text{THF}$, X , and introduce the fractions of activated monomer, α_M , and of deactivated chain ends, α' :

$$M_{\text{act}} = M \cdot \frac{K \cdot X}{1 + K \cdot X} \equiv \alpha_M \cdot M \quad (3-11a)$$

$$P' = I_0 \cdot \frac{K_1 \cdot X}{1 + K_1 \cdot X} \equiv \alpha' \cdot I_0 \quad (3-11b)$$

Substituting these expressions into Equation (3-8), one obtains the equation for X :

$$Al_0 = X + I_0 \cdot \frac{K_1 \cdot X}{1 + K_1 \cdot X} + M \cdot \frac{K \cdot X}{1 + K \cdot X} \quad (3-12a)$$

Equation (3-12a) is a cubic equation with respect to X and it was solved numerically for arbitrary values of concentrations Al_0 , M_0 , and I_0 and equilibrium constants K_1 and K . However, since most experiments were made under the condition $Al_0 \gg I_0$ (at least, $Al_0/I_0 > 10$) it is possible to neglect the second term in Equation (3-12a). Then, instead of a cubic equation one obtains the approximated quadratic equation for X

$$Al_0 = X + M \cdot \frac{K \cdot X}{1 + K \cdot X} \quad (3-12b)$$

The solution of this equation is

$$X = \frac{1}{2} \cdot \left\{ \sqrt{\left(M + Al_0 + K^{-1} \right)^2 - 4 \cdot M \cdot Al_0} - \left(M - Al_0 + K^{-1} \right) \right\} \quad (3-13)$$

Thus, for the fraction of activated monomer,

$$\alpha_M = \frac{M_{\text{act}}}{M} = \frac{K \cdot X}{K \cdot X + 1},$$

one obtains Equation (3-4) of the main text independently of the initiator

$$\alpha_M = \frac{1}{2} \cdot \left\{ 1 + \frac{Al_0 + K^{-1}}{M} - \sqrt{\left(1 + \frac{Al_0 + K^{-1}}{M} \right)^2 - 4 \cdot \frac{Al_0}{M}} \right\} \quad (3-14)$$

Substituting (3-13) into Equation (3-11b) one obtains the expression for the fraction of coordinated chain ends, P'

$$\alpha' = \frac{\sqrt{(M + Al_0 + K^{-1})^2 - 4 \cdot M \cdot Al_0} - (M - Al_0 + K^{-1})}{\sqrt{(M + Al_0 + K^{-1})^2 - 4 \cdot M \cdot Al_0} - (M - Al_0 + K^{-1}) + 2 / K_1} \quad (3-15)$$

Expressions (3-14) and (3-15) are valid always except for very high conversions when the concentration of monomer becomes close to the concentration of initiator. In that case the cubic equation for X should be solved.

Assuming that the reactivity of coordinated centers, P' , is much lower than that of P , the polymerization rate may be expressed as

$$R_p = (k_p \cdot M_{\text{free}} + k'_p \cdot M_{\text{act}}) \cdot P = M \cdot I_0 \cdot [k_p \cdot (1 - \alpha_M) + k'_p \cdot \alpha_M] \cdot (1 - \alpha')$$

Hence, the observed rate constant $k_{p,\text{exp}} = k_{\text{app}}/P$ is

$$k_{p,\text{exp}} = [k_p \cdot (1 - \alpha_M) + k'_p \cdot \alpha_M] \cdot (1 - \alpha') = k'_p \cdot \frac{\lambda + K \cdot X}{1 + K \cdot X} \cdot \frac{1}{1 + K_1 \cdot X} \quad (3-16)$$

where $\lambda = k_p/k'_p$ is the ratio of the propagation rate constants of free and activated monomer and k_{app} is the slope of the first-order time-conversion plot.

In the course of the polymerization the concentration of THF-coordinated Et_3Al , X , increases and hence, the fraction of activated monomer, α_M , also increases whereas the fraction of active chains, $P/I_0 = 1 - \alpha'$, decreases. Due to these two oppositely directed changes in α_M and $(1 - \alpha')$ the resulting behavior of the observed rate constant as a function of initial monomer concentration may be different depending on the relationship between K and K_1 . For example, for not very high K_1 , i.e. when the fraction of active chain ends, P , is not very low, the polymerization rate decreases with increasing initial monomer concentration, M_0 . On the opposite, for high K_1 the observed rate constant, $k_{p,\text{exp}}$, is the higher the higher the ratio M_0/Al_0 . For some relationship between rate constants the dependence of $k_{p,\text{exp}}$ on M_0 may even go through a maximum, however, this effect is not

very pronounced. Also, if the reactivity of free monomer is not extremely low in comparison with that of activated monomer, the dependence of k_{app} on conversion will be not very drastic.

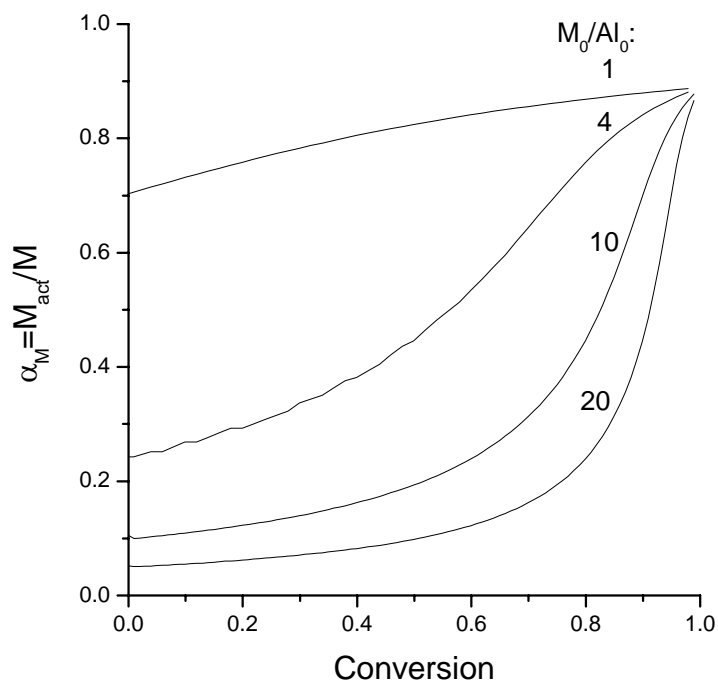


Figure 3-29. Dependence of the fraction of activated monomer on conversion for different initial monomer concentrations. $k_p^2 = 500 \text{ L}\cdot\text{mol}^{-1}\cdot\text{s}^{-1}$, $k_p = 0$, $AI_0 = 10^{-2}$, $I_0 = 10^{-3} \text{ mol}\cdot\text{L}^{-1}$, $K_M = 10^4 \text{ L}\cdot\text{mol}^{-1}$.

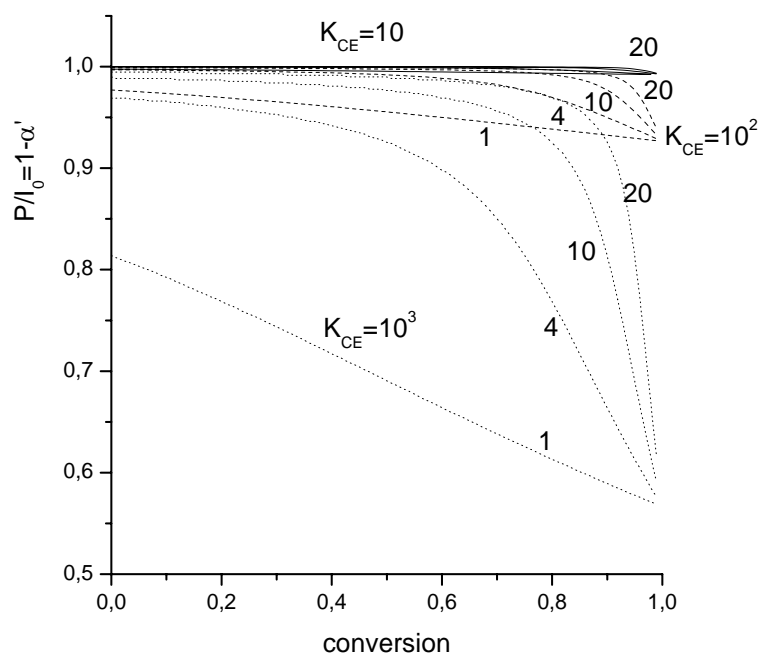


Figure 3-30. Dependence of the fraction of active chain ends on conversion for different initial monomer concentrations and different K_{CE} . $k'_p = 500 \text{ L}\cdot\text{mol}^{-1}\cdot\text{s}^{-1}$, $k_p = 0$, $AI_0 = 10^{-2}$, $I_0 = 10^{-3} \text{ mol}\cdot\text{L}^{-1}$, $K_M = 10^4 \text{ L}\cdot\text{mol}^{-1}$.

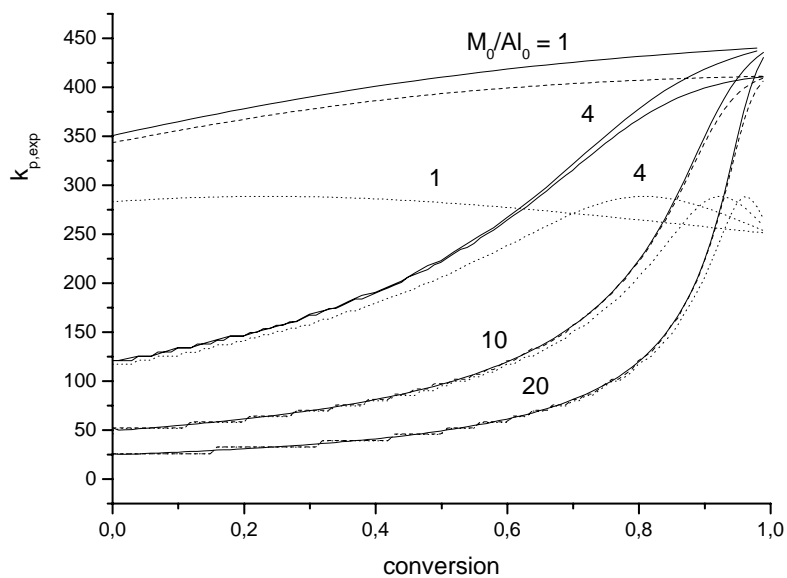


Figure 3-31. Dependence of the observed rate constant on conversion for different initial concentration of monomer and different K_{CE} . [$K_{CE}\cdot(\text{mol}\cdot\text{L}^{-1}) = 10$ (solid), 10^2 (dash) and 10^3 (dot)]. $k'_p = 500 \text{ L}\cdot\text{mol}^{-1}\cdot\text{s}^{-1}$, $k_p = 0$, $AI_0 = 10^{-2}$, $I_0 = 10^{-3} \text{ mol}\cdot\text{L}^{-1}$, $K_M = 10^4 \text{ L}\cdot\text{mol}^{-1}$. Numbers in the figure denote the M_0/AI_0 ratio.

It follows from Equations (3-15) and (3-13) that the observed rate constant, $k_{p,\text{exp}}$, can have an extremum as a function of aluminum concentration Al_0 . The extreme (maximum) value of $k_{p,\text{exp}}$ may be determined from the condition that the derivative of $k_{p,\text{exp}}$ over Al_0 is equal to zero.

$$\frac{dk_{p,\text{exp}}}{dAl_0} = \frac{dk_{p,\text{exp}}}{dX} \cdot \frac{dX}{dAl_0} = 0$$

As follows from Equation (3-12a), dX/dAl_0 is always > 0 . This means that maximum k_{app} is reached when $dk_{p,\text{exp}}/dX = 0$. This condition is satisfied at

$$X = \frac{\sqrt{\lambda^2 + (1-\lambda) \cdot K/K_1 - \lambda} - \lambda}{K} \quad (3-17a)$$

If $\lambda \ll 1$ one obtains from Equation (3-17a) that $k_{p,\text{exp}}$ is maximum at

$$X = (K \cdot K_1)^{-1/2} \quad (3-17b)$$

The concentration of aluminum at the point of maximum $k_{p,\text{exp}}$ should be calculated from Equation (3-12a). The same is valid for the extremal dependence of $k_{p,\text{app}}$ on M , because

$$\frac{dk_{p,\text{exp}}}{dM} = \frac{dk_{p,\text{exp}}}{dX} \cdot \frac{dX}{dM}$$

and dX/dM is always < 0 (that is, $dX/dx = -dX/d(M/M_0) > 0$). Hence, the maximum of $k_{p,\text{exp}}$ is reached at X determined from expressions (3-17).

Independently of the initial concentration of monomer, the final (at full monomer conversion) values of α_M , α' , and $k_{p,\text{exp}}$ are defined only by the concentration of Et_3Al , Al_0 , and the equilibrium constants. As follows from Equation (3-12), for $x \rightarrow 1$ the concentration of coordinated Et_3Al is defined from equation

$$Al_0 = X + I_0 \cdot \frac{K_1 \cdot X}{K_1 \cdot X + 1} \approx X$$

because $I_0 \ll Al_0$. Consequently, the final parameters are

$$\alpha_M \approx \frac{K \cdot Al_0}{K \cdot Al_0 + 1}$$

$$\alpha' \approx \frac{K_1 \cdot Al_0}{K_1 \cdot Al_0 + 1}$$

$$k_{p,\text{exp}} \approx \frac{k_p + k'_p \cdot K \cdot Al_0}{K \cdot Al_0 + 1} \cdot \frac{1}{K_1 \cdot Al_0 + 1}$$

4. Thermo- and pH-Responsive Micelles of Poly(acrylic acid)-*block*-Poly(*N,N*-diethylacrylamide)

Xavier André, Mingfu Zhang, and Axel H. E. Müller*

Makromolekulare Chemie II and Bayreuther Zentrum für Kolloide und Grenzflächen, Universität Bayreuth, D-95440 Bayreuth, Germany. Fax: (+49) 921-553393. Email: axel.mueller@uni-bayreuth.de

Keywords: anionic polymerization; amphiphilic block copolymers; double-stimuli responsive micelles; LCST behavior.

Summary

The bishydrophilic block copolymer poly(acrylic acid)₄₅-*block*-poly(*N,N*-diethylacrylamide)₃₆₀ was obtained after hydrolysis of poly(*tert*-butyl acrylate)₄₅-*block*-poly(*N,N*-diethylacrylamide)₃₆₀ synthesized by sequential anionic polymerization in the presence of Et₃Al. The polymer is stimuli-sensitive with respect to both pH and temperature in aqueous solution, reversibly forming spherical ‘crew-cut’ micelles with PDEAAm-core ($\langle R_h \rangle_z = 21.5$ nm) under alkaline conditions for $T > 35$ °C as well as inverse star-like micelles with expanded PAA-core ($\langle R_h \rangle_z = 43.8$ nm) under acidic conditions for $T < 35$ °C, as indicated by Dynamic Light Scattering.

Published in *Macromolecular Rapid Communications* **2005**, 26, 558-563.

4.1 Introduction

The interest in stimuli-responsive (co)polymers has increased during the last decades. In this main direction, some systems have been studied in order to obtain ‘smart’ materials, the behavior of which depends intrinsically on structural parameters and on the experimental conditions. Statistical, block, or brush copolymers based on the thermo-responsive poly(*N*-isopropylacrylamide) (PNIPAAm) have been widely studied.¹ In water such (co)polymers exhibit a sharp transition from the hydrophilic expanded coil to the hydrophobic collapsed coil at around 32 °C (lower critical solution temperature, LCST) and this typical behavior has made them especially interesting for biomedical applications.²

Beside PNIPAAm, other *N*-substitued poly(acrylamide)s undergo the same phase transition below and above their LCST, which was found to be 32 °C in the case of poly(*N,N*-diethylacrylamide) (PDEAAm) synthesized free-radically.³ By incorporating a hydrophilic comonomer like acrylic acid, it is possible to shift the LCST to higher temperatures closer to the human body temperature, making this material and its derivatives a very interesting class of thermo-responsive polymers. In general such (co)polymers were obtained by free-radical polymerization, by Group Transfer Polymerization (GTP), or by anionic polymerization but the living characters were not demonstrated.^{4,5} Contrary to PDEAAm, poly(*N,N*-dimethylacrylamide) (PDMAAm) does not exhibit an LCST in aqueous solution but the commercially available *N,N*-dimethylacrylamide (DMAAm) represents an interesting model for the investigation of new polymerization processes. Different systems were elaborated to polymerize DMAAm in a living way by anionic polymerization, by Atom Transfer Radical Polymerization (ATRP), by Reversible Addition Fragmentation Transfer (RAFT), or via Nitroxide-Mediated Radical Polymerization (NMP).⁶⁻¹¹ Some advances were reported for the anionic polymerization of DMAAm and DEAAm by the use of Lewis acids (Et₂Zn, Et₃B) and have demonstrated the influence of additives on the tacticity and the solubility of the resulting polymer.^{12,13}

A new strategy was elaborated to synthesize PDMAAm, PDEAAm, poly(*tert*-butyl acrylate)-*block*-PDEAAm (PtBA-*b*-PDEAAm), and poly(*tert*-butyl methacrylate)-*block*-PDEAAm (PtBMA-*b*-PDEAAm) by anionic polymerization in the presence of Et₃Al, in our laboratory and by Nakhmanovich et. al. PDEAAm obtained by this method are rich in heterotactic triads and exhibit a LCST (26.1 < T_c < 32 °C).^{14,15} In this work we report the

synthesis of *PtBA-b-PDEAAm* by the new strategy we have elaborated in our laboratory using sequential anionic polymerization in the presence of Et_3Al . After hydrolysis of the *PtBA* block, the pH- and thermo-responsive behavior in aqueous solution of the resulting poly(acrylic acid)-*block*-poly(DEAAm) (*PAA-b-PDEAAm*) copolymer was studied.

4.2 Experimental Part

Materials. Tetrahydrofuran (THF, Merck) was purified by reflux over CaH_2 and distilled from potassium before use. Et_3Al (Aldrich, 1M in hexane) was used as received. The monomer *tert*-butyl acrylate (*tBA*, BASF) was degassed by three freeze-evacuate-thaw cycles under high vacuum (10^{-5} mbar), and Et_3Al was added dropwise until yellowish color appeared. The mixture was stirred, condensed into an ampoule and stored under dry nitrogen atmosphere. The monomer *tert*-butyl methacrylate (*tBMA*, BASF) was purified using the same procedure described for *tBA*. DEAAm was synthesized by the reaction at $T < 10$ °C in toluene (Merck) of a two-fold excess of diethylamine and acryloyl chloride (96%, Aldrich). The crude DEAAm was then purified five times by fractional distillation from CaH_2 under reduced pressure and it was three times degassed prior to the polymerization. Diphenylhexyllithium (DPH-Li) was prepared by the reaction of *n*-butyllithium (*n*-BuLi, Acros, 1.3M in cyclohexane/hexane: 92/8) and 1,1-diphenylethylene (DPE, 97%, Aldrich, freshly distilled over *n*-BuLi) in situ ($[\text{DPE}]/[\textit{n}\text{-BuLi}] = 1.1$). LiCl (anhydrous $\geq 98\%$, Fluka) was dried in high vacuum at 300 °C for three days and dissolved in dry THF.

Polymerization procedure. The polymerization was performed under dry nitrogen in a thermostated glass autoclave (Büchi). The initiator (DPH-Li) (1.1 mmol; $1.8 \text{ mmol}\cdot\text{L}^{-1}$) was formed in-situ in the THF solution of LiCl at -78 °C (17.5 mmol; $28.2 \text{ mmol}\cdot\text{L}^{-1}$). *tBA* (54.7 mmol; $88.1 \text{ mmol}\cdot\text{L}^{-1}$) was injected via a syringe into the reactor to start the polymerization of the precursor. The characteristic red color of the DPH-Li initiator disappeared instantaneously. 2.2 minutes after full conversion of *tBA*, Et_3Al (8 mmol; $12.9 \text{ mmol}\cdot\text{L}^{-1}$) was added. After another 6.1 minutes, DEAAm (58.4 mmol; $94 \text{ mmol}\cdot\text{L}^{-1}$) ($t = 0$) was injected. A degassed solution of methanol / acetic acid (9/1 v/v) was used as quenching agent. At full conversion an aliquot of the final solution was taken and dried for two days under vacuum to result the crude copolymer. The rest of the copolymer was recovered by precipitation into a large excess of *n*-hexane, filtered and dried for two days

under vacuum. This process removes unreacted *PtBA* precursor, leading to the purified copolymer. Traces of LiCl were removed from *PtBA* precursor by one day stirring in benzene followed by a filtration. The clear solution was freeze-dried from benzene. The synthesis and purification of *PtBMA-b-PDEAAm* copolymer was carried out using the same experimental conditions at $-30\text{ }^{\circ}\text{C}$ and the complete *tBMA* conversion was observed in ca. 20 minutes.

Hydrolysis and micellization procedure. 2.08 g of the purified *PtBA-b-PDEAAm* copolymer were dissolved in 100 mL dichloromethane (Merck, P.A.) and 5.82 g of trifluoroacetic acid (about 5-fold molar excess with respect to the ester groups of *PtBA* block) was added. The hydrolysis was carried out one day at room temperature. After evaporation of the solvent, the hydrolyzed copolymer was washed twice with dichloromethane and dried for two days under vacuum. The resulting *PAA-b-PDEAAm* was

dissolved in fresh standard NaOH solution (Merck, 0.1N) or in HCl solution at room temperature for two days. Prior to any measurement the pH of the copolymer solution was measured using a SCHOTT CG840 pH-meter with a glass electrode.

Characterizations. *PtBA-b-PDEAAm* copolymer was characterized by Size Exclusion Chromatography (SEC) using a RI detector, and a UV detector ($\lambda = 254\text{ nm}$). PSS SDVgel columns (300 x 8 mm, $5\mu\text{m}$): 10^5 , 10^4 , 10^3 and 10^2 \AA were used and $100\mu\text{L}$ of a 0.4.wt.-% polymer solution was injected at room temperature at a elution rate of $0.5\text{ mL}\cdot\text{min}^{-1}$ using THF with 0.25.wt.-% of *tBu*₄NBr as eluent. Polystyrene standards were used to calibrate the columns. Internal standard was ortho-dichlorobenzene. For the *PtBA* precursor characterization, a similar SEC setup was performed in pure THF at an elution rate of $1\text{ mL}\cdot\text{min}^{-1}$ using a poly(*tert*-butyl methacrylate) calibration and toluene as internal standard.

MALDI-TOF mass spectrometry was performed on a Bruker Reflex III equipped with a 337 nm N₂ laser in the reflector mode and 20 kV acceleration voltage. Dihydroxybenzoic acid (DHB) was used as matrix. Samples were prepared from Dimethylacetamide or THF solution by mixing matrix ($10\text{ g}\cdot\text{L}^{-1}$) and sample ($10\text{ g}\cdot\text{L}^{-1}$) in a ratio 10:1. The number-average molecular weights, M_n , were determined in the linear mode and in the reflector mode for the copolymer and the precursor, respectively. ¹H NMR spectrum was recorded on a Bruker AC-250 in DMF-*d*₇ at room temperature.

Dynamic Light Scattering (DLS) was performed on an ALV DLS/SLS-SP 5022F compact goniometer system equipped with an ALV 5000/E correlator and a He/Ne laser ($\lambda = 632.8$ nm). Prior to light scattering measurements, the sample solutions were filtered using 0.45 μm Nylon filter. The turbid acidic solution was not filtered. Measurements were carried out at various scattering angles (30-150°, step: 10°).

The cloud point determination was carried out on a Hitachi U3000 spectrophotometer. The transmittance of the solution was measured at a wavelength of 500 nm using a thermostatically controlled cuvette. The temperature of the solution was precisely measured using a Philips Type K thermo element (Chromel-Alumel, Ni-CrNi).

4.3 Results and Discussion

Synthesis of the Poly(*tert*-butyl acrylate) precursor.

*t*BA was polymerized using the well-known system 1,1-diphenylhexyl-lithium (DPH-Li) / LiCl in THF at -78 °C.¹⁶ The ratio [LiCl]/[initiator] ~ 10 was claimed by Kunkel et al. to be the most effective in terms of initiator efficiency and control of polydispersity.^{17,18} The course of the polymerization was monitored by Fourier-Transform Near-Infrared in-line spectroscopy (FT-NIR), a useful technique which has demonstrated its efficiency in the past to follow the kinetics of various monomers for controlled/living polymerization processes.^{19,20} Experimental details can be found elsewhere.²¹ Polymerization occurs within one minute ($t_{1/2} \sim 6.6$ s). Narrowly distributed polymer is obtained after quenching the reaction mixture: $M_n = 9970$, $M_w/M_n = 1.10$ by SEC in THF using poly(*tert*-butyl methacrylate) calibration; $M_n = 6030$ ($DP_n = 45$), $M_w/M_n = 1.07$ by MALDI-TOF MS. The M_n obtained by MALDI-TOF is somewhat smaller than the theoretical value ($M_{n,theo} = 6620$) which may be attributed to the fact that discrimination of the higher molecular weight chains occurs during the ionization.

Polymerization of *N,N*-diethylacrylamide initiated by a *Pt*BA macroinitiator.

Anionic polymerization of DEAAm was initiated by a *Pt*BA-Li macroinitiator after addition of 7-fold excess of Et_3Al . At the monomer concentration used, the polymerization mixture remains soluble during the reaction. Full conversion was reached after 7.5 minutes

($t_{1/2} \approx 2$ min). As shown in Figure 4.1, the final copolymer shows a bimodal molecular weight distribution due to unreacted precursor. This may be attributed to the short half-life of PtBA-Li active chains.

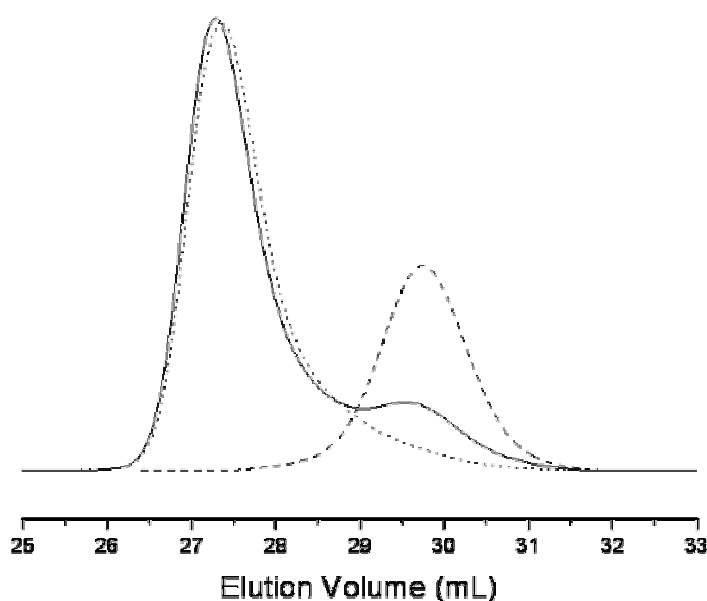


Figure 4-1. SEC traces of the PtBA precursor (---), the crude PtBA-*b*-PDEAAm block copolymer before purification (___), and the purified PtBA-*b*-PDEAAm after precipitation in *n*-hexane (...) in THF (+ salt).

Figure 4-1 shows the molecular weight distribution before and after removing residual precursor. The molecular weights were characterized by SEC using a polystyrene calibration: $M_n = 23,100$, $M_w/M_n = 1.23$ for the crude copolymer, and $M_n = 28,500$, $M_w/M_n = 1.12$ for the purified copolymer. The later copolymer was characterized by MALDI and a molecular weight of $51,750 \text{ g}\cdot\text{mol}^{-1}$ was measured. The structure of the copolymer is $(tBA)_{45}\text{-}b\text{-(DEAAm)}_{360}$ with a molecular weight distribution, $M_w/M_n = 1.12$, determined by SEC. It was reported by Schilli et al. that SEC with PS calibration strongly underestimates the molecular weight of poly(*N*-isopropylacrylamide), proving the importance of the molecular weight determination by an absolute technique.²² From the expected molecular weight, $M_{n,\text{theo}} = 12,700 \text{ g}\cdot\text{mol}^{-1}$, the blocking efficiency is determined as $f = 0.15$. The low

efficiency may be attributed to the short half-life of *PtBA*-Li active chains²³ leading to a backbiting reaction of part of the precursor before the second monomer was added. The backbiting product (a cyclic, enolized β -ketoester) was reported to have a strong UV absorption at 260 nm.²³ Backbiting occurs after 100 % conversion of *tBA*. In fact, the UV signal of the GPC traces of the unreacted *PtBA* precursor shows a weak signal at 260 nm that is not seen in the purified diblock copolymer. Inactive *PtBA* chains terminated by a cycle are removed from the copolymer during the selective precipitation.

One experiment using poly(*tert*-butyl methacrylate)-Li (*PtBMA*-Li) macroinitiator instead of *PtBA*-Li as macroinitiator was attempted. Although the *PtBMA*-Li active chains are more stable than *PtBA*-Li one, some *PtBMA* precursor remains in the crude product and the blocking-efficiency was found to be $f = 0.53$, higher than the blocking efficiency observed in the case of *PtBA*-*b*-PDEAAm. After purification well-defined poly(*tert*-butyl methacrylate)-*block*-PDEAAm is obtained ($M_n = 22,700 \text{ g}\cdot\text{mol}^{-1}$ by MALDI; $M_w/M_n = 1.10$ by SEC).

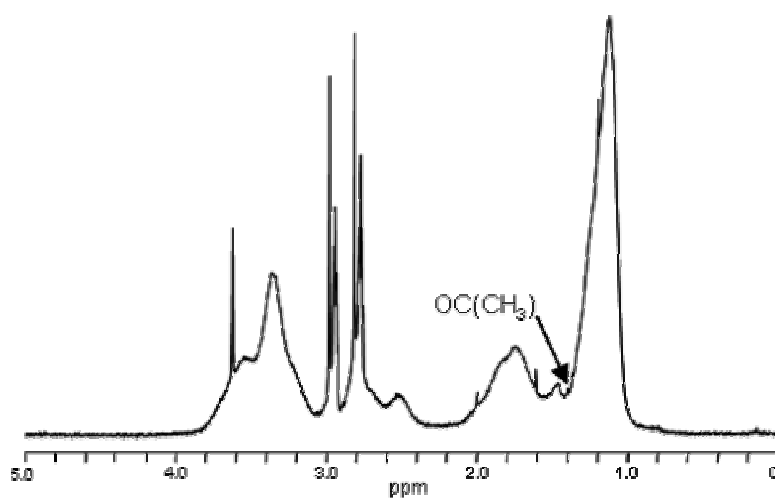


Figure 4-2. ^1H NMR spectrum of the hydrolyzed copolymer PAA-*b*-PDEAAm (in $\text{DMF-}d_7$).

Hydrolysis of the diblock copolymer.

By selective hydrolysis of the *PtBA* block, a copolymer containing poly(acrylic acid) (PAA) and PDEAAm segments can be obtained. As shown in Figure 4-2, the characteristic

strong signal of the *t*Bu protons at 1.44 ppm disappears on the ^1H NMR spectrum demonstrating the efficiency of the hydrolysis procedure. Pure bishydrophilic diblock is obtained: $(\text{AA})_{45}\text{-}b\text{-(DEAAm)}_{360}$ which can easily be dissolved in alkaline water at room temperature. The resulting solutions are transparent ($\text{pH} \geq 9$; $c = 0.6 - 5.2 \text{ g}\cdot\text{L}^{-1}$). Under acidic conditions ($\text{pH} \leq 4$) PAA-*b*-PDEAAm solutions are turbid, indicating the presence of larger aggregates.

Micellization and solution properties.

In selective solvents, amphiphilic block copolymers associate to form spherical, cylindrical, or crew-cut micelles, vesicles, etc., which are in equilibrium with non-associated copolymer molecules.²⁴ The applications of the micellization of amphiphilic block copolymers are various: steric stabilization of latex particles, dispersion of pigments in paints, drug carriers, etc. As mentioned above, most reported works deal with PDEAAm made by free-radical polymerization but for some of these applications the use of well-defined polymers is a requirement in order to have a better control on the phenomena. The controlled/living anionic polymerization of DEAAm and the control of the tacticity of the resulting polymer, which influences strongly the solubility, continue to be a challenge for polymer scientists. The micellization of amphiphilic ionic copolymers in solution is a complicated and time-consuming procedure in particular when the hydrophobic block is long, ‘crew-cut’ micelles with a large core and small corona are obtained. Thus, many factors must be controlled carefully in the preparation method because they may strongly influence the resulting micellar architectures. In contrast with other amphiphilic block copolymers leading to the formation of ‘crew-cut’ micelles, use of intermediate solvent and dialysis procedure are not necessary for PAA-*b*-PDEAAm because both segments are hydrophilic in aqueous solution at room temperature under alkaline conditions.^{25,26} The PAA-*b*-PDEAAm aqueous solutions are clear and dissolution is instantaneous.

As shown in Figure 4-3, a cloud point of ca. 35 °C was observed for the $(\text{AA})_{45}\text{-}b\text{-(DEAAm)}_{360}$ copolymer at $\text{pH} = 12$ in the absence of salt by turbidimetry. The transmission decreases to 82% when the temperature raises above the LCST of PDEAAm suggesting the presence of micelles with PDEAAm forming the core and deprotonated PAA forming the shell.²⁷ As it was reported for copolymers of DEAAm and (meth)acrylic acid

synthesized free-radically, the LCST is shifted to higher temperature (from 32 to 35 °C) by incorporating a hydrophilic comonomer.^{28,29}

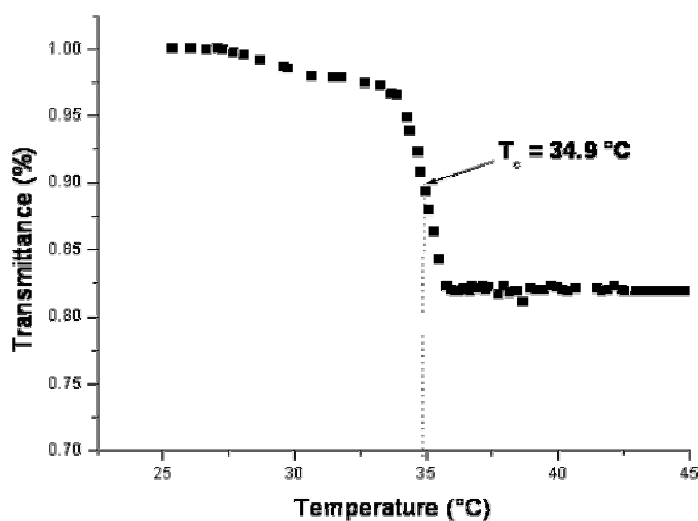


Figure 4-3. Turbidimetric determination of the cloud point in water for $(AA)_{45}\text{-}b\text{-(DEAAm)}_{360}$ (at $\lambda = 500\text{ nm}$, $c = 5.2\text{ g}\cdot\text{L}^{-1}$; $\text{pH} = 12$).

DLS was used to characterize the solution properties of the $(AA)_{45}\text{-}b\text{-(DEAAm)}_{360}$ copolymer below and above its LCST under alkaline ($\text{pH} > 9$), and acidic ($\text{pH} < 4$) conditions. Similar 'Flip-flop' or 'schizophrenic' behaviors in solution were reported by Armes and coworkers.^{30,31} By playing with the hydrophilic/hydrophobic balance and the pH, block copolymers based on 2-(diethylamino)ethyl methacrylate (DEA) [or 4-vinylbenzoic acid (VBA)] and 2-(*N*-morpholino)ethyl methacrylate (MEMA) can form micelles containing hydrophobic PMEMA segment in the core, reverse-micelles containing hydrophobic PDEA (or PVBA) in the core, or molecularly dissolved chains in aqueous solution. Similarly, thermo- and pH-responsive micelles and reverse-micelles of poly(propylene oxide)-*block*-poly[2-(diethylamino)ethyl methacrylate] (PPO-*b*-PDEA) were synthesized by ATRP but the relative low value of LCST (10 to 20 °C for the PPO block) makes such copolymers not so interesting for biomedical applications for example.³² The hydrodynamic radius distribution (CONTIN plot) of the $(AA)_{45}\text{-}b\text{-(DEAAm)}_{360}$ block copolymer at a scattering angle of 30° under basic conditions is shown

in Figure 4-4. At $T = 21\text{ }^{\circ}\text{C}$, unimers ($\langle R_h \rangle_z = 4.7\text{ nm}$) coexisting with large aggregates ($\langle R_h \rangle_z = 101\text{ nm}$) are observed. Since the CONTIN analysis renders intensity-weighted distributions, the proportion of the large particles is strongly exaggerated, as the scattering intensity is strongly dependent on the radius of the particle ($\sim R^6$ for spherical particles). Thus, the weight fraction of the aggregates shown in Figure 4-4 ($T = 21\text{ }^{\circ}\text{C}$), is actually rather small (0.05 wt.-%). The formation of these aggregates is still not well understood. At pH 12.8, PAA should be fully deprotonated to poly(sodium acrylate), which can not lead to the formation of hydrogen bonding (no δ^+ proton). The C_{18} hydrophobic end group of the block copolymer as well as the intrinsic difference of hydrophilicity between the poly(*N,N*-diethylacrylamide) and the poly(sodium acrylate) blocks may play roles in the aggregate formation. The disappearance of the aggregates above the LCST (see below) indicates that this is not due to impurity (dust for example) in the solution.

When the temperature was raised above the LCST ($T = 45\text{ }^{\circ}\text{C}$), a very narrow and unimodal peak is found with a z -average hydrodynamic radius of 21.5 nm. No angular dependence of the value of the z -average R_h is observed for all systems, suggesting a spherical geometry for all assemblies.

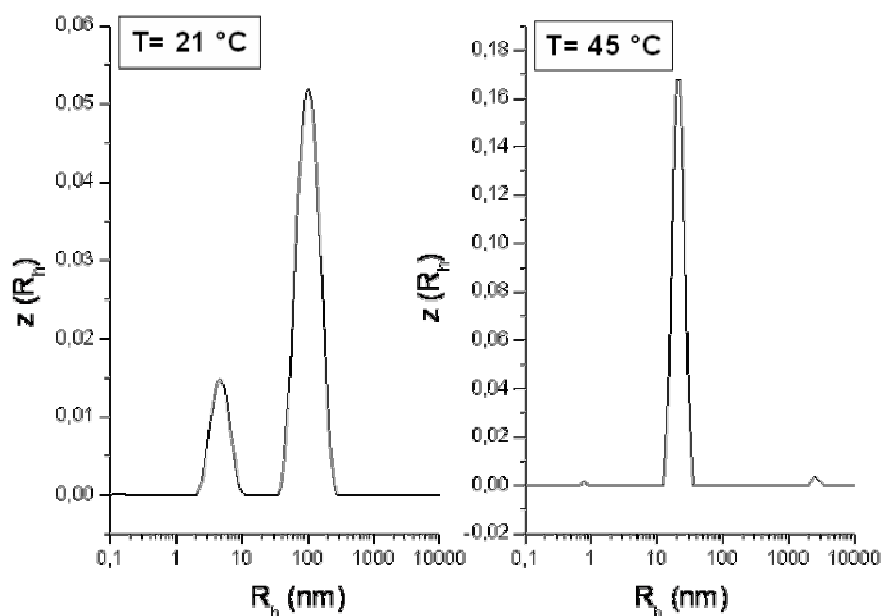


Figure 4-4. Intensity-weighted hydrodynamic radius distribution of $(AA)_{45}\text{-}b\text{-(DEAAM)}_{360}$ in water (pH = 12.8) at 30° scattering angle ($c = 1.3\text{ g}\cdot\text{L}^{-1}$, $[\text{NaCl}] = 0.1\text{ mol}\cdot\text{L}^{-1}$).

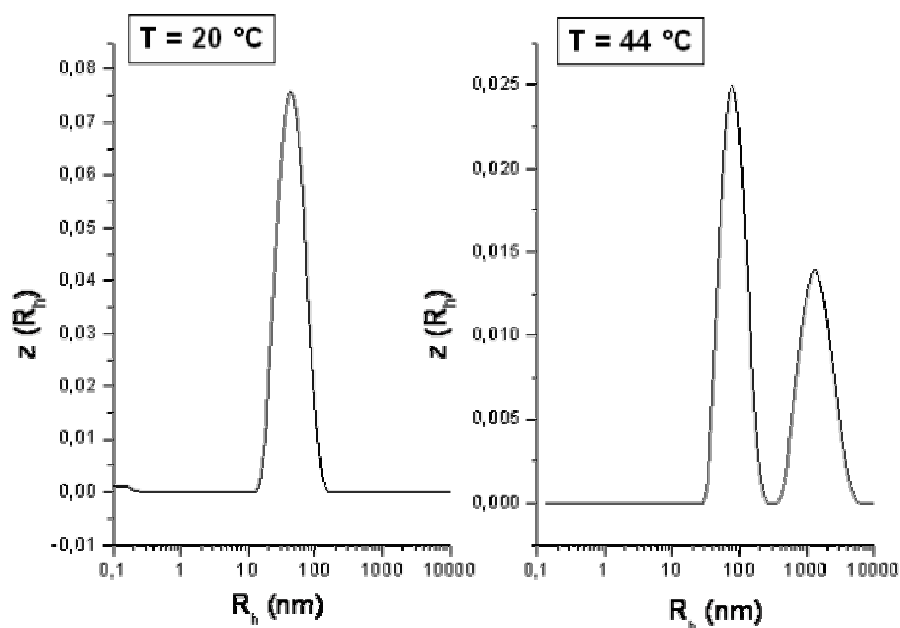


Figure 4-5. Intensity-weighted hydrodynamic radius distribution of $(AA)_{45}\text{-}b\text{-(DEAAM)}_{360}$ in water ($\text{pH} = 3.9$) at 90° scattering angle ($c = 0.9 \text{ g}\cdot\text{L}^{-1}$; $[\text{NaCl}] = 0.1 \text{ mol}\cdot\text{L}^{-1}$).

The existence of inverse micelles containing protonated poly(acrylic acid) segments in the core, and stabilized by a corona made of a long poly(*N,N*-diethylacrylamide) block is indicated by DLS (Figure 4-5). In contrast to the clear solutions containing mainly unimers under alkaline conditions, turbid solutions were obtained under acidic conditions ($\text{pH} = 3.9$) at room temperature. At $T = 20 \text{ }^\circ\text{C}$, polydisperse ‘inverse’ micelles ($\langle R_h \rangle_z = 43.8 \text{ nm}$ at the scattering angle of 90°) are observed suggesting eventually the presence of different assemblies. The presence of another peak ($\langle R_h \rangle_z \approx 300 \text{ nm}$) is also observed only at the scattering angle of 30° and it is attributed to larger aggregates responsible for the turbidity. As expected from the asymmetric composition of the block copolymer, the inverse PAA-core micelles observed are larger than the PDEAAM-core micelles. The formation of the inverse PAA-core micelles may be attributed either to the intrinsic difference of hydrophilicity between the poly(*N,N*-diethylacrylamide) and the poly(acrylic acid) blocks or the C_{18} initiating hydrophobic fragment or a combination of both effects. When the temperature was raised above the LCST ($T = 44 \text{ }^\circ\text{C}$), macroscopic precipitation occurs. A relatively narrower peak is found with a z -average hydrodynamic radius of 25.1 nm (at 30°

scattering angle) coexisting with peaks of very large particles attributed to precipitated copolymer ($\langle R_h \rangle_z \geq 1 \mu\text{m}$). In this case, the precipitation is not a sharp transition and the observed value of the z -average hydrodynamic radius increases with time (81.0 nm at 90° scattering angle after 35 minutes at $T = 44 \text{ }^\circ\text{C}$). The presence and formation of inverse PAA-core micelles is suggested at room temperature, and at $T > \text{LCST}$ the PDEAAm-corona firstly collapses and then self-aggregates till the precipitation is complete because the PDEAAm block becomes more hydrophobic.

4.4 Conclusions

The synthesis of poly(acrylic acid)-*b*-poly(DEAAM) can be achieved by sequential anionic polymerization of *t*BA and DEAAM followed by the hydrolysis of *Pt*BA block. At room temperature such bishydrophilic compounds can be directly dissolved in alkaline water. The existence and the geometry of these thermo-responsive micelles are indicated by DLS measurements: above the LCST of PDEAAM, crew-cut micelles are formed. This elegant and effective strategy allows the reversible formation of spherical crew-cut micelles in aqueous solution without the use of intermediate solvents. The existence of ‘inverse’ micelles with an acrylic acid core is also demonstrated by DLS measurements. Further characterizations of these promising double-stimuli materials are subject to further investigations in our laboratory and will be reported in the future.

Acknowledgment

X. A. wants to thank the French Research Ministry and the French-Bavarian University Center for financial support. We acknowledge the help of Michael Lanzendörfer[†], and Hideharu Mori.

4.5 References

- (1) Park, T. G.; Hoffman, A. S. *Journal of Applied Polymer Science* **1992**, *46*, 659-671.
- (2) Huang, G.; Gao, J.; Hu, Z.; St. John, J. V.; Ponder, B. C.; Moro, D. J. *Controlled Release* **2004**, *94*, 303-311.
- (3) Liu, H. Y.; Zhu, X. X. *Polymer* **1999**, *40*, 6985-6990.
- (4) Eggert, M.; Freitag, R. *Journal of Polymer Science, Part A: Polymer Chemistry* **1994**, *32*, 803-813.
- (5) Idziak, I.; Avoce, D.; Lessard, D.; Gravel, D.; Zhu, X. X. *Macromolecules* **1999**, *32*, 1260-1263.
- (6) Xie, X.; Hogen-Esch, T. E. *Macromolecules* **1996**, *29*, 1746-1752.
- (7) Nakhmanovich, B. I.; Urman, Y. G.; Arest-Yakubovich, A. A. *Macromol. Chem. Phys.* **2001**, *202*, 1327-1330.
- (8) Ding, S.; Radosz, M.; Shen, Y. *Macromolecular Rapid Communications* **2004**, *25*, 632-636.
- (9) Donovan, M. S.; Lowe, A. B.; Sumerlin, B. S.; McCormick, C. L. *Macromolecules* **2002**, *35*, 4123-4132.
- (10) Diaz, T.; Fischer, A.; Jonquieres, A.; Brembilla, A.; Lochon, P. *Macromolecules* **2003**, *36*, 2235-2241.
- (11) Schierholz, K.; Givehchi, M.; Fabre, P.; Nallet, F.; Papon, E.; Guerret, O.; Gnanou, Y. *Macromolecules* **2003**, *36*, 5995-5999.
- (12) Ishizone, T.; Yoshimura, K.; Hirao, A.; Nakahama, S. *Macromolecules* **1998**, *31*, 8706-8712.
- (13) Kobayashi, M.; Okuyama, S.; Ishizone, T.; Nakahama, S. *Macromolecules* **1999**, *32*, 6466-6477.
- (14) Müller, A. H. E.; André, X.; Charleux, B. *e-Polymers* **2003**, P_003.
- (15) Nakhmanovich, B. I.; Urman, Y. G.; Krystal'nyi, E. V.; Arest-Yakubovich, A. A. *Vysokomolekulyarnye Soedineniya, Seriya A i Seriya B* **2003**, *45*, 978-981.
- (16) Fayt, R.; Forte, R.; Jacobs, C.; Jérôme, R.; Ouhadi, T.; Teyssie, P.; Varshney, S. K. *Macromolecules* **1987**, *20*, 1442-1444.
- (17) Kunkel, D. *Ph. D. Thesis*; Johannes-Gutenberg Universität: Mainz, 1992.
- (18) Kunkel, D.; Müller, A. H. E.; Janata, M.; Lochmann, L. *Polym. Prepr. (Am. Chem. Soc., Div. Polym. Chem.)* **1991**, *32*, 301-302.
- (19) Long, T. E.; Liu, H. Y.; Schell, B. A.; Teegarden, D. M.; Uerz, D. S. *Macromolecules* **1993**, *26*, 6237-6242.
- (20) Lanzendoerfer, M. G.; Schmalz, H.; Abetz, V.; Mueller, A. H. E. In *In Situ Spectroscopy of Monomer and Polymer Synthesis*; Storey, R., Ed.; Kluwer Academic/Plenum: New York / Dordrecht, 2003; pp 67-82.
- (21) André, X.; Benmohamed, K.; Yakimansky, A. V.; Müller, A. H. E. *Proceedings, 40th IUPAC International Symposium on Macromolecules*: Paris, France, 2004.
- (22) Schilli, C. M.; Müller, A. H. E.; Rizzardo, E.; Thang, S. H.; Chong, Y. K. *ACS Symposium Series* **2003**, *854*, 603-618.
- (23) Janata, M.; Lochmann, L.; Vlcek, P.; Dybal, J.; Müller, A. H. E. *Makromolekulare Chemie* **1992**, *193*, 101-112.
- (24) Alexandridis, P.; Lindman, B. *Amphiphilic Block Copolymers: Self-Assembly and Applications*; Elsevier: Amsterdam, 2000.
- (25) Zhang, L.; Eisenberg, A. *Journal of Polymer Science, Part B: Polymer Physics* **1999**, *37*, 1469-1484.
- (26) Zhang, L.; Eisenberg, A. *Polymers for Advanced Technologies* **1998**, *9*, 677-699.

- (27) Müller, A. H. E.; Andre, X.; Schilli, C. M.; Charleux, B. *Polymeric Materials: Science and Engineering* **2004**, *91*, 252-253.
- (28) Gan, L. H.; Cai, W.; Tam, K. C. *European Polymer Journal* **2001**, *37*, 1773-1778.
- (29) Liu, S.; Liu, M. *Journal of Applied Polymer Science* **2003**, *90*, 3563-3568.
- (30) Liu, S.; Armes, S. P. *Langmuir* **2003**, *19*, 4432-4438.
- (31) Bütün, V.; Armes, S. P.; Billingham, N. C.; Tuzar, Z.; Rankin, A.; Eastoe, J.; Heenan, R. K. *Macromolecules* **2001**, *34*, 1503-1511.
- (32) Liu, S.; Billingham, N. C.; Armes, S. P. *Angewandte Chemie, International Edition* **2001**, *40*, 2328-2331.

5. Solution Properties of Double-Stimuli Responsive Poly(Acrylic Acid)-*block*-Poly(*N,N*-Diethylacrylamide) Copolymer

Xavier André, Markus Burkhardt, Markus Drechsler, Peter Lindner,[§]

Michael Gradzielski,[‡] and Axel H. E. Müller*

Makromolekulare Chemie II, Universität Bayreuth, D-95440 Bayreuth, Germany

[§]*Institut Max von Laue-Paul Langevin, D-38042 Grenoble CEDEX 9, France*

[‡]*Stranski Laboratorium für Physikalische und Theoretische Chemie,
Technische Universität Berlin, D-10623 Berlin, Germany*

*Email: axel.mueller@uni-bayreuth.de

Abstract

The thermo- and pH-responsive poly(acrylic acid)-*block*-poly(*N,N*-diethylacrylamide), (AA)₄₅-*b*-(DEAAm)₃₆₀, diblock copolymer, synthesized via sequential anionic polymerization, exhibits interesting ‘schizophrenic’ micellization behavior in response to temperature, to pH, and to added salt. Due to its asymmetric composition, two opposite micellar structures were expected and investigated by DLS/SLS, SANS, and cryo-TEM investigations. For pH > 7, the block copolymer is molecularly dissolved and spherical PDEAAm-core micelles ($\langle R_h \rangle_z = 23$ nm, $N_{\text{agg}} = 54$, $\langle R_g \rangle_z / \langle R_h \rangle_z = 0.77 \pm 0.19$) are formed upon heating the solution above the cloud point ($T_c \approx 35$ °C). Crew-cut morphology is observed and the PAA-corona thickness can be easily tuned by variation of both pH and ionic strength. This elegant procedure allows the easy formation of crew-cut micelles made of a glassy PDEAAm-core ($T_g = 85.5$ °C) without the use of intermediate solvents or dialysis procedure. For pH ≤ 4, a turbid solution containing ‘inverse’ PAA-

core star-like micelles are observed at room temperature ($\langle R_h \rangle_z \approx 50$ nm, $N_{\text{agg}} = 69 \pm 5$). Upon heating the solution above T_c , a macroscopic phase separation occurs.

5.1 Introduction

In the recent years, the interest in stimuli-responsive water-soluble materials has increased considerably due to their intrinsic properties, and to the increasing demands of water-based applications instead of traditional solvent-based technologies.¹⁻⁵ Among the wide variety of stimuli to which a so-called ‘smart’ compound can respond,⁶ the thermo- or pH-responsive copolymers are of importance because their applications cover a wide range of domains related to the environment, biochemistry, and medicine. They can be used in various separation techniques,⁷⁻⁹ for biological molecules recognition,¹⁰⁻¹² as protein- or drug-conjugates in therapeutics,¹³⁻¹⁶ or as biomedical implants.² Such polymers are often constituted of a monomer exhibiting a lower critical solution temperature (LCST), and/or hydrophilic neutral or ionic (or ionizable) monomers.^{17,18}

Aqueous solutions of polymers with an LCST are characterized by a phase separation upon heating. Below the LCST the solution is homogeneous and transparent, but when the temperature exceeds the critical value, called the cloud point, a macroscopic phase separation occurs. The LCST corresponds to the minimum of the phase diagram.^{19,20} The most studied thermo-responsive polymer is poly(*N*-isopropylacrylamide) (PNIPAAm),^{21,22} but other poly (*N*-alkylacrylamide)s polymers also undergo a coil-to-globule phase transition above their respective LCST. Homopolymers of *N,N*-diethylacrylamide (DEAAm) have a cloud point at 32 °C when synthesized via free-radical polymerization (atactic polymer).²³ PDEAAm of high stereoregularity synthesized via anionic polymerization may lose their LCST behavior. Indeed, highly syndiotactic PDEAAm made by anionic polymerization was reported not to be soluble in water.²⁴ In contrast, Freitag et al.^{25,26} mentioned that the highly syndiotactic PDEAAm synthesized by Group Transfer Polymerization (GTP) exhibits an LCST at 30 °C. It denotes the importance on the choice of initiator, additive, and solvent on the microstructure and therefore on the solution properties of the final product.

On the other hand, pH-responsive compounds may include all the copolymers containing weak polyelectrolyte segments, and they are also sensitive to the ionic strength

of the solution.²⁷ The charges along the chain lead to complex intra- and intermolecular interactions that have strong impact on structural, dynamic and rheological properties of the system.²⁸

The association properties of copolymers of different architectures has been investigated but most attention was devoted to amphiphilic block copolymers since their structure mimics the low-molecular weight surfactants.²⁹ Similarly to those, amphiphilic block copolymers self-assemble in aqueous solutions.³⁰ In most cases, the association phenomenon leads to the formation of micellar aggregates of different shape or to vesicles which can be in dynamic equilibrium with non-associated copolymer molecules (unimers) if the hydrophobic block has a low glass transition temperature, T_g , and is short enough. If the corona-forming soluble block is much longer than the core-forming block, the aggregates are spherical and are called ‘star’ micelles. In the opposite case, when the corona-forming block is much shorter, ‘crew-cut’ micelles are formed.³¹

The term schizophrenic denotes the ability of such AB block copolymers to form either A-core or inverse B-core micelles by varying the pH, and/or the temperature. This remarkable property was introduced by Armes and coworkers for ‘smart’ pH-dependent micelles of poly[2-(diethylamino)ethyl methacrylate]-*block*-poly[2-(*N*-morpholino)ethyl methacrylate] copolymer synthesized by Group Transfer Polymerization (GTP),^{32,33} and poly(4-vinyl benzoic acid)-*block*-PDEAEMA copolymer synthesized by Atom Transfer Radical Polymerization (ATRP).³⁴ By combining both effects, namely the sensitivity to the pH and the temperature, it is possible to obtain double stimuli-responsive materials whose macroscopic properties can be controlled at the microscopic level by modifying the structure and composition of the polymeric chains, as well as the two external stimuli. Depending on the pH and the temperature, poly(propylene oxide)-*block*-PDEAEMA (PPO-*b*-PDEAEMA) can exist in aqueous solution as molecularly dissolved copolymer, PDEAEMA-core micelles and PPO-core inverse micelles.³⁵ Similarly, double-thermo-responsive block copolymers made of NIPAAm and 3-[*N*-(3-methacrylamidopropyl)-*N,N*-dimethyl]ammonio propane sulfonate (SPP) synthesized via Radical Addition Fragmentation Transfer polymerization (ATRP) were reported by Laschewsky et al. where two kinds of micelles can be formed by tuning the solution temperature.³⁶ Recently, the synthesis of poly[2-(*N*-morpholino)ethyl methacrylate]-*block*-poly[sulfobetainized 2-

(dimethylamino)ethyl methacrylate] copolymer (PMEMA-*b*-PSDMAEMA) was reported via GTP and the authors claimed the possible application as polymeric surfactant, where the molecularly dissolved block copolymer ($30\text{ }^{\circ}\text{C} < T < 40\text{ }^{\circ}\text{C}$) could form either direct PSDMAEMA-core ($T < 10\text{ }^{\circ}\text{C}$), or inverse PMEMA-core micelles ($T > 50\text{ }^{\circ}\text{C}$).³⁷

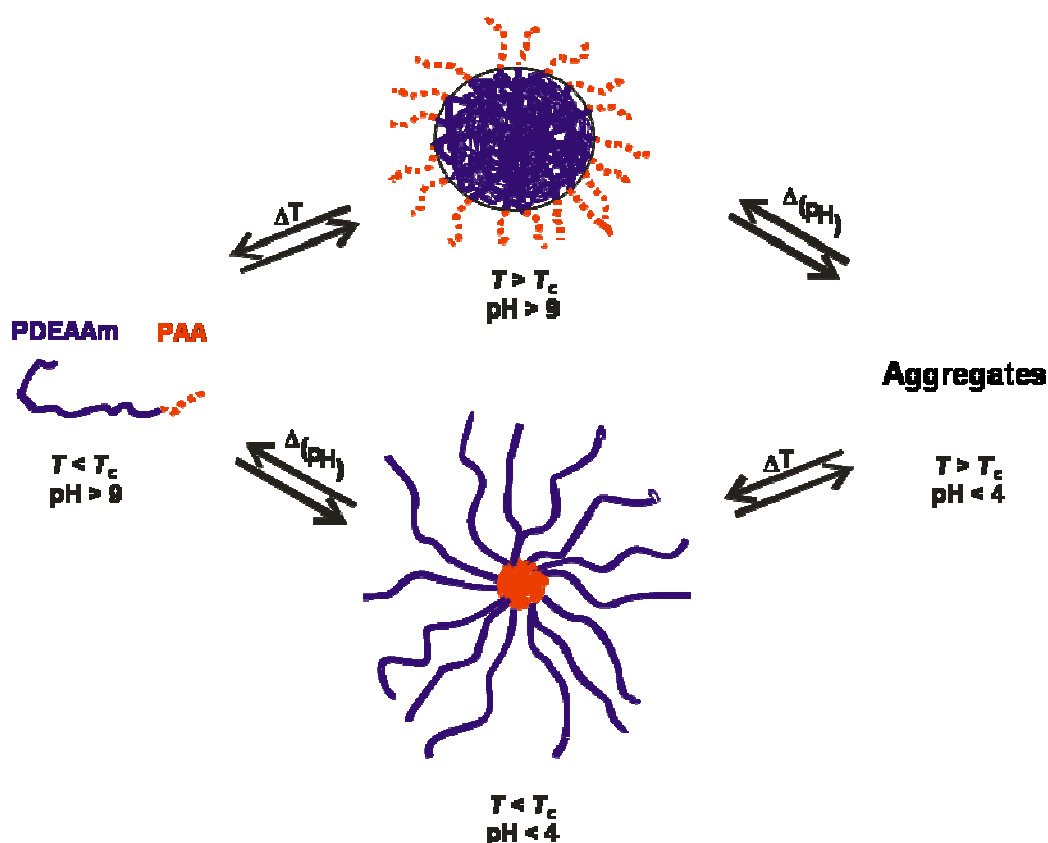


Figure 5-1. Modes of micelle formation for poly(acrylic acid)₄₅-*block*-poly(*N,N*-diethylacrylamide)₃₆₀ in aqueous solution depending on the pH and temperature.

Recently we proposed a new strategy to synthesize PDEAAm, poly(*tert*-butyl acrylate)-*block*-PDEAAm (PtBA-*b*-PDEAAm), and poly(*tert*-butyl methacrylate)-*block*-PDEAAm (PtBMA-*b*-PDEAAm) by anionic polymerization in the presence of Et₃Al.³⁸⁻⁴⁰ The PDEAAm blocks obtained by this method are rich in heterotactic (rm, mr) triads and undergo a coil to globule transition at ca. 31 °C. After hydrolysis of the PtBA or PtBMA block, poly(acrylic acid)-*block*-PDEAAm and poly(methacrylic acid)-*block*-PDEAAm (PAA-*b*-PDEAAm, PMAA-*b*-PDEAAm) were successfully obtained. Preliminary results

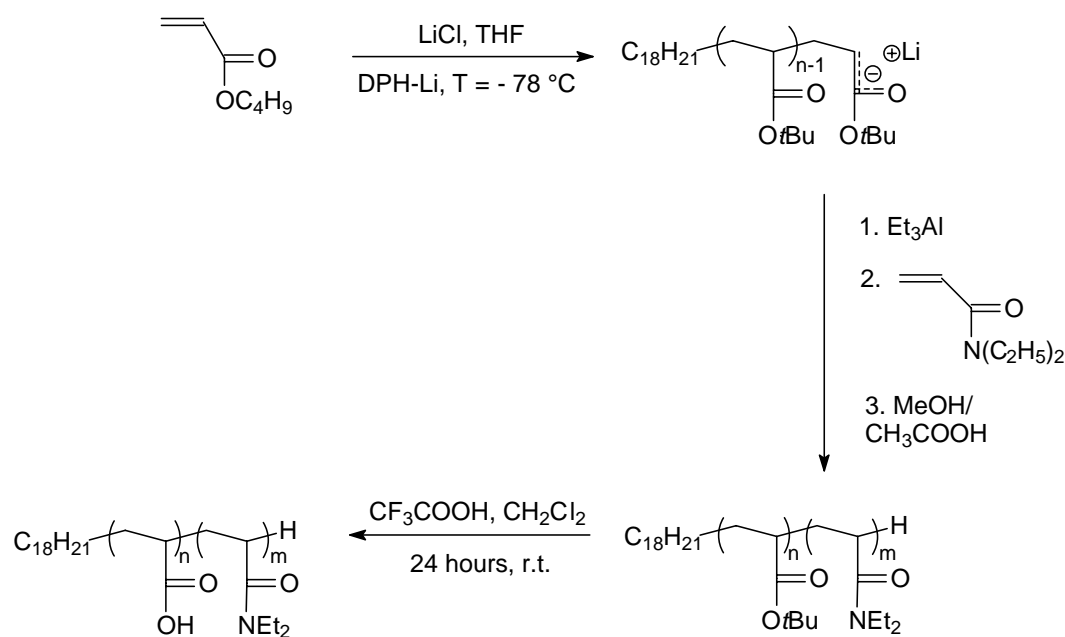
on the pH- and thermo-responsive behavior of PAA-*b*-PDEAAm copolymer in aqueous solution were reported.⁴¹ Because the asymmetric composition of the diblock copolymers synthesized (Figure 5-1), it can form in water either core-cut PDEAAm-core micelles, or inverse star-like PAA-core micelles, depending on both the pH and the temperature. This remarkable behavior corresponds to the various types of schizophrenic micelles reported by Armes et al.

In the present contribution, we report the complete characterization of the bishydrophilic poly(acrylic acid)-*block*-poly(*N,N*-diethylacrylamide) which can exist in four states in aqueous solution, depending on both the temperature and the pH, namely, micelles, inverse micelles, aggregates, and molecularly dissolved chains (unimers), as it shown in Figure 5-1. The influence of the added salt is also investigated. Static and Dynamic Light Scattering methods (SLS, DLS), NMR, Small-angle neutron scattering (SANS) as well as cryogenic Transmission Electron Microscopy (cryo-TEM) experiments are performed under various conditions and the results obtained from different techniques discussed and compared.

5.2 Experimental Part

Materials. Poly(acrylic acid)-*block*-poly(*N,N*-diethylacrylamide) (PAA-*b*-PDEAAm) was prepared via sequential anionic polymerization of *tert*-butyl acrylate and DEAAm using the synthetic strategy reported elsewhere (Scheme 5-1).⁴¹ NaCl (Fluka) was used as received. DCl (35 wt.-% in D₂O, 99 atom D-%), NaOD (30 wt.-% in D₂O, 99 atom D-%), α,α,α -tris-(hydroxymethyl)-methylamin (TRIS, 99.8+%), and tris(hydroxymethyl)-aminomethane hydrochloride (TRIS·HCl, reagent grade) were purchased from Aldrich and used as received.

Scheme 5-1. Synthetic strategy for the synthesis of well-defined poly(acrylic acid)₄₅-*block*-poly(*N,N*-diethylacrylamide)₃₆₀ copolymer



Characterizations methods. ¹H NMR spectra were recorded on a Bruker AC-250 spectrometer in D₂O at different temperatures (25 to 50 °C). The pH of the deuterated solution was adjusted by adding dropwise concentrated NaOD or DCl solutions.

Differential Scanning Calorimetry measurement was performed on a Perkin Elmer DSC 7 equipped with a CCA 7 liquid nitrogen cooling device. The instrument was calibrated using *n*-decane and tin as references. The measurement was carried out from 20 to 300 °C

at a scanning rate of $10 \text{ K}\cdot\text{min}^{-1}$. The heating trace corresponds to the second heating run in order to exclude effects resulting from any previous thermal history of the sample.

Micro-Differential Scanning Calorimetry measurements were performed on a Micro-DSC instrument (Setaram, France). The samples were sealed in ca. 1 mL aluminum pans. As reference a sealed pan with the same amount of water was used. The DSC thermograms were recorded in the temperature range 20-50 °C (scanning rate = $0.1 \text{ K}\cdot\text{min}^{-1}$).

Surface tension was measured on a Lauda tensiometer (platinum ring method). The platinum ring was annealed with a Bunsen burner prior to each measurement in order to ensure wetting by the aqueous solutions. The block copolymer was dissolved in freshly prepared 0.1 N NaOH solution (Merck, Titrisol, pH = 12-13). All solutions were kept at room temperature for 48 h prior to measurement. Each sample was measured three times at $T = 23 \text{ °C}$, and the deviation of each measurement ranged within $0.2 \text{ mN}\cdot\text{m}^{-1}$.

Size Exclusion Chromatography (SEC) measurements were performed at various temperatures (23-40 °C) using a Gynkotek Pump, a Jasco UV-III detector (270 nm), and a Bischoff RI-71 detector. Two PL Aquagel-OH columns (300 x 8 mm, 8 μm): Mixed, and 30 (Polymer Laboratory, Birmingham, United Kingdom) were used. 20 μL of a 0.3 wt.-% copolymer solution were injected at an elution rate of $1.0 \text{ mL}\cdot\text{min}^{-1}$ in a NaN_3 ($0.05 \text{ mol}\cdot\text{L}^{-1}$) / NaH_2PO_4 ($0.2 \text{ mol}\cdot\text{L}^{-1}$) aqueous solution (pH = 7). Poly(methacrylic acid) standards (PSS, Mainz, Germany) were used to calibrate the columns. Internal standard was ethylene glycol.

Small-Angle Neutron Scattering (SANS). Sample solutions for SANS experiments were prepared by dissolving the copolymer in D_2O solutions of DCl (pH = 1.0), TRIS·HCl (pH = 3.6), TRIS/TRIS·HCl 1:1 (pH = 7.7), TRIS (pH = 8.6), and NaOD (pH = 12.7). The typical copolymer concentration was $c = 1.4\text{-}1.5 \text{ g}\cdot\text{L}^{-1}$. The ionic strength was adjusted by adding NaCl. The solutions were stirred at 23 °C for two days prior to the measurement. For pH above 7, the prepared solutions were homogeneous and transparent. For pH below 7, the solutions were turbid. The sample solutions were put into quartz cells with 2 mm path length (Hellma). Prior to measurements the pH of the different solutions was measured using a SCHOTT pH-meter equipped with a glass electrode calibrated with two standard buffer solutions (pH = 4.0 and pH = 10.0). The experiments were carried out at the Institute Max von Laue-Paul Langevin (ILL, Grenoble, France) using the beamline D11. The neutron wavelength was 6 Å, and sample-to-detector distances of 1.1, 4, and 16

m were employed. A total range of the magnitude of the scattering vector, $q = 0.003\text{--}0.45 \text{ \AA}^{-1}$, was covered. The detector sensitivity and the intensity of the primary beam were calibrated by a comparison with the scattering from a 1 mm reference sample of water. The obtained data were radially averaged, corrected for the detector background, the detector dead time, and the scattering from an empty cell, using the GRASP software, version 3.66. Then, they were converted into absolute units by a comparison with the scattering from water.⁴² It should be noted that the SANS curves presented in this study still contain the incoherent background scattering of the solvent and the sample.

Static Light Scattering (SLS). The absolute weight average molecular weight, M_w , the radius of gyration, R_g , and the second virial coefficient, A_2 , were determined by Static Light Scattering (SLS). The dialysis of the (AA)₄₅-*b*-(DEAAm)₃₆₀ copolymer was carried out with a Spectra/Por[®] membrane having 1000 Da as molecular mass cut-off. 1 L of a 0.1 N NaOH (Titrisol, Merck) was prepared on the starting day of the dialysis using fresh Milli-Q water and the concentration of NaCl was adjusted to $0.1 \text{ mol}\cdot\text{L}^{-1}$ to give the solution A. The membrane was firstly conditioned for 1 hour with 50 mL of the solution A, and rinsed with abundant Milli-Q water. The appropriate amount of (AA)₄₅-*b*-(DEAAm)₃₆₀ copolymer (107.4 mg, $4.230 \text{ g}\cdot\text{L}^{-1}$) was dissolved in the proper amount of solution A. 25 mL of this solution were placed inside the dialysis membranes, hermetically closed and kept immersed in the rest of solution A (0.9 L). This system was bubbled with nitrogen for 1 hour and hermetically closed, and stirred for 6 days at 23 °C. The dialyzed solution (inside the membrane) was employed as stock solution, using the solution outside the membrane as solvent to prepare the samples of different concentrations for SLS measurements ($c = 0.94, 1.25, 1.77, 2.46, 4.23 \text{ g}\cdot\text{L}^{-1}$). The refractive index increment (dn/dc) of the copolymer solution was measured on a Chromatix KMX-16 interferometer using a He/Ne laser at $T = 45 \text{ °C}$ against the dialysate. Prior to light scattering measurements, the sample solutions were filtered using a $0.45 \text{ }\mu\text{m}$ Teflon filter. The measurements were carried out on an ALV DLS/SLS-SP 5022F compact goniometer system with an ALV 5000/E correlator equipped with a He/Ne laser ($\lambda = 632.8 \text{ nm}$) and an avalanche diode at 45 °C. Data processing was performed using the ALV/ Static and Dynamic FIT and PLOT 4.23 software. In the range of diluted solutions, the excess scattering intensity ($I - I_{\text{solvent}}$) is generally expressed in a reduced form (Equation 5-1).

$$\frac{Kc}{R_\theta} = \left(\frac{1}{M_w} + 2A_2c \right) \left(1 + \frac{q^2}{3} \langle R_g^2 \rangle_z \right) \quad (5-1)$$

where $R_\theta = R_{\text{tol}} \cdot [(I - I_{\text{sol}})/I_{\text{tol}}]$ is the Rayleigh ratio determined using toluene as a reference,⁴³ c is the copolymer concentration. The magnitude of the scattering vector q , and the optical constant K are defined as,

$$q = \frac{4\pi n_0 \sin(\theta/2)}{\lambda_0} \quad (5-2)$$

$$K = \frac{4\pi^2 n_0^2 (dn/dc)^2}{\lambda_0^4 N_A} \quad (5-3)$$

where n_{tol} and n_0 are the refractive index of toluene and water 1.494, and 1.332, respectively, N_A is the Avogadro's number, λ_0 is the wavelength of the laser (632.8 nm), and θ is the scattering angle (30-150°). Finally, the Zimm procedure has been used to determine M_w , R_g , and A_2 .⁴⁴

Dynamic Light Scattering (DLS). Sample solutions for DLS experiments were prepared by dissolving the (AA)₄₅-*b*-(DEAAm)₃₆₀ copolymer in freshly prepared solutions in the range, 3.9 < pH < 12.7, using MilliQ water. The typical copolymer concentration was 0.9-1.3 g·L⁻¹. The copolymer solutions at different pH (1.0-12.7) were prepared by direct dissolution in fresh MilliQ H₂O at $T = 23$ °C in the presence of NaCl. The salt concentration, NaCl, was varied in the range 0.1-1.0 mol·L⁻¹. The solutions were stirred two days at 23 °C. Depending on the pH value, clear or turbid solutions were obtained. The clear copolymer solutions were filtered using a 0.45 μm Nylon filter, whereas turbid ones were not filtered. The z -average hydrodynamic radii, R_h , of the micelles were determined at different temperatures by DLS using an ALV DLS/SLS-SP 5022F compact goniometer system with an ALV 5000/E correlator equipped with a He/Ne laser ($\lambda = 632.8$ nm) and an avalanche diode. The autocorrelation function, $g_2(t)$, of the scattered light was analyzed using the regularized fit ALV-software to obtain the mean decay rate Dq^2 for each

measurement, where D is the mean diffusion coefficient of the micelles and q the scattering vector (Equation 5-2). The obtained intensity autocorrelation functions, $g_2(t)$, were converted to decay rate distributions, $G(\Gamma)$, via the CONTIN procedure^{45,46} according to the following equation:^{47,48}

$$g_2(t) - 1 = \left(\int_{\Gamma_{\min}}^{\Gamma_{\max}} e^{-\Gamma t} G(\Gamma) d\Gamma \right)^2 \quad (5-4)$$

This analysis yields a discrete, intensity-weighted distribution function of logarithmically equidistantly spaced decay times ($\tau = 1/\Gamma$). The mean hydrodynamic radius (R_h) was calculated using the Stokes-Einstein equation (Eq. 5-5):

$$R_h = \frac{kT}{6\pi\eta_0 D} \quad (5-5)$$

where k is the Boltzmann constant, T the absolute temperature, and η_0 the viscosity of H₂O or D₂O at the temperature T .

Cryogenic Transmission Electron Microscopy (Cryo-TEM). Sample solutions for cryo-TEM experiments were prepared by dissolving the (AA)₄₅-*b*-(DEAAm)₃₆₀ copolymer in a freshly-prepared aqueous NaOH solution (Titrisol Merck 1N) and in a Certipur Merck buffer solution (pH = 4). No salt was added. The solutions were stirred at 23 °C for two days prior to the measurement. For pH = 12.6, the solution was homogeneous and transparent ($c = 4.9 \text{ g}\cdot\text{L}^{-1}$), whereas the solution at pH = 4.0 was slightly turbid ($c = 2.1 \text{ g}\cdot\text{L}^{-1}$). A drop of each sample was put on a holey carbon filmed copper grid (Quantifoil R2/2, Quantifoil Micro Tools GmbH, Jena, Germany), where most of the liquid was removed with blotting paper leaving a thin film stretched over the grid holes. The specimens were instantly vitrified by rapid immersion into liquid ethane and cooled to approximately 90K by liquid nitrogen in a temperature-controlled freezing unit (Zeiss Cryobox, Zeiss NTS GmbH, Oberkochen, Germany). The temperature was monitored and

kept constant in the chamber during all the sample preparation steps. After freezing the specimens, the remaining ethane was removed using blotting paper. The specimen was inserted into a cryotransfer holder (CT3500, Gatan, München, Germany) and transferred to a Zeiss 922 OMEGA EFTEM (Zeiss NTS GmbH, Oberkochen, Germany) operated at an acceleration voltage of 200 kV. Examinations were carried out at temperatures around 90K. Zero-loss filtered images ($\Delta E = 0$ eV) were taken under reduced dose conditions ($100 - 1000 \text{ e} \cdot \text{nm}^{-2}$). All images were registered digitally by a bottom mounted CCD camera system (Gatan, Ultrascan 1000) combined and processed with a digital imaging processing system (Gatan, Digital Micrograph 3.9 for GMS 1.4).

Conventional TEM was performed on the same instrument by negative staining with uranyl acetate on a carbon-coated copper grid. (Mesh size 200, Science Service München, Germany).

5.3 Results and Discussion

In the following, the solutions properties of the $(AA)_{45}\text{-}b\text{-(DEAAm)}_{360}$ block copolymer is discussed. As reported before,⁴¹ the polymer has $M_n = 49,300$ (MALDI-TOF mass spectrometry) and $M_w/M_n = 1.12$ (SEC in NMP). As stated before, such double-stimuli block copolymer can exist in four states in aqueous solution. Figure 5-1 shows the possible modes of aggregate formation for the PAA-*b*-PDEAAm in dependence of pH and temperature. The different states are accompanied by a change of the macroscopic appearance of the solution as it is shown in Figure 5-2.

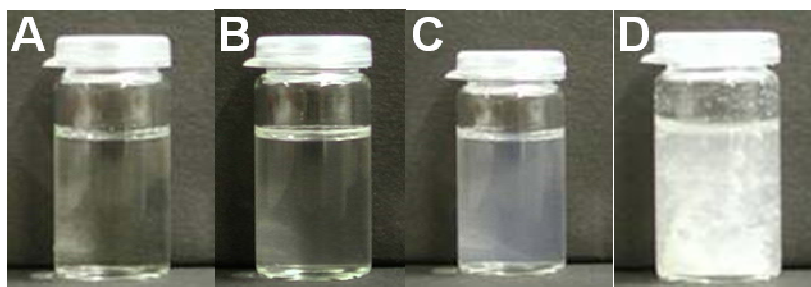


Figure 5-2. $(AA)_{45}\text{-}b\text{-(DEAAm)}_{360}$ in aqueous solution at pH = 12.0 at $T = 23$ (A) and 45 °C (B) ($c = 1.3 \text{ g} \cdot \text{L}^{-1}$), and pH = 3.9 at $T = 23$ (C) and 45 °C (D) ($c = 0.9 \text{ g} \cdot \text{L}^{-1}$).

Aqueous solutions at $T = 23\text{ }^{\circ}\text{C}$.

(i) **Characterization of the unimers at $\text{pH} \geq 8$.** Dynamic Light Scattering (DLS) was previously used for the characterization of the coil-to-globule transition of PNIPAAm⁴⁹⁻⁵¹ and PDEAAm in aqueous solutions.⁵² At $T = 21\text{ }^{\circ}\text{C}$, the solution is clear and transparent (Figure 5-2A). DLS results indicate the coexistence of two species, one with $R_h = 4\text{ nm}$, attributed to unimer and one with $R_h = 98\text{ nm}$, attributed to loose aggregates (see Figure 4-4).⁴¹ As it is shown in Figure 5-3, no angular dependence of the value, $R_h = 4\text{ nm}$, attributed to unimers is observed, indicating that, as expected, the molecules are in the Rayleigh scattering region (diameter $< \lambda/20$).⁴⁴ In order to eliminate the influence of form factors for large molecules, the R_h values measured at different angles have to be extrapolated for $q^2 \rightarrow 0$. Only a very weak angular dependence of the peak is observed. This peak may be attributed to the correlation due to interaction of polyelectrolytes molecules ('slow modes').

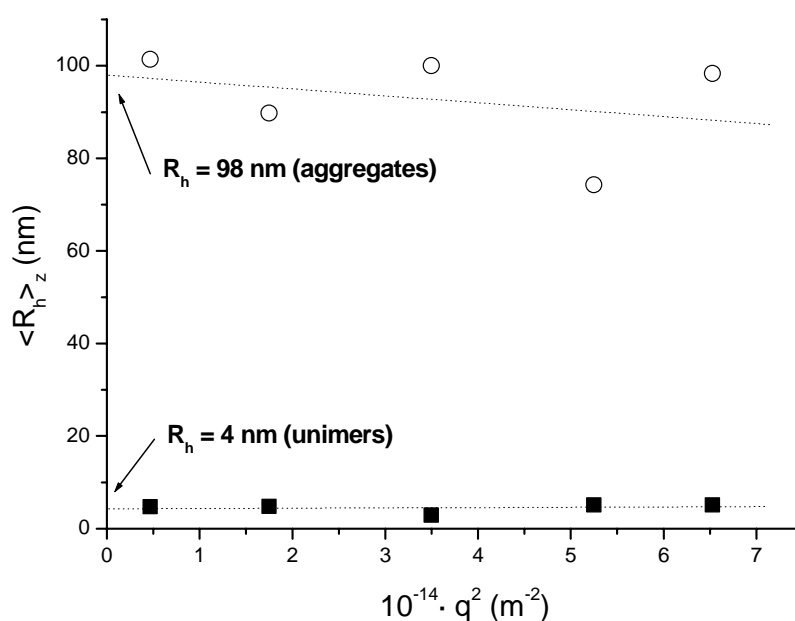


Figure 5-3. Angular dependence of the z -average hydrodynamic radius, $\langle R_h \rangle_z$, of the aggregates (—), and of the unimers (!) at $T = 21\text{ }^{\circ}\text{C}$ (CONTIN analysis, $c = 1.3\text{ g}\cdot\text{L}^{-1}$, $\text{pH} = 12.8$, $[\text{NaCl}] = 0.1\text{ mol L}^{-1}$).

At $T < T_c$, the presence of aggregates is not well understood because the poly(sodium acrylate) can not lead to the formation of hydrogen bonds (no δ^+ proton). It is clear that the amide groups of PDEAAm can only be acceptor in contrast to those of PNIPAAm, which can be proton donor as well as proton acceptor.⁵³ The C_{18} hydrophobic end group of the block copolymer (see Scheme 5-1) as well as the intrinsic difference of hydrophilicity between the poly(*N,N*-diethylacrylamide) and the poly(sodium acrylate) blocks may play roles in the aggregate formation. Nevertheless, since the CONTIN analysis renders intensity-weighted distributions, the amount of large particles is strongly exaggerated (see Figure 4-4), as the scattering intensity is strongly dependent on the radius of the particle ($\sim R^6$ for spherical particles) and their weight fraction is actually rather small (0.05 wt.-%).

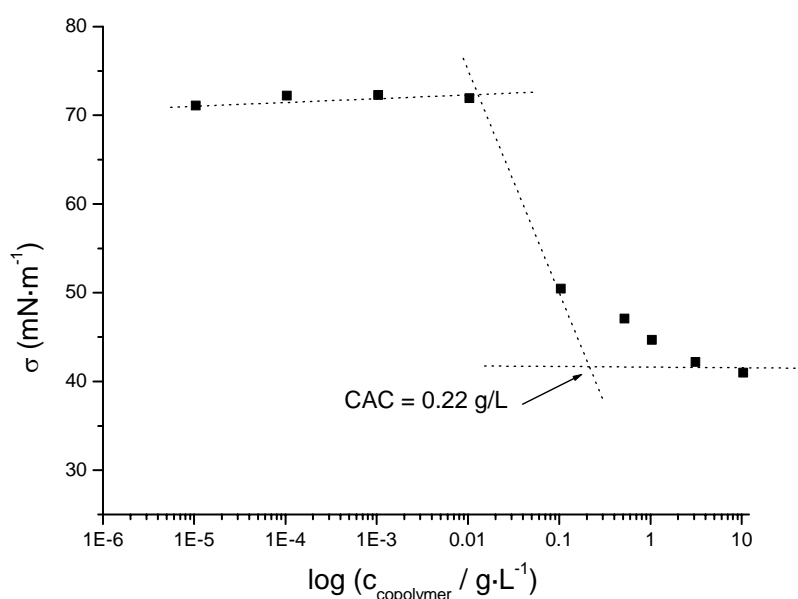


Figure 5-4. Surface tension measurement at 23 °C in 0.1N NaOH solution (pH = 12, without added salt).

To further elucidate this experimental observation, surface tension measurements were performed at room temperature (Figure 5-4). A lowering of the surface tension is observed indicating the presence of a surface active macromolecule. At a concentration of $c = 0.22 \text{ g L}^{-1}$ the graph shows a kink typical for Critical Aggregation Concentrations (CAC). We expect that upon reaching this value loose aggregates are being formed, which may explain

the observation of a peak in the CONTIN plot (see figure 4-4) at higher radius. The formation of these assemblies may be induced by the presence of a hydrocarbon C_{18} initiator fragment attached to the PAA segment. Certainly, this strongly hydrophobic moiety increases the surface activity and the aggregation tendency of the bishydrophilic block copolymers.

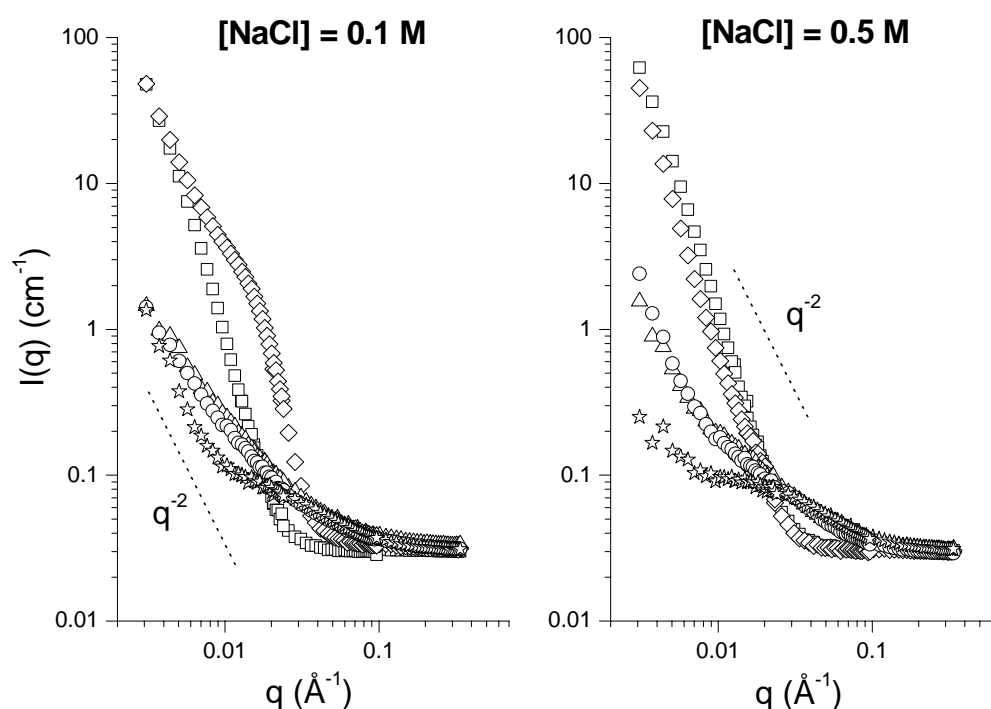


Figure 5-5. SANS curves at $T = 23$ °C for the $(AA)_{45}\text{-}b\text{-(DEAAm)}_{360}$ in aqueous solutions at different salt concentrations: pH = 1.0 (∇), 3.6 (M), 7.7 (8), 8.6 (v), and 12.7 (ψ). Experimental conditions: $c = 1.4\text{-}1.5$ $\text{g}\cdot\text{L}^{-1}$.

At room temperature ($T = 23$ °C, full symbols) and $\text{pH} \geq 7.7$, the SANS curves do not show any defined structure and a strong upturn is observed in the low q region (Figure 5-5). It could be due either due to the presence of large residual particles or to critical scattering. This effect was reported for other polyelectrolytes systems.^{54,55} Fitting the log-log plot of the scattering profiles at low q , slopes of -1.4, -1.4 and -2.2 are calculated for pH = 7.7, 8.6 and 12.7, respectively with the lowest salt concentration. Theoretically, the

slope or fractal exponent corresponding to linear Gaussian chains in solution is 2.⁵⁶ Thus, there is no need to use more complicated models to describe the system under these conditions. The experimental results also indicate that the larger aggregates are more present at lower pH value, suggesting that their formation is ruled by the lower ionization degree of the PAA block and is not due to correlation of PAA chains.

In the range of dilute solutions the overall apparent radius of gyration $R_{g,app}$, and the apparent particles molecular weight, $M_{w,app}$, can be extrapolated from the scattering intensity in the low q range, using the Guinier method⁵⁷ (Equations 5-6 and 5-7),

$$I(q) = I(0) \cdot e^{-q^2 R_{g,app}^2 / 3} \quad (5-6)$$

$$M_{w,app} = \frac{I(0) \rho_{Polymer}^2 N_A}{(\rho_P - \rho_S)^2 c} \quad (5-7)$$

where $I(0)$ is the scattered intensity extrapolated at $q \rightarrow 0$, c is the copolymer concentration, ρ_S and ρ_P being the solvent and polymer scattering length densities, respectively, $\rho_{polymer}$ the polymer density ($1.1 \text{ g}\cdot\text{L}^{-1}$). The following scattering length densities were used $\rho_S = 63.7 \cdot 10^9 \text{ cm}^{-2}$ for D_2O , and $\rho_P = 6.42 \cdot 10^9 \text{ cm}^{-2}$, $6.22 \cdot 10^9 \text{ cm}^{-2}$, $1.30 \cdot 10^{10} \text{ cm}^{-2}$, for the diblock copolymer, the PDEAAm block, and the C_{18} -PAA block, respectively (see Scheme 5-1).

The Guinier procedure in the linear region ($2 \cdot 10^{-4} < q^2 < 6 \cdot 10^{-4} \text{ \AA}^{-2}$, see Figure 5-19 in Supporting Information) renders a consistent molecular weight of $4.4 \cdot 10^4 \text{ g}\cdot\text{mol}^{-1}$ and a gyration radius, $R_g = 4 \text{ nm}$ for the sample where no upturn is observed ($\text{pH} = 12.7$, $[\text{NaCl}] = 0.5 \text{ mol}\cdot\text{L}^{-1}$). This value can be correlated to the values obtained by DLS, which were attributed to unimers. Additionally, the M_w can be easily compared to the value obtained by MALDI-TOF mass spectrometry ($N_{agg} \sim 1$, Table 5-1). The addition of salt tends to destroy the aggregates whose presence can be explained by the insufficient screening of the negative charges on the PAA segment. For lowest salt concentration, a surprisingly low M_w of $1.2 \cdot 10^4 \text{ g}\cdot\text{mol}^{-1}$ is found, due possibly to electrostatic repulsive interactions which

tend to decrease the scattering intensity. The strong upturns are due to the presence of a small amount of larger entities. By decreasing the pH of the solution, the PAA segment becomes less ionized and the scattering intensity increases suggesting the formation of larger structures which are discussed below. Furthermore, the addition of salt has no effect on the scattering curves and their formation can be assumed firstly to be ruled by another driving force.

Table 5-1. Radius of gyration, molecular weight, and aggregation number obtained from SANS data evaluation at different pH and salt concentrations at $T = 23\text{ }^{\circ}\text{C}$

pH	[NaCl] = 0.1 mol·L ⁻¹			[NaCl] = 0.5 mol·L ⁻¹		
	$R_{g,app}^a$ (nm)	$10^{-5} \cdot M_{w,app}^b$ (g·mol ⁻¹)	N_{agg}^c	$R_{g,app}^a$ (nm)	$10^{-5} \cdot M_{w,app}^b$ (g·mol ⁻¹)	N_{agg}^c
12.7	4.6	(0.11)	-	4.0	0.44	1
8.6	6.7	0.80	1	6.3	0.73	1
7.7	6.8	0.89	~1	6.3	0.81	1
3.6	12.6	27.2 ^d	697 ^e	9.8	2.52 ^d	65 ^e
1.0	10.6	2.67 ^d	68 ^e	10.8	2.88 ^d	74 ^e

^a Calculated from the slope of the Guinier plots, $\ln I(q)$ vs q^2 to $q^2 \rightarrow 0$, maximum relative error = $\pm 35\%$ (Figure 5-19 in Supporting Information). ^b Calculated from the intercept of the Guinier plots, $I(0)$, using the scattering length density of the diblock copolymer, $\rho_p = 6.42 \cdot 10^9\text{ cm}^{-2}$, maximum relative error = $\pm 11.6\%$. ^c Aggregation number, $N_{agg} = M_{w,app} / M_{w,unimer}$, $M_{w,MALDI} = 56,300\text{ g}\cdot\text{mol}^{-1}$ for PANa-*b*-PDEAAm. ^d Calculated from the intercept of the Guinier plots, $I(0)$, using the scattering length density of the PAA block copolymer, $\rho_p = 1.30 \cdot 10^{10}\text{ cm}^{-2}$, maximum relative error = $\pm 6.9\%$. ^e Aggregation number, $N_{agg} = M_{w,app} / M_{w,PAA}$, $M_{w,PAA} = 3,900\text{ g}\cdot\text{mol}^{-1}$.

(ii) Characterization of the star-like micelles at pH ≤ 4 . Under acidic conditions, the solution is turbid at $20 \leq T \leq 35\text{ }^{\circ}\text{C}$ ($T < T_c$) as it is shown in Figure 5-2C. Polydisperse ‘inverse’ micelles ($R_h = 40\text{-}50\text{ nm}$) were observed by DLS suggesting eventually the presence of different assemblies (see Figure 4-5).⁴¹ We attributed them to inverse star-like PAA-core micelles stabilized by a corona made of a long PDEAAm block. As expected from the asymmetric composition of the block copolymer, the inverse PAA-core micelles

observed are larger than the PDEAAM-core micelles (about twice the size of the PDEAAM-core micelles). The values observed for R_h of these entities are clearly q -dependent and a hydrodynamic radius of 47 nm can be extrapolated to $q^2 \rightarrow 0$ (Figure 5-6). The corresponding CONTIN plot at $\theta = 90^\circ$ is shown in Figure 4-5. They coexist with larger aggregates ($R_h > 300$ nm) responsible for the turbidity.⁴¹ The formation of the inverse PAA-core micelles may be attributed either to the intrinsic difference of hydrophilicity between the poly(*N,N*-diethylacrylamide) and the poly(acrylic acid) blocks or the C₁₈ initiating hydrophobic fragment or a combination of both effects. In addition, the high local concentration of the incompatible segments might lead to microphase separation even in solution.

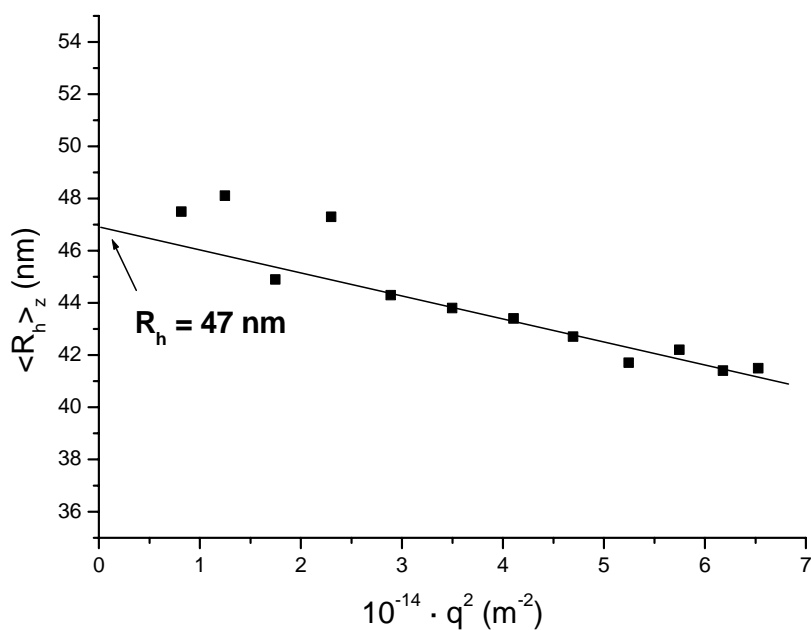


Figure 5-6. Angular dependence of the z -average hydrodynamic radius, $\langle R_h \rangle_z$, of the peak attributed to the inverse star-like PAA-core micelles at $T = 20$ °C (CONTIN analysis, $c = 0.9 \text{ g}\cdot\text{L}^{-1}$, $\text{pH} = 3.9$, $[\text{NaCl}] = 0.1 \text{ mol}\cdot\text{L}^{-1}$).

At $\text{pH} \leq 4$, the SANS scattering intensity at $T = 23$ °C shown in Figure 5-5 increases by a factor 20 in comparison to that observed for unimers ($\text{pH} \geq 7.7$), suggesting the presence of new structures, larger than the unimers. A Guinier procedure leads therefore to higher

$M_{w,app,core}$ and $R_{g,app}$ assuming that the C₁₈-PAA segments form the core (Table 5-1). The typical Guinier plot $\ln I(q)$ vs. q^2 is shown in Supporting Information (Figure 5-19). The micellar aggregates at $\text{pH} \leq 4$ and at room temperature can be characterized as follow: $R_{g,app} \approx 10\text{-}11$ nm and $M_{w,app,core} = 270,000 \pm 19,000$ g·mol⁻¹. These larger structures are constituted of ca. 69 ± 5 unimers (N_{agg}). These entities correspond to the star-like micelles observed by DLS under the same conditions ($R_h \approx 40\text{-}50$ nm). No influence of the added salt is observed, because all the chains are protonated for $\text{pH} \leq 4$. Furthermore, the ionic strength should not have an influence on the structural parameter of the star-like micelles because the core is assumed to be constituted of PAA chains surrounded by pH-independent PDEAAm corona.

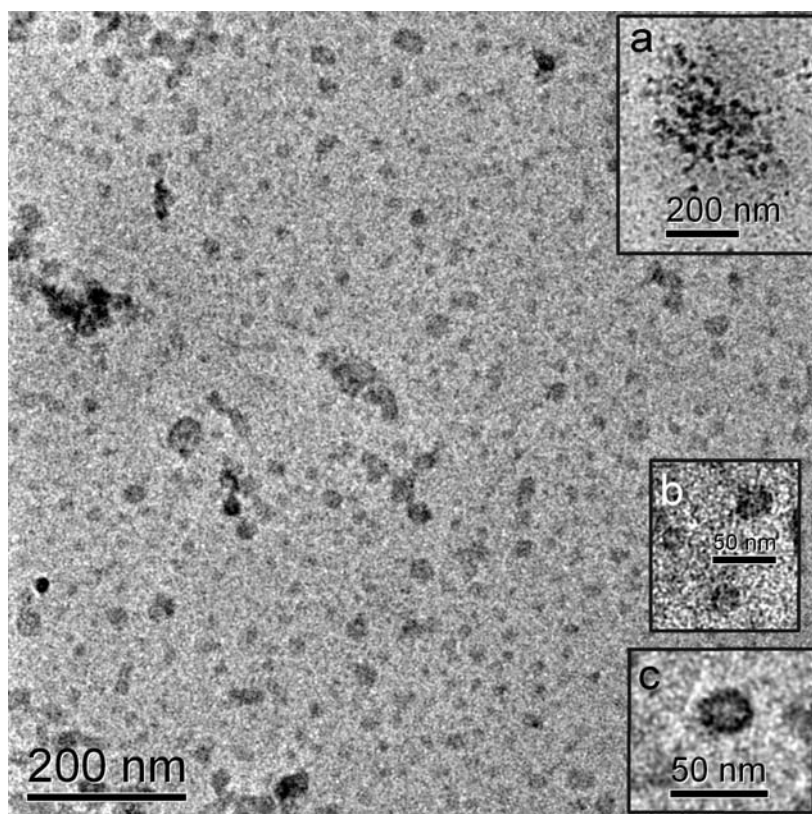


Figure 5-7. Cryo-TEM image taken from the aqueous solution of the (AA)₄₅-*b*-(DEAAm)₃₆₀ at $T = 23$ °C and $\text{pH} = 4.0$ ($c = 2.1$ g·L⁻¹): (a) loose aggregates, (b) PAA-core micelles, (c) PAA-core 'donut' type micelles.

The cryo-TEM micrograph of the (AA)₄₅-*b*-(DEAAm)₃₆₀ copolymer at $T = 23$ °C and $\text{pH} = 4$ (Figure 5-7) shows particles, $10 \leq \text{radius} \leq 15$ nm, which might correspond to the

polydisperse PAA-core micellar aggregates observed by DLS and SANS. These entities coexist with larger aggregates (diameter ≈ 200 nm) also observed in DLS experiments. They may be constituted of micelles which self-assemble to form super-structures. These particles made of a PAA-core show different shapes and no conclusion on the geometry can be drawn due to the low contrast between the PAA-core, the PDEAAm corona and the background of the frozen water. Insert (c) in Figure 5-7 may suggest a ‘donut’ structure where the PAA-core appears with lower contrast, probably due to the presence of water inside the core.

Aqueous solutions at $T = 45$ °C.

(i) Characterization of the PDEAAm crew-cut micelles at $\text{pH} \geq 8$. Under alkaline conditions, the formation of PDEAAm-core micelles is characterized by a slight decrease of the transmitted light at 500 nm (100 to 82%) when the temperature is raised above the LCST of the PDEAAm block (Figures 2A and 2B). This suggests the formation of micelles with PDEAAm forming the core at $T > T_c$ and PAA forming the corona. The thermo- and pH-responsive properties of $(AA)_{45}\text{-}b\text{-(DEAAm)}_{360}$ in aqueous solution were reported in a previous contribution.⁴¹ This elegant strategy allows the formation of crew-cut micelles without the use of intermediate solvents as it was reported in the literature for various block copolymers based on polystyrene-*block*-poly(acrylic acid),^{58,59} poly(ethylene glycol)-*block*-poly(ϵ -caprolactone),⁶⁰ or polystyrene-*block*-poly(vinylpyridinium bromide).⁶¹ The micellization of highly asymmetric block copolymers is complicated and time-consuming, especially when the hydrophobic block is glassy (glass transition temperature, T_g , higher than room temperature) or when the hydrophilic content is too low.^{62,63} In this case, the geometry of the formed supramolecular assemblies (micelles), is closely dependent on the micellization procedure (stirring, heating, or dialysis).⁶⁴ In our case, the T_g of a PDEAAm polymer of similar microstructure was measured by DSC to be 85.5 °C which is between the two reported values for poly(N,N -dibutylacrylamide), $T_g = 60$ °C, and poly(N,N -dimethylacrylamide), $T_g = 89$ °C. The T_g of poly(N -isopropylacrylamide) was found at relatively higher values, $T_g = 124$,⁶⁵ and 130 °C,⁶⁶ due to the possibility in bulk to form hydrogen bonding.

To characterize the simple formation of micelles upon heating a solution containing molecularly dissolved molecules (unimers), aqueous SEC of the copolymer sample was

performed at 24 °C and 40 °C (pH = 7). SEC allows the separation of the compounds according to their hydrodynamic volume and was used to study the micellization in various cases.^{67,68} The formation of micellar aggregates made of similar PAA-*b*-PNIPAAm copolymers synthesized by RAFT polymerization was suggested using aqueous SEC.⁶⁹ Interest was focused on the relative amounts of micelles and non-associated chains (unimers) and their relative size distribution. All these studies remain difficult because the exchange dynamics between unimers and micelles have to be considered. Kinetically frozen systems or systems ruled by slow exchange dynamics give more realistic information.⁷⁰ At 23 °C, only one peak is observed, whereas two peaks were found at 40 °C, namely one in the high molecular weight region and one at the same elution volume as the peak observed at 23 °C (Figure 5-8). This can be attributed to the formation of micelles at $T > T_c$. The presence of the peak corresponding to the unimers at higher elution volume can be understood considering that at pH = 7, the poly(acrylic acid) segment is not completely ionized and the equilibrium is not sufficiently shifted to the formation of micelles.²⁹ The solution was prepared at a concentration of 4 g·L⁻¹ (ca. 10⁻⁴ mol·L⁻¹), which during passage through the columns is diluted by a factor of ca. 100, thus leading to a concentration in the range of 40 mg·L⁻¹ or 10⁻⁶ mol·L⁻¹. Thus, the actual concentration might be in the range of the CMC (see above). The more probable explanation consists in assuming that the system is frozen under the time-scale, i.e. is ruled by a very slow exchange dynamics between unimers and micelles.

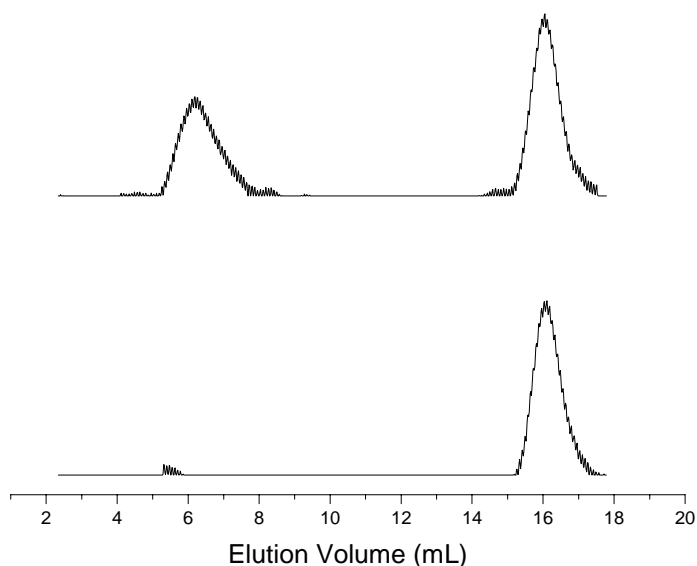


Figure 5-8. SEC traces (RI detector) of (AA)₄₅-b-(DEAAM)₃₆₀ at $T = 24$ °C (bottom) and 40 °C (top) in water + 0.05 M NaN₃/ 0.2 M NaH₂PO₄ (pH = 7).

Additionally, temperature-sweep ¹H NMR spectroscopy was used to characterize the thermally-induced phase transition in D₂O varying temperature from 25 °C to 50 °C. This method is suitable for investigation of local phenomena within the unimer/micelles solution. The application of NMR spectroscopy on block copolymer micelles is based on the fact that the peak intensity is related to its mobility.⁷¹⁻⁷³ The mobility of insoluble segment (core) is reduced when the micelle is formed, and therefore, its intensity reduced. As it shown in Figure 5-9, the peak intensity attributed to the NCH₂- and -CH₃ groups (DEAAM units), decreased while increasing the temperature, suggesting the formation of PDEAAM-core micelles with PAA forming the corona. The methine proton of the PAA block can not be assigned in the spectra.

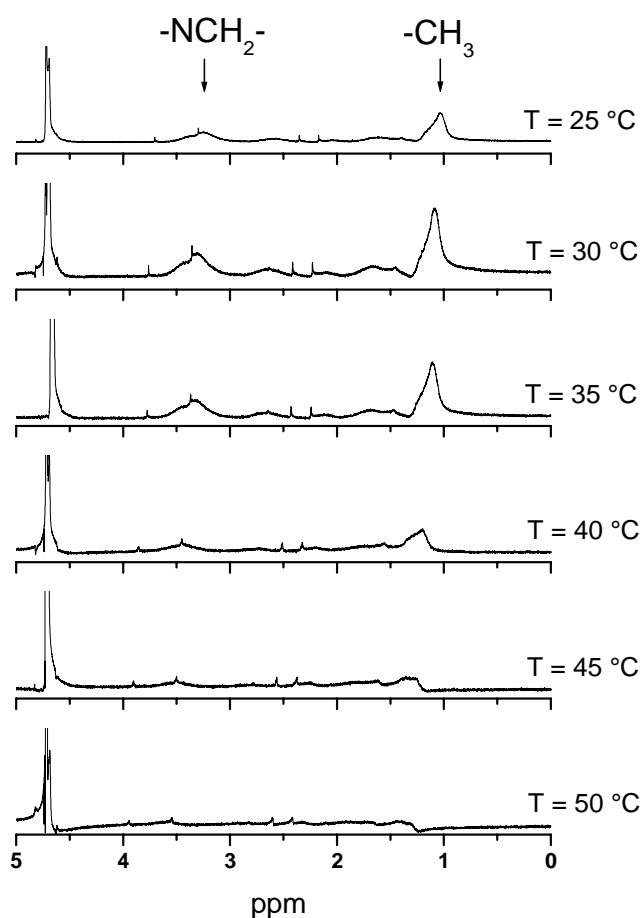


Figure 5-9. Temperature sweep ^1H NMR $(\text{AA})_{45}\text{-}b\text{-(DEAAM)}_{360}$ at $\text{pH} = 11.7$ in $\text{D}_2\text{O}/\text{NaOD}$ at various temperatures. ^1H NMR spectra were recorded with 32 scans, $c \approx 1.0$ wt.-%.

The reported value for the cloud point, $T_c = 35$ °C, measured by turbidimetric titration,^{41,74} is confirmed by micro-Differential Scanning Calorimetry ($\mu\text{-DSC}$),⁵³ if we take into account the onset temperature at a heating rate of $0.1 \text{ K}\cdot\text{min}^{-1}$ (Figure 5-10). For comparison, the DSC traces of an equivalent homopolymer of DEAAM, which was synthesized by anionic polymerization using the same method ($\text{RLi}/\text{Et}_3\text{Al}$ in THF), presents a cloud point at ca. 30-31 °C (onset = 30.6 °C). By incorporation of a hydrophilic comonomer, the cloud point can be shifted to higher values (onset = 35.7 °C), as it was reported for DEAAM copolymerized with methacrylic acid,¹⁸ or acrylic acid.²³ Furthermore, by comparing the heating and cooling DSC traces, a slight hysteresis is

observed for the transition temperature. This effect was reported by Freitag et al. for stereoregular PDEAAm (rich in isotactic triads).⁷⁵

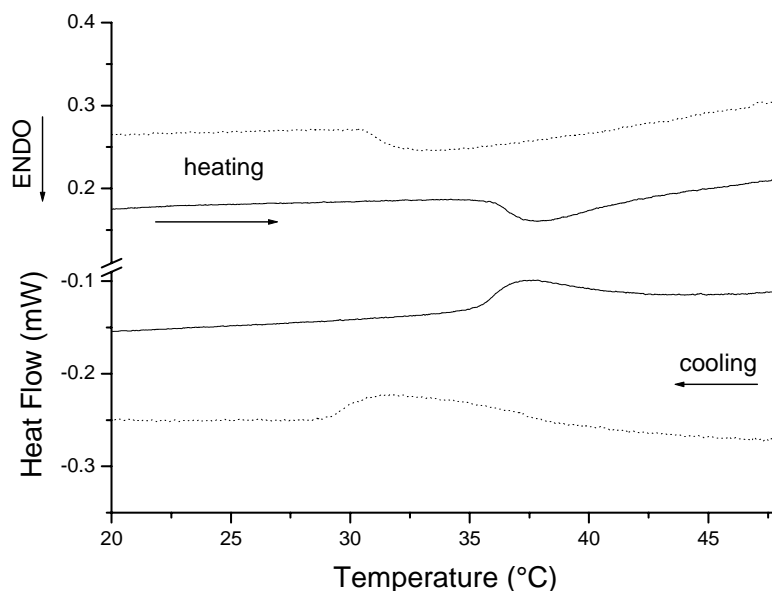


Figure 5-10. Micro-DSC traces of $(AA)_{45}\text{-}b\text{-(DEAAm)}_{360}$ in aqueous solution at pH = 12.0 (—), and $(DEAAm)_{92}$ in pure water (...). Scanning rate = $0.1 \text{ K}\cdot\text{min}^{-1}$, $c = 0.5 \text{ wt.}\%$.

Upon increasing the temperature, the transition from a solution containing the molecularly dissolved block copolymer (unimers, $R_h \approx 4 \text{ nm}$) with a small portion of large particles which ($R_h \approx 100 \text{ nm}$) to a solution containing micelles ($20 \leq R_h \leq 25 \text{ nm}$) is indicated by DLS measurements at various temperatures (Figure 5-11). These aggregates are still present after 2 hours of centrifugation at 4000 rpm. The scattering intensity is nearly constant for $T < 34\text{-}37 \text{ }^\circ\text{C}$ (19.7 kHz), whereas above this temperature, a dramatic increase in the scattering intensity is observed (200.3 and 214.7 kHz at 47.5, and 58.1 $^\circ\text{C}$, respectively). Nevertheless, this increase is only a factor 10 which is too low if we assume an aggregation number, N_{agg} , of approx. 50 (see below). We attribute this to the overlapping at $T > T_c$ of the contribution of the loose aggregates with that of the micelles. Furthermore, by increasing the temperature above 45 $^\circ\text{C}$, a slight decrease in the hydrodynamic radius is observed. The PDEAAm-core contains water which is slowly expelled, as it becomes more hydrophobic. It indicates first that the PDEAAm contains water at temperature close to T_c , and secondly that the transition is not sharp at the

molecular level. The normalized autocorrelation functions as well as the corresponding hydrodynamic radius distributions (CONTIN) at 47.5 and 58.1 °C are shown in Supporting Information (Figure 5-21). By varying the copolymer concentration from 0.4 to 1.3 g·L⁻¹, the *z*-average hydrodynamic radius of the micelles is constant, $R_h = 21.5$ nm (CONTIN from the single autocorrelation function at $\theta = 90^\circ$), suggesting a closed association.

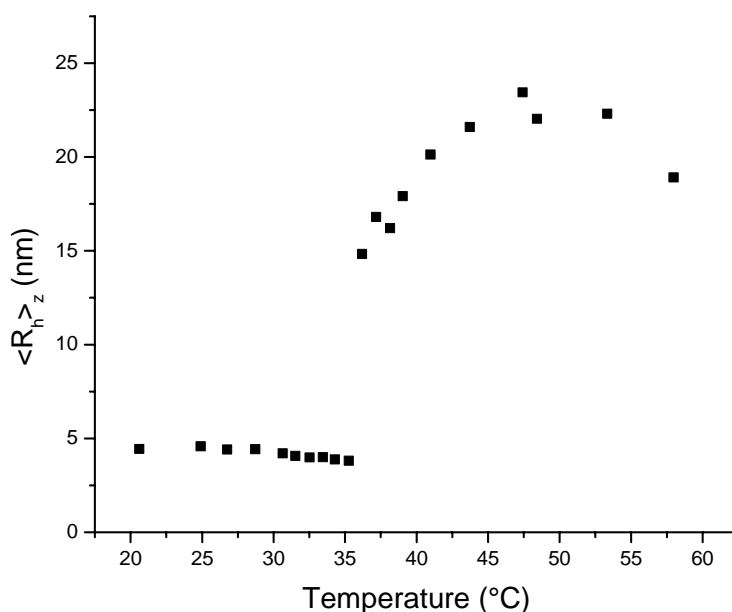


Figure 5-11. Effect of the temperature on the hydrodynamic radius, $\langle R_h \rangle_z$, of (AA)₄₅-b-(DEAAm)₃₆₀ in NaOH solution measured by DLS (CONTIN analysis of the autocorrelation function at 30° scattering angle). Below $T \approx 36$ °C, the peak attributed to a small fraction of aggregates ($\langle R_h \rangle_z \approx 100$ nm) is not indicated on the figure. Experimental conditions: [NaCl] = 0.1 mol·L⁻¹, $c = 1.27$ g·L⁻¹, pH = 12.8.

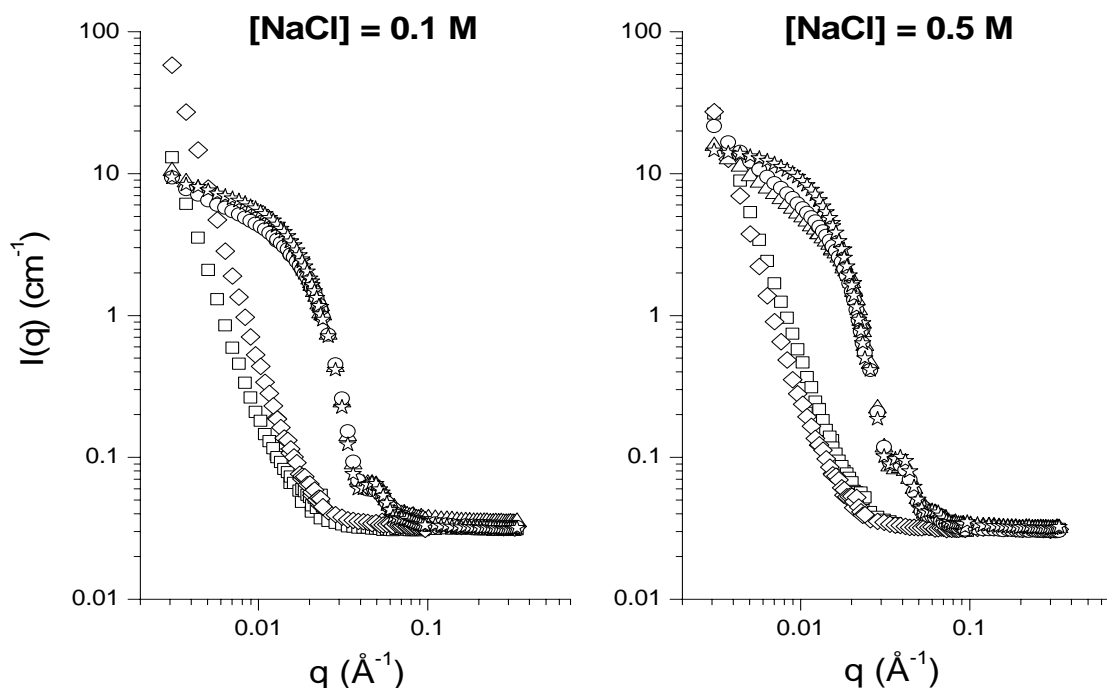


Figure 5-12. SANS curves at $T = 45$ °C for the $(AA)_{45}\text{-}b\text{-(DEAAm)}_{360}$ in aqueous solutions at different salt concentrations: pH = 1.0 (∇), 3.6 (M), 7.7 (δ), 8.6 (ν), and 12.7 (ψ). Experimental conditions: $c = 1.4\text{-}1.5$ g·L $^{-1}$.

To further characterize the structure of the micelles observed by DLS, SANS experiments were performed by varying pH, temperature and the salt concentration. SANS is a powerful technique for investigating the internal structure of micelles.⁵⁶ Micelles made of amphiphilic block copolymers were successfully investigated, like those based on polyisobutylene-*block*-poly(methacrylic acid),⁷⁶ polystyrene-*block*-poly(acrylic acid),⁷⁷ and poly(methyl methacrylate)-*block*-poly(acrylic acid).⁷⁸ SANS was also used to characterize the various schizophrenic micelles reported by Armes and coworkers.^{32,79,80} In general, structural information can be obtained by this method, such as the overall micelle size, R_g , the core radius, R_{core} , the corona thickness, δ_c , and the number of macromolecules forming each micelle, i.e. the aggregation number, N_{agg} .

Table 5-2. Influence of the pH on the structural parameters of the micellar aggregates at $T = 45\text{ }^{\circ}\text{C}$ ($\text{pH} \geq 7.7$).a) $[\text{NaCl}] = 0.1\text{ mol}\cdot\text{L}^{-1}$

pH	R_h^a (nm)	$R_{g,\text{calc}}^b$ (nm)	$R_{g,\text{app}}^c$ (nm)	R_{eff}^d (nm)	R_{core}^e (nm)	δ_c^f (nm)	σR_{core}	$10^{-6}\cdot M_{w,\text{app,core}}^g$ ($\text{g}\cdot\text{mol}^{-1}$)	N_{agg}^h
12.7	23.7	18.4	10.7	11.2	11.5	5.3	0.13	3.78	74
8.6	21.5	16.7	9.5	9.9	10.8	5.9	0.16	2.56	50
7.7	16.9	13.1	9.9	10.4	11.0	2.1	0.14	2.95	58

b) $[\text{NaCl}] = 0.5\text{ mol}\cdot\text{L}^{-1}$

pH	R_h^a (nm)	$R_{g,\text{calc}}^b$ (nm)	$R_{g,\text{app}}^c$ (nm)	R_{eff}^d (nm)	R_{core}^e (nm)	δ_c^f (nm)	σR_{core}	$10^{-6}\cdot M_{w,\text{app,core}}^g$ ($\text{g}\cdot\text{mol}^{-1}$)	N_{agg}^h
12.7	27.3	21.2	13.7	14.8	14.3	6.9	0.10	8.56	167
8.6	26.9	20.8	12.3	11.9	13.0	7.8	0.15	4.53	88
7.7	29.2	22.6	11.4	11.3	12.9	9.7	0.14	3.84	75

^a From DLS at 90° scattering angle. ^b Calculated radius of gyration assuming a spherical shape, $R_{g,\text{calc}} = 0.775\cdot R_h$.⁷⁷ ^c Calculated from the slope of the Guinier plots, $\ln I(q)$ vs q^2 to $q^2 \rightarrow 0$, maximum relative error = $\pm 32\%$ (Equation 5-6). ^d From Equation 5-12. ^e By fitting the $I(q)$ vs q curve using a polydisperse sphere model. ^f Corona thickness, $\delta_c = R_{g,\text{calc}} - R_{\text{core}}$. ^g Calculated from the intercept of the Guinier plots, $I(0)$, using the scattering length density of the PDEAAm block, $\rho_p = 6.22\cdot 10^9\text{ cm}^{-2}$, maximum relative error = $\pm 0.1\%$ (Eq. 5-7). ^h Aggregation number, $N_{\text{agg}} = M_{w,\text{app,core}}/M_{w,\text{PDEAAm}}$, with $M_{w,\text{PDEAAm}} = 51,300\text{ g}\cdot\text{mol}^{-1}$.

At $T = 45\text{ }^{\circ}\text{C}$, all curves look similar for $\text{pH} \geq 7.7$ and exhibit the typical shape of spherical aggregates (Figure 5-12). The scattered intensity at low q is about ten times higher than that at room temperature, suggesting the formation of larger entities. Under these conditions, we assume that the PDEAAm-core is responsible for the scattering intensity and the corresponding scattering length density ($\rho_p = 6.22\cdot 10^9\text{ cm}^{-2}$) was used for the calculations of $M_{w,\text{app,core}}$ from the Guinier approximations (Equations 5-6 and 5-7). The core radii, R_{core} , were calculated using a polydisperse sphere model with a Schulz

distribution, assuming a density, $\rho_{\text{polymer}} = 1.1 \text{ g}\cdot\text{cm}^{-3}$ for each block, and a volume fraction of 0.11, for which the scattering intensity is given by:

$$I(q) = \int f(R_{\text{core}}) \cdot P(q, R_{\text{core}}) \cdot dR_{\text{core}} \quad (5-8)$$

where $P(q, R_{\text{core}})$ was taken to be the form factor of a homogeneous sphere with radius R_{core} :

$$P(q, R_{\text{core}}) = |F(q, R_{\text{core}})|^2 = V_p^2 \cdot \Delta\rho^2 \cdot \left\{ \frac{3 \cdot [\sin(q \cdot R_{\text{core}}) - q \cdot R_{\text{core}} \cdot \cos(q \cdot R_{\text{core}})]}{(q \cdot R_{\text{core}})^3} \right\}^2 \quad (5-9)$$

where V_p is the particle volume and $\Delta\rho$ is the difference between the scattering length densities of particle (here the PDEAAm-core) and solvent (D_2O). For the distribution of the particle radii, R , a Schulz distribution was used:

$$f(R_{\text{core}}) = \left(\frac{Z+1}{\langle R_{\text{core}} \rangle} \right)^{Z+1} \cdot \frac{R_{\text{core}}^Z}{\Gamma(Z+1)} \cdot \left(-\frac{(Z+1) \cdot R_{\text{core}}}{\langle R_{\text{core}} \rangle} \right) \quad (5-10)$$

where the parameter Z is directly given by the variance σ of the distribution according to:

$$\sigma^2 = \frac{\langle R_{\text{core}}^2 \rangle}{\langle R_{\text{core}} \rangle^2} = \frac{1}{Z+1} \quad (5-11)$$

Table 5-2 summarizes the results obtained by the different methods for the measurements at $T = 45\text{ }^{\circ}\text{C}$ by varying the pH and for the two salt concentrations investigated: $[\text{NaCl}] = 0.1$ and $0.5\text{ mol}\cdot\text{L}^{-1}$. The experimental data are perfectly fitted by the curve as it is shown in Figure 5-13 for the measurement at $\text{pH} = 12.7$ for both salt concentration investigated. The resulting data can be compared to the theoretical value expected for the from the core-shell theory where an effective core-radius, R_{eff} , is calculated from the amount of the hydrophobic PDEAAm block at $T > T_c$ and $\text{pH} \geq 7.7$, according to Equation 5-12.^{81,82}

$$R_{\text{eff}} = \left(\frac{3}{4 \cdot \pi} \cdot \frac{M_{n,\text{PDEAAm}}}{\rho_{\text{PDEAAm}}} \cdot N_A \cdot N_{\text{agg}} \right)^{1/3} \quad (5-12)$$

where ρ_{PDEAAm} the PDEAAm block density, $10^6\text{ g}\cdot\text{m}^{-3}$. As summarized in Table 5-2, for both salt concentrations investigated, the effective core radii calculated from this relation fit perfectly with the values extrapolated from the spherical model, R_{core} . It indicates us the validity of the model used.

The $R_{g,\text{app}}$ extrapolated from the slope of the Guinier plots (Figure 5-20 in Supporting Information) are somewhat lower than the calculated R_{core} and R_{eff} . It is well known that the Guinier approximation tends to underestimate R_g .⁸³ The overall micelle radius of gyration, R_g , and hydrodynamic radius, R_h , can be estimated from SLS/DLS measurements. Knowing theses parameters, the corona thickness can be calculated (see Table 5-2).

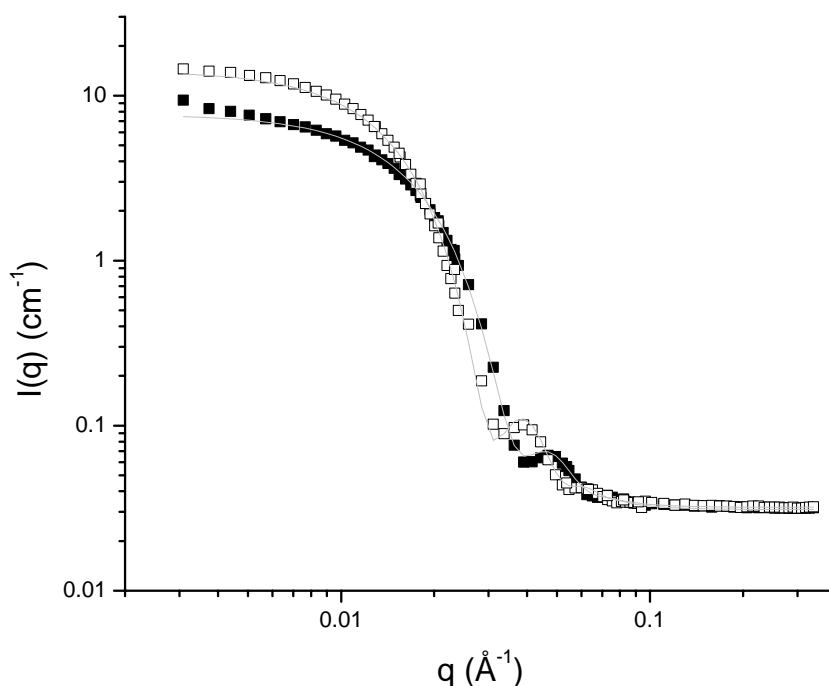


Figure 5-13. Effect of the salt concentration on the scattered neutrons profile of $(AA)_{45}\text{-}b\text{-(DEAAm)}_{360}$ in water ($\text{pH} = 12.7$) at $T = 45\text{ }^{\circ}\text{C}$ for $[\text{NaCl}] = 0.1$ (■), and $0.5\text{ mol}\cdot\text{L}^{-1}$ (□). The solid gray lines represent the polydisperse spherical model fit used to evaluate the radius of the core, R_{core} .

To further elucidate the solution properties of the PDEAAm-core micellar aggregates, SLS and DLS were performed simultaneously. The polyelectrolyte solution of $(AA)_{45}\text{-}b\text{-(DEAAm)}_{360}$ was dialyzed against a NaCl and NaOH aqueous solutions, $0.1\text{ mol}\cdot\text{L}^{-1}$ each. In the case of amphiphilic copolymers of different architectures, containing an ionic segment (polyelectrolyte), the presence of electrostatic interactions can lead to the so-called ‘polyelectrolyte effect’ which is promoted at low salt concentration. It is due to the charges borne along the chain which induce repulsive interactions and the extension of the polymer chains. The addition of salt tends to screen this effect.⁸⁴ It is characterized by the presence of strong upturns in the scattering curves at low q values or that of slow modes in the relaxation time distribution.⁵⁴ The ratio of the polyelectrolyte monomer units concentration to salt concentration (Λ) was introduced by Förster et al. to quantify the influence of the salt concentration on the polyelectrolyte chains behavior.⁸⁵ The polyelectrolyte effect appears for flexible systems when this ratio is larger than unity,

whereas for dense polyelectrolytes such as stars or brushes, charge renormalization shifts the critical ratio to values much larger than unity.^{86,87} The typical salt concentration used in our experiments was $0.1 \text{ mol}\cdot\text{L}^{-1}$ with a maximum copolymer concentration of $4.23 \text{ g}\cdot\text{L}^{-1}$ ($c = 7.7\cdot 10^{-5} \text{ mol}\cdot\text{L}^{-1}$), which lead to a value of $\Lambda = 0.03$, and furthermore, neither upturns in the scattering intensities at low q , nor slow modes were detected. Taking into account all these observations, the addition of salt has been estimated to be sufficient to screen intermicellar electrostatic interactions.

Another aspect of importance for the study of low-molecular surfactant, or amphiphilic block copolymers is the CMC. The lowest copolymer concentration used ($0.94 \text{ g}\cdot\text{L}^{-1}$, $1.7\cdot 10^{-5} \text{ mol}\cdot\text{L}^{-1}$) is one order of magnitude larger than the minimal value determined for the CMC ($4.0\cdot 10^{-6} \text{ g}\cdot\text{L}^{-1}$). Thus, the micellization equilibrium is shifted towards micelles and the amount of unimers in solution is considered to be very small, and therefore their contribution to the light-scattering intensity is negligible. After 6 days of dialysis under continuous stirring, the Donnan equilibrium was reached,⁸⁶ and the solutions were prepared by diluting the appropriate amounts of dialysate with the remaining solution outside the membrane. This clarification method gave consistent results for the scattered light, with no anomalous angular dependence in the case of the dialyzed samples and a good constancy in repeated scans of the same sample.^{88,89} An experiment without dialysis procedure renders a negative second virial coefficient that was not well understood because alkaline water at $T > T_c$ is a good solvent of the PANa corona. A series of five different concentrations ($c = 0.94, 1.25, 1.77, 2.46, 4.23 \text{ g}\cdot\text{L}^{-1}$) was used for the measurements. The pH of the solution was measured to be 12.8. Prior to the measurement, the refractive index increment was determined as $dn/dc = 0.1732 \pm 8.8\cdot 10^{-3} \text{ mL}\cdot\text{g}^{-1}$. The analysis of the scattering intensities using a Zimm plot⁹⁰ (Figure 5-14) yields a molecular weight, $M_w = 2.96\cdot 10^6 \text{ g}\cdot\text{mol}^{-1}$ (error = ± 2.5 and 1.9 % by extrapolation at $c \rightarrow 0$, and at $q^2 \rightarrow 0$, respectively), and a z-average radius of gyration for the overall micelles, $R_g = 17.5 \pm 4.0 \text{ nm}$. The value of the second virial coefficient is, $A_2 = (2.40 \pm 0.17)\cdot 10^{-8} \text{ mol}\cdot\text{L}\cdot\text{g}^{-2}$, which is close to the values reported by Eisenberg and coworkers for poly(styrene)-*block*-poly(acrylic acid) micelles ($10^{-8} < A_2 < 10^{-7} \text{ mol}\cdot\text{L}\cdot\text{g}^{-2}$).⁸⁸

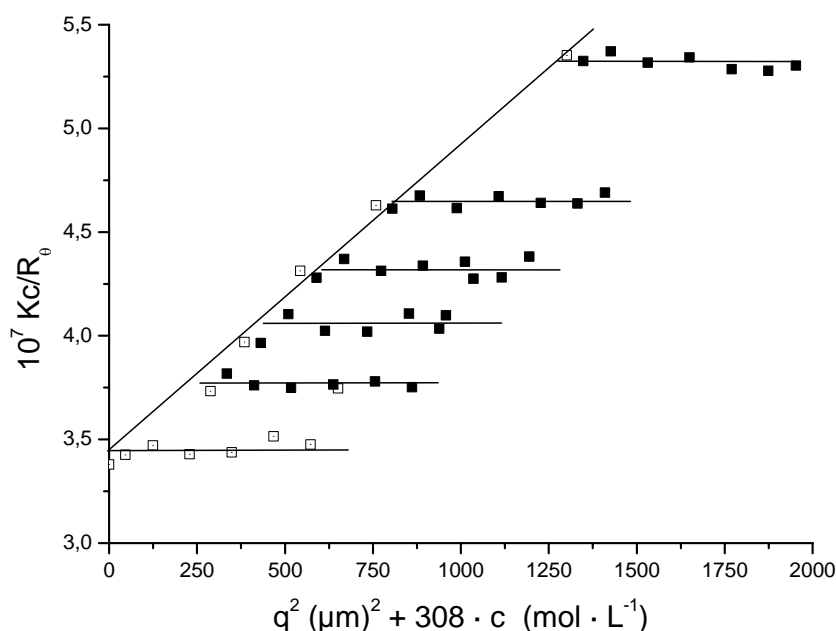


Figure 5-14. Zimm plot of $(AA)_{45}\text{-}b\text{-(DEAAM)}_{360}$ micelles in dialyzed solution of NaCl ($0.1 \text{ mol}\cdot\text{L}^{-1}$) and NaOH at $45 \text{ }^\circ\text{C}$ ($\text{pH} = 12.8$, concentration range $0.94\text{-}4.23 \text{ g}\cdot\text{L}^{-1}$). The extrapolated data at $c \rightarrow 0$ and $q^2 \rightarrow 0$ are shown on the figure as open squares (∇).

DLS was performed simultaneously to SLS to yield more information about the hydrodynamic size and the size distribution of the formed micelles. The characteristic autocorrelation functions obtained at $T = 45 \text{ }^\circ\text{C}$ for various scattering angles, θ , are presented in Figure 5-22 (Supporting Information) for a copolymer concentration of $1.25 \text{ g}\cdot\text{L}^{-1}$. The CONTIN analysis renders a monomodal distribution of the relaxation times as shown in Figure 4-4. The linear dependence of the decay rate Γ ($\Gamma = 1/\tau$, with τ the average relaxation time) on q^2 passes through the origin, indicating that the relation, $\Gamma = D \cdot q^2$, is satisfied, and that the peak corresponds to real diffusive particles.^{91,92} The slopes give the apparent translational diffusion coefficient D of the micellar aggregates in water under these conditions. In the range of dilute solutions, the concentration dependence of D is given by: $D = D_0 \cdot (1 + k_D \cdot c)$ where k_D is the dynamic second virial coefficient and c the copolymer concentration.⁹³ From the values of D obtained at different concentrations, $0.94 \leq c \leq 4.23 \text{ g}\cdot\text{L}^{-1}$, the translational diffusion coefficient, D_0 , at infinite dilution ($c \rightarrow 0$) can be extrapolated (Figure 5-15). The obtained value, $D_0 = (1.74 \pm 0.02) \cdot 10^{-11} \text{ m}^2\cdot\text{s}^{-1}$,

was used to determine the hydrodynamic radius of the micelles according to the Stokes-Einstein equation (Eq. 5-5). A consistent z -average hydrodynamic radius, R_h , of 22.6 ± 0.5 nm can be calculated.

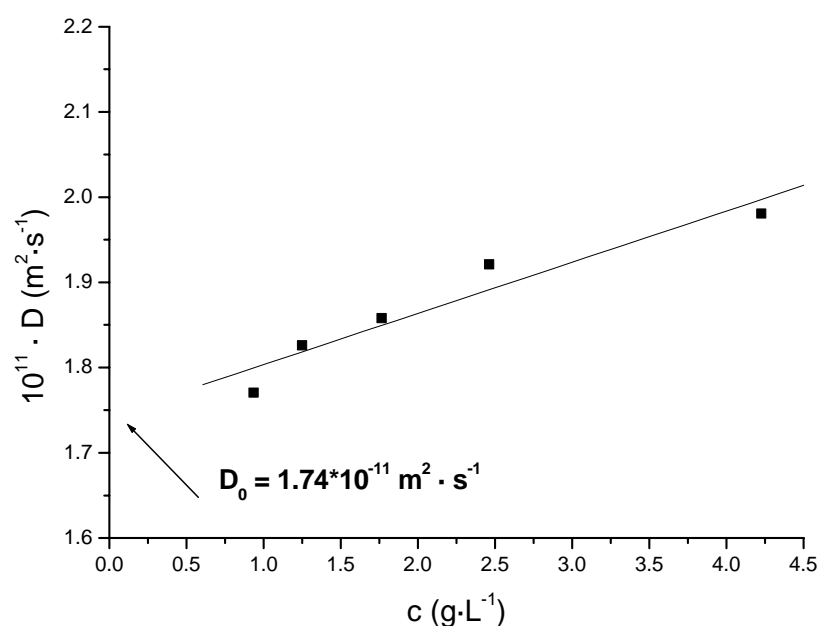


Figure 5-15. Dependence of the translational diffusion coefficient, D , on the copolymer concentration for the solutions of $(AA)_{45}\text{-}b\text{-(DEAAm)}_{360}$ in water at $T = 45$ °C (pH = 12.8, $[\text{NaCl}] = 0.1 \text{ mol}\cdot\text{L}^{-1}$).

From the values obtained by these techniques, the aggregation number, N_{agg} , the overall micellar radius, R_g , the core radius, R_{core} , and the hydrodynamic radius, R_h , are obtained. The ratio $F = R_g / R_h$, is a characteristic parameter, which depends on the polydispersity and morphology of the micellar aggregates formed (spheres, vesicles, rods).⁹⁴ The theoretical value for spherical micelles with a dense core is $F = 0.775$.⁷⁷ Under alkaline conditions and at a temperature above the cloud point of the PDEAAm segment ($T > T_c$), an aggregation number $N_{\text{agg}} = 54$ and a ratio $F = 0.77 \pm 0.19$ can be calculated due to the relative error of 20 % in the determination of R_g . The N_{agg} value obtained from SLS/DLS measurements is somewhat lower than that obtained from SANS investigations in D_2O under the same conditions (pH = 12.7, $[\text{NaCl}] = 0.1 \text{ mol}\cdot\text{L}^{-1}$): $N_{\text{agg}} = 74$. This can be

explained by the difference of hydration in H₂O and D₂O, the association of D₂O with the copolymer reduces the effective contrast term, K^n (See Equation 5-7), hence a higher apparent molecular weight is calculated.

To confirm the spherical structure of the PDEAAm-core micelles in alkaline solution, cryo-TEM preparation was performed at 45 °C, i.e., above the cloud point of the PDEAAm block, $T_c \approx 35$ °C (Figure 5-16). Relatively narrow distributed spherical micellar aggregates with a number-averaged radius of 24 nm are observed with a polydispersity index, $D_w/D_n = 1.12$. This observation corroborates SLS/DLS measurements, where monomodal micelles with a z -average hydrodynamic radius of 23 nm (PDI = 0.01) were observed, and with SANS investigations where the application of a sphere model renders consistent results. The low contrast difference or the low thickness of the corona does not allow the accurate observation of the core/corona structure. Furthermore, the formation of a loop due to the presence of the C₁₈ hydrophobic sticker is presumable, lowering thus the PANa corona thickness.

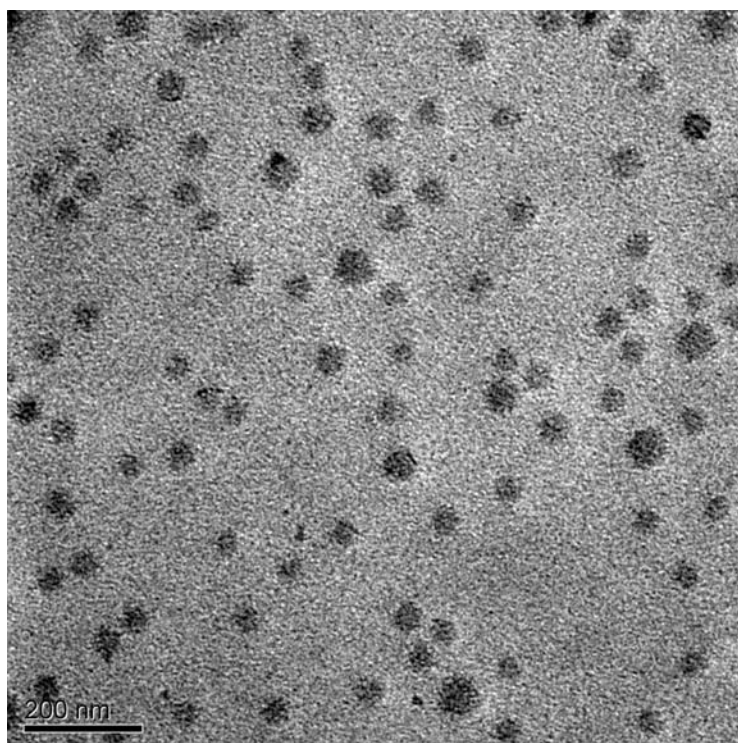


Figure 5-16. Cryo-TEM image of the (AA)₄₅-*b*-(DEAAm)₃₆₀ micelles vitrified from an aqueous solution at $T = 45$ °C showing individual PDEAAm-core micelles ($c = 4.9$ g·L⁻¹, pH = 12.6).

Some studies were reported by Groenewegen et al.^{95,96} on the ionic strength influence in the case of PS-*b*-PAA copolymers. In the absence of salt, the ionized polyelectrolyte segment ($\alpha = 100\%$) is completely expanded in aqueous solution. Counter-ions are generally localized in the polyelectrolyte chains or confined in the PA-Na corona. The osmotic pressure exerted by the counter-ions trapped in the corona is responsible of the extension of the chains. When the ionization degree, α , decreases, i.e. lower pH values, the average radius of the micelles decreases. The salt plays a key-role in the extension of the polyelectrolyte chains and also on the localization of the counter-ions. For $\alpha = 100\%$, the corona collapses while adding salt. The internal part of the corona is not affected while the external corona behaves like a neutral polymer. When $\alpha < 0.1$, the addition of salt exerts a contraction of the chains until precipitation for higher salt concentrations.⁹⁵⁻⁹⁷

For the lowest salt concentration ($[\text{NaCl}] = 0.1 \text{ mol}\cdot\text{L}^{-1}$), while increasing the pH from 7.7 to 12.7, no significant effect is observed on $M_{w,\text{app,core}}$ and R_{core} . Indeed, a small increase of R_{core} by 5% is observed and the $M_{w,\text{app,core}}$ increases from 3.0 to $3.8\cdot 10^6 \text{ g}\cdot\text{mol}^{-1}$, thus the aggregation number increases only from 58 to 74.⁹⁸ The relative polydispersity of the core radii can be described by the ratio, σ/R_{core} , where σ is the standard deviation and is not affected by the variation of pH for the lowest salt concentration.

The salt concentration has an effect on both the scattered intensity and the shape of the SANS curves. Indeed, by increasing the salt concentration, the particles are more defined, as indicated by the more pronounced oscillations in the scattering pattern, and the scattered intensity increases twice (Figure 5-12). For $[\text{NaCl}] = 0.5 \text{ mol}\cdot\text{L}^{-1}$, the values of the core radii are affected by the augmentation of the pH value, i.e. an increase of 10% is observed by increasing the pH (12.9 to 14.3 nm). This is accompanied with the increase of the core molecular weight, corresponding to an increase of N_{agg} from 75 to 167, i.e. by a factor of 2. Well-defined particles are obtained at pH = 12.7 with a core radius, $R_{\text{core}} = 14.3 \text{ nm}$ ($\sigma/R_{\text{core}} = 0.10$).

No information about the corona can be deduced from SANS data due to the limited q -range. The corona thickness, δ_c , can be calculated as $\delta_c = R_g - R_{\text{core}}$. Since not all samples were measured by SLS, we use the ratio $F = R_g/R_h$ ⁷⁷ to calculate R_g from the hydrodynamic radius determined by DLS (Table 5-2). By increasing the pH from 7.7 to 12.7, the z -average hydrodynamic radius of the overall micelle, R_h , measured in D_2O increases from 16.9 to 23.7 nm for the lowest salt concentration, and decreases from 29.2 to 27.3 nm for

the highest salt concentration. In this case, the PDEAAm-core is compact, $11.0 \leq R_{\text{core}} \leq 14.3$ nm, surrounded by a PAA-corona responsible for the stabilization ($2.1 \leq \delta_c \leq 9.7$ nm). For 100% extension and a $DP_n = 45$, a maximum corona thickness of 11 nm can be estimated.⁹⁹ Thus, the corona is not fully stretched. This is in fact not expected in the presence of salt, shielding the charges. In addition the presence of the C₁₈ hydrophobic fragment on the PAA block side may induce the formation of a loop. Nevertheless, the corona expansion can be tuned by the PAA block ionization degree (e.g., variation of pH) and/or the ionic strength. In all cases, the corona-forming block (PAA) is much shorter than the core-forming block (PDEAAm), and ‘crew-cut’ micelles are observed.^{31,100}

These observations are consistent with a PDEAAm-core/PAA-corona micellar structure where the core is constituted of pH-independent PDEAAm chains. The key-role of the added salt is of importance for the expansion polyelectrolyte segment (PAA) forming the corona and also on the aggregation number of the micelles.

(ii) Characterization of the aggregates at pH ≤ 4 . To further elucidate the phase transition, the dependence of the *z*-average hydrodynamic radius, R_h , on both temperature and time was studied. Figure 5-17 shows this double dependence. The temperature was raised above T_c within 5 minutes and maintained constant at $T = 43\text{-}44$ °C for 60 minutes. A macroscopic precipitation occurs and it is not a sharp transition, in this case. Indeed, the observed value of the *z*-average hydrodynamic radius increases with time until complete phase separation. The peak of very large particles attributed to precipitated copolymer particles ($R_h > 1$ μm) is not shown in Figure 5-17. Also, the peak attributed to larger aggregates responsible for the turbidity at $T < 35$ °C is not represented in the figure.

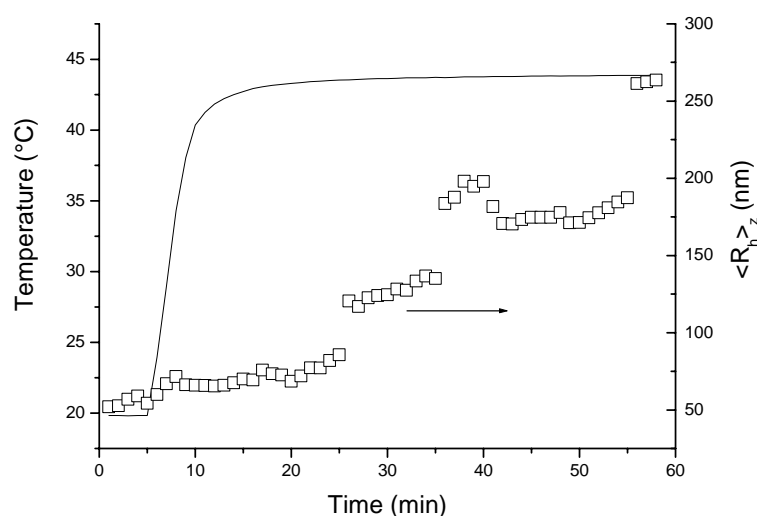


Figure 5-17. Dependence of the measured z -average hydrodynamic radius, $\langle R_h \rangle_z$ on the temperature and the time. Experimental conditions: $c = 0.9 \text{ g}\cdot\text{L}^{-1}$, $[\text{NaCl}] = 0.1 \text{ mol}\cdot\text{L}^{-1}$, $\text{pH} = 3.9$, $\theta = 90^\circ$.

Table 5-3. Influence of pH and salt concentration on the structural parameters of the micellar aggregates at $T = 45^\circ\text{C}$ at $\text{pH} < 4$

pH	[NaCl] = 0.1 mol·L ⁻¹			[NaCl] = 0.5 mol·L ⁻¹		
	$R_{g,\text{app}}^a$ (nm)	$10^4 \cdot M_{w,\text{app}}^b$ (g·mol ⁻¹)	N_{agg}^c	$R_{g,\text{app}}^a$ (nm)	$10^4 \cdot M_{w,\text{app}}^b$ (g·mol ⁻¹)	N_{agg}^c
3.6	9.0	9.05	2	8.2	5.28	1
1.0	7.9	4.24	1	9.3	9.48	2

^a Calculated from the slope of the Guinier plots, $\ln I(q)$ vs q^2 to $q^2 \rightarrow 0$, maximum relative error = $\pm 30\%$ (Eq. 5-6). ^b Calculated from the intercept of the Guinier plots, $I(0)$, using the scattering length density of the PAA-*b*-PDEAAm block copolymer, $\rho_p = 6.42 \cdot 10^9 \text{ cm}^{-2}$, maximum relative error = $\pm 30\%$ (Eq. 5-7). ^c Aggregation number, $N_{\text{agg}} = M_{w,\text{app}} / M_{w,\text{unimer}}$, with $M_{w,\text{unimer}} = 55,200 \text{ g}\cdot\text{mol}^{-1}$ for PAA-*b*-PDEAAm.

By SANS, the scattered intensity at $\text{pH} < 7$ is comparable to that observed at room temperature for $\text{pH} > 7$. Thus, the roughly estimated $M_{w,\text{app}}$ and $R_{g,\text{app}}$ (by Guinier method)

are similar to those observed at room temperature: $M_{w,app} \approx 50,000-100,000 \text{ g}\cdot\text{mol}^{-1}$, and $R_{g,app} \approx 8-9 \text{ nm}$ (Table 5-3). These values are purely speculative because they do not correspond to real entities because a macroscopic phase separation occurs. We discussed previously that the precipitation is not a sharp process and it is not surprising that SANS analyses render results similar to that observed at $T = 23 \text{ }^\circ\text{C}$. By gravity, the precipitated copolymer is localized at the bottom of the cuvette and remaining unimers in solution scatter.

Finally, the ‘cross’ transition, namely the pH-induced transition of a PDEAAm-core micelles solution at $T = 45 \text{ }^\circ\text{C}$ by addition of HCl. The solution becomes instantaneously turbid and a broad peak is found at $\text{pH} = 5-6$ with a z -average hydrodynamic radius of 199 nm at 90° scattering angle. A strong angular dependence of the value of the z -average R_h is observed for all systems, suggesting the presence of a multitude of assemblies (non-defined structure) and macroscopic phase separation occurs for further addition of HCl ($\text{pH} \leq 4$).

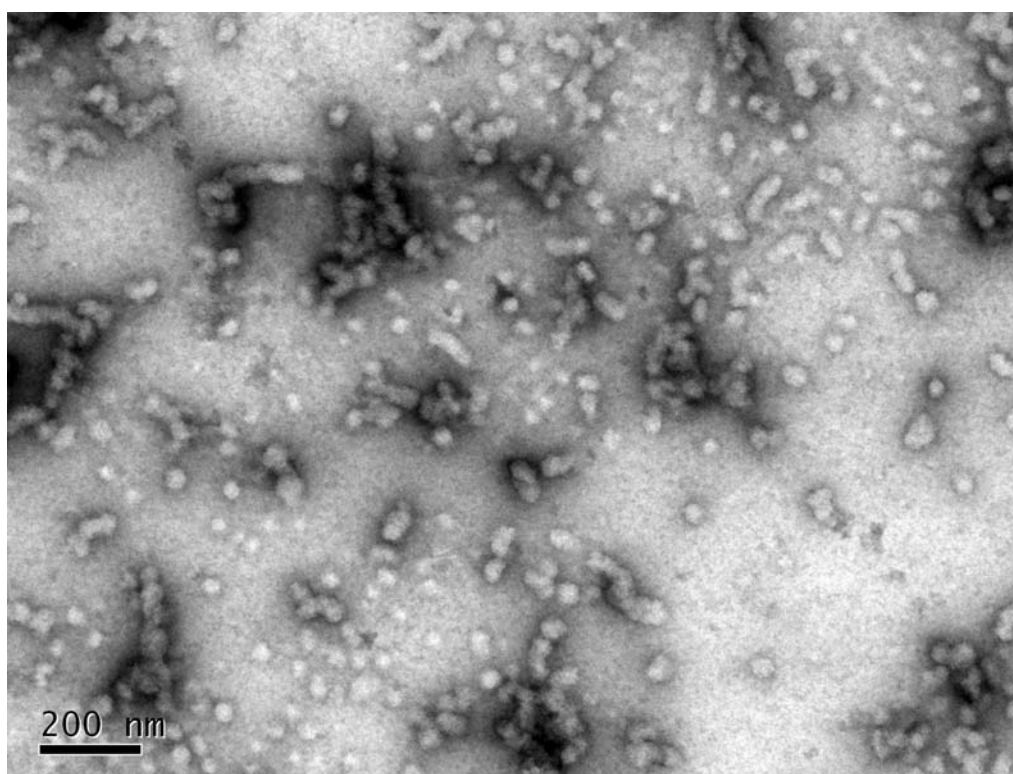


Figure 5-18. TEM image of $(AA)_{45}\text{-}b\text{-(DEAAm)}_{360}$ from an aqueous solution at $T = 45 \text{ }^\circ\text{C}$ prepared by negative staining with uranyl acetate on carbon-coated copper grid. Experimental conditions: $c = 1 \text{ g}\cdot\text{L}^{-1}$, $\text{pH} = 4$, no added salt.

The TEM image (Figure 5-18) of the aqueous solution at pH = 4 and $T = 45\text{ }^{\circ}\text{C}$ shows the aggregated micelles (randomly-formed ‘super-micellar’ aggregates), which coexists with remaining PDEAAm-core micelles. It corresponds to the step before the complete macroscopic phase separation (Figure 5-2D). This is not surprising as we mentioned above that the macroscopic precipitation is not a sharp transition.

5.4 Conclusions

Small Angle Neutrons Scattering was used in combination with Static/Dynamic Light Scattering and Cryo-TEM methods to examine the schizophrenic behavior in aqueous solution of the asymmetric poly(acrylic acid)₄₅-*block*-poly(*N,N*-diethylacrylamide)₃₆₀ copolymer synthesized via sequential anionic polymerization. Under alkaline conditions, the bishydrophilic block copolymer is molecularly dissolved at room temperature (unimers) and forms spherical PDEAAm-core micelles upon heating above the PDEAAm block cloud point ($T_c \approx 35\text{ }^{\circ}\text{C}$) by turbidimetric titration and micro-DSC. The spherical shape of these entities as well as their structure (PDEAAm-core/PAA-corona) is confirmed by SANS, DLS/SLS, and Cryo-TEM investigations. Crew-cut morphology is observed in all cases and the PAA-corona thickness can be adjusted by variation of its ionization degree and the ionic strength. Under acidic conditions, PAA-core micelles are observed at room temperature and disappear progressively upon heating above the cloud point where a macroscopic phase separation is observed. The addition of HCl to a solution containing PDEAAm-core micelles at $T = 45\text{ }^{\circ}\text{C}$ lead to the formation of super-micellar aggregates of non-defined structure which correspond to the step before macroscopic phase separation. This new kind of schizophrenic micelles can be used as ‘smart’ emulsifier for the stabilization of polymer dispersions.^{101,102}

Acknowledgement

This work was supported by the European Union within MC RTN POLYAMPHI and by DFG within the ESF EUROCORES Programme SONS. X. A. acknowledges financial support by the French Research Ministry, and the French-Bavarian University Center. The Institute Laue-Langevin (ILL), Grenoble, is gratefully acknowledged for providing the SANS beam time. Sabine Wunder, Anette Krökel, Adriana Boschetti, and Karl-Heinz

Lauterbach are gratefully acknowledged for aqueous SEC, temperature-sweep NMR, DSC, and dn/dc measurements, respectively. We appreciate Prof. B. A. Wolf (Johannes-Gutenberg Universität, Mainz, Germany) for fruitful discussions.

Supporting Information Available: Guinier plots (SANS) at $T = 23$ °C and $T = 45$ °C, normalized field correlation function and corresponding hydrodynamic radius distribution (CONTIN) of the block copolymer in water at $T = 48$ and 58 °C ($\theta = 30^\circ$), normalized autocorrelation function of the block copolymer in water at $T = 45$ °C at various θ . This material is available free of charge via the Internet at <http://pubs.acs.org>.

5.5 References

- (1) Tsvetanov, C.; Müller, A. H. E.; Universität Bayreuth: Bayreuth, Germany, 2000.
- (2) Hiratani, H.; Alvarez-Lorenzo, C. *Journal of Controlled Release* **2002**, *83*, 223-230.
- (3) Ringsdorf, H. *J. Polym. Sci. Polymer Symp.* **1975**, *51*, 135-153.
- (4) Hussein, G. A.; Christensen, D. A.; Rapoport, N. Y.; Pitt, W. G. *Journal of Controlled Release* **2002**, *83*, 303-305.
- (5) Pruitt, J. D.; Hussein, G.; Rapoport, N.; Pitt, W. G. *Macromolecules* **2000**, *33*, 9306-9309.
- (6) Roy, I.; Gupta, M. N. *Chemistry & Biology* **2003**, *10*, 1161-1171.
- (7) Kikuchi, A.; Okano, T. *Progress in Polymer Science* **2002**, *27*, 1165-1193.
- (8) Kikuchi, A.; Okano, T. *Macromolecular Symposia* **2004**, *207*, 217-227.
- (9) Ying, L.; Kang, E. T.; Neoh, K. G. *Langmuir* **2002**, *18*, 6416-6423.
- (10) Elaissari, A.; Delair, T.; Pichot, C. *Progress in Colloid & Polymer Science* **2004**, *124*, 82-87.
- (11) Costioli, M. D.; Fisch, I.; Garret-Flaudy, F.; Hilbrig, F.; Freitag, R. *Biotechnology and Bioengineering* **2003**, *81*, 535-545.
- (12) Costioli, M. D.; Ecole Polytechnique Fédérale de Lausanne: Lausanne, Switzerland, 2004; p 167.
- (13) Yokoyama, M.; Okano, T.; Sakurai, Y.; Kataoka, K. *J. Control. Release* **1994**, *32*, 269-277.
- (14) Kabanov, A. V.; Alakhov, V. Y. *J. Control. Release* **1994**, *28*, 15-35.
- (15) Katayama, Y.; Sonoda, T.; Maeda, M. *Macromolecules* **2001**, *34*, 8569-8573.
- (16) Meng, F.; Hiemstra, C.; Engbers, G. H. M.; Feijen, J. *Macromolecules* **2003**, *36*, 3004-3006.
- (17) Virtanen, J.; Holappa, S.; Lemmetyinen, H.; Tenhu, H. *Macromolecules* **2002**, *35*, 4763-4769.
- (18) Liu, S.; Liu, M. *Journal of Applied Polymer Science* **2003**, *90*, 3563-3568.
- (19) Heskins, M.; Guillet, J. E. *Journal of Macromolecular Science, Chemistry* **1968**, *2*, 1441-1455.
- (20) Durand, A.; Hourdet, D. *Polymer* **2000**, *41*, 545-557.
- (21) Chee, C. K.; Rimmer, S.; Shaw, D. A.; Soutar, I.; Swanson, L. *Macromolecules* **2001**, *34*, 7544-7549.
- (22) Chee, C. K.; Rimmer, S.; Soutar, I.; Swanson, L. *ACS Symposium Series* **2001**, *780*, 223-237.
- (23) Liu, H. Y.; Zhu, X. X. *Polymer* **1999**, *40*, 6985-6990.
- (24) Kobayashi, M.; Okuyama, S.; Ishizone, T.; Nakahama, S. *Macromolecules* **1999**, *32*, 6466-6477.
- (25) Freitag, R.; Baltes, T.; Eggert, M. *Journal of Polymer Science, Part A: Polymer Chemistry* **1994**, *32*, 3019-3030.
- (26) Eggert, M.; Freitag, R. *Journal of Polymer Science, Part A: Polymer Chemistry* **1994**, *32*, 803-813.
- (27) Schiessel, H. *Macromolecules* **1999**, *32*, 5673-5680.
- (28) Løyen, K.; Iliopoulos, I.; Olsson, U.; Audebert, R. *Progress in Colloid & Polymer Science* **1995**, *98*, 42-46.
- (29) Alexandridis, P.; Lindman, B. *Amphiphilic Block Copolymers: Self-Assembly and Applications*; Elsevier: Amsterdam, 2000.
- (30) Riess, G. *Progress in Polymer Science* **2003**, *28*, 1107-1170.

- (31) Gao, Z.; Varshney, S. K.; Wong, S.; Eisenberg, A. *Macromolecules* **1994**, *27*, 7923-7927.
- (32) Bütün, V.; Billingham, N. C.; Armes, S. P. *Journal of the American Chemical Society* **1998**, *120*, 11818-11819.
- (33) Bütün, V.; Armes, S. P.; Billingham, N. C.; Tuzar, Z.; Rankin, A.; Eastoe, J.; Heenan, R. K. *Macromolecules* **2001**, *34*, 1503-1511.
- (34) Liu, S.; Armes, S. P. *Angewandte Chemie, International Edition* **2002**, *41*, 1413-1416.
- (35) Liu, S.; Billingham, N. C.; Armes, S. P. *Angewandte Chemie, International Edition* **2001**, *40*, 2328-2331.
- (36) Arotcarena, M.; Heise, B.; Ishaya, S.; Laschewsky, A. *Journal of the American Chemical Society* **2002**, *124*, 3787-3793.
- (37) Weaver, J. V. M.; Armes, S. P.; Buetuen, V. *Chemical Communications (Cambridge, United Kingdom)* **2002**, 2122-2123.
- (38) André, X.; Benmohamed, K.; Müller, A. H. E. *Macromolecules* **2005**, submitted.
- (39) André, X.; Benmohamed, K.; Yakimansky, A. V.; Müller, A. H. E. *Proceedings, 40th IUPAC International Symposium on Macromolecules*: Paris, France, 2004.
- (40) Müller, A. H. E.; André, X.; Schilli, C. M.; Charleux, B. *Polymeric Materials: Science and Engineering* **2004**, *91*, 252-253.
- (41) André, X.; Zhang, M.; Müller, A. H. E. *Macromolecular Rapid Communications* **2005**, *26*, 558-563.
- (42) Dewhurst, C. D., GRASP v3.66 ed.; Institut Laue-Langevin: Grenoble, France, 2003.
- (43) Moreels, E.; De Ceuninck, W.; Finsy, R. *Journal of Chemical Physics* **1987**, *86*, 618-623.
- (44) Kratochvil, P. In *Classical light scattering from Polymer Solutions*; Jenkins, A. D., Ed.; Elsevier: Amsterdam, Oxford, 1987; p 187.
- (45) Ju, R. T. C.; Frank, C. W.; Gast, A. P. *Langmuir* **1992**, *8*, 2165-2171.
- (46) Bodycomb, J.; Hara, M. *Macromolecules* **1995**, *28*, 8190-8197.
- (47) Provencher, S. W. *Makromol. Chem.* **1979**, *180*, 201.
- (48) Provencher, S. W. *Computer Phys. Commun.* **1982**, *27*, 229.
- (49) Fujishige, S.; Kubota, K.; Ando, I. *J. Phys. Chem.* **1989**, *93*, 3311-3313.
- (50) Kubota, K.; Fujishige, S.; Ando, I. *J. Phys. Chem.* **1990**, *94*, 5154-5158.
- (51) Wang, X.; Wu, C. *Macromolecules* **1999**, *32*, 4299-4301.
- (52) Lessard, D. G.; Ousalem, M.; Zhu, X. X.; Eisenberg, A.; Carreau, P. J. *Journal of Polymer Science, Part B: Polymer Physics* **2003**, *41*, 1627-1637.
- (53) Idziak, I.; Avoce, D.; Lessard, D.; Gravel, D.; Zhu, X. X. *Macromolecules* **1999**, *32*, 1260-1263.
- (54) Borsali, R.; Nguyen, H.; Pecora, R. *Macromolecules* **1998**, *31*, 1548-1555.
- (55) Matsuoka, H.; Schwahn, D.; Ise, N. *Macromolecules* **1991**, *24*, 4227-4228.
- (56) Higgins, B. *Polymers and Neutron Scattering*; Oxford Science and Publications: Oxford, 1994.
- (57) Guinier, A.; Fournet, G. *Small-Angle Scattering of X-rays*, 1955.
- (58) Zhang, L.; Eisenberg, A. *Macromolecules* **1999**, *32*, 2239-2249.
- (59) Zhang, L.; Shen, H.; Eisenberg, A. *Macromolecules* **1997**, *30*, 1001-1011.
- (60) Kim, K. H.; Cui, G. H.; Lim, H. J.; Huh, J.; Cheol-Hee, A.; Jo, W. H. *Macromolecular Chemistry and Physics* **2004**, *205*, 1684-1692.
- (61) Selb, J.; Gallot, Y. *Makromolekulare Chemie* **1981**, *182*, 1491-1511.

- (62) Zhang, L.; Eisenberg, A. *Journal of the American Chemical Society* **1996**, *118*, 3168-3181.
- (63) Zhang, L.; Eisenberg, A. *Macromolecules* **1996**, *29*, 8805-8815.
- (64) Burguière, C. *Ph. D. Thesis*; Université Pierre et Marie Curie: Paris, France, 2001.
- (65) Schilli, C. M. *Ph. D. Thesis*; Universität Bayreuth: Bayreuth, 2003.
- (66) Brandrup, J.; Immergut, E. H.; Editors. *Polymer Handbook, Fourth Edition*, 1998.
- (67) Prochazka, K.; Bednar, B.; Tuzar, Z.; Kocirik, M. *Journal of Liquid Chromatography* **1988**, *11*, 2221-2239.
- (68) Prochazka, K.; Bednar, B.; Tuzar, Z.; Kocirik, M. *Journal of Liquid Chromatography* **1989**, *12*, 1023-1041.
- (69) Schilli, C. M.; Zhang, M.; Rizzardo, E.; Thang, S. H.; Chong, Y. K.; Edwards, K.; Karlsson, G.; Müller, A. H. E. *Macromolecules* **2004**, *37*, 7861-7866.
- (70) Desjardins, A.; Eisenberg, A. *Macromolecules* **1991**, *24*, 5779-5790.
- (71) Spevacek, J.; Hanykova, L.; Ilavsky, M. *Macromolecular Chemistry and Physics* **2001**, *202*, 1122-1129.
- (72) Spevacek, J.; Geschke, D.; Ilavsky, M. *Polymer* **2000**, *42*, 463-468.
- (73) Starovoytova, L.; Spevacek, J.; Ilavsky, M. *Polymer* **2005**, *46*, 677-683.
- (74) Costa, R. O. R.; Freitas, R. F. S. *Polymer* **2002**, *43*, 5879-5885.
- (75) Baltes, T.; Garret-Flaudy, F.; Freitag, R. *J. Polym. Sci., Part A: Polym. Chem.* **1999**, *37*, 2977-2989.
- (76) Pergushov, D. V.; Remizova, E. V.; Gradzielski, M.; Lindner, P.; Feldthusen, J.; Zezin, A. B.; Müller, A. H. E.; Kabanov, V. A. *Polymer* **2004**, *45*, 367-378.
- (77) Moffitt, M.; Yu, Y.; Nguyen, D.; Graziano, V.; Schneider, D. K.; Eisenberg, A. *Macromolecules* **1998**, *31*, 2190-2197.
- (78) Kriz, J.; Masar, B.; Pospisil, H.; Plestil, J.; Tuzar, Z.; Kiselev, M. A. *Macromolecules* **1996**, *29*, 7853-7858.
- (79) Lee, A. S.; Gast, A. P.; Bütün, V.; Armes, S. P. *Macromolecules* **1999**, *32*, 4302-4310.
- (80) Liu, S.; Armes, S. P. *Langmuir* **2003**, *19*, 4432-4438.
- (81) Förster, S.; Zisenis, M.; Wenz, E.; Antonietti, M. *Journal of Chemical Physics* **1996**, *104*, 9956-9970.
- (82) Schuch, H.; Klingler, J.; Rossmanith, P.; Frechen, T.; Gerst, M.; Feldthusen, J.; Müller, A. H. E. *Macromolecules* **2000**, *33*, 1734-1740.
- (83) Glatter, O.; Kratky, O.; Editors. *Small Angle X-ray Scattering*, 1982.
- (84) Dautzenberg, H.; Jaeger, W.; Kötz, J.; Philipp, B.; Seidel, C.; Stscherbina, D. *Polyelectrolytes - Formation, Characterization and Application*; Hanser Publishers: Munich, Vienna, New York, 1994.
- (85) Förster, S.; Schmidt, M.; Antonietti, M. *Polymer* **1990**, *31*, 781-792.
- (86) Förster, S.; Abetz, V.; Müller, A. H. E. *Advances in Polymer Science* **2004**, *166*, 173-210.
- (87) Förster, S.; Hermsdorf, N.; Böttcher, C.; Lindner, P. *Macromolecules* **2002**, *35*, 4096-4105.
- (88) Khougaz, K.; Astafieva, I.; Eisenberg, A. *Macromolecules* **1995**, *28*, 7135-7147.
- (89) Rivas, B. L.; Pereira, E. D.; Horta, A.; Renamayar, C. S. *European Polymer Journal* **2004**, *40*, 203-209.
- (90) Zimm, B. H. *Journal of Chemical Physics* **1948**, *16*, 1099-1116.
- (91) Stepanek, P. *Journal of Chemical Physics* **1993**, *99*, 6384-6393.
- (92) Petrov, P.; Rangelov, S.; Novakov, C.; Brown, W.; Berlinova, I.; Tsvetanov, C. B. *Polymer* **2002**, *43*, 6641-6651.

-
- (93) Schmidt, M. *Macromolecules* **1984**, *17*.
- (94) Burchard, W. *Advances in Polymer Science* **1983**, *48*, 1-124.
- (95) Groenewegen, W.; Egelhaaf, S. U.; Lapp, A.; van der Maarel, J. R. C. *Macromolecules* **2000**, *33*, 3283-3293.
- (96) Groenewegen, W.; Lapp, A.; Egelhaaf, S. U.; Van der Maarel, J. R. C. *Macromolecules* **2000**, *33*, 4080-4086.
- (97) Van der Maarel, J. R. C.; Groenewegen, W.; Egelhaaf, S. U.; Lapp, A. *Langmuir* **2000**, *16*, 7510-7519.
- (98) Sfika, V.; Tsitsilianis, C.; Kiriya, A.; Gorodyska, G.; Stamm, M. *Macromolecules* **2004**, *37*, 9551-9560.
- (99) Zhang, L.; Barlow, R. J.; Eisenberg, A. *Macromolecules* **1995**, *28*, 6055-6066.
- (100) Zhang, L.; Eisenberg, A. *Science (Washington, D. C.)* **1995**, *268*, 1728-1731.
- (101) André, X.; Müller, A. H. E.; Charleux, B. *Proceedings, 40th IUPAC International Symposium on Macromolecules*: Paris, France, 2004.
- (102) André, X.; Benmohamed, K.; Wunder, S.; Zhang, M.; Müller, A. H. E.; Charleux, B. *in preparation*.

5.6 Supporting Information

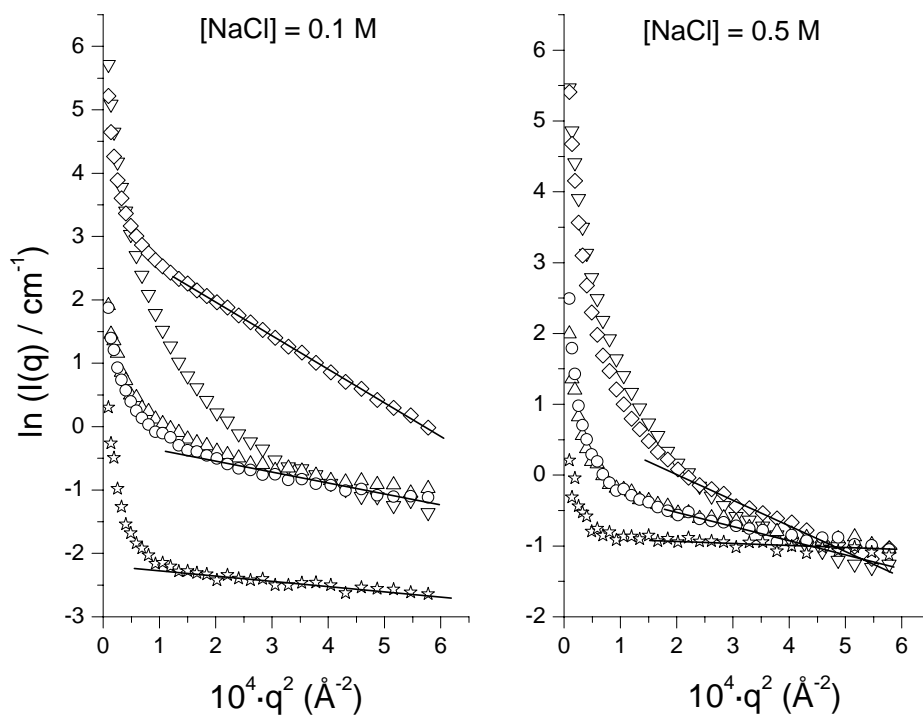


Figure 5-19. Guinier plots for the $(AA)_{45}\text{-}b\text{-(DEAAm)}_{360}$ in aqueous solutions at $T = 23\text{ }^\circ\text{C}$ for different salt concentrations and $\text{pH} = 1.0$ (X), 3.6 (M), 7.7 (8), 8.6 (v), and 12.7 (ψ), $c = 1.4\text{-}1.5\text{ g}\cdot\text{L}^{-1}$.

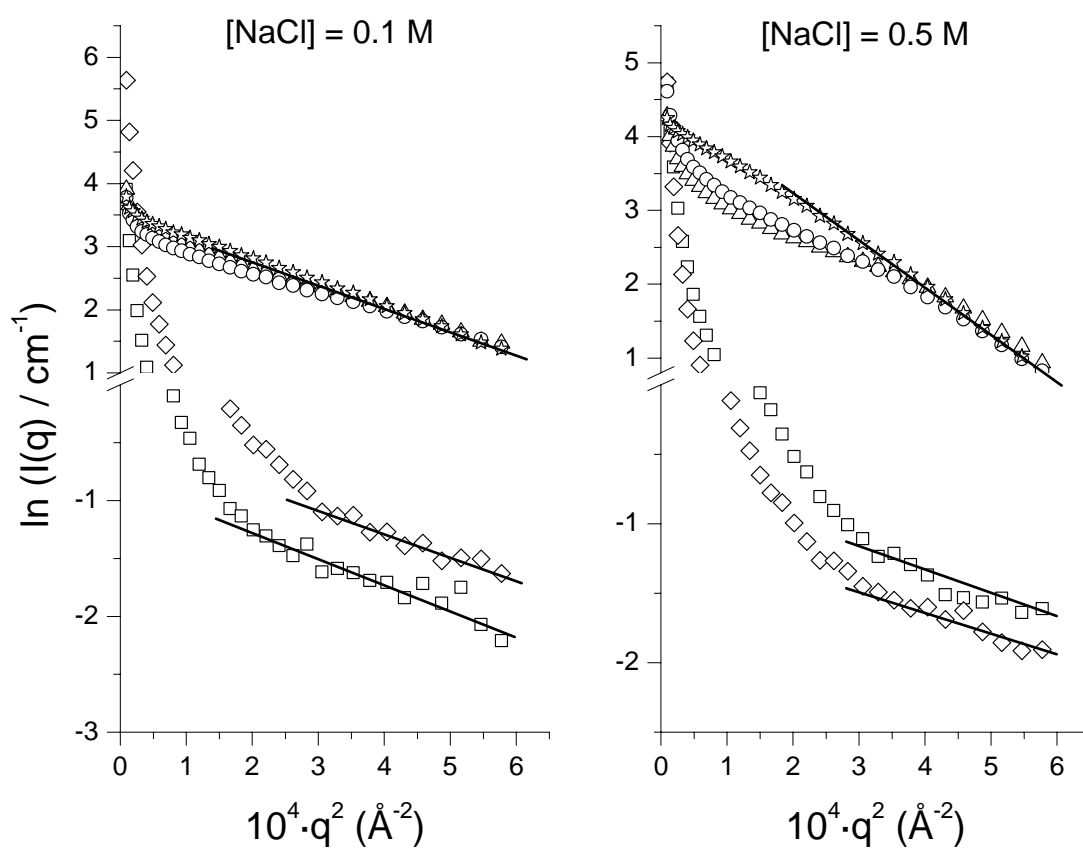


Figure 5-20. Guinier plots for the $(AA)_{45}\text{-}b\text{-(DEAAm)}_{360}$ in aqueous solutions at $T = 45\text{ }^{\circ}\text{C}$ for different salt concentrations and $\text{pH} = 1.0$ (X), 3.6 (M), 7.7 (8), 8.6 (v), and 12.7 (ψ), $c = 1.4\text{-}1.5\text{ g}\cdot\text{L}^{-1}$.

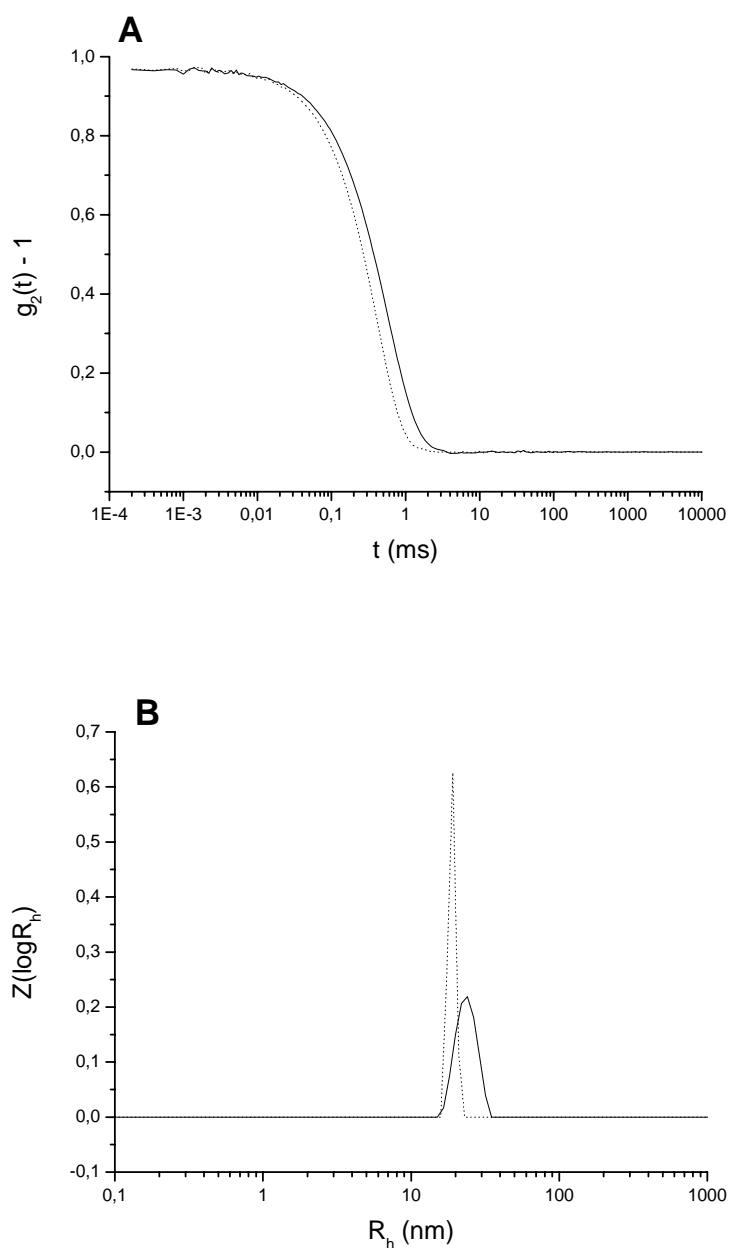


Figure 5-21. (A) Normalized autocorrelation function of $(AA)_{45}\text{-}b\text{-(DEAAm)}_{360}$ copolymer in NaOH solution at (—) 47.5, and (...) 58.1 °C for $\theta = 30^\circ$ ($[\text{NaCl}] = 0.1 \text{ mol}\cdot\text{L}^{-1}$, $c = 1.27 \text{ g}\cdot\text{L}^{-1}$, $\text{pH} = 12.8$). (B) Corresponding intensity-weighted hydrodynamic radius distributions of $(AA)_{45}\text{-}b\text{-(DEAAm)}_{360}$ (CONTIN analysis, $\theta = 30^\circ$).

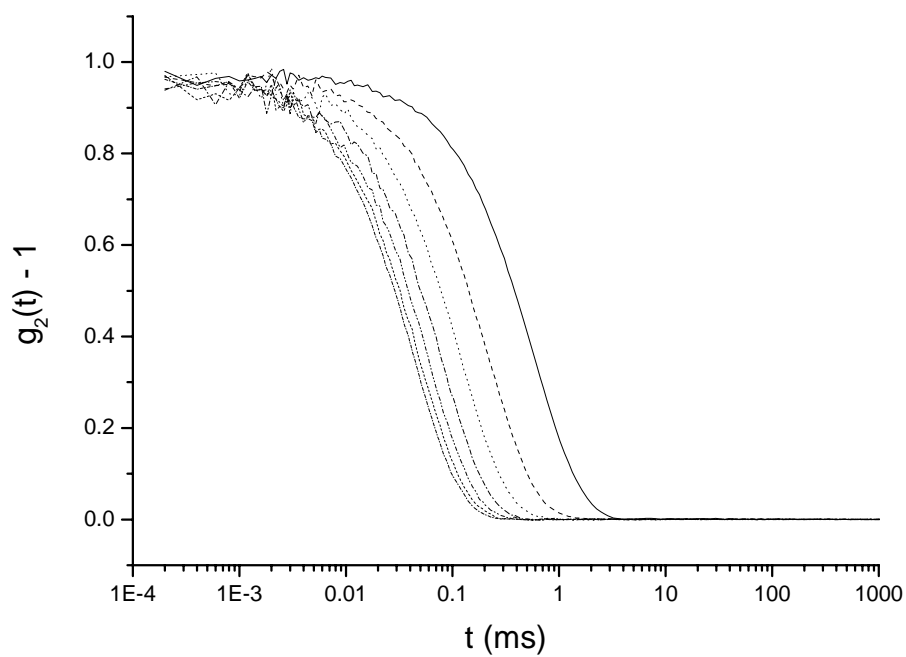


Figure 5-22. Normalized autocorrelation function of $(AA)_{45}\text{-}b\text{-(DEAAm)}_{360}$ copolymer in water at $T = 45\text{ }^\circ\text{C}$ for $\theta = 30^\circ$ (—), 50° (---), 70° (···), 90° (-·-), 110° (- - -), 130° (- - -), and 150° (···) ($[\text{NaCl}] = 0.1\text{ mol}\cdot\text{L}^{-1}$, $c = 1.25\text{ g}\cdot\text{L}^{-1}$, $\text{pH} = 12.8$).

6. Remarkable Stabilization of Latex Particles by a New Generation of Double-Stimuli Responsive Poly[(Meth)acrylic Acid]-*block*-Poly(*N,N*-diethylacrylamide) Copolymers

Xavier André, Khaled Benmohamed, Sabine Wunder,

Axel H. E. Müller, and Bernadette Charleux^{‡,*}

*Makromolekulare Chemie II, Universität Bayreuth, Universitätstrasse 30,
95440 Bayreuth, Germany*

[‡]*Laboratoire de Chimie des Polymères, UMR 7610 associée au CNRS, Université Pierre et Marie Curie, 4 place Jussieu, 75252 Paris CEDEX 05, France*

*E-mail: charleux@ccr.jussieu.fr

Abstract

We report the remarkable feature of narrowly distributed ‘smart’ bishydrophilic/amphiphilic poly[(meth)acrylic acid]-*block*-poly(*N,N*-diethylacrylamide) [P(M)AA-*b*-PDEAAm] copolymers to act as emulsion stabilizer and to generate *in-situ* stable latexes of different natures, e.g. polystyrene (PS), poly(methyl methacrylate) (PMMA), and poly(*n*-butyl acrylate) (P*n*BA). The main advantage using these copolymers is that they are molecularly dissolved in water at room temperature under alkaline conditions, independently of their composition. Above their cloud point ($T_c \approx 35$ °C), the PDEAAm segment becomes hydrophobic and the block copolymer is amphiphilic. Thus, it can be used as stabilizer in emulsion polymerization process and it represents a considerable advance in comparison to the usual amphiphilic block copolymers used, like polystyrene-*block*-poly(acrylic acid), whose solubility in water is limited to very high hydrophilic/hydrophobic balance. Additionally, considering the relatively high glass transition temperature of the PDEAAm block, $T_g = 85.5$ °C, all the reagents except the

water-soluble initiator should be introduced at room temperature before heating the solution above T_c . This ‘one-pot’ method avoids the monomer droplet nucleation and the micellar nucleation is enhanced. The produced latexes were surprisingly stable for a long period of time, independently of the polymer nature and its glass transition temperature. This is true for glassy PS and PMMA and for soft PnBA latexes. The accurate determination of the particle size and particle size distribution was determined routinely by Dynamic Light Scattering (DLS) and Transmission Electron Microscopy (TEM), and also by Asymmetric Flow Field-Flow Fractionation (AF-FFF). The best stabilization is observed for the latexes stabilized with a symmetric block copolymer-to-monomer weight ratio of 2 %. In fact, the block copolymer desorption was expected and further investigations indicate that the stabilization is purely electrostatic. The P(M)AA segment is located at the particle surface whereas the PDEAAm one seems to be buried inside the particle by strong entanglements (PS and PMMA) or by covalent linkages to the polymer chains in the case of PnBA latex. Thus, the PDEAAm block can not act as steric stabilizer and the produced latexes are highly sensitive to freeze-thaw cycles. The produced latexes are pH-responsive and their flocculation is triggered by the decrease of pH. The formation of stable monomer-in-water emulsions at room temperature after heating the solution above T_c allowed the formation of stable submicrometer particles via miniemulsion procedure.

6.1 Introduction

The interests in intelligent or smart water-soluble materials have increased in the last years. They may include the amphiphilic block copolymers, which mimic the structure of low molecular weight surfactant and can self-assemble in aqueous solutions and form a variety of associated structures, whose nature depends essentially on the structural parameters (composition, architecture) and on the experimental conditions.¹ When including an intrinsically stimulus-responsive monomer, their behavior can additionally be triggered by appropriate external-environmental changes, such as pH,² temperature,³ ionic strength,⁴ electric field,⁵ or UV irradiation.⁶

The specific volume change in solutions of thermo-responsive amphiphilic water-soluble (co)polymers is of importance for biotechnological applications (drug carriers, enzyme immobilizations, polymer-protein conjugates etc.).⁷⁻⁹ Such materials are based on

a thermo-responsive monomer like *N*-isopropylacrylamide (NIPAAm),¹⁰ *N,N*-diethylacrylamide (DEAAm),¹¹ vinylcaprolactam,¹² methyl vinyl ether,¹³ or 2-(dimethylamino)ethyl methacrylate (DMAEMA),¹⁴ and undergo a coil-to-globule transition above their respective lower critical solution temperature (LCST).¹⁵ Copolymerization with an ionic or ionizable monomer renders stimuli-responsive copolymers, the amphiphilic properties of which can be triggered at the molecular level by a small variation of the temperature, the pH or the ionic strength of the solution.^{11,16}

Such materials can be used as stabilizers for latexes particles. The use of ionic or neutral amphiphilic block copolymers (macromolecular surfactant) in the stabilization of colloidal suspensions and emulsion polymerization processes was already reported. By using amphiphilic block copolymers, it was possible to enhance the final latex properties (electrosteric stabilization) in comparison to latex stabilized by a low molecular weight surfactant like sodium dodecyl sulfate (SDS),¹⁷ and to avoid the use of an hydrophilic comonomer, whose traces in the final latex is considered as an impurity for many applications.¹⁸⁻²⁰ Nevertheless, some drawbacks are encountered due to the limitation of the method inherent with the structure of the block copolymer itself. Indeed, the solubilization of amphiphilic block copolymer is rather complicated and time-consuming and is generally possible for copolymers containing a rather short hydrophobic block.²¹⁻²⁴ In some cases, a dialysis procedure together with the use of a common solvent are necessary for the solubilization of amphiphilic block copolymers in solution.^{25,26}

By including a stimulus-responsive ‘smart’ segment in the block copolymer structure, it is possible to use such compounds as intelligent surfactant, instead of the traditional ones used with permanent amphiphilic properties, like polystyrene-*block*-poly(acrylic acid), poly(hydrogenated butadiene)-*block*-poly(styrene sulfonate), or graft copolymer based on poly(ethylene glycol).

The emulsifying properties of poly(methyl vinyl ether)-*block*-poly(isobutyl vinyl ether) obtained by living cationic polymerization were demonstrated at room temperature in water/decane mixtures but were lost when the temperature was raised above the LCST of the poly(methyl vinyl ether) segment ($T_c \approx 36$ °C).¹³ Recently two groups have described the efficient stabilization of polystyrene latex particles by block copolymers based on DMAEMA. The pH-dependent surface activity exhibited by PS latexes stabilized by a PDMAEMA-*block*-poly(methyl methacrylate) suggests potential applications as stimulus-

responsive particulate emulsifiers for oil-in-water emulsions.^{27,28} But only the pH-dependence of the produced latex was investigated, whereas the polymer is also temperature-responsive. Indeed, the cloud point of PDMAEMA homopolymers was reported to be $32 \leq T_c \leq 50$ °C, depending on the polymerization degree.^{29,30} But in these cases, the poly(isobutyl vinyl ether) or PMMA segment is permanently hydrophobic and the direct solubilization is limited to copolymers with a low hydrophobic content.

To our knowledge, double-stimuli responsive bishydrophilic/amphiphilic block copolymers have not been used as stabilizer in emulsion polymerization up to now. The direct solubilization in aqueous solution of ‘smart’ amphiphilic block copolymers of highly hydrophobic content may represent an advantage and is possible by application of the appropriate stimulus, which renders a bishydrophilic block copolymer. Furthermore, the properties and state of the final latexes stabilized using these new compounds can be tuned by the change of one or more external stimulus(i), e.g. the pH and the temperature.

Herein we want to investigate the ability of new pH- and thermo-responsive diblock copolymers based on acrylic or methacrylic acid and *N,N*-diethylacrylamide to act as stabilizer for the emulsion polymerization of styrene (St), methyl methacrylate (MMA) and *n*-butyl acrylate (*n*BA). Well-defined poly(acrylic acid)-*block*-poly(*N,N*-diethylacrylamide) (PAA-*b*-PDEAAm), and poly(methacrylic acid)-*block*-poly(*N,N*-diethylacrylamide) (PMAA-*b*-PDEAAm) were synthesized via the sequential anionic polymerization of *tert*-butyl (meth)acrylate and *N,N*-diethylacrylamide.^{31,32} From the bishydrophilic block copolymer soluble in water under alkaline conditions at room temperature (molecularly dissolved block copolymer, unimer), direct PDEAAm-core micelles, and inverse PAA- or PMAA-core micelles can be obtained by tuning the pH or the temperature of the copolymer solution.³³ The stability of the produced latexes as well as the particle size and their particle size distribution is presented. Different monomers are used and the effect of different parameters such as the block copolymer concentration and composition, the pH and the temperature are investigated. DLS and TEM are used as routine methods for the characterization of the latexes.

6.2 Experimental Part

Materials. Styrene (St), methyl methacrylate (MMA), and *n*-butyl acrylate (*n*BA) (Acros, 99%) were distilled under vacuum before used and stored at 4 °C. Potassium persulfate ($K_2S_2O_8$, Aldrich 99+%), sodium metabisulfite ($Na_2S_2O_5$, Fluka $\geq 98\%$), potassium carbonate (K_2CO_3 , Merck $\geq 99\%$), tris(hydroxymethyl)aminomethane hydrochloride (TRIS·HCl, Aldrich, reagent grade) and hexadecane (Aldrich, $\geq 99\%$) were used as received. α,α' -azobisisobutyronitrile (AIBN, Fluka, 98+%) was recrystallized from benzene/hexane. Deionized water was used for all experiments. Sodium dodecyl sulfate (SDS, Acros 98%, used as received), narrowly distributed poly(acrylic acid) (PAA), poly(*N,N*-diethylacrylamide) (PDEAAm), poly(acrylic acid)-*block*-poly(*N,N*-diethylacrylamide) (PAA-*b*-PDEAAm), and poly(methacrylic acid)-*block*-poly(*N,N*-diethylacrylamide) (PMAA-*b*-PDEAAm) copolymers were used as macromolecular surfactant (stabilizer) (Figure 6-1). The polymers and block copolymers were synthesized via sequential anionic polymerization in tetrahydrofuran (THF) and their respective synthesis reported elsewhere.³² The absolute number-average polymerization degrees, DP_n , were determined by MALDI-TOF mass spectrometry.

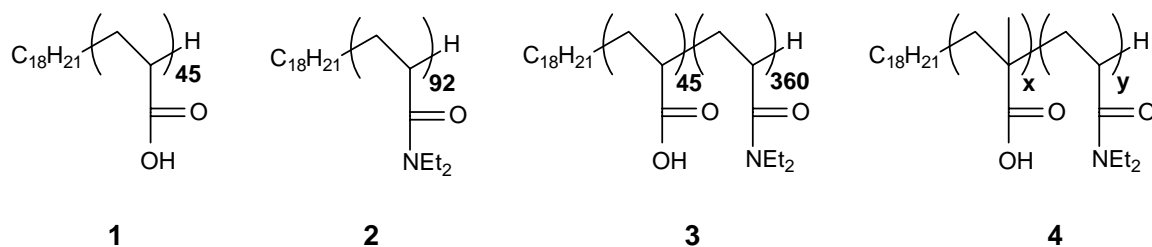


Figure 6-1. Structure of the poly(acrylic acid) (1), poly(*N,N*-diethylacrylamide) (2), poly(acrylic acid)-*block*-poly(*N,N*-diethylacrylamide) (3), and poly(methacrylic acid)-*block*-poly(*N,N*-diethylacrylamide) (4) (co)polymers.

Batch emulsion polymerization procedure. Batch emulsion polymerizations were carried out in a 100 mL three-neck-round-bottom flask equipped with a reflux condenser and a nitrogen inlet. In the ‘one-pot’ method, the surfactant or the block copolymer (10.5 mg , $1.0 \text{ to } 3.5 \cdot 10^{-2} \text{ mmol} \cdot \text{L}^{-1}$), the salt (K_2CO_3 , 56.3 mg , $20.3 \text{ mmol} \cdot \text{L}^{-1}$), and the monomer (2 g , ca. $0.95 \text{ mol} \cdot \text{L}^{-1}$) were added to 18 g of deionized water at room temperature ($\text{pH} =$

11.0-11.5). Latexes with a 10 % solid content were targeted in all cases. The reaction mixtures were immersed in a thermoregulated oil bath at 70 °C, magnetically stirred at ca. 300 rpm, and deoxygenated by nitrogen bubbling for 45 min under continuous stirring. A deoxygenated aqueous solution of the initiator potassium persulfate ($\text{K}_2\text{S}_2\text{O}_8$, 26 mg in 2g of water, $5.0 \text{ mmol}\cdot\text{L}^{-1}$) was added to start the polymerization ($t = 0$). After 4 hours, the solution was quenched by plunging the flask into an ice-bath. In one experiment (run B), styrene was added to the pre-formed aqueous micellar solution of $(\text{AA})_{45}\text{-}b\text{-(DEAAm)}_{360}$ at 70 °C, i.e. ‘pre-micellization’ method.

Batch emulsion polymerizations of styrene were carried out at 23 °C under acidic and alkaline conditions (pH = 4.0, and 11.0, respectively) using the ‘one-pot’ procedure described above. The solutions containing the reagents except the initiator were deoxygenated for 45 minutes under continuous stirring (300 rpm) at 23 °C. The initiators dissolved in deoxygenated water were added, $\text{Na}_2\text{S}_2\text{O}_5$ first (20.5 mg, $4.7 \text{ mmol}\cdot\text{L}^{-1}$), immediately followed by $\text{K}_2\text{S}_2\text{O}_8$ (27.1 mg, $4.4 \text{ mmol}\cdot\text{L}^{-1}$). This step corresponded to time zero of the polymerization reaction. The reaction was quenched by plunging the flask into an ice-bath after 48 hours of reaction.

Miniemulsion polymerization procedure. Batch miniemulsion polymerization was performed at 70 °C in a 100 mL three-neck-round-bottom flask equipped with a reflux condenser and a nitrogen inlet. Hexadecane was used as hydrophobe (5 wt.-% with respect to styrene) to stabilize the droplets from Ostwald ripening. Styrene (St, 2.0 g, $0.97 \text{ mmol}\cdot\text{L}^{-1}$) with AIBN (14.9 mg, $4.1 \text{ mmol}\cdot\text{L}^{-1}$), and hexadecane (0.1 g, $5.0 \text{ mmol}\cdot\text{L}^{-1}$) was added to a clear aqueous solution containing K_2CO_3 (53.7 mg, $20.3 \text{ mmol}\cdot\text{L}^{-1}$) and the copolymer, $(\text{AA})_{45}\text{-}b\text{-(DEAAm)}_{360}$ (39.6 mg, $1.1 \text{ mmol}\cdot\text{L}^{-1}$). The turbid initial emulsion (pH = 11.4) was strongly sheared at room temperature by ultrasonification (Branson 450 Sonifier; 20% power) for 10 minutes in order to get a stable emulsion with submicronic monomer droplets. The process leads to an increase of the solution temperature to ca. 40 °C. This emulsion was then deoxygenated by nitrogen bubbling for 45 minutes and plunged into the pre-heated oil bath at 70 °C ($t = 0$). The reaction was quenched by plunging the flask into an ice-bath after 6 hours of reaction.

Characterization of the latexes. The latexes were characterized by their polymer content τ_{poly} ($\text{g}\cdot\text{L}_{\text{latex}}^{-1}$) obtained from gravimetric analyses taking into account the weight

of polymer and that of block copolymer. The final density of particles or particles number, N_p (L_{latex}^{-1}) was calculated according to

$$N_p = \frac{6 \cdot \tau_{\text{poly}}}{\pi \cdot d \cdot D^3} \quad (6-1)$$

with D the particle diameter expressed in cm and d the density of polystyrene, polymethylmethacrylate, and poly(*n*-butyl acrylate), 1.05, 1.19, and 0.90 $\text{g}\cdot\text{cm}^{-3}$, respectively.

The z -average particle average diameters, $D_{p,\text{DLS}}$ (nm), were measured using an ALV DLS/SLS-SP 5022F compact goniometer system with an ALV 5000/E correlator equipped with a He/Ne laser ($\lambda = 632.8$ nm) and an avalanche diode. The solutions were prepared by diluting a few drops of latex with pure water (pH = 7). Prior to light scattering measurements, the solutions were filtered using 1.0 μm Millipore glass fiber filter (hydrophilic). The sample cells were thermostated 10 minutes at 23 °C (room temperature) or at 45 °C before the measurement. A 2nd order cumulant analysis was used for data evaluation of the autocorrelation function at the scattering angle, $\theta = 90^\circ$. The relative polydispersity indexes of the latex particles, μ_2/Γ^2 , were determined from the cumulant analysis of the normalized intensity autocorrelation function, $g_2(t)$, according to Equation 6-2 where Γ is the decay rate.

$$\ln(g_2(t)) = \ln(A) - \Gamma t + \frac{\mu_2}{2} t^2 - \frac{\mu_3}{6} t^3 + \dots \quad (6-2)$$

Transmission electron microscopy (TEM) images were taken on a Zeiss 922 OMEGA EFTEM (Zeiss NTS GmbH, Oberkochen, Germany) with an accelerating potential of 200 kV. The latex diluted in pure water (0.02 wt.-%, non-filtered) was deposited onto a copper grid covered with a carbon membrane. After 2 minutes drying at room temperature, the sample was inserted into the microscope and the analysis was carried out at low temperature ($T = -150$ °C). The number-average particle diameter, D_n , the weight-average

particle diameter, D_w , and the z-average particle diameter, D_z , were calculated from the mean value of 200 particles according to

$$\begin{aligned} D_n &= \frac{\sum n_i D_i}{\sum n_i} \\ D_w &= \frac{\sum n_i D_i^4}{\sum n_i D_i^3} \\ D_z &= \frac{\sum n_i D_i^5}{\sum n_i D_i^4} \end{aligned} \quad (6-3)$$

The latex particle diameters and their particle size distributions were determined by Asymmetric Flow Field-Flow Fractionation (AF-FFF)^{34,35} using a Postnova Analytics HRFFF-10000 system equipped with a UV detector ($\lambda = 210$ nm), and a Multiangle Light Scattering (MALS, Wyatt DAWN EOS, $\lambda = 632.8$ nm) detector with a 0.2 v/v % aqueous solution of FL-70[®] detergent (Fisher Scientific) as eluent at $T = 23$ °C. The MALS detectors at various angles were calibrated using pure HPLC grade toluene (Merck), and normalized using an aqueous solution of dextran (MW = 65,000, $\langle R_g^2 \rangle^{1/2} = 7$ nm). The following experimental conditions were applied: latex concentration = ca. 0.02 wt.-% (filtered using 0.2 μ m nylon filters); dimension of the channel, 0.35 mm; membrane cutoff molecular weight, 10⁴; injection volume, 100 μ L; measuring time, 30 min; cross-flow gradient, 68-0% within 40 min; laminar flow out, 1.0 mL \cdot min⁻¹. The collected data were processed with the Astra for Windows software version 4.73 (Wyatt Technology, Santa Barbara, CA, USA) using a linear Berry fit.^{36,37} The number-average, weight-average, and z-average particle diameters, D_n , D_w , and D_z , respectively, were derived from the corresponding root-mean-square radii of gyration. The errors on the extrapolated values were less than 10 % in all cases. The polydispersity was determined as follows: PDI = D_w/D_n .

Scanning Electron Microscopy (SEM) image was taken on a LEO 1530 apparatus with an accelerating potential of 0.8 kV. The silica wafer was deep coated from the diluted latex solution (0.01 wt.-%).

Location of the copolymer in the latex. The crude PS latex stabilized with 1.9 % of (AA)₄₅-*b*-(DEAAM)₃₆₀ copolymer-to-styrene weight ratio (run D in Table 6-1) was destabilized by three freeze-thaw cycles and separated from the serum using a Heraeus Megafuge 1.0R centrifuge at 4,000 rpm for 30 minutes at $T = 23$ °C. The turbid solution (serum) was removed and the compacted solid phase redispersed in pure water, and centrifuged a second time using the same conditions. The washing solution was added to the firstly extracted serum. The latexes before (crude) and after centrifugation were dried under vacuum for two days at room temperature. Cast films were prepared on CaF₂ plates from the dried latexes by dissolving them in chloroform (CHCl₃, 2.2 wt.-%). After evaporation of the CHCl₃, infrared spectra were recorded on a Bruker 55/S FT-IR spectrometer at $T = 23$ °C and constructed from 128 scans (resolution 4 cm⁻¹) after subtraction of the empty plates spectrum. Elementary analysis (EA) of the crude and the centrifuged latexes were performed by Ilse Beetz Mikroanalytisches Laboratorium (Kronach, Germany).

6.3 Results and Discussion

Emulsion polymerization in the presence of PDEAAM-core micelles: $T > T_c$, pH \geq 8.

The emulsion polymerizations of styrene (St) methyl methacrylate (MMA), and *n*-butyl acrylate (*n*BA) initiated by K₂S₂O₈ were carried out in alkaline water at $T = 70$ °C in the presence of amphiphilic (AA)₄₅-*b*-(DEAAM)₃₆₀ or (MAA)_{*x*}-*b*-(DEAAM)_{*y*} block copolymers as macromolecular stabilizers. As reported elsewhere, this type of bishydrophilic copolymer is molecularly dissolved in alkaline water at room temperature (pH \geq 8) and forms PDEAAM-core micelles upon heating the temperature above the cloud point of the PDEAAM segment, $T_c \approx 35$ °C.³¹ Under such emulsion polymerization conditions, all the acrylic acid units are in the potassium salt form ($pK_{a,PAA} = 6.15$)²⁰ and the block copolymer is amphiphilic ($T > T_c$).

(i) Influence of the emulsion preparation method. Determining the adequate polymerization procedure for the synthesis of latexes is the starting point of this study. Indeed, the case of bishydrophilic block copolymers is rather different from that of other amphiphilic block copolymers described in the literature.³⁸ In the latter case, the direct

solubilization in the aqueous medium was achieved only when the hydrophobic segment was short enough and a heating procedure was necessary. In contrast, the bishydrophilic copolymers used in this study are molecularly dissolved at room temperature in alkaline water and form amphiphilic assemblies upon heating above the cloud point of the PDEAAm segment. The initial state of an emulsion might determine the final state because it has a direct influence on the nucleation step. A priori, the formation of frozen micelles can be envisaged due to the relatively high glass transition temperature of the PDEAAm homopolymer ($T_g = 85.5 \text{ }^\circ\text{C}$),³⁹ in their frozen state, the block copolymer unimers are kinetically frozen and it can lead to the incomplete stabilization of the system and a multi-loci nucleation after injection of the water-soluble initiator.

Table 6-1. Batch emulsion polymerization of styrene using $\text{K}_2\text{S}_2\text{O}_8$ as a radical initiator at $70 \text{ }^\circ\text{C}$ and various amounts of the $(\text{AA})_{45}\text{-}b\text{-(DEAAm)}_{360}$ copolymer as stabilizer^a

Run	[copolymer]		Conv. ^c ($\text{g}\cdot\text{L}^{-1}$)	particle diameter TEM ^d			particle diameter DLS ^f			
	wt.-% vs St ^b	10^{-5} $\text{mol}\cdot\text{L}_{\text{latex}}^{-1}$		D_n (nm)	D_z (nm)	D_w/D_n^e TEM	D_z (nm)	μ_2/Γ^2	$10^{16}\cdot N_p^g$ ($\text{L}_{\text{latex}}^{-1}$)	$10^{16}\cdot N_{m,\text{app}}^h$ ($\text{L}_{\text{latex}}^{-1}$)
A	0.5	1.0	84.5	218	350	1.45	402	0.138	1.34	10.8
B ⁱ	0.5	1.0	52.5	191	967	2.66	458	0.299	1.24	11.0
C	1.1	2.0	73.5	262	725	2.82	286	0.080	0.67	22.0
D	1.9	3.5	80.9	124	141	1.10	180	0.186	7.02	39.8

^a Reagents and conditions: $[\text{St}]_0 = 0.95 \text{ mol}\cdot\text{L}^{-1}$, $[\text{K}_2\text{S}_2\text{O}_8]_0 = 5\cdot 10^{-3} \text{ mol}\cdot\text{L}^{-1}$, $[\text{K}_2\text{CO}_3] = 20\cdot 10^{-3} \text{ mol}\cdot\text{L}^{-1}$, $T = 70 \text{ }^\circ\text{C}$, solid content: 10 wt.-% St/ H_2O , pH = 11.2 using the one-pot method. ^b Block copolymer $[(\text{AA})_{45}\text{-}b\text{-(DEAAm)}_{360}]$ -to-styrene weight ratio. ^c Styrene conversion after 4 hours of reaction calculated by gravimetric analysis. ^d D_n is the number-average diameter and D_z the z-average mean diameter of the polystyrene particles calculated from TEM with 200 particles according to Equation 6-3. ^e D_w/D_z is the polydispersity index. ^f z-average hydrodynamic radius measured at pH = 7 by DLS at $\theta = 90^\circ$ and $T = 23 \text{ }^\circ\text{C}$ using a second-order cumulant analysis. ^g Final number of particles, N_p , calculated from $D_{n,\text{TEM}}$ (see Equation 6-1). ^h Apparent total number of micelles, $N_{m,\text{app}}$, calculated from Equation 6-4. ⁱ Pre-micellization method.

Therefore, two experimental procedures were investigated. In the first one (run A, Table 6-1), all reagents except the water-soluble radical initiator ($K_2S_2O_8$) were introduced to the deionized water at room temperature ($T = 23\text{ }^\circ\text{C}$), allowing the different equilibria to take place during deoxygenating and heating up the solution to $70\text{ }^\circ\text{C}$: ‘one-pot’ method. On the other hand (run B, Table 6-1), styrene was added to the pre-formed micellar solution at $T = 70\text{ }^\circ\text{C}$: ‘pre-micellization’ method. In both cases, the addition of initiator represents the time zero of the reaction. The emulsion polymerizations proceed in a normal way where the turbid appearance is replaced by the characteristic milky one after ca. 10 minutes of reaction. The homogeneous polymerization mixtures are quenched in an ice-bath after 4 hours. High monomer conversion ($> 80\%$) is reached in the case of the PS latex produced with the ‘one-pot’ method whereas only 50% of monomer conversion is calculated for the other method.

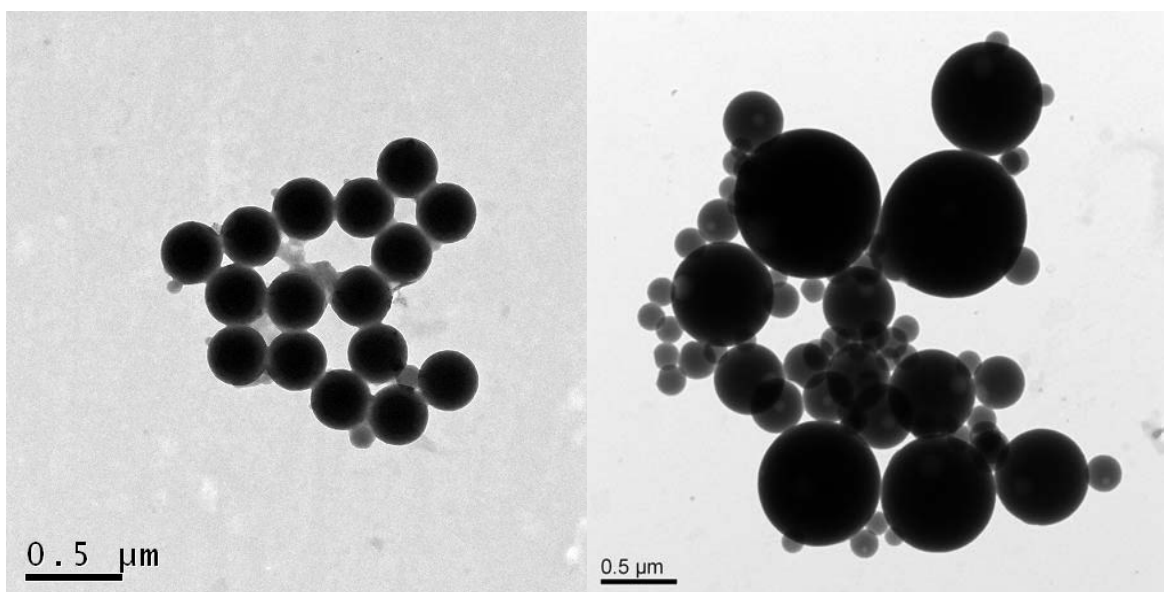


Figure 6-2. TEM images of PS latexes stabilized with 0.5 wt.-% of $(AA)_{45}\text{-}b\text{-(DEAAm)}_{360}$ copolymer-to-styrene ratio using (A) the ‘one-pot’, and (B) the ‘pre-micellization’ methods, runs A and B, respectively. See Table 6-1 for experimental conditions.

Both analytical methods used as routine in this study (DLS, TEM) indicate that the PS latex particles synthesized using the ‘pre-micellization’ are broadly dispersed in comparison to the one synthesized using the one-pot method, $D_w/D_n = 2.66$ and 1.45,

respectively for a same amount of $(AA)_{45}\text{-}b\text{-}(\text{DEAAM})_{360}$ copolymer (see Table 6-1, runs A and B). The TEM images of both runs are shown in Figure 6-2. In the case of pre-formed micelles, the bimodal particle size distribution suggests that two nucleation loci existed, i.e. in the pre-formed micelles and in the large monomer droplets. The polymerization rate is considerably lowered in that case may be due to the lower amount of particles (N_p) but the experimental results (Table 6-1) do not reflect this tendency.

In the ‘pre-micellization’ initial state (before addition of the water-soluble initiator), the frozen state of the micelles may prevent them from monomer swelling, ensuring therefore the nucleation in the monomer droplets. In contrast, the ‘one-pot’ procedure allows the formation of the micelles in the presence of monomer, ensuring their swelling together with dynamics exchanges of the unimers between micelles and polymer particles in formation. The ‘one-pot’ method avoids the monomer droplet nucleation and the micellar nucleation is enhanced. Thus, this method was used systematically in this study.

(ii) Latex stability. From the colloidal point of view, the important result is that the polystyrene latexes are all stable for long period of time. All latexes produced using the $(AA)_{45}\text{-}b\text{-}(\text{DEAAM})_{360}$ copolymer as stabilizer are stable at 70 °C during the polymerization, and at 23 °C. No flocculation process is observed, even after 12 months indicating the efficiency of the stabilization during the storage at room temperature. This phenomenon is remarkable since the $(AA)_{45}\text{-}b\text{-}(\text{DEAAM})_{360}$ copolymer is water-soluble when the temperature remains below the cloud point of the PDEAAM segment ($T_c \approx 35$ °C) and consequently should desorb from the particle surface. Using a poly(methacrylic acid)₅₂-block-poly(*N,N*-diethylacrylamide)₅₅, $(\text{MAA})_{52}\text{-}b\text{-}(\text{DEAAM})_{55}$, as emulsion stabilizer, the same feature was observed, i.e. the produced PS latexes are stable for months at room temperature (see Table 6-2).

Table 6-2. Emulsion polymerization of styrene (St) and methyl methacrylate (MMA) using various amounts of (MAA)_x-*b*-(DEAAm)_y copolymer as stabilizer^a

Run	Copolymer	monomer	[copolymer]		Conv. (%)	particle diameter ^d DLS		$D_{n,TEM}^e$ (nm)	particles density $10^{16} \cdot N_p^f$ (L ⁻¹ latex)
			wt.-% vs St ^b	$10^5 \cdot \text{mol L}^{-1}$		D_z (nm)	μ_2/Γ^2		
E	(MAA) ₅₂ - <i>b</i> -(DEAAm) ₅₅	MMA	0.5	3.6	91.0	226	0.106	153	4.18
F	(MAA) ₅₂ - <i>b</i> -(DEAAm) ₅₅	MMA	1.0	8.1	78.0	208	0.244	93	15.8
G	(MAA) ₅₂ - <i>b</i> -(DEAAm) ₅₅	MMA	2.1	16.2	72.3	125	0.176	110	8.76
H	(MAA) ₅₂ - <i>b</i> -(DEAAm) ₅₅	St	0.5	3.8	48.3	122	0.126	81	15.1
I	(MAA) ₅₂ - <i>b</i> -(DEAAm) ₅₅	St	1.0	7.8	83.3	162	0.048	153	3.81
J	(MAA) ₅₂ - <i>b</i> -(DEAAm) ₅₅	St	2.1	16.6	81.8	101	0.089	73	34.7
K	(MAA) ₅₄ - <i>b</i> -(DEAAm) ₂₈	St	1.9	20.5	85.4	257	0.152	169	3.01
L	(MAA) ₅₅ - <i>b</i> -(DEAAm) ₈₂	St	2.0	11.7	86.9	126	0.185	84	24.1
M	(MAA) ₅₈ - <i>b</i> -(DEAAm) ₁₁₂	St	1.9	9.2	78.0	180	0.248	91	17.5
N	(MAA) ₅₆ - <i>b</i> -(DEAAm) ₁₄₁	St	2.0	8.0	81.5	130	0.089	105	11.5
O	(MAA) ₇₃ - <i>b</i> -(DEAAm) ₂₅	St	2.7	18.4	84.5	134	0.033	123	7.59
P	(MAA) ₇₈ - <i>b</i> -(DEAAm) ₃₈	St	1.9	15.4	76.2	124	0.024	105	11.2
Q	(MAA) ₇₇ - <i>b</i> -(DEAAm) ₂₀₇	St	2.1	5.7	88.9	135	0.176	101	14.1

^a Reagents and conditions: [monomer] = ca. 1 mol·L⁻¹ (St or MMA), [K₂S₂O₈] = 5·10⁻³ mol·L⁻¹, [K₂CO₃] = 20·10⁻³ mol·L⁻¹ in deionized water at $T = 70$ °C, solid content: 10 wt.-% St/H₂O, pH = 11.2 using the one-pot method. ^b Copolymer (MAA)_x-*b*-(DEAAm)_y to styrene weight ratio. ^c Monomer conversion after 4 hours of reaction calculated by gravimetric analysis. ^d z -average hydrodynamic radius, D_z , measured at pH = 7 by DLS at $\theta = 90^\circ$ and $T = 23$ °C using a 2nd cumulant analysis. ^e By TEM, D_n is the average number radius calculated from the mean value of 200 particles. ^f Number of particles per liter of latex, calculated from $D_{n,TEM}$, see Equation 6-1.

Furthermore, using $(AA)_{45}\text{-}b\text{-}(\text{DEAAm})_{360}$ and $(\text{MAA})_x\text{-}b\text{-}(\text{DEAAm})_y$ block copolymers as macromolecular stabilizer, it is possible to synthesize stable polystyrene (PS), poly(methyl methacrylate (PMMA), and poly(*n*-butyl methacrylate) (*Pn*BA) latexes. Using various amounts of $(\text{MAA})_{52}\text{-}b\text{-}(\text{DEAAm})_{55}$, the produced PS and PMMA latex particles are in the same size range ($70 < D_{n,\text{TEM}} < 150$) and their particle size distributions remain narrow for both core-nature (runs E-G and H-J). These results suggest that the PDEAAm segment of the block copolymer might be strongly anchored at the particle, maybe, owing to their glassy state at room temperature, which might favor an irreversible trapping. Such hypothesis was checked using *n*BA as a monomer for the emulsion polymerization.

The conventional batch emulsion polymerization of *n*-butyl acrylate is carried out to study the influence of the particle nature and of the T_g on the stabilization process. In contrast to atactic polystyrene and poly(methyl methacrylate) synthesized via free-radical polymerization, whose T_g are above room temperature, 100 and 105 °C, respectively,⁴⁰ poly(*n*-butyl acrylate) is a soft polymer ($T_g = -54$ °C).⁴⁰ Using 2.0 % of $(AA)_{45}\text{-}b\text{-}(\text{DEAAm})_{360}$ to *n*BA weight ratio, 88.9 % of monomer conversion is reached in 4 hours and the latex is stable at room temperature ($D_{z,\text{DLS}} = 270$ nm, $\mu_2/\Gamma^2 = 0.347$). From the colloidal view point, it is important to note that the latexes are stable independently of the monomer employed: styrene, methyl methacrylate or *n*-butyl acrylate. Consequently, the T_g of the final polymer is supposed to have a negligible effect on the surprising stabilization observed due to the a priori non-desorption of the block copolymer from the particle. The stabilization mechanism is discussed further below and especially the role of the C₁₈ hydrophobic fragment present on each chain and on the P(M)AA side (see location of the copolymer).

(iii) Accurate determination of the particle size. As a prerequisite before studying the influences of both the copolymer structure and the copolymer concentration, the accurate determination of the particle size is of importance because the final particle number, N_p , is not directly measured but derived from the final particle size. The final number of particles (particles density, N_p , Equation 6-1) is generally considered as a function of the weight fraction of stabilizer with respect to the monomer in the emulsion formulation. Indeed, the efficiency of a stabilizer is closely related to the highest surface area stabilized per

macromolecular chain, and consequently, for the same amount of stabilizer (weight content), the larger the final latex particle number, the better the efficiency.

As summarized in Table 6-1, considering the z -average values, huge differences can be observed between the results obtained by DLS and TEM: $D_{z,DLS} > D_{z,TEM}$. The differences observed, can not be explained by the thickness of the hydrophilic poly(potassium acrylate) shell. Indeed, for 100% extension and a $DP_n = 45$, a theoretical corona thickness of 11 nm can be estimated.⁴¹ It is well known that DLS is inaccurate for broad particle size distribution, the value being strongly overestimated due to the contribution of the large particles to the scattered intensity.^{31,42} This remains particularly true for PS latexes synthesized using a block copolymer-to-styrene weight ratio lower than 2 % (runs A, B, and C). We consider that narrowly distributed particles are obtained when $0.02 \leq \mu_2/\Gamma^2 \leq 0.1$ and only in that case, $D_{z,DLS} \approx D_{z,TEM}$. The PS latex stabilized with 1.9 wt.-% of block copolymer relative to styrene (run D, Table 6-1) was further characterized by AF-FFF coupled with MALS detection.⁴³ As shown in Figure 6-3, a monomodal particle size distribution is observed. By application of the Berry method and a first-order fit of the light scattering data, the z -average root-mean-square radius of gyration was determined to be, $\langle R_g^2 \rangle_z^{1/2} = 57.9 \pm 5.8$ nm which confirms the value obtained from TEM: $D_z = 141$ nm, $D_w/D_n = 1.10$ (Table 6-1). Thus, in this work, particles diameters were measured by DLS at pH = 7 for monodisperse particles, or by TEM for polydisperse particles. The particle number or particle density, N_p in L_{latex}^{-1} , was calculated from Equation 6-1.

The emulsion polymerization of styrene was carried out using SDS as a stabilizer (run T, Table 6-3). In that case, a z -average particle diameter of 70 nm was measured by DLS with a μ_2/Γ^2 ratio of 0.035 which corresponds to a $D_{z,TEM} = 77$ nm ($D_w/D_n = 1.04$) calculated with 200 particles. The corresponding TEM image is shown in Supporting Information (Figure 6-8). This observation confirms our experimental assumption, e.g. the value measured by DLS is correct for narrowly dispersed particles ($\mu_2/\Gamma^2 \leq 0.1$).

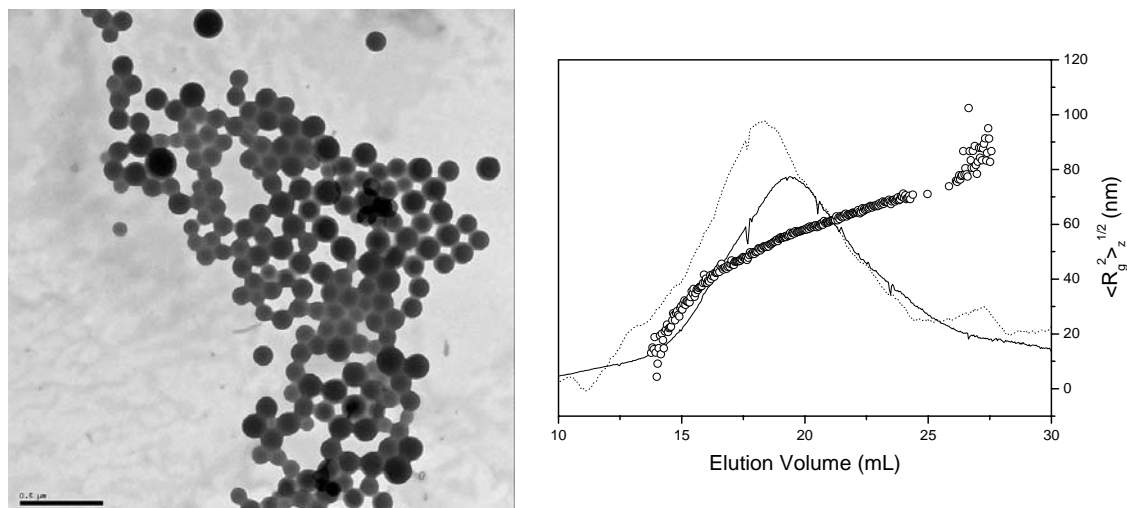


Figure 6-3. TEM image (left) and AF-FFF-MALS measurement in water+FL-70[®] (right) of the PS latex stabilized with 1.9 % of (AA)₄₅-*b*-(DEAAm)₃₆₀ copolymer-to-styrene weight ratio (run D). Experimental conditions: see Table 6-1. (—) 90° light scattering signal, (···) UV at $\lambda = 210$ nm, (○) z -average root-mean-square radius of gyration distribution obtained using the Berry method and first-order fit of the light scattering data.

(iv) **Influence of the PDEAAm block length on N_p .** The PS latexes (runs H, I, and J, Table 6-2) synthesized with (MAA)₅₂-*b*-(DEAAm)₅₅ are stable and their particle size is remarkably lower than that of the PS latexes synthesized using the more asymmetric (AA)₄₅-*b*-(DEAAm)₃₆₀, (runs A, C, and D, Table 6-1). Therefore, due to the glassy PDEAAm segment which is long in that case, it could have a huge effect on the initial emulsion state, on the copolymer mobility at $T > T_c$, on the nucleation mechanism, and on the different equilibria. Thus, the influence of the PDEAAm block length was studied using poly(methacrylic acid)-*block*-poly(*N,N*-diethylacrylamide) (PMAA-*b*-PDEAAm) of various PDEAAm block lengths as macromolecular stabilizer in the emulsion polymerization of styrene using the one-pot method (Table 6-2).

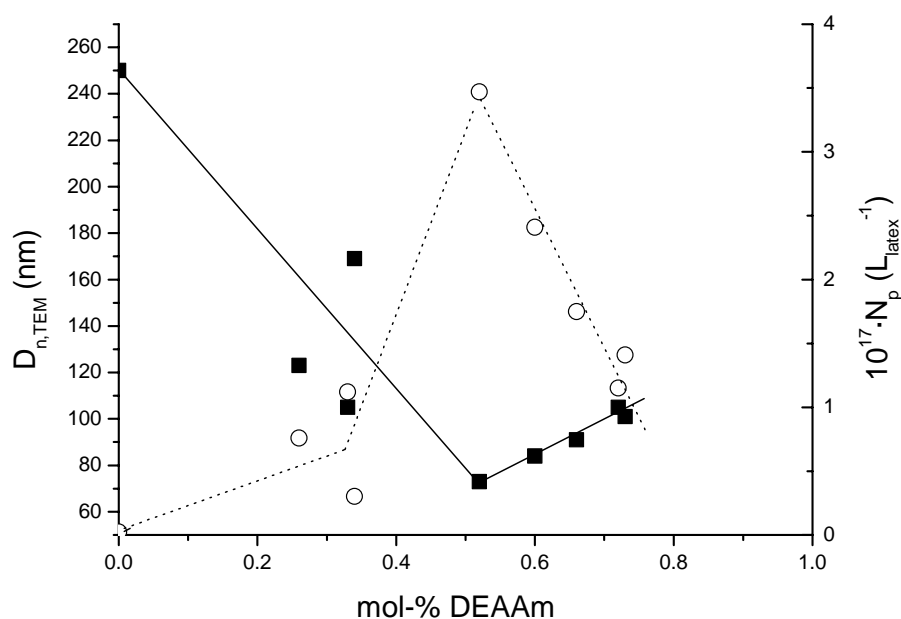


Figure 6-4. Dependence of the PS particle diameter (■) and of the corresponding particles number, N_p , calculated from Equation 6-1 (○) on the DEAAm composition (mol.-%). The data points for DEAAm = 0 mol.-% correspond to the PS latex produced a pure poly(acrylic acid)₄₅. Experimental conditions: block copolymer and homopolymer = 2 wt.-% relative to styrene, $T = 70$ °C, solid content: 10 wt.-% St/H₂O, see Tables 6-2 and 6-3.

Figure 6-4 shows the effect of the DEAAm mol-% on the PS particle size and on the particle number, considering that the PMAA blocks are similar for a series of block copolymers containing 54-77 methacrylic acid units (runs J to Q). The polymerization of styrene using a pure poly(acrylic acid)₄₅ (0 mol-% DEAAm) synthesized via the same method leads to the formation of a stable latex (Table 6-3, run R). The investigations on the stabilization mechanism are detailed below. For a DEAAm-content between 0 and 50 mol-%, the number-average particle size decreases while increasing the number of DEAAm units. A minimum is found for a block copolymer containing 55 DEAAm units (mol-% DEAAm = 0.52, $D_{n,TEM} = 73$ nm), corresponding to the larger amount of particles. In the second part of the plot, for DEAAm mol-% > 50%, the particle size increases gradually but remains rather small in comparison with the particle diameter observed in the first part of the plot. In contrast, the polymerization of styrene using a pure PDEAAm ($DP_n = 92$) does not lead to a stable latex and no data points are shown in the figure. It suggest

that the stabilization of the particles is enhanced by increasing the number of hydrophobic DEAAm units (at $T > T_c$), allowing a better adsorption onto the particles.

Table 6-3. Emulsion polymerization of styrene using various stabilizers at 70 °C^a

Run	stabilizer	[stabilizer]		Conv. ^c (%)	particle diameter ^d DLS	
		wt.-% vs St ^b	10 ⁵ ·mol·L ⁻¹		D_z (nm)	μ_2/Γ^2
R	poly(acrylic acid) ₄₅	1.2	34.6	19.9	250	0.012
S	poly(DEAAm) ₉₂	2.0	16.9	39.2	coagulum	-
T	SDS	2.0	703	84.7	70	0.035

^a Reagents and conditions: $[St]_0 = 0.95 \text{ mol}\cdot\text{L}^{-1}$, $[K_2S_2O_8]_0 = 5\cdot 10^{-3} \text{ mol}\cdot\text{L}^{-1}$, $[K_2CO_3] = 20\cdot 10^{-3} \text{ mol}\cdot\text{L}^{-1}$, $T = 70 \text{ }^\circ\text{C}$, pH = 11.2, solid content: 10 wt.-% St/H₂O. ^b Stabilizer or polymer to styrene weight ratio. ^c After 4 hours of reaction calculated by gravimetric analysis. ^d z-average hydrodynamic radius, D_z , measured at pH = 7 by DLS at $\theta = 90^\circ$ and $T = 23 \text{ }^\circ\text{C}$ using a 2nd order cumulant analysis.

Thus, depending on the block copolymer composition, it is possible to adjust the efficiency of the stabilization (lower particle size, larger particle number). Furthermore, it indicates first the importance of the hydrophilic block in the stabilization process. Indeed, a polymerization using a pure PDEAAm leads to a latex which flocculates during the polymerization (run S, Table 6-3) and its contribution to the stabilization is not sufficient at room temperature (steric stabilization). Secondly, it indicates that both segments should be present (block copolymer structure) to obtain a perfect stabilization of the latexes.

(v) Effect of the Block Copolymer Concentration on N_p . The influence of the diblock copolymer-to-monomer weight ratio was studied in the case of the highly asymmetric (AA)₄₅-*b*-(DEAAm)₃₆₀ and the symmetric (MAA)₅₂-*b*-(DEAAm)₅₅. In addition to the effect of structural factors on N_p , i.e. the hydrophobic block length, the relationship between N_p and the molar concentration of stabilizer can give other information. For a given monomer, the proportionality between N_p and $[\text{surfactant}]^\alpha$ initially set up by Smith

and Ewart for low-molecular weight surfactants is valid over a wide range of surfactant concentrations above the critical micelle concentration (CMC). Theoretically, N_p should be proportional to $[\text{surfactant}]^{0.6}$, which applies well for styrene emulsion polymerization at surfactant concentration above the CMC. The CMC of (AA)₄₅-*b*-(DEAAm)₃₆₀ copolymer was determined to be below 10^{-7} - 10^{-8} mol·L⁻¹ by extrapolation of the value determined at room temperature.³⁹ All the emulsion polymerizations reported in the present work were carried out at a surfactant concentration above the CMC ($c \geq 10^{-5}$ mol·L⁻¹). On the other hand, a slope = 1 is characteristic of a kinetically-frozen system: micellar nucleation and each micelle forms a particle.⁴⁴ The concentration of the block copolymer was varied, keeping the other parameters constant. The final particle number, N_p , was calculated according to Equation 6-1. As suggested in Tables 6-1 and 6-2, by increasing the block copolymer concentration the particles size decreased and the particle size distribution narrowed for PS stabilized by (AA)₄₅-*b*-(DEAAm)₃₆₀, and for PS or PMMA stabilized by (MAA)₅₂-*b*-(DEAAm)₅₅.

In all cases, the best stabilization (larger N_p , smaller D) is observed with 2 wt.-% copolymer-to-monomer ratio. Linear relationships are not observed but a scattering of the experimental points. Due to the highly sensitivity of the system to small experimental variations, i.e. the temperature, it can involve even greater differences on the final latexes. Even if the procedure leads to the production of stable latexes, a crucial problem of reproducibility is however encountered. The most reasonable explanation in that case is that, due to the broad particle size distribution, a non negligible error on N_p is done.

From the aggregation number of (AA)₄₅-*b*-(DEAAm)₃₆₀ micelles determined by static light scattering in the absence of styrene, $N_{\text{agg}} = 54$,³⁹ it is possible to calculate the apparent micelles number for each run, $N_{\text{m,app}}$ (Equation 6-4), before the nucleation step and to compare them with the final particle number, N_p . As summarized in Table 6-1, the apparent micelles number is always larger than the final particle number, indicating first that either a large number of non-nucleated micelles was used to stabilize the latex particles or a small portion of micelles was nucleated, and secondly that the system is apparently not frozen even if $T_{\text{g,PDEAAm}} = 85.5$ °C. Increasing the number of micelles by increasing the block copolymer amount, leads to a better stabilization of the latex (smaller particles and narrower particle size distribution). The same behavior was reported by Save et al.⁴⁵ for polystyrene latex particles stabilized by a cationic polystyrene-*block*-

poly(vinylbenzyltriethylammonium chloride) copolymer, but in that case the hydrophobic segment (PS) was only constituted of 12 units and styrene was introduced to the pre-formed micellar solution. In contrast, Burguière et al.²⁰ reported that the micelles stabilized by an anionic polystyrene-*block*-poly(sodium acrylate) served as seed in the emulsion polymerization of styrene ($N_{m,app}/N_p = 1-2$).

$$N_m = \frac{[copolymer]N_A}{N_{agg}} \quad (6-4)$$

Origin of the stabilization and location of the block copolymer.

The location of the copolymer either in the water phase, on the particle surface, or in the latex particle is of importance in this system because the knowledge of this factor can explain the stabilization process. Due to the presence of the hydrophobic C₁₈ diphenylhexyl- fragment present on each P(M)AA block, it is necessary to investigate separately the role of each segment on the stabilization process. Furthermore, the pH- and thermo-responsive properties of the produced latexes are studied.

(i) Blank tests. The emulsion polymerization of styrene using a narrowly distributed poly(acrylic acid)₄₅, or a poly(*N,N*-diethylacrylamide)₉₂, are carried out using the same one-pot procedure alike for the block copolymers. The PS latex produced using poly(*N,N*-diethylacrylamide)₉₂ are stable at $T = 70$ °C during the polymerization (conversion = 39.2 %, run F). In that case, it is more a suspension than an emulsion and it flocculates at 23 °C. At 70 °C the homopolymer of DEAAm is hydrophobic and is either not sufficiently adsorbed onto the hydrophobic PS surface (and lost in the aqueous phase at $T < T_c$), or buried into the particle. In both cases it can not act as a stabilizer especially at room temperature. It suggests also the key-role of the electrostatic contribution in the stabilization mechanism.

In contrast, the PS latex synthesized using a poly(acrylic acid)₄₅ is still stable after the polymerization at room temperature, whereas a low monomer conversion of 20 % is reached after 4 hours, due to the lower particle number: $D_{z,DLS} = 250$ nm, $\mu_2/\Gamma^2 = 0.012$, $N_p = 2.08 \cdot 10^{15}$ L_{latex}⁻¹ (run E). The TEM image of this PS latex is shown in Figure 6-4.

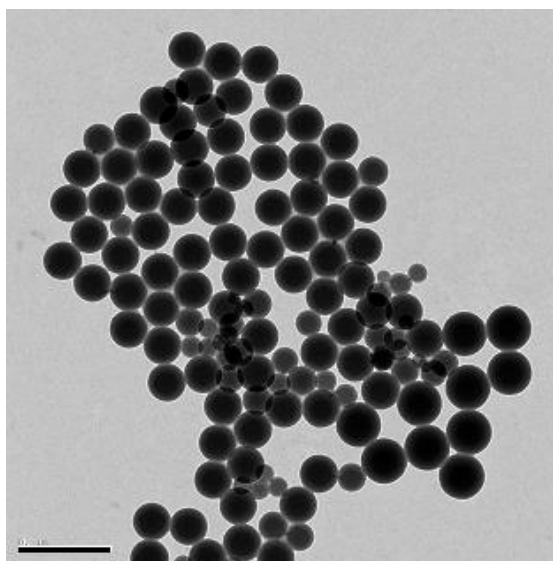


Figure 6-5. TEM image of the PS latex stabilized with 2.0 % of poly(acrylic acid)₄₅-to-styrene weight ratio (run R, Table 6-3).

It is important to note that both homopolymers were synthesized via anionic polymerization using diphenylhexyl-lithium as initiator which corresponds to the C₁₈ hydrophobic fragment present on each chain (Figure 6-1). Thus, as the latex produced with a pure PAA is stable, the presence of this hydrophobic group can explain the remarkable stabilization of the latexes obtained with the pure PAA homopolymer, the later being adsorbed onto the particle surface via the C₁₈ fragment. The same conclusion was reported by Liu et al.⁴⁶ for monodisperse PS latexes produced with a benzyloxy end-capped PDMAEMA homopolymer as stabilizer in water at pH = 3 and $T = 70\text{ }^{\circ}\text{C}$ ($T > T_c$). As the latexes remain stable at room temperature, the authors suggested that the hydrophobic benzyloxy group could be absorbed or anchored into the PS particle and the PDMAEMA chains were supposed to be extended into the aqueous phase ($T < T_c$) and enhancing the stabilization.

(ii) Freeze-thaw tests. As preliminary observations, the PS and PMMA latexes flocculate after three freeze-thaw cycles whereas the P n BA latex does after only one cycle. Macromolecular nonionic surfactant such as poly(ethylene oxide) or poly(propylene oxide)

are known to stabilize sterically latex dispersions and to improve their freeze-thaw and their shear stability.⁴⁷ The non-resistance to the freeze-thaw tests indicates the importance of the electrostatic contribution to the stabilization and the absence or non-efficiency of a steric one. Indeed, freeze-thaw treatment destroys in general the electrostatic repulsive interactions stabilizing the emulsion. Thus, the stabilization at room temperature can not be explained by a pure steric mechanism as it was observed for latexes sterically stabilized by high PEO chains.⁴⁸ It supports the previous assumption that the PDEAAm block is not adsorbed onto the surface but buried inside the particle.⁴⁹ The non-resistance to freeze-thaw tests excludes definitely the presence of the PDEAAm block onto the particles and a possible expansion in the aqueous phase.

The analysis of the latex particles cleaned by centrifugation can give information about the location of the block copolymer and the nature of its anchorage or adsorption onto the particle. Figure 6-6 suggests that the copolymer could be partially removed from the PS particles by centrifugation at room temperature (run D, 1.9 wt.-% of (AA)₄₅-*b*-(DEAAm)₃₆₀ relative to styrene). A discrepancy in the absorbance of the characteristic carbonyl stretching vibrations of carboxylate and amide functions (1635 and 1678 cm⁻¹) is observed for the latex after centrifugation. It may indicate that a part of the block copolymer is strongly anchored into the particles (buried) at room temperature ($T < T_c$) and can not be completely removed by centrifugation. The strong peaks at 1583 and 1601 cm⁻¹ are attributed to polystyrene (see Figure 6-9 in Supporting Information). Nevertheless, elementary analysis (EA) of the same latex does not indicate any removal of the block copolymer: N-% = 0.20 and 0.19 in the crude latex, and in the centrifugated latex, respectively. A theoretical N-% of 0.21 can be calculated from the amounts of the different reagents in the latex formulation. The difference between EA and FT-IR may be attributed to the low content of N to analyze. Further investigations including the surfaces analysis by X-Ray Photoelectron Spectroscopy (XPS) will be carried out.

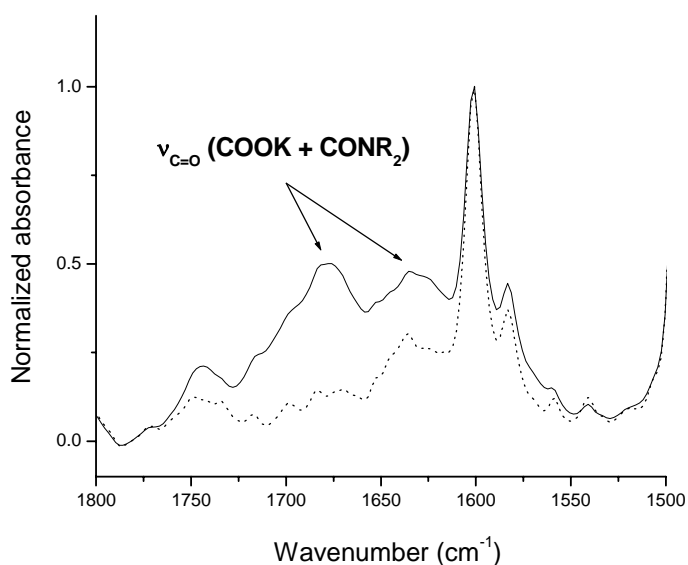


Figure 6-6. FT-IR spectra of the PS latex stabilized with 1.9 % of PAA-*b*-PDEAAm-to-styrene weight ratio before (—) and after centrifugation (---). The arrow indicates the stretching spectral region of C=O (amide and carboxylate). Run D, experimental conditions, see Table 6-1.

(iii) Influence of the pH and the temperature on the particle size. The influence of the pH and the temperature on the particle size is of importance because it gives some information on the location of the copolymer.

DLS was used to characterize the double influence of the latex particles of different nature (Table 6-4). At pH = 7, the solutions of diluted latexes are turbid and the increase of the temperature above the cloud point of the PDEAAm block (T_c) has no influence on the PS and PMMA particle size but their particle size distributions are narrower in every case.

At pH = 2 and room temperature, the solutions are still turbid and present larger aggregates which are visible in the solution ($D_{z,DLS} > 1 \mu\text{m}$). Increasing the temperature above T_c leads to the precipitation of the particles. This phenomenon is not reversible since no redissolution is observed after 24 hours of stirring at 5 °C. Alike, by adding a few drops of concentrated NaOH (pH = 12.8), the redissolution is not observed. Thus, we attribute this to the presence of the PDEAAm segment into the particle, the P(M)AA one stabilizing the interfaces. The PDEAAm segment is either covalently bonded to PS during the free-radical polymerization process by a chain transfer to the block copolymer (N-CH₂ groups

for example) or strongly anchored by entanglements (glassy core, $T < T_g$). Thus, the produced latexes are only pH-responsive since flocculation can be tuned by a decrease in the pH value.

Table 6-4. Influence of the temperature and the pH on the latex particles size^a

Latex nature /type	Copolymer	$D_{n,TEM}^b$ (nm)	D_z at pH = 7 ^c		D_z at pH = 2 ^d	
			DLS		DLS	
			$T = 23\text{ °C}$ (nm, μ_2/Γ^2)	$T = 45\text{ °C}$ (nm, μ_2/Γ^2)	$T = 23\text{ °C}$ (nm, μ_2/Γ^2)	$T = 45\text{ °C}$ (nm, μ_2/Γ^2)
PS emulsion	(AA) ₄₅ - <i>b</i> - (DEAAm) ₃₆₀	124	180 (0.186)	183 (0.143)	1764 ^e (0.050)	precipitation
PS mini-emulsion	(AA) ₄₅ - <i>b</i> - (DEAAm) ₃₆₀	192	200 (0.051)	198 (0.038)	3292 ^f (0.283)	precipitation
PnBA emulsion	(AA) ₄₅ - <i>b</i> - (DEAAm) ₃₆₀	215 ^g	270 (0.347)	243 (0.036)	253 ^f (0.297)	220 ^f (0.197)
PMMA emulsion	(MAA) ₅₂ - <i>b</i> - (DEAAm) ₅₅	110	125 (0.176)	128 (0.103)	9546 ^e (0.549)	precipitation

^a Latexes synthesized using the one-pot method at $T = 70\text{ °C}$ and pH = 11.0-11.5, block copolymer to monomer weight ratio = 2 %, solid content > 60 g·L⁻¹. ^b By TEM, average-number diameter, D_n , calculated from the mean value of 200 particles, at pH = 7. ^c By dilution of the latex in pure water, DLS at $\theta = 90^\circ$ using a 2nd-order cumulant method. ^d By addition of two drops of concentrated HCl. ^e Turbid solution containing particles in suspension. ^f Turbid and homogeneous solution. ^g Mean value of 15 particles, $D_z = 299\text{ nm}$, $D_w/D_n = 1.32$.

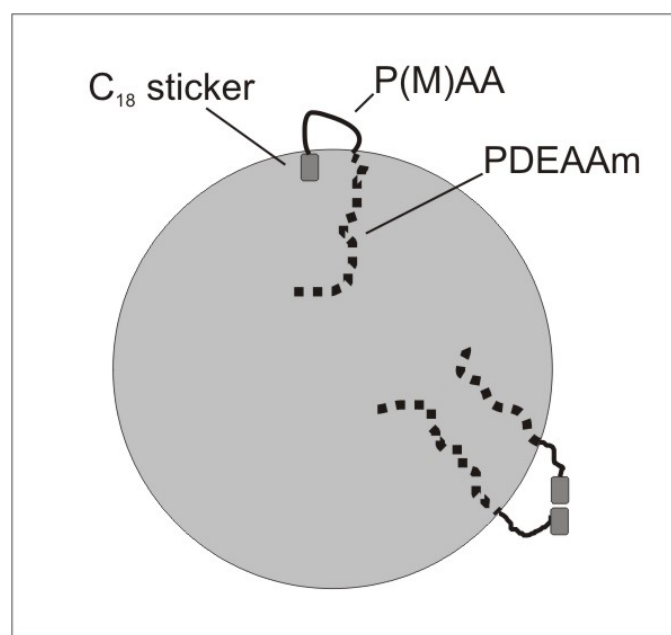
In the case of PnBA latex, the situation is drastically different. At pH = 7, the increase of temperature leads to a decrease of the particle size (10%) and a narrowing of the particle size distribution. The solution at pH = 2 and room temperature is turbid but does not contain visible precipitated structures. In this case, a diminution of 6 % in the particle size is observed in comparison to the $D_{z,DLS}$ measured at room temperature and pH = 7 whereas its particle size distribution is not influenced by the lowering of the pH value. At pH = 2, by increasing the temperature above T_c , the particle size decreases by 13 % and the PSD is

narrowed. The pH-effect is not so pronounced: the neutralization of the PAA block leads to a diminution of the particle size by 6.3 and 9.5% at 23 °C and 45 °C, respectively.

Both pH- and temperature-induced transitions are supposed to be reversible in the case of *PnBA* latex, even if the non-resistance to freeze-thaw test indicates that the PDEAAM block is not present on the surface, which should theoretically lead to the steric stabilization. In that case, the loss of the PDEAAM segment can not be explained by the formation of strong entanglements due to a glassy core as it was speculated for PS and PMMA cores. Indeed, the T_g of *PnBA* is lower than room temperature ($T_g = -54$ °C),⁴⁰ and only the covalent linkage of the PDEAAM segment with the *PnBA* polymer can explain the experimental observations. It may occur by a chain transfer to the block copolymer (*N*-CH₂ groups for example) because the transfer-to-polymer rate constant is relatively high in the case of free-radical polymerization of *nBA*.⁴⁰

(iv) Postulated stabilization mechanism. From the observations mentioned above, a stabilization mechanism can be postulated. At $T > T_c$, during the emulsion polymerization, the PDEAAM block is hydrophobic, and at room temperature ($T > T_c$), is buried inside the polymer particle by strong entanglements (PS or PMMA) or covalently linked inside the particle with the polymer chains (*PnBA*). This is confirmed by the non-resistance to freeze-thaw cycles of all types of latexes produced indicates the non-efficient or absence of steric contribution to the stabilization. The P(M)AA segment is present onto the particle surface and ensures the electrostatic stabilization of the latexes. Flocculation can be triggered by the neutralization of the P(M)AA block. Due to the presence of the C₁₈ hydrophobic fragment on the side of the P(M)AA block, the formation of a loop is possible if the later is anchored onto the particle surface. The production of stable latex stabilized by a pure C₁₈-PAA supports this assumption. In that case, it could form also a reversible network onto the particle surface by combination of two C₁₈ hydrophobic stickers. The stabilization by fully stretched P(M)AA chains is improbable taking into account the non-stabilization of the latexes at low pH. Indeed, at low pH, the neutralized PAA chains should act as steric stabilizer. The possible modes of location for the P(M)AA-*b*-PDEAAM copolymer at the surface of the latex particle are shown in Scheme 6-1.

Scheme 6-1. Postulated location of the poly[(meth)acrylic acid]-*block*-poly(*N,N*-diethylacrylamide) copolymer on the latex particle



Emulsion Polymerization at room temperature ($T = 23\text{ }^{\circ}\text{C}$).

The $(\text{AA})_{45}\text{-}b\text{-(DEAAm)}_{360}$ copolymer forms PAA-core micelles ($D_{z,\text{DLS}} \approx 100\text{ nm}$) in aqueous solutions at room temperature ($T < T_c$) and $\text{pH} \leq 4.1$. They are coexisting with larger aggregated structures responsible for the turbidity.³⁹ This copolymer was specially chosen for preliminary emulsion polymerization tests because of the long PDEAAm block, thus an enhancement of the steric stabilization was expected.

In the absence and presence of styrene at $\text{pH} = 4.1$, the initial solution is turbid under continuous stirring (run U). Experimental data can be found in Supporting Information (Table 6-5). After addition of the initiating redox-system ($\text{K}_2\text{S}_2\text{O}_8/\text{Na}_2\text{S}_2\text{O}_5$), the reaction is carried out during 48 hours at $T = 23\text{ }^{\circ}\text{C}$. The solution is then more turbid than at time zero but no milky appearance is observed. A low monomer conversion is reached in that case (4 %), that we attribute to the extremely low particle number. The latex flocculates immediately without stirring.

The same experiment is repeated at $\text{pH} = 11.0$ in the presence of molecularly dissolved block copolymer (run V). After 48 hours of reaction, the solution shows a milky aspect and low monomer conversion is reached (8.6 %). A phase separation is observed. In the same conditions ($\text{pH} = 11.2$, $T = 23\text{ }^{\circ}\text{C}$), the styrene emulsion is not stabilized by the PDEAAm

homopolymer (run W) and a phase separation occurs. Surprisingly, the non-efficiency observed in these cases suggests that the presence of the diphenylhexyl- fragment has no effect on the stabilization. In that case, the C₁₈ fragment is the only hydrophobic part of the block copolymer, both PAA and PDEAAm segments being hydrophilic, and the hydrophobic part is too small to ensure efficient stabilization.

Thus, the PAA block is not sufficiently adsorbed onto the particles due to the chemical heterogeneity between PS and PAA, and/or the steric stabilization of the PDEAAm block is insufficient or inexistent. The MMA or *n*BA batch polymerizations have to be carried out using the same PAA-core micelles or using a more hydrophobic PMAA-core to enhance the compatibility between the core and the adsorbed block. The direct transposition of the remarkable latex stability observed in the presence of PDEAAm-core micelles to the PAA-core micelles is not possible but it seems to be due to some pure chemical problems.

Stabilization of monomer/water liquid emulsion and miniemulsion polymerization.

In the absence of monomer, the K₂CO₃ aqueous solution of molecularly dissolved bishydrophilic (AA)₄₅-*b*-(DEAAm)₃₆₀ copolymer is clear and transparent (pH = 11.0-11.5, $T < T_c$). Upon the addition of styrene (10 % solid content), two phases are observed which disappear under stirring at room temperature, where a turbid emulsion is observed. Phase separation is observed instantaneously without stirring. After ca. 10 minutes at $T = 70$ °C ($T > T_c$), the solution is still turbid but no phase separation occurs without stirring. Furthermore the monomer-in-water emulsions remain stable for months at room temperature after the heating procedure, even if a phase separation was expected.

It reveals the ability of the bishydrophilic/amphiphilic block copolymer to stabilize monomer emulsions at $T > T_c$. The heating procedure is necessary and furthermore, the temperature-induced transition is irreversible in the presence of an hydrophobic oil phase, in contrast to the reversible transition observed in pure aqueous solutions between molecularly dissolved block copolymers (unimers) at $T < 35$ °C, and PDEAAm-core micelles at $T > 35$ °C. The remarkable stabilization of oil-in-water emulsions (decane in water) was already reported by DuPrez and coworkers in the case of thermo-responsive poly(methyl vinyl ether)-*block*-poly(*iso*-butyl vinyl ether) copolymer and poly(*N*-vinyl caprolactam)-*graft*-poly(tetrahydrofuran) but in these cases, the copolymer is amphiphilic

or hydrophobic depending on the temperature but not bishydrophilic at room temperature, because it contains a permanent hydrophobic segment.^{13,50} In contrast, the system based on P(M)AA-*b*-PDEAAm copolymers is drastically different and represents the first example of the efficient stabilization of oil-in-water emulsions by a bishydrophilic/amphiphilic block copolymer.

At $T > T_c$, the PDEAAm becomes hydrophobic and has more affinity for the organic phase. After the heating procedure, it becomes less hydrophobic ($T < T_c$) but desorption from the organic phase might be a limiting kinetic factor.

This remarkable feature of such bishydrophilic/amphiphilic block copolymer represents a significant improvement in the field of oil/water emulsions. This remarkable feature opens the possibility to carry out miniemulsion polymerizations. In contrast to conventional emulsion polymerization, the organic medium containing the monomer and the water-insoluble initiator is dispersed as submicrometer droplets in the aqueous solution by ultrasonification.^{51,52} Hexadecane is generally used to stabilize the droplets from Ostwald ripening whereas the stabilizer prevents the droplet coalescence. It allows the formation of hybrid particles containing, for instance an organic or inorganic compound whose water-solubility is too low for diffusion from the monomer droplets to the growing latex particles in a conventional emulsion polymerization.

The batch miniemulsion polymerization of styrene using AIBN ($5 \cdot 10^{-3} \text{ mol} \cdot \text{L}^{-1}$) as a radical initiator and (AA)₄₅-*b*-(DEAAm)₃₆₀ as a stabilizer in water at 70 °C was attempted. The milky styrenic emulsion is stable after ultrasonication where no phase separation occurs. Indeed, this procedure leads to an increase of the temperature above the PDEAAm cloud point ($T > T_c$). After 6 hours of reaction at 70 °C, stable PS dispersion is obtained (monomer conversion = 66.9 %, $\tau_{\text{poly}} = 60.5 \text{ g} \cdot \text{L}^{-1}$) which stays stable for months at room temperature. As shown in Figure 6-7, relatively monodisperse PS particles can be observed by TEM: $D_{n,\text{TEM}} = 192 \text{ nm}$ ($D_w/D_n = 1.07$) which correspond to a *z*-average diameter of 200 nm ($\mu_2/\Gamma^2 = 0.051$) by DLS at $\theta = 90^\circ$ using a 2nd order cumulant analysis. The PS latex particles were also characterized by AF-FFF: $D_n = 152 \text{ nm}$, $D_z = 158 \text{ nm}$, $D_w/D_n = 1.01$ (Figure 6-7).

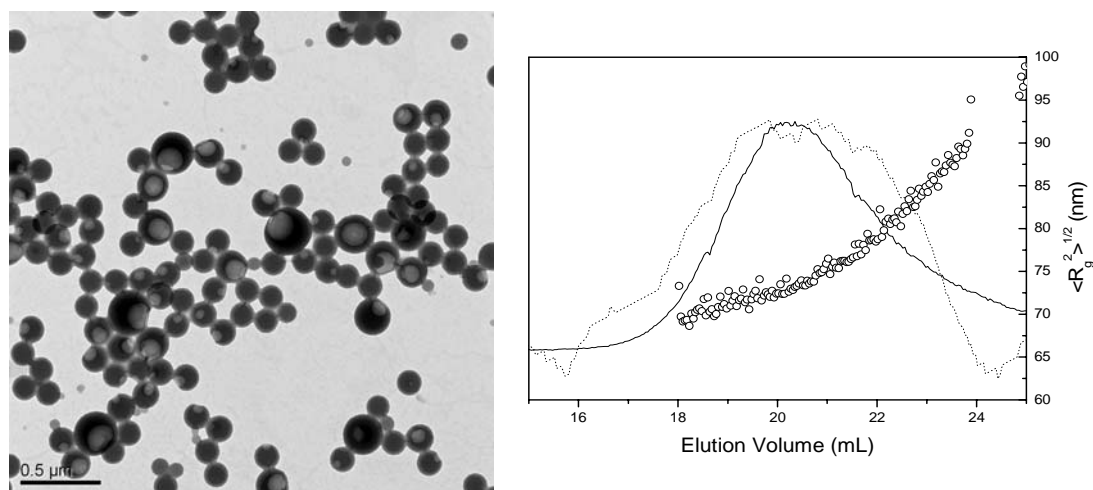


Figure 6-7. TEM image (left) and AF-FFF-MALS measurement in water+FL-70[®] (right) of the PS latex synthesized via miniemulsion using (AA)₄₅-*b*-(DEAAm)₃₆₀ as macromolecular stabilizer (2.0 % of copolymer-to-styrene weight ratio). (—) 90° light scattering signal, (···) UV at $\lambda = 210$ nm, (○) *z*-average root-mean-square radius of gyration distribution obtained using the Berry method and first-order fit of the light scattering data.

In terms of latex stabilization, no improvement is seen by miniemulsion process, if we take into account the particles number ($N_p = 0.8 \cdot 10^{16} \text{ L}_{\text{latex}}^{-1}$). A PS latex synthesized via conventional emulsion process (run D, Table 6-1) using the same amount of copolymer is characterized by a particles density of $7.0 \cdot 10^{16} \text{ L}_{\text{latex}}^{-1}$. The improvement resides in the fact that the particles are in that case monodisperse and that the process itself opens an elegant synthetic way for the formation of hybrid submicrometer particles containing an encapsulated inorganic or organic compound.

6.4 Conclusions

This contribution represents the first example of the efficient use of a double-stimuli-responsive block copolymer made of poly[(meth)acrylic acid]-*block*-poly(*N,N*-diethylacrylamide) copolymers as emulsifier and latex stabilizer. The bishydrophilic nature of the block copolymers under alkaline conditions at room temperature allows the solubilization of compounds with high hydrophobic content. This feature represents a great improvement in comparison to the traditionally used amphiphilic copolymers with a permanent hydrophobic segment. By using the amphiphilic properties of the diblock copolymer in alkaline water above the cloud point of the PDEAAM block ($T > T_c$), which form PDEAAM/PAA core-shell spherical micellar aggregates, it was possible to carry out batch emulsion polymerizations of styrene, methyl methacrylate and *n*-butyl acrylate at 70 °C. Stable latexes were obtained. In term of control of particles size and particle size distribution, some improvements could be envisaged.

Nevertheless, we wanted to focus on the remarkable stability of the produced latexes for months during the storage at room temperature when the block copolymer is water-soluble. The stabilization mechanism was studied and reveals that the hydrophobic diphenylhexyl-group is not involved in the stabilization and is anchored onto the particle surface or forms a reversible network at their surface. The PDEAAM is in every case buried in the latex particles and lost for the stabilization. It is strongly anchored into the particle either by entanglements in the case of PS and PMMA latexes, or by covalent linkages in the case of *Pn*BA latex. The PM(AA) shell ensures the stabilization by electrostatic contribution and the obtained latexes are pH-responsive. Under acidic conditions, no stabilization of PS particles is observed using the reverse PAA/PDEAAM core-shell micelles at room temperature.

The stable monomer-in-water emulsions obtained at room temperature after heating the solution above the cloud point of the PDEAAM block allows the formation of stable submicrometer particles via miniemulsion procedure. Such results are really new and interesting and would require further investigations.

Acknowledgment. We thank Peter Igney, Astrid Göpfert (TEM), and Clarissa Abetz (SEM) for their help as well as Andreas Walther, Julien Nicolas, and Maud Save for

helpful discussions. The French Research Ministry, the French-Bavarian University Center, and the University of Bayreuth are gratefully acknowledged for financial supports to X. A.'s 'Co-tutelle' Ph. D. program. Kh. B. acknowledges an Erasmus scholarship from the European Union.

Supporting Information Available: TEM images of PS latex stabilized with 2.0 wt.-% of SDS-to-styrene ratio, polystyrene FT-IR spectrum, and experimental conditions of the batch emulsion polymerizations at $T = 23$ °C using a redox system as initiator (PDF). This material is available free of charge via the Internet at <http://www.pubs.acs.org>.

6.5 References

- (1) Alexandridis, P.; Lindman, B. *Amphiphilic Block Copolymers: Self-Assembly and Applications*; Elsevier: Amsterdam, 2000.
- (2) Buetuen, V.; Armes, S. P.; Billingham, N. C.; Tuzar, Z.; Rankin, A.; Eastoe, J.; Heenan, R. K. *Macromolecules* **2001**, *34*, 1503-1511.
- (3) Kulkarni, S.; Schilli, C.; Müller, A. H. E.; Hoffman, A. S.; Stayton, P. S. *Bioconjugate Chemistry* **2004**, *15*, 747-753.
- (4) Brannon-Peppas, L.; Peppas, N. A. *Chemical Engineering Science* **1991**, *46*, 715-722.
- (5) Slater, G. W.; Noolandi, J.; Eisenberg, A. *Macromolecules* **1991**, *24*, 6715-6720.
- (6) Porcar, I.; Perrin, P.; Tribet, C. *Langmuir* **2001**, *17*, 6905-6909.
- (7) Schilli, C.; Müller, A. H. E.; Rizzardo, E.; Thang, S. H.; Chong, B. Y. K. *Polymer Preprints (American Chemical Society, Division of Polymer Chemistry)* **2002**, *43*, 687-688.
- (8) Elaissari, A.; Delair, T.; Pichot, C. *Progress in Colloid & Polymer Science* **2004**, *124*, 82-87.
- (9) Prazeres, T. J. V.; Santos, A. M.; Martinho, J. M. G.; Elaissari, A.; Pichot, C. *Langmuir* **2004**, *20*, 6834-6840.
- (10) Park, T. G.; Hoffman, A. S. *Journal of Biomaterials Science, Polymer Edition* **1993**, *4*, 493-504.
- (11) Liu, S.; Liu, M. *Journal of Applied Polymer Science* **2003**, *90*, 3563-3568.
- (12) Makhaeva, E. E.; Tenhu, H.; Khokhlov, A. R. *Macromolecules* **2002**, *35*, 1870-1876.
- (13) Verdonck, B.; Goethals, E. J.; Du Prez, F. E. *Macromolecular Chemistry and Physics* **2003**, *204*, 2090-2098.
- (14) Bütün, V.; Lowe, A. B.; Billingham, N. C.; Armes, S. P. *Journal of the American Chemical Society* **1999**, *121*, 4288-4289.
- (15) Baltes, T.; Garret-Flaudy, F.; Freitag, R. *J. Polym. Sci., Part A: Polym. Chem.* **1999**, *37*, 2977-2989.
- (16) Hiratani, H.; Alvarez-Lorenzo, C. *Journal of Controlled Release* **2002**, *83*, 223-230.
- (17) Gilbert, R. *Emulsion Polymerization - A Mechanistic Approach*; Academic Press: London, 1995.
- (18) Bo, G.; Wesslen, B.; Wesslen, K. B. *Journal of Polymer Science, Part A: Polymer Chemistry* **1992**, *30*, 1799-1808.
- (19) Mueller, H.; Leube, W.; Tauer, K.; Foerster, S.; Antonietti, M. *Macromolecules* **1997**, *30*, 2288-2293.
- (20) Burguiere, C.; Pascual, S.; Bui, C.; Vairon, J.-P.; Charleux, B.; Davis, K. A.; Matyjaszewski, K.; Betremieux, I. *Macromolecules* **2001**, *34*, 4439-4450.
- (21) Selb, J.; Gallot, Y. *Makromolekulare Chemie* **1981**, *182*, 1775-1786.
- (22) Selb, J.; Gallot, Y. *Makromolekulare Chemie* **1981**, *182*, 1513-1523.
- (23) Selb, J.; Gallot, Y. *Makromolekulare Chemie* **1981**, *182*, 1491-1511.
- (24) Burguière, C. *Ph. D. Thesis*; Université Pierre et Marie Curie: Paris, France, 2001.
- (25) Zhang, L.; Eisenberg, A. *Journal of the American Chemical Society* **1996**, *118*, 3168-3181.
- (26) Kim, K. H.; Cui, G. H.; Lim, H. J.; Huh, J.; Cheol-Hee, A.; Jo, W. H. *Macromolecular Chemistry and Physics* **2004**, *205*, 1684-1692.

-
- (27) Amalvy, J. I.; Unali, G. F.; Li, Y.; Granger-Bevan, S.; Armes, S. P.; Binks, B. P.; Rodrigues, J. A.; Whitby, C. P. *Langmuir* **2004**, *20*, 4345-4354.
- (28) Amalvy, J. I.; Percy, M. J.; Armes, S. P.; Leite, C. A. P.; Galembeck, F. *Langmuir* **2005**, *21*, 1175-1179.
- (29) Buetuen, V.; Armes, S. P.; Billingham, N. C. *Macromolecules* **2001**, *34*, 1148-1159.
- (30) Butun, V.; Armes, S. P.; Billingham, N. C. *Polymer* **2001**, *42*, 5993-6008.
- (31) André, X.; Zhang, M.; Müller, A. H. E. *Macromolecular Rapid Communications* **2005**, *26*, 558-563.
- (32) André, X.; Benmohamed, K.; Müller, A. H. E. *Macromolecules* **2005**, submitted.
- (33) Müller, A. H. E.; André, X.; Schilli, C. M.; Charleux, B. *Polymeric Materials: Science and Engineering* **2004**, *91*, 252-253.
- (34) Giddings, J. C. *Science (Washington, DC, United States)* **1993**, *260*, 1456-1465.
- (35) Ratanathanawongs, S. K.; Giddings, J. C. *ACS Symposium Series* **1993**, *521*, 13-29.
- (36) Frankema, W.; van Bruijnsvoort, M.; Tijssen, R.; Kok, W. T. *Journal of Chromatography, A* **2002**, *943*, 251-261.
- (37) Andersson, M.; Wittgren, B.; Wahlund, K.-G. *Analytical Chemistry* **2003**, *75*, 4279-4291.
- (38) Burguière, C.; Pascual, S.; Bui, C.; Vairon, J.-P.; Charleux, B.; Davis, K. A.; Matyjaszewski, K.; Bétrémieux, I. *Macromolecules* **2001**, *34*, 4439-4450.
- (39) André, X.; Burkhardt, M.; Drechsler, M.; Lindner, P.; Gradzielski, M.; Müller, A. H. E. **2005**, in preparation.
- (40) Brandrup, J.; Immergut, E. H.; Editors. *Polymer Handbook, Fourth Edition*, 1998.
- (41) Zhang, L.; Barlow, R. J.; Eisenberg, A. *Macromolecules* **1995**, *28*, 6055-6066.
- (42) Nicolas, J.; Charleux, B.; Guerret, O.; Magnet, S. *Macromolecules* **2004**, *37*, 4453-4463.
- (43) Pich, A.; Richter, S.; Adler, H.-J.; Datsyuk, V.; Voronov, S. *Macromolecular Symposia* **2001**, *164*, 11-24.
- (44) Rager, T.; Meyer, W. H.; Wegner, G. *Macromol. Chem. Phys.* **1999**, *200*, 1672-1680.
- (45) Save, M.; Manguian, M.; Chassenieux, C.; Charleux, B. *Macromolecules* **2005**, *38*, 280-289.
- (46) Liu, Q.; Yu, Z.; Ni, P. *Colloid and Polymer Science* **2004**, *282*, 387-393.
- (47) Brown, R.; Stützel, B.; Sauer, T. *Macromolecular Chemistry and Physics* **1995**, *196*, 2047-2064.
- (48) Jain, M.; Piirma, I. *Polymeric Materials Science and Engineering* **1986**, *54*, 358-361.
- (49) Mura, J.-L.; Riess, G. *Polymers for Advanced Technologies* **1995**, *6*, 497-508.
- (50) Verbrugghe, S.; Bernaerts, K.; Du Prez, F. E. *Macromolecular Chemistry and Physics* **2003**, *204*, 1217-1225.
- (51) Barrere, M.; Landfester, K. *Macromolecules* **2003**, *36*, 5119-5125.
- (52) Barrere, M.; Landfester, K. *Polymer* **2003**, *44*, 2833-2841.

6.6 Supporting Information

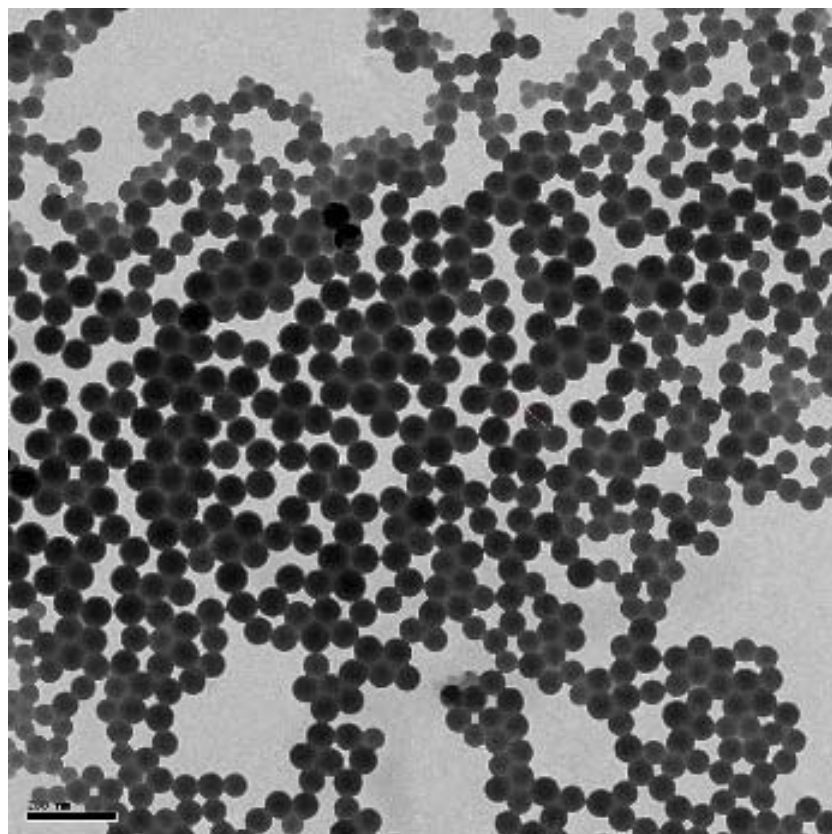


Figure 6-8. TEM images of PS latex stabilized with 2.0 wt.-% of sodium dodecyl sulfate (SDS)-to-styrene ratio using the one-pot method. Experimental conditions: $[\text{St}]_0 = 0.95 \text{ mol} \cdot \text{L}^{-1}$, $[\text{K}_2\text{S}_2\text{O}_8]_0 = 5 \cdot 10^{-3} \text{ mol} \cdot \text{L}^{-1}$, $[\text{SDS}] = 7 \cdot 10^{-3} \text{ mol} \cdot \text{L}^{-1}$, $[\text{K}_2\text{CO}_3] = 20 \cdot 10^{-3} \text{ mol} \cdot \text{L}^{-1}$, $T = 70 \text{ }^\circ\text{C}$, solid content: 10 wt.-% St/H₂O (pH = 11.2).

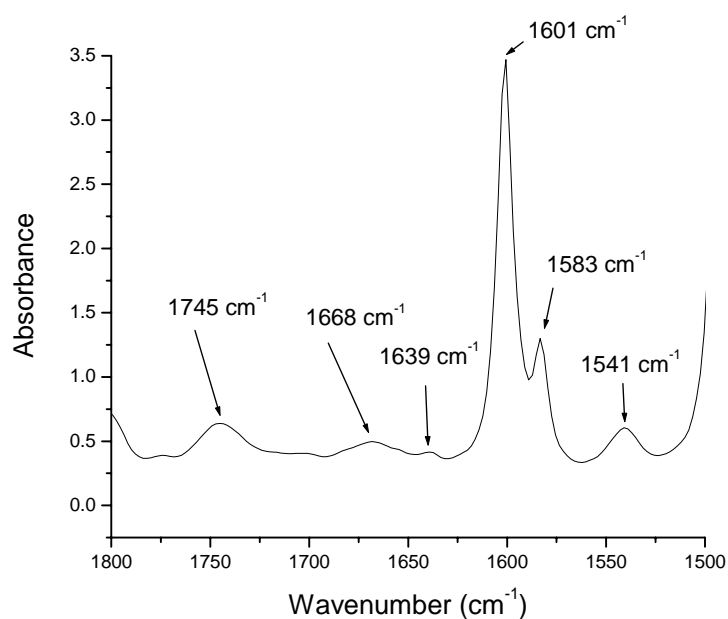


Figure 6-9. FT-IR analysis of a PS film (Nicolet[®], thickness = 76.2 μm).

Table 6-5. Batch emulsion polymerization of styrene using $\text{K}_2\text{S}_2\text{O}_8/\text{Na}_2\text{S}_2\text{O}_5$ as a radical initiating system at 23 °C and various stabilizers^a

Run	(co)polymer	salt	pH	[stabilizer]		Conv. ^c (%)	Aspect
				wt.-% vs St ^b	$10^{-5} \text{ mol}\cdot\text{L}^{-1}$		
U	$(\text{AA})_{45}\text{-}b\text{-}(\text{DEAAm})_{360}$	TRIS·HCl	4.1	2.1	4.5	3.7	coagulum
V	$(\text{AA})_{45}\text{-}b\text{-}(\text{DEAAm})_{360}$	K_2CO_3	11.0	2.0	4.3	8.6	phase separation
W	$(\text{DEAAm})_{92}$	K_2CO_3	11.2	2.1	15.9	~ 2.0	phase separation

^a Reagents and conditions: $[\text{St}]_0 = 0.95 \text{ mol}\cdot\text{L}^{-1}$, $[\text{K}_2\text{S}_2\text{O}_8]_0 = [\text{Na}_2\text{S}_2\text{O}_5]_0 = 5\cdot 10^{-3} \text{ mol}\cdot\text{L}^{-1}$, $[\text{salt}] = 20\cdot 10^{-3} \text{ mol}\cdot\text{L}^{-1}$, $T = 23 \text{ }^\circ\text{C}$, solid content: 10 wt.-% St/ H_2O . ^b Copolymer to styrene weight ratio. ^c Monomer conversion after 48 hours of reaction calculated by gravimetric analysis.

7. Summary

Thermo- and pH-responsive block copolymers based on (meth)acrylic acid and *N,N*-diethylacrylamide were synthesized and their aqueous solution behavior was studied. Such bishydrophilic block copolymers represent an interesting class of stimuli-responsive water-soluble materials whose macroscopic properties can be triggered at the molecular level by tuning the temperature, the pH and the ionic strength of the solution.

A new method was introduced for the synthesis of well-defined poly(*N,N*-diethylacrylamide) (PDEAAM) via living anionic polymerization using ethyl α -lithioisobutyrate (EiBLi) in the presence of triethylaluminium (Et₃Al) as Lewis acid in tetrahydrofuran (THF) at -78 °C. Kinetic investigations were performed using *in-situ* Fourier-transform near-infrared (FT-NIR) fiber-optic spectroscopy. This is the first mechanistic study of the anionic polymerization of a dialkylacrylamide. The polymerization follows first order kinetics with respect to the effective concentration of active chains, $[P^*]_0$, but shows complex kinetics with respect to the actual monomer and initial aluminum concentrations. Upon addition of Et₃Al, the polymerization rate constant, k_p decreases, which is explained by the formation of an amidoenolate chain end/Et₃Al complex of lower reactivity. It involves two equilibria: between noncoordinated and Et₃Al-coordinated chain ends (deactivation of chain ends) as well as between free and Et₃Al-activated monomer (activated monomer mechanism). These two effects are in a delicate balance that depends on the ratio of the concentrations of Et₃Al, monomer, and chain ends. Thus, the polymerization rate of this system is governed simultaneously by the complex interplay between the activation of monomer (dependent on monomer and Et₃Al concentrations) and the deactivation of chain ends (dependent on the ratio of concentrations of Et₃Al to initiator). Polymers with narrow molecular weight distribution are obtained, indicating that the rate of interconversion between the different chain end species is greater than the polymerization rate. In contrast, such well-defined polymers are not found in the absence of Et₃Al. PDEAAM polymers, synthesized using organolithium initiator in the presence of Et₃Al, are rich in heterotactic (*mr*) triads and exhibit Lower Critical Solution Temperatures (LCST) in water with a cloud point at $T_c \approx 31$ °C.

By extending this synthetic concept and using poly(*tert*-butyl acrylate)-Li, and poly(*tert*-butyl methacrylate)-Li as macroinitiators, well-defined poly(*tert*-butyl acrylate)-

block-PDEAAm, and poly(*tert*-butyl methacrylate)-*block*-PDEAAm block copolymers were obtained. Although the blocking efficiencies remained below 70 % a separation of block and homopolymers was easily possible.

The narrowly distributed (AA)₄₅-*b*-(DEAAm)₃₆₀ block copolymer obtained after hydrolysis of the protecting *tert*-butyl groups exhibits interesting ‘schizophrenic’ micellization behavior in response to temperature, to pH, and ionic strength of the aqueous media. Due to its asymmetric composition, two opposite micellar structures are expected. Indeed, the existence of different micellar aggregates, i.e. ‘crew-cut’ micelles with a PDEAAm core and inverse star-like micelles with PAA core, was proven by several analytical techniques, like Small-Angle Neutron Scattering (SANS), Dynamic and Static Light Scattering (DLS, SLS) and Cryo Transmission Electron Microscopy (cryo-TEM). Furthermore, all the transitions were found to be reversible.

Finally, the synthesized bishydrophilic block copolymers were used for batch emulsion polymerizations of styrene, methyl methacrylate and *n*-butyl acrylate. In all cases, latexes with remarkable long-term stabilities were obtained, which is a very interesting feature from the colloidal point of view. The stabilization efficiency was found to be essentially adjustable by the pH due to the loss of the PDEAAm segment inside the latex particle. A detailed analysis of the particle size and particle size distribution was carried out using a variety of methods, including DLS, TEM and Asymmetric Flow Field-Flow Fractionation (AF-FFF).

Zusammenfassung

Es wurden thermo- und pH-responsive bishydrophile Blockcopolymeren aus (Meth)acrylsäure und *N,N*-Diethylacrylamid synthetisiert. Solche Blockcopolymeren stellen eine interessante Klasse stimuli-responsiver Polymeren dar, deren makroskopische Eigenschaften auf dem molekularen Niveau durch Änderungen von Temperatur, pH-Wert oder Ionenstärke, eingestellt werden können.

Es wurde eine neue Synthesemethode zur Herstellung wohldefinierter Poly(*N,N*-diethylacrylamid) (PDEAAm) mittels lebender anionischer Polymerisation unter Verwendung von Ethyl- α -lithioisobutyrat (EiBLi) in Gegenwart von Triethylaluminium (Et_3Al) als Lewis-Säure in Tetrahydrofuran (THF) bei $-78\text{ }^\circ\text{C}$ eingeführt. Kinetische Untersuchungen an diesem System unter Einsatz der *in-situ* Fourier-Transform Nahinfrarot- (FT-NIR) Spektroskopie ermöglichten die erste vollständige mechanistische Studie der anionischen Polymerisation eines Dialkylacrylamids. Die Polymerisationsreaktion folgt einer Kinetik erster Ordnung mit Bezug auf die effective Konzentration an aktiven Kettenenden, $[\text{P}^*]_0$, aber zeigt eine komplexere Kinetik hinsichtlich der tatsächlichen (actual) Monomerkonzentration und der anfänglichen Aluminiumkonzentration. Bei Zugabe von Et_3Al nimmt die Wachstumskonstante k_p ab, was durch die Ausbildung eines Komplexes aus Et_3Al und dem Amidoenolat-Kettenende bedingt ist. Es beinhaltet zwei Gleichgewichte: zum einen das zwischen unkoordiniertem und mit Et_3Al koordiniertem Kettenende (Deaktivierung des Kettenendes) und zum anderen das Gleichgewicht zwischen freiem und mit Et_3Al aktiviertem Monomer. Diese zwei Effekte halten sich die Waage und sind durch die Verhältnisse der Konzentration an Et_3Al , Monomer und Kettenenden bedingt. Daher ist die Polymerisationsrate dieses Systems gleichzeitig durch das komplexe Wechselspiel zwischen Monomeraktivierung (abhängig von Monomer und Et_3Al Konzentration) und der Deaktivierung der Kettenenden (abhängig von dem Verhältnis an Et_3Al zu Initiatorkonzentration) bestimmt. Die Polymerisation führt zu engen Molekulargewichtsverteilungen, was darauf hindeutet, dass in Anwesenheit von Et_3Al die Umwandlungsgeschwindigkeit der verschiedenen denkbaren Kettenendenspezies deutlich größer ist als die Wachstumsgeschwindigkeit. Ohne Zusatz von Et_3Al können solche gute Ergebnisse bei anionischer Polymerisation von Dialkylacrylamiden nicht erzielt werden. Die synthetisierten PDEAAm-Polymeren sind

reich an heterotaktischen (*mr*) Diaden und zeigen in Wasser ein 'Lower Critical Solution Temperature' (LCST) Verhalten mit einem Trübungspunkt von $T_c \approx 31^\circ\text{C}$.

Das synthetische Konzept zur kontrollierten Polymerisation von Dialkylacrylamiden wurde im Folgenden auf die Synthese von Blockcopolymeren ausgeweitet. Durch Verwendung geeigneter Makroinitiatoren, Poly[*tert*-butyl(meth)acrylat]-Li, konnten definierte Poly[*tert*-butyl(meth)acrylat]-*block*-PDEAAm Blockcopolymer hergestellt werden. Obwohl die Blockeffektivitäten kleiner als 70% sind, konnte verbleibendes Homopolymer leicht von den erwünschten Diblockcopolymeren abgetrennt werden.

Auf Grund seiner asymmetrischen Zusammensetzung zeigt das durch Eliminierung der *tert*-Butylgruppe erhaltene bishydrophile Blockcopolymer Polyacrylsäure₄₅-*b*-poly(*N,N*-diethylacrylamid)₃₆₀ ein besonders interessantes 'schizophrenes' Mizellierungsverhalten. Abhängig von den Umgebungsparametern, wie Temperatur, pH-Wert und Ionenstärke, bilden sich zwei gegensätzliche Mizellarchitekturen in wässriger Lösung aus. Zum einen bilden sich bei Temperaturerhöhung in alkalischer Lösung 'crew-cut'-Mizellen mit einem großen PDEAAm-Kern. Bei Erniedrigung des pH-Werts hingegen zeigen sich sternförmige Mizellen mit einem Kern aus PAA. Das Vorliegen dieser Mizellstrukturen wurde durch verschiedene analytische Techniken, wie z.B. Neutronenkleinwinkelstreuung (SANS), dynamische und statische Lichtstreuung (DLS, SLS) und kryogene Transmissionselektronenmikroskopie (cryo-TEM) nachgewiesen. Es zeigte sich außerdem eine bemerkenswerte Reversibilität der möglichen Übergänge an mizellaren Strukturen, die durch geeignete externe Stimuli induziert werden.

Zuletzt wurden die zuvor synthetisierten bishydrophilen Blockcopolymer für eine Reihe verschiedener Emulsionspolymerisationen mit unterschiedlichen Monomeren eingesetzt. In allen Fällen wiesen die Latices eine beeindruckende Langzeitstabilität auf, was unter kolloidchemischen Gesichtspunkten äußerst interessant ist. Die Untersuchungen zeigten des Weiteren, dass die Stabilisierungseffektivität stark durch den pH-Wert beeinflusst wird, da sich der PDEAAm Block in dem Partikel befindet. Die ausführliche Analyse der Teilchengrößen und der Teilchengrößenverteilungen erfolgte durch eine Vielzahl unterschiedlicher Methoden einschließlich DLS, TEM und Feldflussfraktionierung (AF-FFF).

Résumé

Des copolymères à blocs composés d'acide acrylique, d'acide méthacrylique et d'acrylamide de *N,N*-diéthyle sensibles à la température et au pH ont été synthétisés. De tels copolymères à blocs représentent une classe intéressante de matériaux hydrosolubles sensibles à des stimuli externes, dont les propriétés macroscopiques peuvent être déclenchées au niveau moléculaire en faisant varier la température, le pH et la force ionique de la solution.

Une nouvelle méthode de polymérisation anionique a été utilisée pour la synthèse de poly(acrylamide de *N,N*-diéthyle) (PDEAAm) de structure bien définie en utilisant comme amorceur l' α -isobutyrate-lithium d'éthyle (EiBLi) en présence de triéthylaluminium (Et_3Al) comme acide de Lewis dans le tétrahydrofurane (THF) à -78°C .

Les cinétiques de polymérisation ont été suivies par analyse spectroscopique dans le proche infra-rouge (FT-NIR) en temps réel, ce qui conduit à la première étude mécanistique de la polymérisation anionique d'un acrylamide de dialkyle. La polymérisation suit une cinétique du premier ordre par rapport à la concentration en chaînes actives, $[\text{P}^*]_0$, et une cinétique de polymérisation complexe par rapport à la concentration instantanée en monomère et à la concentration initiale en triéthylaluminium. L'addition de Et_3Al entraîne la diminution de la constante de vitesse de polymérisation, k_p , diminution expliquée par la formation d'un complexe entre la chaîne active et l'aluminium d'alkyle, dont la réactivité est diminuée. Deux équilibres sont impliqués: entre les chaînes actives libres et complexés par l'aluminium d'alkyle et entre le monomère libre et activé par l'aluminium. Ces deux effets s'opposent et dépendent du rapport instantané des concentrations en Et_3Al , monomère et chaînes actives. De ce fait, la vitesse de polymérisation de ce système est déterminée simultanément par un mécanisme complexe entre l'activation du monomère (dépendant des concentrations en monomère et en Et_3Al) et la désactivation des chaînes actives (dépendant du rapport des concentrations d' Et_3Al sur l'amorceur). En présence d' Et_3Al , les vitesses d'inter-conversion entre les différentes espèces de chaînes actives sont plus grandes que les vitesses de polymérisation correspondantes. De ce fait, les polymères synthétisés ont une distribution étroite des masses molaires alors que les polymères synthétisés sans aluminium présentent des distributions larges.

La principale caractéristique de cette méthode (amorceur organolithium/ Et_3Al) est que les PDEAAs synthétisés sont riches en triades hétérotactiques (mr) et présentent une ‘Lower Critical Solution Temperature’ (LCST) dans l’eau, $T_c \approx 31\text{ }^\circ\text{C}$.

Par extension de cette stratégie de synthèse, en utilisant des macroamorceurs tels que le poly(acrylate de *tert*-butyle)-Li et le poly(méthacrylate de *tert*-butyle) en présence d' Et_3Al , des poly(acrylate de *tert*-butyle)-*bloc*-PDEAAm et poly(méthacrylate de *tert*-butyle)-*bloc*-PDEAAm de structure bien définie ont été obtenus. Les efficacités d’amorçage observées sont faibles ($f < 0.7$). Néanmoins, la séparation du précurseur est facilement réalisable et des copolymères à blocs purs sont obtenus après purification.

Un intérêt particulier a été porté à l’étude des propriétés des copolymères à blocs hydrosolubles dérivés en réponse à différents stimuli. Ces copolymères ont été obtenus après hydrolyse des groupes protecteurs *tert*-butyle. En raison de sa structure asymétrique, le copolymère à blocs poly(acide acrylique)₄₅-*b*-poly(*N,N*-diéthylacrylamide)₃₆₀ de structure bien définie forme dans l’eau des agrégats micellaires *schizophrènes* en variant de manière indépendante la température, le pH ou la force ionique de la solution aqueuse. L’existence de micelles en brosse contenant un cœur de PDEAAm ainsi que celle de micelles inverses contenant un cœur de poly(acide acrylique) a été démontré par différentes techniques d’analyse comprenant la diffusion de neutrons aux petits angles (SANS), la diffusion de lumière statique et dynamique (SLS/DLS) et la cryo-Microscopie Electronique en Transmission (cryo-TEM). De plus, toutes les transitions observées par application du stimulus sont réversibles.

Dans la dernière partie, les copolymères à blocs hydrosolubles synthétisés ont été utilisés comme stabilisants pour les polymérisations radicalaires en émulsion de différents monomères. Dans tous les cas, les latex obtenus sont stables pendant de longues périodes, ce qui représente une caractéristique très intéressante du point de vue colloïdal. L’efficacité de la stabilisation s’est avérée réglable principalement par le pH, car le PDEAAm se trouve ancré dans la particule de latex. Les analyses détaillées de la taille des particules et de leur distribution en taille ont été effectuées par une variété de différentes méthodes comprenant la diffusion dynamique de la lumière (DLS), la microscopie électronique en transmission (TEM) et ‘l’Asymmetric Flow Field-Flow Fractionation’ (AF-FFF).

8. Appendix

8.1 Fundamentals of anionic polymerization

Like free-radical polymerization, anionic polymerization proceeds via a chain reaction mechanism. In general, the elementary steps for chain reactions are: initiation, propagation, chain transfer and chain termination. In contrast to free radical polymerization, the active chain ends in anionic polymerization carry a negative charge. Due to Coulomb interaction chain termination by combination or disproportionation is prohibited. In the absence of other termination reactions (with impurities, protic functional groups on monomers or solvents, etc.) chains can keep their active sites until all monomer is consumed. Upon addition of a next batch of monomer, polymerization proceeds, and the reaction is called a "living" polymerization. When the livingness criteria are present, a complete control of the system is possible: prediction of the molecular weight, the control of the microstructure, and the design of various architectures.^{1,2} After a starting period, the kinetics of the polymerization are governed by the rate law of the propagation step, which is, under the assumption of equal chain end reactivity, first order in monomer and active chain end concentration. The latter is constant during the course of polymerization and equal to the effective initiator concentration or active chain concentration, $[P^*]_0 = f \cdot [I]_0$, at the time of initiation, where f is the initiator efficiency ($0 < f < 1$) and $[I]_0$, the initial concentration of initiator. With an instantaneous initiation reaction, fast mixing of the reaction components, an irreversible propagation reaction and only one type of growing species, each chain has the same time and same probability to incorporate monomers, resulting in a narrow molecular weight distribution. The mathematical description for the molecular weight distribution of an ideal living polymerization is the Poisson distribution with polydispersity index, $M_w/M_n \approx 1 + 1/P_n$.³ In practical cases, polymers with $M_w/M_n < 1.10$ are said to be narrowly distributed.

Suitable monomers for anionic polymerization possess usually electron-withdrawing substituents which increase the electrophilic character of the double bond and stabilize the regenerated active anionic center. Because of the high reactivity of anions and the different reactive species present in the polymerization medium, the reaction conditions (solvent, temperature, counter-ion, additives) have to be adjusted to specific requirements.

Depending on the solvent nature, the active chains can be either free ions, loose ion pairs, tight ion pairs, or aggregates (Figure 8-1). Each kind possesses its reactivity regarding the polymerization. Thus, the polymerization kinetics is ruled by the equilibria between the species and the rate of interconversion between them. In order to observe living polymerization either only one propagating species should exist or the rate of interconversion between alternate species must be greater than the rate of propagation. Solvation or aggregation of the active chains can occur which influences strongly the microstructure and tacticity of the final product as well as the polymerization kinetics (initiation and propagation).

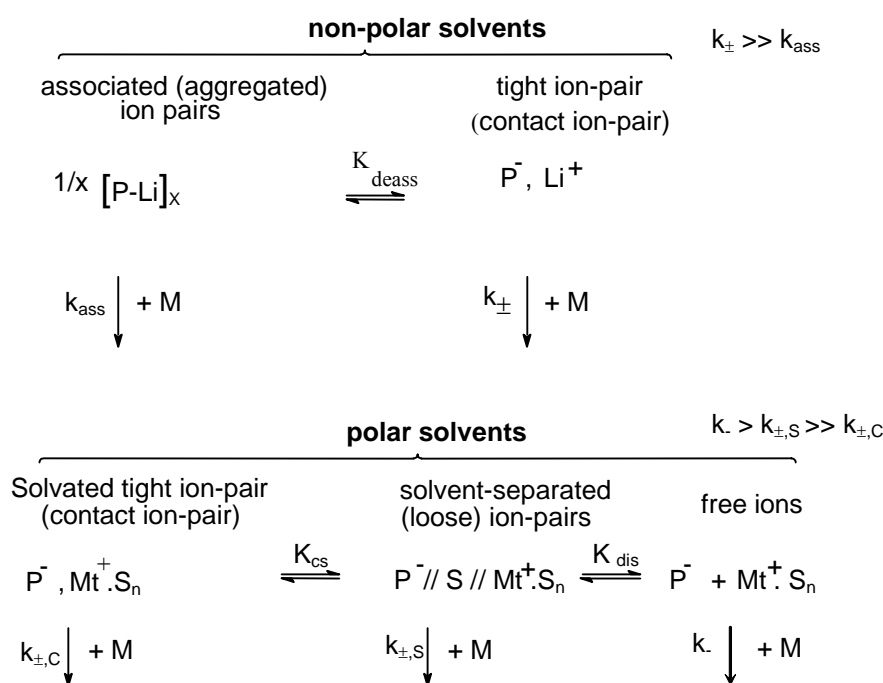


Figure 8-1. States of initiators and chain ends in non-polar and polar solvents (P = polymer chain, M = monomer, Mt = metal, x = aggregation number, S = solvent).

While increasing the polarity of the solvent, the equilibrium is shifted to the side of the ion pairs resulting in the formation of more reactive species. Nevertheless with sodium as counterion, solvent separated (loose) and free ions have similar rate constants for the propagation step. In non-polar solvents, the kinetics is complicated because of the presence of multiple aggregates having different reactivities. For acrylic monomers, the

polymerization can not occur in a living way without additive.^{4,5} The temperature plays also a key-role where low temperature in polar solvents shifts the equilibrium to the dissociation ($10^{-7} < K_{\text{diss}} < 10^{-4}$, $\Delta H < 0$). The concentration in active chains plays a key-role on the equilibrium, where higher concentrations shift the equilibrium to the formation of aggregates. The presence of additive has a strong influence on the equilibria and on the reactivity of each species. For that reason the experimental conditions have to be adjusted for any single case to observe the livingness of the polymerization. Usually, the anionic polymerizations are carried out in solvents which have no strong electrophilic groups like halogens or carbonyl functions, i.e. aromatic or aliphatic hydrocarbons or ethers. Due to their solubility in hydrocarbons and in polar solvents in addition to their sufficiently high reactivity towards most monomers, alkyl lithium initiators (*n*-, *sec*-, *tert*-butyl lithium) have been extensively employed as initiators for anionic polymerization.⁶

The reactivity of initiators or active chain ends depends strongly on their actual molecular structure and on the structure of the anion-cation ion pairs in solution. The influence of the molecular structure of the carbanion-bearing organic fragment is often described in terms of the $\text{p}K_{\text{a}}$ value of the corresponding conjugated C-H acid. Highly reactive initiators are generally strong bases, i.e. their conjugated acids are weak and the $\text{p}K_{\text{a}}$ value of the acid-base equilibrium is high. If there are any reagents present in the polymerization system, which have lower $\text{p}K_{\text{a}}$ values, they will be deprotonated and the initiator or the active chain terminated. In order to initiate the polymerization of a specific monomer, the initiator should be equally or more basic than the resulting anionic chain end. However, *basicity* is only a rough estimate of the reactivity of initiators, since it is defined in terms of thermodynamic equilibria and thus can not explain kinetic phenomena, especially steric factors. High activation barriers can still prevent the reaction from proceeding. Kinetic factors are summarized in the term of *nucleophilicity*, which is much harder to quantify.

The synthesis of linear block copolymers with living polymerization methods is very elegantly accomplished by sequential monomer addition.⁶ Special care is required that each living chain is a good initiator for the next type of monomer. In order to initiate the polymerization of a specific monomer, the initiator or the macroinitiator should be equally or more basic than the resulting anionic chain end. For example, block copolymers of styrene and methyl methacrylate cannot be synthesized starting with methyl methacrylate,

because the living MMA chains are not nucleophilic enough to start the polymerization of styrene. If the initiator is too nucleophilic, side reactions may occur, as it is the case in the transfer from polystyryl anions to MMA where the PS^- anions can attack the ester group of MMA. The reactivity of polystyryl anions can be reduced by capping the chain end with one unit of the non-homopolymerizable *1,1*-diphenyl ethylene (DPE).

In addition to basicity and nucleophilicity, the nature of the counterion (Li^+ , Na^+ , K^+ etc.) and the state of the ion pair formed from anion and cation in solution has a great influence on the reactivity. In non-polar solvents there is a little rather no solvation of the carbanion or its counterion and lithium alkyls usually stabilize themselves by formation of aggregates of several molecules with electron-deficient three-center two-electron bonds. The actual structure of such aggregates in solution (whether they are defined dimeric, tetrameric or hexameric compounds or micellar clusters of differing number of monomers) and how they react in the polymerization process (whether they have to dissociate before adding monomer or if the clusters themselves can add monomer) is currently under debate.⁷

In polar solvents, the counterions can be solvated, because the usual polar solvents are Lewis bases (electron donors). Solvation increases the distance between the carbanion and the metal counterion, which leads to a higher rate of polymerization, because the charge density at the carbanion increases and the monomer has more space to attack the carbanion. Detailed kinetic and spectroscopic studies revealed the existence of three different species present in polar solvents, namely tight ion-pairs (external solvation), solvent-separated or loose ion pairs (exactly one shell of solvent molecules between the counterion and the carbanion) and free ions, where each species has a different rate constant of propagation. In polar solvents like THF, the polymerizations are generally carried out at $T < -60$ °C where contact ion pairs are predominantly involved in the chain growth. Even if the fraction of more reactive solvent-separated ion pairs and free ions increases at lower temperature, their relative $k_p(T)$ are smaller than the k_p of the contact ion pair. Since the rates of dissociation, solvation, and association are some orders of magnitude larger than that of chain propagation, the molecular weight distribution remains narrow. Further, the structure of the chain end can be modified by the use of various ligands (ethers, tertiary amines, Lewis bases, Lewis acids ...) which modify the polymerization kinetics as well as the regioselectivity of monomer incorporation.

The bulk and solution properties of the polymers strongly depend on their microstructure, i. e. the way the monomer units are incorporated into the chain. It is the case for polydienes, poly(alkyl acrylate)s, poly(alkyl methacrylate)s, and poly(alkyl acrylamide)s. The microstructure of polydienes prepared by anionic polymerization is determined by the reaction conditions. In non-polar solvents with Li as counterion, polymers with high 1,4- content are obtained whereas predominant 1,2-addition occurs in polar solvents. This can be explained with Figure 8-2. Monomer addition leads to a *s*-cis fashion, leading to a *cis*-chain end with the metal cation bound to the C-4 and the resulting microstructure will be 1,4 but the *cis*/*trans* ratio depends on the rate of the next monomer addition step and the rate of *cis*/*trans* isomerization (the *trans* configuration is thermodynamically more stable). If isomerization is slow compared to monomer addition, a high content of *cis*-1,4 microstructure is the result. In polar solvents, the metal cation is separated from the chain end because of solvation, allowing charge delocalization to C-2. Addition of monomer to C-2 leads to 1,2-microstructure with pendant vinyl group.

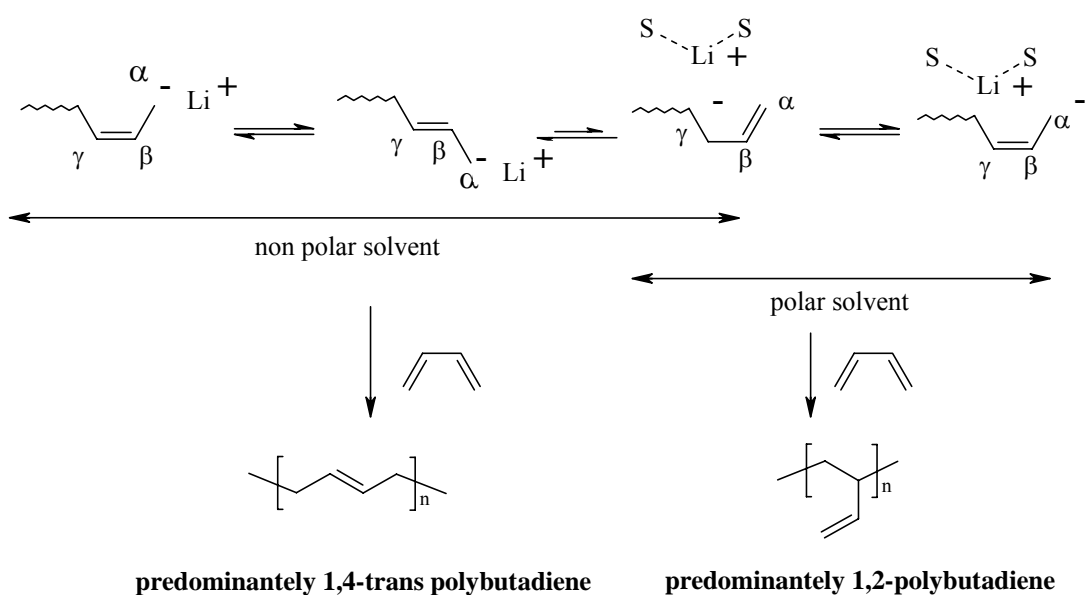


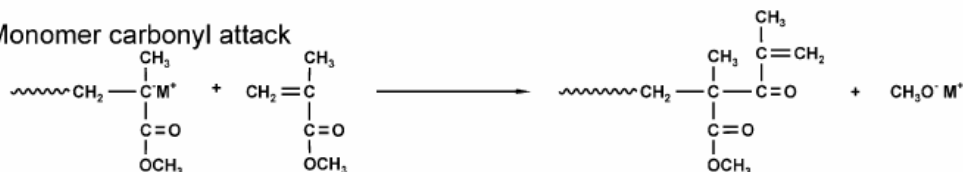
Figure 8-2. Solvent depending structure of polybutadiene (PB) active centers and formation of 1,2-PB and 1,4-PB.

In certain polymerization systems especially that of alkyl methacrylate monomers, the control of the resulting tacticity is possible: Li^+ in THF leads to a high amount of syndiotactic addition, Cs^+ in THF to predominant heterotactic addition while Li^+ or MgBr^+ in toluene leads to predominantly isotactic addition. During several decades, a large number of monomers could not be polymerized in a living fashion due to interaction with the reactive initiators (metal amides, alkoxides, or organometallic compounds). The polar ester group undergoes many side reactions during both initiation and propagation.⁸⁻¹⁰ Figure 8-3 summarizes the side reactions which can occur. Stronger and less sterically hindered nucleophiles can undergo reaction with the carbonyl group instead of the vinyl unsaturation resulting in a vinyl ketone and lithium methoxide. Side reactions lead to low initiator efficiency and broadening of the molecular weight distribution. This vinyl group can subsequently react with a living polymer chain forming a carbanionic center with lower reactivity which acts as a “dormant” species.^{6,11} An initiator with higher electron delocalization and steric hindrance of the reactive center is preferable and easily obtained by the reaction of *sec*-butyl lithium (*s*-BuLi) or *n*-butyl lithium (*n*-BuLi) with *1,1*-Diphenylethylene (DPE) *in-situ* at low temperature in the reaction solvent, e.g. in THF.¹²

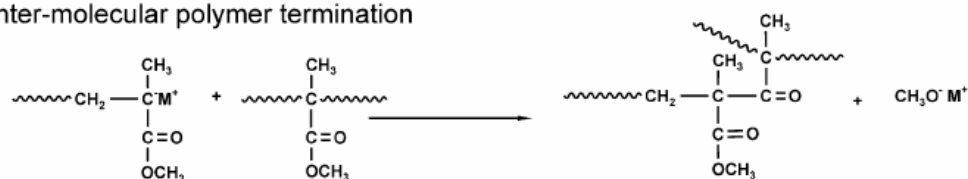
1. Initiator destruction



2. Monomer carbonyl attack



3. Inter-molecular polymer termination



4. Intra-molecular back-biting termination

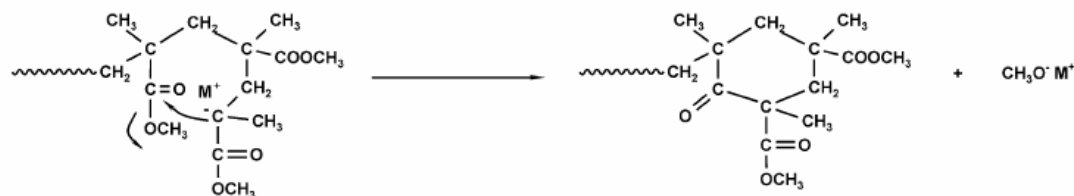


Figure 8-3. Side reactions in the polymerization of methyl methacrylate with a lithium alkyl initiator.¹²

The coupling between two chains is rarely observed since the inter-molecular polymer termination is thermodynamically unfavorable.^{13,14} Another aspect in the livingness of the alkyl acrylate and alkyl methacrylate monomers remains the relative short livingness of the active chains. After complete monomer conversion the nucleophilic attack of the carbanion on the carbonyl of the pre-antepenultimate monomer unit (x-2) occurs and a six-member ring is formed. This so-called “back-biting” product, a cyclic, enolized β -ketoester, can be easily detected in Size Exclusion Chromatography (SEC) coupled with UV detection for poly(alkyl acrylate)s and poly(alkyl methacrylate)s at 260 and 310 nm, respectively.^{15,16} As a side product of this reaction, lithium methanolate is formed which is unable to reinitiate the polymerization of methyl methacrylate at low temperature. Several systems were proposed to achieve the synthesis of poly(alkyl acrylate) and poly(alkyl methacrylate) in a living/controlled fashion via anionic polymerization in THF: alkali metal alkoxides,¹⁷⁻²¹ LiCl,²²⁻²⁶ LiClO₄,^{27,28} Et₂Zn,²⁹ or Et₃B,³⁰ and in toluene: trialkylaluminium compounds in

the presence of lewis bases (12-crown-4, methyl pivalate, methylbenzoate, and *N,N,N',N'*-tetramethylenediamine),³¹⁻³⁶ or tetraalkylammonium.^{31,37}

References

- (1) Szwarc, M. *Living Polymers and Mechanisms of Anionic Polymerization*, 1983.
- (2) Hsieh, H. L. *ACS Symposium Series* **1998**, 696, 28-33.
- (3) Flory, P. J. *J. Am. Chem. Soc.* **1940**, 62, 1561.
- (4) Bywater, S. *Macromolecules* **1998**, 31, 6010-6013.
- (5) Bywater, S.; Worsfold, D. J. *Journal of Organometallic Chemistry* **1967**, 10, 1-6.
- (6) Hsieh, H. L.; Quirk, R. P. *Anionic Polymerization*; Marcel Dekker, Inc.: New York, Basel, Hong Kong, 1996.
- (7) Arest-Yakubovich, A. A. *J. Polym. Sci., Part A: Polym. Chem.* **1997**, 35, 3613-3615.
- (8) Graham, R. K.; Dunkelberger, D. L.; Goode, W. E. *Journal of the American Chemical Society* **1960**, 82, 400-403.
- (9) Graham, R. K.; Panchak, J. R.; Kampf, M. J. *Journal of Polymer Science* **1960**, 44, 411-419.
- (10) Graham, R. K.; Dunkelberger, D. L.; Cohn, E. S. *Journal of Polymer Science* **1960**, 42, 501-510.
- (11) Young, R. N.; Quirk, R. P.; Fetters, L. J.; Luston, J.; Vass, F. *Anionic Polymerization*; Springer-Verlag: Berlin, Heidelberg, New York, Toronto, 1984; Vol. 56.
- (12) Baskaran, D. *Progress in Polymer Science* **2003**, 28, 521-581.
- (13) Müller, A. H. E.; Gerner, F. J.; Kraft, R.; Hoecker, H.; Schulz, G. V. *Polymer Preprints (American Chemical Society, Division of Polymer Chemistry)* **1980**, 21, 36-37.
- (14) Gerner, F. J.; Hoecker, H.; Müller, A. H. E.; Schulz, G. V. *European Polymer Journal* **1984**, 20, 349-355.
- (15) Janata, M.; Lochmann, L.; Vlcek, P.; Dybal, J.; Müller, A. H. E. *Makromolekulare Chemie* **1992**, 193, 101.
- (16) Maurer, A.; *Ph. D. Thesis*, Johannes Gutenberg Universität: Mainz, Germany, 1998.
- (17) Vlcek, P.; Lochmann, L. *Progress in Polymer Science* **1999**, 24, 793-873.
- (18) Lochmann, L.; Janata, M.; Machova, L.; Vlcek, P.; Mitera, J.; Müller, A. H. E. *Polymer Preprints (American Chemical Society, Division of Polymer Chemistry)* **1988**, 29, 29-30.
- (19) Lochmann, L.; Kolarik, J.; Duskocilova, D.; Vozka, S.; Trekoval, J. *Journal of Polymer Science, Polymer Chemistry Edition* **1979**, 17, 1727-1737.
- (20) Lochmann, L.; Müller, A. H. E. *Makrom. Chem.* **1990**, 191, 1657.
- (21) Wang, J. S.; Jerome, R.; Bayard, P.; Patin, M.; Teyssie, P. *Macromolecules* **1994**, 27, 4635.
- (22) Varshney, S. K.; Hautekeer, J. P.; Fayt, R.; Jérôme, R.; Teyssié, P. *Macromolecules* **1990**, 23, 2618-2622.
- (23) Fayt, R.; Forte, R.; Jacobs, C.; Jérôme, R.; Ouhadi, T.; Teyssié, P.; Varshney, S. K. *Macromolecules* **1987**, 20, 1442-1444.

-
- (24) Kunkel, D.; Müller, A. H. E.; Lochmann, L.; Janata, M. *Makromol. Chem., Macromol. Symp.* **1992**, *60*, 315.
- (25) Kunkel, D. *Ph. D. Thesis*; Johannes-Gutenberg Universität: Mainz, 1992.
- (26) Kunkel, D.; Müller, A. H. E.; Janata, M.; Lochmann, L. *Polym. Prepr. (Am. Chem. Soc., Div. Polym. Chem.)* **1991**, *32*, 301-302.
- (27) Baskaran, D.; Sivaram, S. *Macromolecules* **1997**, *30*, 1550-1555.
- (28) Baskaran, D.; Müller, A. H. E.; Sivaram, S. *Macromolecules* **1999**, *32*, 1356-1361.
- (29) Ishizone, T.; Yoshimura, K.; Hirao, A.; Nakahama, S. *Macromolecules* **1998**, *31*, 8706-8712.
- (30) Ishizone, T.; Yoshimura, K.; Yanasc, E.; Nakahama, S. *Macromolecules* **1999**, *3*, 955.
- (31) Schlaad, H.; Schmitt, B.; Müller, A. H. E.; Jüngling, S.; Weiss, H. *Macromolecules* **1998**, *31*, 573-577.
- (32) Schmitt, B.; Schlaad, H.; Müller, A. H. E. *Macromolecules* **1998**, *31*, 1705-1709.
- (33) Schmitt, B.; Schlaad, H.; Müller, A. H. E.; Mathiasch, B.; Steiger, S.; Weiss, H. *Macromolecules* **2000**, *33*, 2887-2893.
- (34) Baskaran, D.; Müller, A. H. E.; Sivaram, S. *Macromolecular Chemistry and Physics* **2000**, *201*, 1901-1911.
- (35) Marchal, J.; Gnanou, Y.; Fontanille, M. *Makromol. Chem., Macromol. Symp.* **1996**, *107*, 27.
- (36) Anderson, B. C.; Andrews, G. D.; Arthur Jr., P.; Jacobson, H. W.; Melby, L. R.; Playtis, A. J.; Sharkey, W. H. *Macromolecules* **1981**, *14*, 1599.
- (37) Schlaad, H.; Müller, A. H. E. *Macromolecules* **1998**, *31*, 7127.

8.2 Fundamentals of free-radical emulsion polymerization

A typical formulation may include the dispersing medium (water), one or more hydrophobic monomer(s) (or slightly water-soluble), an emulsifier or stabilizer (surfactant), and a water-soluble free-radical initiator. Mechanical stirring allows the emulsification. Above its Critical Micellar Concentration (*CMC*), the emulsifier molecules form micelles containing monomer which are in equilibrium with non-associated molecules (unimers of emulsifier). At time zero (t_0), the system is constituted by emulsifier micelles containing monomer (diameter, $D_p \sim 5\text{-}10\text{ nm}$, number $\sim 10^{18}\text{ cm}^{-3}$), and large monomer droplets ($D_p \sim 1000\text{ nm}$, number $\sim 10^{10}\text{ cm}^{-3}$). The different structures are stabilized by the emulsifier localized at the interfaces.

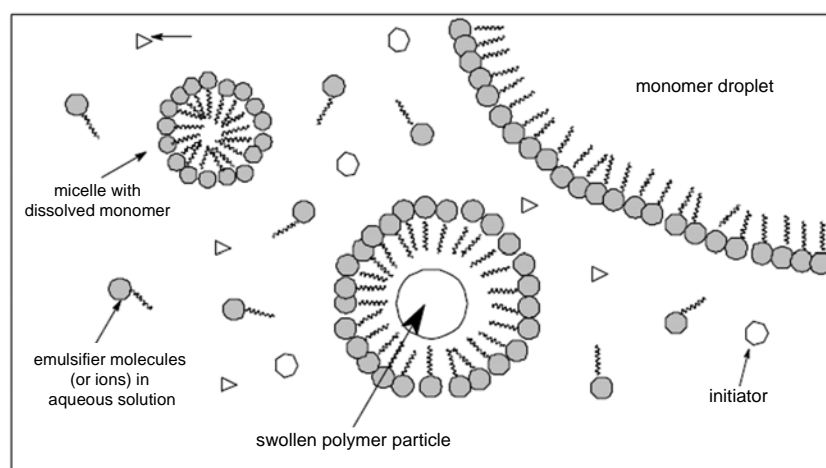


Figure 8-4. Schematic picture of an emulsion polymerization system after initiation.

After injection of the water-soluble initiator, radicals are produced in the aqueous phase and react with dissolved monomer molecules (water solubility of styrene at $50\text{ }^\circ\text{C} \approx 4 \cdot 10^{-3}\text{ mol}\cdot\text{L}^{-1}$).¹ A schematic picture of the system after initiation is shown in Figure 8-4. When a critical degree of polymerization is reached, the resulting oligomeric radicals become less water-soluble and enter into the micelles. The oligoradicals do not enter the monomer droplets because of the higher amount of micelles (higher specific surface area). The diffusion of monomers from the emulsified droplets, through the aqueous medium, into the micelles allows the polymerization inside the micelles, which are called particles. The process can be divided in three parts:

- The nucleation step (stage I), where the particles are formed. The particles number and the polymerization rate increase with the time. The micelles containing no radical act as emulsifier-reservoir for the growing particles. The end of the nucleation step is characterized by the disappearance of the micelles.
- Particles growth (stage II), where the particles number and the polymerization rate are constant. The monomer concentration inside the particles, $[M]_p$, is constant because of the monomer diffusion from the droplets to the particles via the aqueous phase.
- The termination (stage III), where the droplets have disappeared and the polymerization rate decreases.

The nucleation step is of importance because it determines the final latex particles number, N_p . Multiple equilibria have to be considered to describe the mechanisms. Different theories were established to understand the particles formation (nucleation step) and to predict the final N_p . The emulsifier concentration and the monomer solubility in water are two key-factors.¹ The nucleation step is over when no new particles are formed (end of stage I). The newly-formed oligoradicals can either terminate with oligoradicals in the aqueous phase or enter into a pre-existing particle. The latter mechanism is more probable at higher monomer conversion. Under the assumption of an exclusively micellar nucleation (entry of an oligoradical into a micelle, for an emulsifier concentration above its *CMC*), Smith, and Ewerts established a relation between N_p , the emulsifier concentration, $[S]$, and the initiator concentration, $[I]$:²

$$N_p \propto [I]^{\frac{2}{5}} \cdot [S]^{\frac{3}{5}} \quad (8-1)$$

It was demonstrated that the relation is not only valid for pure micellar nucleation mechanism. The theory is valid for any nucleation mechanism under the assumption that the particle nucleation ends when particle surfaces are completely saturated by the stabilizer.⁴ After formation of the particles, the polymerization occurs in the particles where the concentrations in propagating radicals and in monomer are maintained constant. The decomposition of the initiator is slow and continuous in the aqueous phase. Inside the

particle, the growing macroradical, P_n^* , can propagate, or can be terminated by another radical or by transfer to monomer. The monomeric radical, M^* , can either propagate within the particle or exit from it (desorption). The polymerization rate, R_p , can be expressed as follow:

$$R_p = -\frac{d[M]_{\text{latex}}}{dt} = [M]_0 \cdot \frac{dX_p}{dt} = k_p \cdot [M]_p \cdot [P^*]_{\text{latex}} \quad (8-2)$$

where $[M]_{\text{latex}}$, $[M]_p$, are the monomer concentrations in the latex and in the particles, respectively, $[M]_0$ the initial monomer concentration, X_p , the monomer conversion, and $[P^*]_{\text{latex}}$, the total concentration in radicals. By introducing the parameter, n , which is the average number of radical per particle, it is possible to obtain a simplified expression of the polymerization rate (A is the Avogadro's number):

$$R_p = \frac{k_p \cdot (n \cdot N_p)}{A} [M]_p \quad (8-3)$$

n is the determining experimental parameter. Two models are proposed:^{2,5} the 0/1 model where bimolecular termination occurs instantaneously as soon as a second oligoradical enters into the particle ($n \leq 0.5$), and the pseudo-bulk model, for large particles, when termination is slow (more than one radical in the particle, $n \geq 0.5$) or when desorption is faster than termination ($n \ll 0.5$).

References

- (1) Gilbert, R. *Emulsion Polymerization - A Mechanistic Approach*; Academic Press: London, 1995.
- (2) Smith, W. V.; Ewart, R. H. *Journal of Chemical Physics* **1948**, 592.
- (3) Roe, C. P. *Industrial & Engineering Chemistry* **1968**, 60, 20.
- (4) Lovell, P. *Emulsion Polymerization and Emulsion Polymers*, 1997.

8.3 Curriculum vitae

Date of Birth	11 th of May 1977, in Lyon, France
Education	10/1995-07/2000: Bachelor of Science Degree in chemistry, Université Pierre et Marie Curie, Paris VI, France. 10/2000-07/2001: Master's Degree in chemistry, University Pierre et Marie Curie, Paris VI, France. Topic: <i>Synthesis of New pH- and Thermo-Responsive Block Copolymers via Anionic Polymerization.</i> 09/2001-2005: French-German Ph. D. thesis (<i>Thèse en Cotutelle</i>) at the department Makromolekulare Chemie II in Bayreuth University, and at the Laboratoire de Chimie des Polymères in University Pierre et Marie Curie, Paris VI, France. Topic: <i>New Double-Responsive Block copolymers based on N,N diethylacrylamide: synthesis, Kinetics, Micellization, and Application as Emulsion Stabilizers</i> Supervisors: Prof. Dr. Axel Müller and Prof. Dr. Bernadette Charleux
Professional experience	07/1999-08/1999: Industrial training at RHODIA, Aubervilliers, France. 04/2000-07/2000: Industrial training at RHODIA, Saint-Fons, France.
Scholarships and awards	French-Bavarian Institut's scholarship French Research Minister's scholarship National Science Foundation's travel grant (July 2003) European Polymer Federation's student grant (June 2003)
Languages	French (mother tongue), German, and English
Activities	Traveling, tennis, cinema, literature, first aid diploma

Bayreuth, June 2005.

8.4 List of publications

The following publications are enclosed in this PhD thesis:

- Xavier André, Khaled Benmohamed, Alexander V. Yakimansky, Galina L. Litvinenko, Axel H. E. Müller: 'Anionic Polymerization and Block Copolymerization of *N,N*-Diethylacrylamide in the Presence of Triethylaluminium: Kinetic Investigation Using In-Line FT-NIR Spectroscopy', *Macromolecules* **2006**, 39, 2773-2787.
- Xavier André, Axel H. E. Müller: 'New Thermo- and pH-Responsive Micelles of Poly(acrylic acid)-*block*-Poly(*N,N*-diethylacrylamide)', *Macromol. Rapid. Comm.* **2005**, 26, 558-563.
- Xavier André, Markus Burkhardt, Peter Lindner, Michael Gradzielski, Axel H. E. Müller: 'Solution properties of Double-Stimuli Micelles of Poly(acrylic acid)-*block*-Poly(*N,N*-diethylacrylamide)', *Langmuir*, **2006**, to be submitted.
- Xavier André, Khaled Benmohamed, Sabine Wunder, Axel H. E. Müller, Bernadette Charleux: 'Remarkable Stabilization of Latex Particles by a New Generation of Double-Stimuli Responsive Micelles made of Poly[(meth)acrylic acid)-*block*-Poly(*N,N*-diethylacrylamide) Copolymers', *Macromolecules* **2006**, to be submitted.

Within the scope of my PhD thesis the following publications have been additionally published.

- Axel H. E. Müller, Xavier André, Christine M. Schilli, Bernadette Charleux: 'Double-Stimuli Responsive Block Copolymers of Acrylic Acid, *N,N*-diethylacrylamide, and *N*-isopropylacrylamide', *Pol. Mater. Sci. Eng.* **2004**, 91, 252-253.
- Matteo D. Costioli, Daniel Berdat, Ruth Freitag, Xavier André, Axel H. E. Müller: 'Investigation of the Telomerisation Kinetics of *N*-isopropylacrylamide using 3-mercaptopropionic Hydrazide as Chain Transfer Agent', *Macromolecules* **2005**, 38, 3630-3637.

- Sharmila Mutukrishna, Günther Jutz, Xavier André, Hideharu Mori, Axel H. E. Müller: 'Synthesis of Hyperbranched Glycopolymers via Self-Condensing Atom Transfer Radical Copolymerization of Sugar-Carrying Acrylate', *Macromolecules* **2005**, 38, 9-18.
- Hideharu Mori, Andreas Walther, Xavier André, Michael G. Lanzendörfer, Axel H. E. Müller: 'Synthesis of Highly Branched Cationic Polyelectrolytes via Self-Condensing Atom Transfer Radical Copolymerization with 2-(Diethylamino)ethyl Methacrylate', *Macromolecules* **2004**, 37, 2054-2066.
- Axel H. E. Müller, Xavier André, Bernadette Charleux: 'Anionic Block Copolymerization of *N,N*-diethylacrylamide. Applications for Double-Stimuli Responsive Micelles', *e-Polymer* **2003**, P_003.
- Galina Litivienko, Xavier André, Christopher Barner-Kowollik, Axel H. E. Müller, 'An Analytical Solution for the Mechanism of the Reversible Addition Fragmentation Chain Transfer (RAFT) Polymerization', *in preparation*.

8.5 Presentations at international conferences

The results obtained during my Ph. D. thesis were presented at different international conferences.

- Makromolekulares Kolloquium 2005, Freiburg, Germany (February 2005): *Poster presentation*

‘Double Stimuli-Responsive Micelles of Poly[(Meth)acrylic Acid]-*block*-Poly(*N,N*-diethylacrylamide): Efficient Use as Stabilizer in Emulsion Polymerization Processes’

- 228th ACS National Meeting, Philadelphia, PA, USA (August 2004): *Oral presentation*
‘Double-Stimuli Responsive Block Copolymers of Acrylic Acid, *N,N*-diethylacrylamide, and *N*-isopropylacrylamide’

- 40th IUPAC International Symposium on Macromolecules, Paris, France (July 2004): *Poster presentation*

‘Remarkable Stabilization of Latex Particles by Thermo- and pH-Responsive Block Copolymers of Poly[(Meth)acrylic Acid]-*block*-Poly(*N,N*-Diethylacrylamide)’

- 40th IUPAC International Symposium on Macromolecules, Paris, France (July 2004): *Oral presentation*

‘Anionic Block Copolymerization of *N,N*-Diethylacrylamide in the Presence of $AlEt_3$. Kinetic Investigations Using In-Situ FT-NIR Spectroscopy’

- 5th International Symposium on Polymers in Dispersed Media 2004, Lyon, France (April 2004): *Poster presentation*

‘Stabilization of Latex Particles by a New Generation of Amphiphilic Thermo- and pH-Responsive Micelles of Poly[(Meth)acrylic Acid]-*block*-Poly(*N,N*-Diethylacrylamide) Copolymers’

- Bayreuth Polymer Symposium, Bayreuth, Germany (September 2003): *Poster presentation*
'Double-Stimuli Responsive Micelles of Poly[(meth)acrylic acid]-*block*-Poly(*N,N*-diethylacrylamide)'
- 16th IUPAC International Symposium on Ionic Polymerization, Boston, MA, USA (July 2003): *Poster presentation*
'Anionic Block Copolymerization of *N,N*-diethylacrylamide in the Presence of Triethylaluminium. Kinetic Study using inline FT-NIR Spectroscopy'
- European Polymer Federation Congress 2003, Stockholm, Sweden (June 2003): *Poster presentation*
'Anionic Block Copolymerization of *N,N*-diethylacrylamide. Applications for Double-Stimuli Responsive Micelles'
- 5th Minerva Students Symposium, Naurod, Germany (April 2003): *Poster presentation*
'New Thermo- and pH-Responsive Amphiphilic Micelles of Poly(Acrylic Acid)-*block*-Poly(*N,N*-diethylacrylamide)'

Acknowledgments – Remerciements – Danksagung

Je remercie Monsieur le Professeur Axel Müller de m'avoir accueilli au sein de son laboratoire Makromolekulare Chemie II à l'université de Bayreuth et d'avoir encadré ma thèse. Tout en me laissant libre dans la conduite de mes travaux et en me confiant des responsabilités au sein de votre laboratoire, vous avez toujours été à mon écoute et m'avez guidé tout au long de ses quatre années. Je remercie également Madame le Professeur Bernadette Charleux d'avoir co-encadré ma thèse au Laboratoire de Chimie des Polymères à l'université Pierre et Marie Curie et de m'avoir permis de réaliser cette thèse en co-tutelle. Je tiens tout particulièrement à vous remercier pour votre grande confiance, pour vos nombreux conseils et suggestions, pour la liberté que vous m'avez donnée, ainsi que pour votre grande patience car la distance n'a pas rendu les contacts évidents. Je tiens à remercier conjointement mes deux directeurs de thèse, 'meine Doktormutter und meinen Doktorvater', pour l'opportunité qu'ils m'ont donnée de travailler sur ce projet commun aux deux laboratoires et par ce fait d'aborder des domaines variés de la chimie et physico-chimie des polymères. Merci aussi pour m'avoir permis de présenter mes résultats dans de nombreuses conférences internationales.

Je remercie Messieurs les Professeurs Jean-Pierre Vairon et Patrick Hémerly de m'avoir accueilli au sein du laboratoire de Chimie des Polymères pendant mon Master et pendant les différents séjours de recherche passés à Paris au cours de ma thèse. Je tiens également à remercier Monsieur le Professeur Jean-Pierre Vairon pour son soutien, sa confiance et de m'avoir permis de réaliser ce programme d'échange avec l'université de Bayreuth.

Je remercie Monsieur le Professeur Robert Jérôme pour l'honneur qu'il m'a fait en acceptant d'être rapporteur de mon travail. Par ailleurs, je remercie Messieurs les Professeurs Dominique Hourdet et Helmut Alt d'avoir accepté de participer à ce jury. Je remercie également Monsieur le Professeur Michael Gradzielski pour son aide scientifique inestimable et sa disponibilité sans limites. Mes remerciements vont aussi à Hideraru Mori et à Mingfu Zhang qui m'ont accompagné par leurs nombreuses discussions scientifiques, leurs suggestions et conseils, leur disponibilité et leurs qualités humaines inestimables. Je remercie également Michael Lanzendörfer[†] pour son introduction à la spectroscopie NIR et pour ses mesures MALDI de grande qualité. Je remercie également Monsieur le Professeur Volker Abetz pour ses conseils avisés et sa disponibilité.

Je tiens à remercier très chaleureusement les deux stagiaires qui ont travaillé avec moi: Khaled Benmohamed qui tout au long de son stage Erasmus a manifesté un intérêt sans bornes pour les synthèses de copolymères à blocs par voie anionique. Merci pour toute ton aide, pour le temps que tu as passé devant la rampe à vide ou dans le labo anionique (en plein été!), mais surtout pour ton amitié et la confiance réciproque que nous avons acquise. Je remercie aussi Peter Igney pour l'aide qu'il m'a apporté durant l'été 2004, pour son enthousiasme et son désir de comprendre.

Je tiens à remercier Thomas Breiner et Valéry Rebizant pour leur aide lors de mes toutes premières polymérisations anioniques. Un grand merci aussi à Nemesio Martinez-Castro pour sa complicité, son amitié et son soutien sans failles tout au long de ses années, dont quelques unes communes dans ce fameux labo anionique (au fond du couloir...). Merci aussi à Andreas Walther pour les nombreuses discussions scientifiques, les corrections apportées à ce manuscrit, son soutien, son amitié et sa confiance.

Mes remerciements vont aussi à Sabine Wunder, sans qui les appareils d'analyse ne fonctionneraient pas aussi bien (voire pas du tout!), pour son aide dans les responsabilités que nous avons eues en commun, sa grande patience et ses qualités humaines. Un remerciement tout particulier est destiné à Astrid Göpfert et Markus Drechsler pour les nombreuses images de (cryo)-TEM, ainsi que pour leur professionnalisme et leur bonne humeur à toute épreuve. Je tiens à remercier également Markus Burkhardt pour son aide pendant les séjours de mesures à Grenoble et pour l'interprétation des courbes de neutrons à Bayreuth.

Un remerciement tout particulier va à Cornelia Lauble, pas seulement pour les mesures de MALDI, mais aussi pour la bonne ambiance dans le labo anionique. Merci aussi à Annette Krökel pour toute son aide et d'avoir pris soin de la RMN.

Je tiens à remercier Alexander Yakimanski (Sascha), Dmitry Pergushov et Galina Litivienko pour les nombreuses discussions intéressantes que nous avons eues, leur bonne humeur, leur professionnalisme et les quelques trop rares moments passés ensemble. Merci à Rami Abdel Rahem pour ses fructueux conseils, sa disponibilité et sa gentillesse de tous les instants. Je remercie également tout particulièrement Matteo Costioli, Daniel Berdat, Jérôme Crassous et Markus Ruppel pour les discussions scientifiques trop rares que nous avons eues, mais surtout pour leur bonne humeur, leur franchise et leur confiance. Merci aussi à Kerstin Matussek, Manuela Fink et Denise Danz pour les mesures de MALDI. Je

remercie également Clarissa Abetz pour les mesures de SEM, Adriana Boschetti pour celles de DSC, Karl-Heinz Lauterbach pour celles de dn/dc.

Merci aux administrateurs réseau qui se sont succédés à la rude et trop ingrate tâche: Holger Schmalz, Hans Lechner, Chih-Cheng Peng, Felix Plamper et Pierre Millard. Merci aussi à Gaby Rösner-Oliver pour toute son aide sans bornes au secrétariat du MCII. Merci à tous les Français chimistes expatriés à Bayreuth pour de plus ou moins longues périodes ainsi qu'aux francophiles et/ou francophones du MCII ou d'ailleurs, pour leur bonne humeur, leur sympathie et leur soutien. Merci à tous les autres membres actuels ou anciens du MCII qui ont contribué à la bonne ambiance qui y a régné.

Mes remerciements vont aussi aux nombreuses personnes qui m'ont aidé à Paris, en particulier Chuong Bui, Carine Burguière et Julien Nicolas, sans oublier Patrice Castignolles, Michel Moreau, Maud Save, Laurent Bouteiller, Christophe Chassenieux, Francois Ganachaud, et Bernard Coutin pour les nombreuses discussions, suggestions et critiques constructives de mon travail. Merci à tous les autres membres du laboratoire pour la bonne ambiance qui y a régné.

Je remercie tout particulièrement ma famille qui m'a toujours soutenu au long de mes études universitaires.

Mes remerciements vont aussi à l'Institut Universitaire Franco-Bavarois et au Ministère de la Recherche Français pour les aides financières apportées à ma thèse en co-tutelle.

Erklärung

Hiermit erkläre ich, dass ich die Arbeit selbständig verfasst und keine anderen als die angegebenen Quellen und Hilfsmittel benutzt habe.

Ferner erkläre ich, dass ich nicht anderweitig mit oder ohne Erfolg versucht habe, eine Dissertation einzureichen oder mich einer Doktorprüfung zu unterziehen.

Bayreuth, den 29. Juni 2005.

A handwritten signature in black ink, appearing to read 'Xavier André', with a long horizontal stroke extending to the right.

Xavier André.